

THE BIOGEOCHEMISTRY OF COBALT IN THE SARGASSO SEA

By

Mak A. Saito

B.A. Oberlin College, 1994

Submitted in partial fulfillment of the requirement for the degree of

Doctor of Philosophy

at the

MASSACHUSETTS INSTITUTE OF TECHNOLOGY

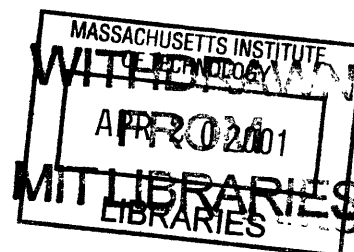
and the

WOODS HOLE OCEANOGRAPHIC INSTITUTION

February, 2001

© 2000 Mak A. Saito
All rights reserved

Lundgren



The author hereby grants to MIT and WHOI permission to reproduce paper and electronic copies of this thesis in whole or part and to distribute them publicly.

Signature of Author

Joint Program in Chemical Oceanography
Massachusetts Institute of Technology and
Woods Hole Oceanographic Institution
November 2000

Certified by

James W. Moffett
Thesis Supervisor

Sallie W. Chisholm
Thesis Supervisor

Accepted by

Margaret K. Tivey
Chair, Joint Committee for Chemical Oceanography
Woods Hole Oceanographic Institution

THE BIOGEOCHEMISTRY OF COBALT IN THE SARGASSO SEA

ABSTRACT

by Mak A. Saito

Processes that enable marine phytoplankton to acquire trace metals are fundamental to our understanding of primary productivity and global carbon cycling. This thesis explored the biogeochemistry of cobalt using analytical chemistry and physiological experiments with the dominant phytoplankton species, *Prochlorococcus*.

A high sensitivity method for Co speciation was developed using hanging mercury drop cathodic stripping voltammetry. Dissolved Co at the Bermuda Atlantic Time Series station (BATS) in the Sargasso Sea was bound by strong organic complexes with a conditional stability constant of $\log K = 16.3 \pm 0.9$. A depth profile of Co at BATS revealed a nutrient-like profile. Biweekly time series measurements of total cobalt near Bermuda from the MITESS sampler were 0-47 pM throughout 1999, and averaged 20 ± 10 pM in 1999. A transect of total cobalt from BATS to American coastal waters ranged from 19-133 pM and correlated negatively with salinity ($r^2 = 0.93$), suggestive of coastal waters as an input source.

Prochlorococcus strains MED4-Ax and SS120 showed an absolute requirement for Co, despite replete Zn. ^{57}Co uptake rates and growth rates were enhanced by additions of filtered low Co cultures, suggesting that a ligand is present that facilitates Co uptake. Bottle incubations from a *Synechococcus* bloom in the Pacific showed production of 425 pM strong cobalt ligand. These and other lines of evidence support the hypothesis that a cobalt ligand, or cobalophore, is involved in cobalt uptake.

Co-limited *Prochlorococcus* cultures exhibited an increase in the fraction of cells in G2 relative to other cell cycle stages during exponential growth, and the durations of this stage increased with decreasing cobalt concentrations. This effect was not observed with Fe, N, or P-limited cultures, suggestive of a specific biochemical function of cobalt that would interfere with the late stages of the cell cycle.

The ligand Teta was explored as a means to induce cobalt limitation. The CoTeta complex was not bioavailable to the Sargasso Sea microbial assemblage in short-term experiments. Bottle incubations with Teta did not induce cobalt limitation of *Prochlorococcus*. These results are consistent with the lower conditional stability constant for CoTeta ($\log K = 11.2 \pm 0.1$) relative to natural cobalt ligands in seawater, and with culture studies that suggest uptake of cobalt via strong organic ligands.

Thesis Supervisors:

James W. Moffett

Title: Associate Scientist, Marine Chemistry and Geochemistry Department,
Woods Hole Oceanographic Institution

Sallie W. Chisholm

Title: Professor of Civil and Environmental Engineering, and Professor of Biology
Massachusetts Institute of Technology

Wonder and knowledge are both to be cherished

-Stephen Jay Gould

This thesis is dedicated to my parents

Acknowledgements

After five years of work on a thesis there are many people who I would like to thank for their assistance and support along the way. First, I would like to thank my advisors. Jim has been a constant source of support and advice over the years. His dedication to the objectives of this work has been critical to its successful completion. And he taught me to be a sea-going oceanographer; may we smoke cigars on the fantail again soon. I'd like to thank Penny for her detailed constructive criticisms that have strengthened my arguments. Also I valued our philosophical discussions early in my graduate career, which made the many long evenings in the lab seem all the more worthwhile.

I am fortunate to have had a committee comprised of experts in the various areas of my thesis research. John Waterbury, in addition to generously offering me lab space to do my culture work, also suggested that we undertake the difficult task of isolating an axenic strain of *Prochlorococcus*. After many months of work we succeeded in this goal and made some of the most important experiments in Chapter 4 possible. Bill Sunda, whose 1995 study with Sue Huntsman laid the groundwork for this thesis, spent many hours discussing science with me (even over dimsum). Tina Voelker introduced me to the field of aquatic chemistry with the 1.76 class, and has been very helpful in talking over details of the chemical aspects of this thesis work. Also, having the opportunity to be a teaching assistant with Tina really solidified my understanding of the field and I will always be appreciative of our interactions during that intense time. Ed Boyle has been helpful in so many ways over the past five years: from what I learned in his classes, to discussing my cobalt data, and most recently, letting me make measurements on his samples from the MITESS sampler. In particular, his advice to me after my thesis proposal to make sure I obtained high-quality total cobalt measurements was key to motivating the work in Chapter 3.

I also want to thank many people in the scientific community here at WHOI and up at MIT. Thanks to Ed Sholkovitz for chairing my defense and for welcoming me to WHOI as a student in his lab during my first summer. Freddi Valois has been helpful around the lab and was a source of great stories. Rob Olson was generous in reading my cell cycle draft. Maureen Conte and J.C. Weber provided me with great samples from the Atlantic. Dave Kulis was kind enough to let me use the Anderson lab fluorometer for several years. A big thanks needs to go to the captain and crew of the R/V Oceanus for their assistance on the many cruises to the Sargasso. Thanks also to the captain and crew of the R/V Melville for their help on our recent San Diego - Peru cruise.

I'm truly appreciative for the friends I've had here who've made the past five years fun. My labmates in the Moffett Lab, Kathy Barbeau, Liz Kujawinski, Rachel Wisniewski, Jordan Watson, Carrie Tuit, and Ian Rummel. And friends in the Chisholm lab: Gabrielle Rocap, Liz Mann, Kent Bares, Lisa Moore, Matt Sullivan, Nathan Ahlgren, Stephanie Shaw, Claire Ting, Phoebe Lam and many others whose friendship and instruction in the lab have been invaluable. Philippe "pHunkerbell" Tortell who's become

a good friend and sounding board on our cruises together. I have to thank housemates and friends over the years, Kirsten, Anna Estes, Ann Pearson, Lihini, Chris (ask him about his tattoo) Reddy, Albert, Rose, and Millfield house, of course. I also have to thank the musical outlets I've had over the past years, for those who know me well, know that without music there can be no science: Aporia, my bandmates from that boston-based band of the future (Aaron, Heidi, T. Rex Wolff, Ian, and David). And down here in Woods Hole I want to thank Manny of Pie in the Sky and the Captain Kidd for their open-mike nights that gave me something to look forward to. Thanks to TSG and the Posterboyz too...

Thanks to my friends and advisors from Oberlin. Oberlin is a mecca for many things – for me it was a place for inspiration, love of learning, and music. In particular, David Egloff has been a great mentor during and after Oberlin.

Finally, I want to thank my parents and family. My mother and father have always made our education a priority, without question. Mhari (bobafette) for being so cool, and understanding during these crazy years. My grandparents and aunt Margaret in Scotland, for welcoming us in the summers for the past 20 years, I did a lot of growing up there. I want to thank my late grandfather, Bill, who taught me how to be practical, to work with my hands, and about life in general.

The work in this thesis was supported by a grant from the National Science Foundation (#OCE-9618729) for cyanobacteria metal interactions in the Sargasso Sea. I have been funded through WHOI on an NSF coastal traineeship (#DGE-9454129) for my first year, followed by an EPA STAR Graduate Fellowship for the subsequent years. Additional funding was supplied by the WHOI Educational Endowment Funds and by the WHOI Ditty Bag fund for part of the DNA/cell cycle work.

TABLE OF CONTENTS

CHAPTER 1	13
Introduction: Hypotheses on the Biogeochemistry of Cobalt	13
Preface	13
References	19
CHAPTER 2	35
Complexation of cobalt by natural organic ligands in the Sargasso Sea as determined by a new high-sensitivity electrochemical cobalt speciation method suitable for open ocean work.....	35
Abstract.....	36
1. Introduction	37
2. Theory.....	39
3. Materials and Methods	45
4. Results	49
5. Discussion.....	54
Conclusions	59
Acknowledgements	60
References	61
CHAPTER 3	93
Total Cobalt in the Western North Atlantic and the Sargasso Sea	93
Abstract.....	93
Introduction	94
Methods	96
Results and Discussion	99
Conclusions	107
Acknowledgements	109
References	110
CHAPTER 4	145
Cobalt limitation, uptake, and metal substitution in <i>Prochlorococcus</i>.....	145
Abstract.....	146
Introduction	147
Materials and Methods	148
Results	152
Discussion.....	155
References	158
CHAPTER 5	181
The Influence of Cobalt Limitation on the Cell Cycle of <i>Prochlorococcus</i>	181
Abstract.....	182
Introduction	183
Methods	185

Results	188
Discussion.....	191
Conclusions	197
References	199
CHAPTER 6.....	223
The Effects of the Cobalt Ligand Teta on <i>Prochlorococcus</i> in Culture and in the Sargasso Sea.....	223
Abstract.....	223
Introduction	224
Materials and Methods	226
Results	230
Discussion.....	234
APPENDIX I	264
Purification of <i>Prochlorococcus marinus</i> isolates (Waterbury and Saito)	
Introduction	264
References	269
APPENDIX II.	283
The fraction of cobalt as B₁₂ in photosynthetic cyanobacteria	283
References	284
APPENDIX III.....	285
The relationship between fluorescence per cell and <i>in vivo</i> fluorescence.....	285
Methods	286
Results and Discussion	286
References	289
APPENDIX IV.	297
Long-term cobalt limitation studies of <i>Prochlorococcus</i> in NTA and EDTA media: Raw data.....	297

TABLE OF FIGURES

Figure 1-1	Cobalt concentrations in aqueous environments	24
Figure 1-2	Cobalt and zinc in the northeast Pacific	26
Figure 1-3	Cobalt and zinc substitution in <i>E. huxleyi</i> and <i>Synechococcus</i>	28
Figure 1-4	The influence of complexation on primary productivity	30
Figure 1-5	Metal chemistry in the Archean ocean	32
Figure 2-1	Cobalt blank determination	64
Figure 2-2	Calibration of conditional stability constant for CoHDMG ₂	66
Figure 2-3	Oxidation of Co(II)EDTA	68
Figure 2-4	Total dissolved cobalt at BATS and sensitivity effects	70
Figure 2-5	Total ligand concentrations and conditional stability constants at BATS	72
Figure 2-6	Example CLE-ACSV titration and non-linear fit	74
Figure 2-7	Hydrographic and cell number data	76
Figure 2-8	Correlation between total cobalt and CoL	78
Figure 2-9	Comparison of CSVspectra before and after UV-irradiation	80
Figure 2-10	Model calculations of Co, Ni, DMG, and L	82
Figure 2-11	Kinetic study of cobalt and nickel Teta complexes	84
Figure 2-12	Calibration of CoTeta and NiTeta	86
Figure 3-1	Eh-pH diagram for inorganic cobalt in seawater	114
Figure 3-2	Recovery of cobalt with addition of base	116
Figure 3-3	Cruise track of western north Atlantic transect	118
Figure 3-4	Comparison of total dissolved cobalt depth profiles	120
Figure 3-5	Transect of total dissolved cobalt from BATS to shelf	122
Figure 3-6	Distribution of <i>Prochlorococcus</i> and <i>Synechococcus</i> on BATS transect	124
Figure 3-7	Time series of total cobalt in the Sargasso (MITES samples)	126
Figure 3-8	Time series data and hydrographic data	128
Figure 3-9	Cruise track of south Atlantic transect	130
Figure 3-10	Total cobalt, phosphate, temperature and salinity on south Atlantic transect	132
Figure 3-11	Correlation between total cobalt and phosphate in south Atlantic	134
Figure 3-12	Ratios of Co, Zn and Cd to carbon near Bermuda	136
Figure 4-1	Uptake of cobalt into <i>Prochlorococcus</i> in NTA, EDTA, and DTPA media	162
Figure 4-2	The influence of conditioned media on cobalt uptake in <i>Prochlorococcus</i>	164
Figure 4-3	Cobalt limitation of <i>Prochlorococcus</i> in long-term culturing studies	166
Figure 4-4	Addition of conditioned media to <i>Prochlorococcus</i> cultures	168
Figure 4-5	Nickel inhibition of cobalt limited <i>Prochlorococcus</i> cultures	170
Figure 4-6	Total dissolved cobalt and labile cobalt at the Costa Rica Upwelling Dome, Pacific	172
Figure 4-7	Production of cobalt ligands by the microbial/particulate community in Pacific	174
Figure 4-8	Cobalt and zinc non-substitution in <i>Prochlorococcus</i> MED4-Ax	176
Figure 4-9	Cobalt and cadmium substitution in <i>Prochlorococcus</i> SS120	178
Figure 5-1	Growth of cobalt limited <i>Prochlorococcus</i> MED4-Ax	202
Figure 5-2	Flow cytometry signatures of Sybr green stained <i>Prochlorococcus</i> cells	204
Figure 5-3	DNA analysis of cobalt limited cultures	206
Figure 5-4	Histograms of DNA in cobalt replete and limited cultures	208
Figure 5-5	Durations of cell cycle stages under cobalt limitation	210
Figure 5-6	Temporal variation in durations of cell cycle stages under cobalt limitation	212
Figure 5-7	DNA analysis of iron limited cultures	214
Figure 5-8	DNA analysis of ammonia and phosphate limited cultures	216
Figure 5-9	Cell size during ammonia and phosphate limitation	218
Figure 6-1	The possible influence of complexation on primary productivity	246
Figure 6-2	Structures of CoTeta and CoHDMG ₂	248
Figure 6-3	The lability of CoTeta as measured using cathodic stripping voltammetry	250
Figure 6-4	Cobalt limitation of <i>Prochlorococcus</i> MED4-Ax using Teta	252

Figure 6-5	Short-term uptake of $^{57}\text{CoTeta}$ in the Sargasso Sea	254
Figure 6-6	Inability of Teta to induce cobalt limitation in the Sargasso Sea	256
Figure 6-7	Long-term $^{57}\text{CoTeta}$ uptake in the Sargasso Sea	258
Figure 6-8	The influence of sunlight exposure on cobalt uptake in the Sargasso Sea	260
Figure I-1	Isolation of <i>Prochlorococcus</i> , plating in stationary phase	270
Figure I-2	Growth rates of recently picked colonies in 100% and 75% media	272
Figure I-3	The effect of inoculum size on the survival of <i>Prochlorococcus</i> cultures	274
Figure I-4	Inoculum volume, vitamin, and conditioned media effects	276
Figure I-5	Production of colored dissolved organic material upon filtration	278
Figure I-6	Fluorescence spectra of dissolved organic material	280
Figure III-1	Flow cytometry and <i>in vivo</i> fluorescence data on a cobalt limited culture	290
Figure III-2	Correlation between cell number and <i>in vivo</i> fluorescence	292
Figure III-3	Flow cytometry and <i>in vivo</i> fluorescence data on a cobalt limited culture	294
Figure IV-1	Raw data <i>Prochlorococcus</i> SS120 under cobalt limitation (NTA media)	298
Figure IV-2	Raw data <i>Prochlorococcus</i> MED4-Ax under cobalt limitation (EDTA media)	300

LIST OF TABLES

Table 2-1	The accuracy of total cobalt electrochemical measurements verified	88
Table 2-2	Conditional Stability Constants for DMG and TETA calibrated using EDTA	89
Table 2-3	Co-Speciation incubations – BATS September and October 1999	90
Table 2-4	Comparison of totals of equilibrated bottles to UV-Total Cobalt	91
Table 2-5	Stability Constants of strong synthetic cobalt and nickel ligands	92
Table 3-1	Selected Thermodynamic data for pe-pH diagram	138
Table 3-2	Sargasso Sea, Shelf Water and Extrapolated Zero Salinity Concentrations (nM)	138
Table 3-3	Crustal composition of transition elements	139
Table 3-4	Regression slopes of Co vs PO ₄ (μmol mol ⁻¹)	139
Table 3-5	Particulate metal:carbon ratios near Bermuda (from Sherrell and Boyle, 1992)	140
Table 3-6	Particulate metal:carbon ratios near Bermuda (from Sherrell and Boyle, 1992)	140
Table 3-7	Particulate metal:phosphate ratios near Bermuda (from Sherrell and Boyle, 1992)	140
Table 3-8	Total Dissolved Cobalt Concentrations in the Sargasso Sea and northwest Atlantic Ocean	141
Table 3-9	Cobalt Time Series at the Bermuda Testbed Mooring (MITESS)	142
Table 3-10	Total Cobalt along a south Atlantic surface transect (5m)	143
Table 4-1	Growth rates of <i>Prochlorococcus</i> zinc and cobalt limitation experiment shown in Figure 8.	180
Table 5-1	Pro-1 media composition for trace metal limitation made with Sargasso Seawater	220
Table 5-2	The influence of environmental factors on the cell cycle of phytoplankton	221
Table 6-1	Cobalt requirements and substitutions in marine phytoplankton	262
Table 6-2	Conditional Stability Constants for DMG and Teta calibrated using EDTA	262
Table 6-3	Stimulation of <i>Prochlorococcus</i> by Teta additions	263
Table 6-4	Application of Liebig's Law of the Minimum to the Sargasso Sea	263
Table I-1	Pro-1 media composition for plating made with 75% Sargasso Seawater	282

Chapter 1

Introduction: Hypotheses on the Biogeochemistry of Cobalt

Preface

Cobalt is an important micronutrient for marine phytoplankton and is part of several current hypotheses about the ecology and biogeochemistry of the oceans. Yet, the biogeochemistry of cobalt in the upper ocean has been much less explored than that of its more famous compatriot, iron. In particular, the organic complexation of cobalt, the strength and kinetics of the ligands, and biogenic sources of cobalt ligands are areas that have been unstudied, in part due to the formidable analytical challenge associated with the picomolar quantities of cobalt in the open oceans (Figure 1). I was inspired to undertake this study of cobalt for my thesis because of three hypotheses implicating an important role for cobalt in marine biogeochemistry: first, there is the potential for limitation of primary productivity by Co, and the potential for co-limitation of carbon uptake and either Cd, Co, or Zn. Second, given that the chemical form of cobalt in the open ocean was unknown, we were interested in the possibility of strong cobalt ligands existing in seawater and their potential use as uptake ligands. Third, there was the hypothesis that the use of cobalt by marine cyanobacteria could be traced through evolution back to the Archean ocean where Co was abundant and Zn was scarce. While the work in this thesis was completed with all of these hypotheses in mind, I have primarily focused on the second. Chapter 2 documents the extensive method development of an analytical technique to measure the speciation of cobalt in seawater. Chapter 3 applied this method to quantifying the distribution of total cobalt across temporal and spatial gradients in the Atlantic. Subsequent chapters explored the biogeochemistry of Co from an interdisciplinary perspective, using low-metal physiological studies with an abundant cyanobacterium, *Prochlorococcus*, hypothesized to influence the chemistry of cobalt in seawater. Chapter 4 uses cultures of *Prochlorococcus* to examine the uptake mechanism of cobalt. Chapter 5 takes a different

tack and looks at the influence of cobalt limitation on the DNA cell cycle of *Prochlorococcus* to get an indication of the physiological effects of cobalt limitation. One of the aims of Chapter 5 was to examine the possibility that cobalt limitation causes an effect in the prokaryotic *Prochlorococcus* cells that zinc limitation would cause in Eukaryotic cells (Falchuk et al., 1975); as a means to examine the potential for the evolution of metal requirements over geologic timescales. Finally, in Chapter 6 chemical and biological methods were combined to examine the uptake of cobalt in the Sargasso Sea, by using a strong cobalt ligand and conducting a variety of experiments to see if it is possible to induce cobalt limitation in natural populations of *Prochlorococcus*.

* * * *

The importance of trace metals in regulating the productivity and species composition of phytoplankton communities is a burgeoning field. With the advent of clean analytical techniques and the subsequent discoveries of the iron limitation and nutrient-like profiles for iron in major oceanic regimes (Martin and Fitzwater, 1988; Martin et al., 1989; researchers have discussed and modeled the potential impact of nutrient induced fluctuations in the biological pump on atmospheric CO₂ (Joos et al., 1991; Peng and Broecker, 1991). More recently, attention has turned to two more subtle hypotheses that connect trace metals to the biological pump. First, there is the hypothesis that iron may limit the growth of *Trichodesmium sp.* which in turn would limit the rate of nitrogen fixation in the surface ocean (Falkowski, 1997; Rueter et al., 1992; Wu et al., 2000). Second, the potential for marine phytoplankton to be carbon limited or carbon-zinc/cobalt co-limited has been demonstrated in the laboratory (Lane and Morel, 2000; Morel et al., 1994; Riebesell et al., 1994). Although this co-limitation has yet to be shown in the field, there is evidence for each piece separately: CO_{2(aq)} limitation was reported along a transect in the Atlantic ocean (Hein and Sand-Jensen, 1977), and a data set of Martin et al. (Martin et al., 1989) that was reinterpreted by Sunda and Huntsman

(1995, Figure 2) shows that zinc has linear, nutrient-like, relationship with phosphorus, and that cobalt also co-varies with phosphorus once zinc is depleted¹.

Given the very low oceanic concentrations of cobalt, cadmium and zinc, it is possible that they could be limiting growth of certain phytoplankton species. Growth studies of two important phytoplankton species, the eukaryotic coccolithophore *Emiliana huxleyi* and the prokaryote *Synechococcus*, showed that *E. huxleyi* can substitute zinc for cobalt; *Synechococcus* is unable to do so (Figure 3). Moreover, *E. huxleyi* appears to require high cobalt concentrations for maximal growth, and *Synechococcus* cannot survive without cobalt (absolute requirement). These results are significant because they suggest that variability in the relative amounts of cobalt and zinc could influence the species composition of phytoplankton communities. For example, an increase in cobalt concentration might result in a coccolithophore bloom and thereby increase the $\text{CaCO}_{3(s)}$ flux to the sediments.

This area of study - the influence of trace metals on oceanic primary productivity and community structure - requires an understanding of the speciation of biolimiting metals. This is because the strong organic complexes can account for a significant part of the total metal in seawater. The organic complexation of metals like Fe and Zn (Bruland, 1989; Rue and Bruland, 1995) has important, but as yet poorly understood, implications for their bioavailability². For cobalt, an important micronutrient, there is no published evidence of organic complexation in oceanic waters much less a recognized source of ligands. The influence of metal speciation on limitation of primary productivity is shown in Figure 4; where cellular quotas for the elements that constitute biomass have been extended to the trace metals. In this figure, complexation of metals by strong organic ligands that are not bioavailable brings Fe, Co and Zn into the range that makes them

¹ While there has not been evidence of CO_2 limitation coupled with cobalt, cadmium, or zinc limitation in the field, there is evidence that changes in CO_2 concentration in seawater can influence the cadmium uptake rate in phytoplankton off the coast of California (Cullen et al., 1999).

² The term bioavailable is used in this thesis to describe a metal chelate that an organism can acquire directly. Siderophores are metal ligand complexes that are known to be bioavailable to marine bacteria (Lewis et al., 1994; Reid et al., 1993) yet are not bioavailable to eukaryotic phytoplankton (Hutchins et al., 1999; Murphy et al., 1976). Other metal ligand complexes have been assumed to be non-bioavailable, such as strong copper ligands which are believed to protect algae from toxic effects of copper (Moffett and Brand, 1997).

important, if not the fundamental, controls on primary productivity. Hence, understanding the speciation chemistry, and the bioavailability of those metal-organic complexes, is a crucial component of understanding metal limitation of primary productivity.

These metal-organic complexes should also increase the solubility of metals in the ocean and prevent them scavenging onto the surfaces of settling particles (Johnson et al., 1997). Iron speciation results in the Iron Ex-II experiment suggests that this might be a biologically related phenomenon: iron additions resulted in a large increase in iron ligand concentration, consistent with a strategy of solubilizing and retaining recently deposited iron in surface waters (Rue and Bruland, 1997). The composition of these organic iron ligands in seawater is unknown. It is known that marine heterotrophic and phototrophic bacteria can produce siderophores (Reid et al., 1993; Wilhelm et al., 1996; Wilhelm et al., 1998), yet determining their presence in seawater is a formidable challenge in the presence of high concentrations of dissolved organic carbon. Extracellular uptake ligands for metals other than iron have not been discovered. Given that the concentrations of cobalt in seawater tend to be about an order of magnitude less than that of iron, and that the photosynthetic cyanobacteria cannot survive without cobalt, the evolution of a cobalt uptake ligand seems like a logical strategy.

Thus far, I have described the first two hypotheses pertaining to cobalt: the potential influence of cobalt on primary productivity, and the possibility of cobalt ligands in seawater. The third hypothesis relates to the origin of cobalt requirements in life, based on the chemical conditions in which the prokaryotes evolved. The Earth's surface is known to have been reducing before the production of oxygen by oxygenic photosynthesis. The photosynthetic prokaryotes are thought to have evolved before this conversion of the Earth's surface, and are also thought to have been the likely causative factor. The utilization of sulfides as a source of electrons by green sulfur bacteria in their primitive photosynthetic capability would not have produced oxygen (Truper, 1982) and could eventually have drawn down the sulfide concentrations in the oceans to growth limiting levels. The evolution of oxygenic photosynthesis, producing oxygen as a by-

product, would have resulted in the oceans and atmosphere gradually becoming oxic as reduced compounds in both environments were gradually oxidized (e.g. red beds of ferric oxides). This process also dramatically decreased the abundance of reduced sulfides by oxidation with biogenic oxygen.

This conversion of the Earth's surface from reduced to oxidized conditions drastically changed the trace metal composition of the oceans due to two factors: 1) elimination of sulfide complexes and precipitates, and 2) creation of oxide precipitates. The loss of sulfides from the water column due to its reaction with oxygen greatly changed the solubility of the transition elements (see Figure 5), with zinc, cadmium, and copper at extremely low dissolved concentrations due to precipitation as sulfide minerals. The appearance of oxygen in seawater drastically altered the seawater redox conditions, changing them from reduced to oxidized. As a result, iron and cobalt both went from being in high concentration to extremely scarce due to oxidation to Fe(III) and Co(III) both of which form oxides and are highly insoluble. In summary, the transition metal chemistry of the oceans flipped upon the conversion of Earth's surface from a reduced environment to an oxidized environment. Organisms that evolved before and after this change would have been subject to intense selection pressure to utilize different metals and/or evolve more efficient uptake systems. This logic as proposed by Sunda and Huntsman (1995) could explain why we observe an absolute requirement for cobalt in the prokaryotic photosynthetic organisms, but not in the eukaryotic organisms. Moreover, this begs the question of what biochemical differences exist between these kingdoms that would result in a shift in cobalt requirements. Researchers studying vitamin B₁₂, which has a cobalt atom held within a corrin ring, have invoked this evolutionary argument for the 'choice' of cobalt in the molecule (Scott, 1990). Yet my calculations of the B₁₂ quota (Wilhelm and Trick, 1995) relative to the cobalt quota (Sunda and Huntsman, 1995) show that the component of cobalt as B₁₂ in the cell is minor (< 4%, see Appendix II. for calculations). Chapter 5 explores the possibility that there are zinc proteins in eukaryotic cells which might have ancestral cobalt analogues in our prokaryotic organism of study, *Prochlorococcus*.

The work in this thesis aims to explore these hypotheses with a combination of new analytical techniques developed in the thesis work, and field and laboratory observations and experiments conducted under stringent trace-metal clean conditions. We have made good progress on developing the analytical methodology to measure complexation of cobalt at the picomolar level. Gaining a sense of the veracity of these hypotheses is an immense task that is larger than what a thesis can hope to answer. Nevertheless, exploration of these questions has inevitably led us to fascinating phenomena and new exciting questions.

References

- Boyd, P. et al., 2000. A mesoscale phytoplankton bloom in the Polar Southern Ocean stimulated by iron fertilization. *Nature*, 407: 695-702.
- Bruland, K.W., 1989. Complexation of zinc by natural organic ligands in the central North Pacific. *Limnol. Oceanogr.*, 34(2): 269-285.
- Cullen, J.L., TW; Morel, FMM; Sherrell, RM, 1999. Modulation of cadmium uptake in phytoplankton by seawater CO₂ concentration. *Nature*, 402(6758): 165-167.
- DeBaar, H.J.W., 1994. von Liebig's Law of the Minimum and Plankton Ecology (1899-1991). *Prog. Oceanogr.*, 33: 347-386.
- Falchuk, K.H., Fawcett, D.W. and Vallee, B.L., 1975. DNA Distribution in the Cell Cycle of *Euglena gracilis*. *Journal of Cell Science*, 17.: 57-78.
- Falkowski, P.G., 1997. Evolution of the nitrogen cycle and its influence on the biological sequestration of CO₂ in the ocean. *Nature*, 387: 272-274.
- Graneli, E. and C. Haraldsson. 1993. Can an increased leaching of trace metals from acidified areas influence phytoplankton growth in coastal waters? *Ambio*. 22. 308-311.
- Hein, M. and Sand-Jensen, K., 1977. CO₂ increases oceanic primary productivity. *Nature* 6642: 526-527.
- Hutchins, D. and Bruland, K., 1998. Iron-limited diatom growth and Si:N uptake ratios in a coastal upwelling regime. *Nature*, 393: 561-564.
- Hutchins, D.A., Witter, A.E., Butler, A. and Luther, G.W., 1999. Competition among marine phytoplankton for different chelated iron species. *Nature*, 400: 858-861.
- Johnson, K.S., Gordon, R.M. and Coale, K.H., 1997. What controls dissolved iron in the world ocean? *Mar. Chem*, 57: 137-161.
- Joos, F., Sarmiento, J.L. and Siegenthaler, U., 1991. Estimates of the effect of Southern Ocean fertilization on atmospheric CO₂ concentrations. *Nature*, 349: 772-775.
- Knauer, G.A., Martin, J.H. and Gordon, R.M., 1982. Cobalt in north-east Pacific waters. *Nature*, 297: 49-51.

- Lane, T.W. and Morel, F.M.M., 2000. A biological function for cadmium in marine diatoms. *Proc. Natl. Acad. Sci.*, 97(9): 4627-4631.
- Lewis, B. et al., 1995. Voltammometric Estimation of Iron(III) Thermodynamic Stability Constants for Catecholate Siderophores Isolated from Marine Bacteria and Cyanobacteria. *Marine Chemistry*, 49: 179-188.
- Martin, J.H. and Fitzwater, S.E., 1988. Iron deficiency limits phytoplankton growth in the north-east Pacific subarctic. *Nature*, 331: 341-343.
- Martin, J.H., Gordon, R.M., Fitzwater, S. and Broenkow, W.W., 1989. VERTEX: phytoplankton/iron studies in the Gulf of Alaska. *Deep-Sea Res.*, 36(5): 649-680.
- Moffett, J.W., 1995. Temporal and spatial variability of copper complexation by strong chelators in the Sargasso Sea. *Deep-Sea Research I*, 42(8): 1273-1295.
- Moffett, J.W. and Brand, L.E., 1997. Production of strong, extracellular Cu chelators by marine cyanobacteria in response to Cu stress. *Limnol. Oceanogr.*, 41(3): 388-395.
- Morel, F.M.M. et al., 1994. Zinc and carbon co-limitation of marine phytoplankton. *Nature*, 369: 740-742.
- Murphy, T.P., Lean, D.R.S. and Nalewajko, C., 1976. Blue-Green Algae: Their Excretion of Iron-Selective Chelators Enables Them to Dominate Other Algae. *Science*, 192: 900-902.
- Peng, T.H. and Broecker, W.S., 1991. Dynamical limitations on the Antarctic iron fertilization strategy. *Nature*, 349: 227-229.
- Reid, R.T., Live, D.H., Faulkner, D.J. and Butler, A., 1993. A siderophore from a marine bacterium with an exceptional ferric ion affinity constant. *Nature*, 366: 455-458.
- Rueter, J., Hutchins, D., Smith, R. and Unsworth, N., 1992. Iron Nutrition of *Trichodesmium*. In: E.J.C.e. al. (Editor), *Marine Pelagic Cyanobacteria: Trichodesmium and other Diazotrophs*. Kluwer Academic Publishers, pp. 289-304.
- Riebesell, U., Wolf-Gladrow, D.A. and Smetacek, V., 1994. Carbon dioxide limitation of marine phytoplankton growth rates. *Nature*, 361: 249-251.

- Rue, E.L. and Bruland, K.W., 1995. Complexation of iron(III) by natural ligands in the Central North Pacific as determined by a new competitive ligand equilibration/adsorptive cathodic stripping voltammetric method. *Mar. Chem.*, 50: 117-138.
- Rue, E.L. and Bruland, K.W., 1997. The role of organic complexation on ambient iron chemistry in the equatorial Pacific Ocean and the response of a mesoscale iron addition experiment. *Limnol. Oceanogr.*, 42(5): 901-910.
- Saito, M.A. and Twiss, M.R., 1998. Total cobalt and copper concentrations in Lake Erie surface waters, International Association for Great Lakes Research, Hamilton, Ontario. Canada.
- Scott, A.I., 1990. Mechanistic and Evolutionary Aspects of Vitamin B12 Biosynthesis. *Acc. Chem. Res.*, 23: 308-317.
- Sunda, W.G. and Huntsman, S.A., 1995. Cobalt and Zinc interreplacement in marine phytoplankton: biological and geochemical implications. *Limnol. Oceanogr.*, 40: 1404-1417.
- Takahashi, T., Broecker, W.S. and Langer, S., 1985. Redfield Ratio Based on Chemical Data from Isopycnal Surfaces. *J. Geophys. Res.*, 90(C4): 6907-6924.
- Truper, H.G. (Editor), 1982. Microbial Processes in the Sulfur Cycle Through Time. Mineral Deposits and the Evolution of the Biosphere. Springer-Verlag, New York, 332 pp.
- Wilhelm, S., Maxwell, D. and Trick, C., 1996. Growth, iron requirements, and siderophore production in iron-limited *Synechococcus* PCC 7002. *Limnology and Oceanography*, 41: 89-97.
- Wilhelm, S.W., MacAuley, K. and Trick, C.G., 1998. Evidence for the importance of catechol-type siderophores in the iron limited growth of a cyanobacterium. *Limnol. Oceanogr.*, 43(5): 992-997.
- Wilhelm, S.W. and Trick, C.G., 1995. Effects of vitamin B12 concentration on chemostat cultured *Synechococcus* sp. strain PCC 7002. *Can. J. Microbiol.*, 41: 145-151.

Wu, J., Sunda, W., Boyle, E.A. and Karl, D.M., 2000. Phosphate Depletion in the Western North Atlantic Ocean. *Science*, 289(5480): 752-762.

Figure 1-1

Total cobalt concentrations in various aqueous environments around the world. Open ocean total dissolved cobalt concentrations can be as low as 4×10^{-12} M. CASS Coastal refers to National Research Council Canada-Institute for National Measurements coastal seawater standard. The CASS standard is unfiltered and hence the particulates could bias the cobalt concentration. Coastal and oceanic data from Knauer et al. (1982), Martin and Fitzwater (1988), and Martin et al. (1989). Lake Erie data from Saito and Twiss (Saito and Twiss, 1998). River Nissan data from Graneli and Haraldsson (1993).

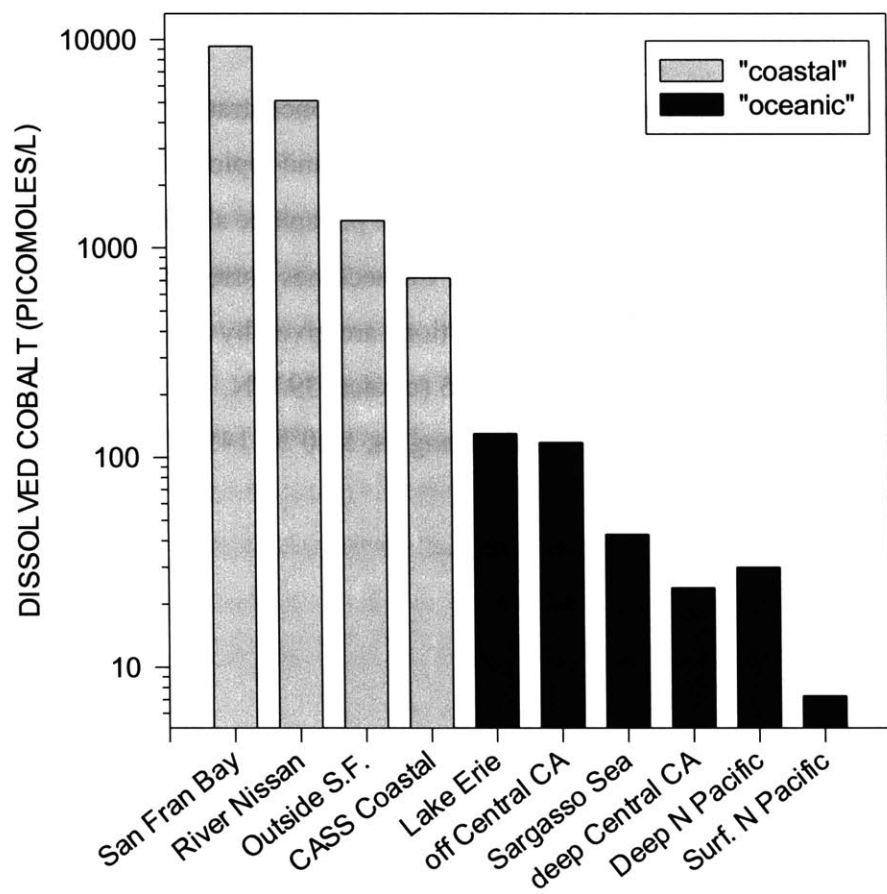


Figure 1-2

Dissolved cobalt and zinc as a function of phosphate concentration for the North Pacific. (data from Martin et al., 1988 and Martin et al., 1989, and replotted by Sunda and Huntsman, 1995). Note that zinc is correlated with phosphate above $1\text{ }\mu\text{mol/kg}$ (A), whereas Co is not. (B) When Zn is depleted, Co becomes correlated suggesting that it is substituting for Zn as a required nutrient. Stations are given by the symbols: T-4 (downwards triangles, 33.3°N , 139.1°W), T-5 (circles, 39.6°N , 140.8°W), T-6 (filled squares, 45.0°N , 142.9°W), T-7 (upwards triangles, 50.0°N , 145.0°W), and T-8 (open squares, 55.5°N , 147.5°W).

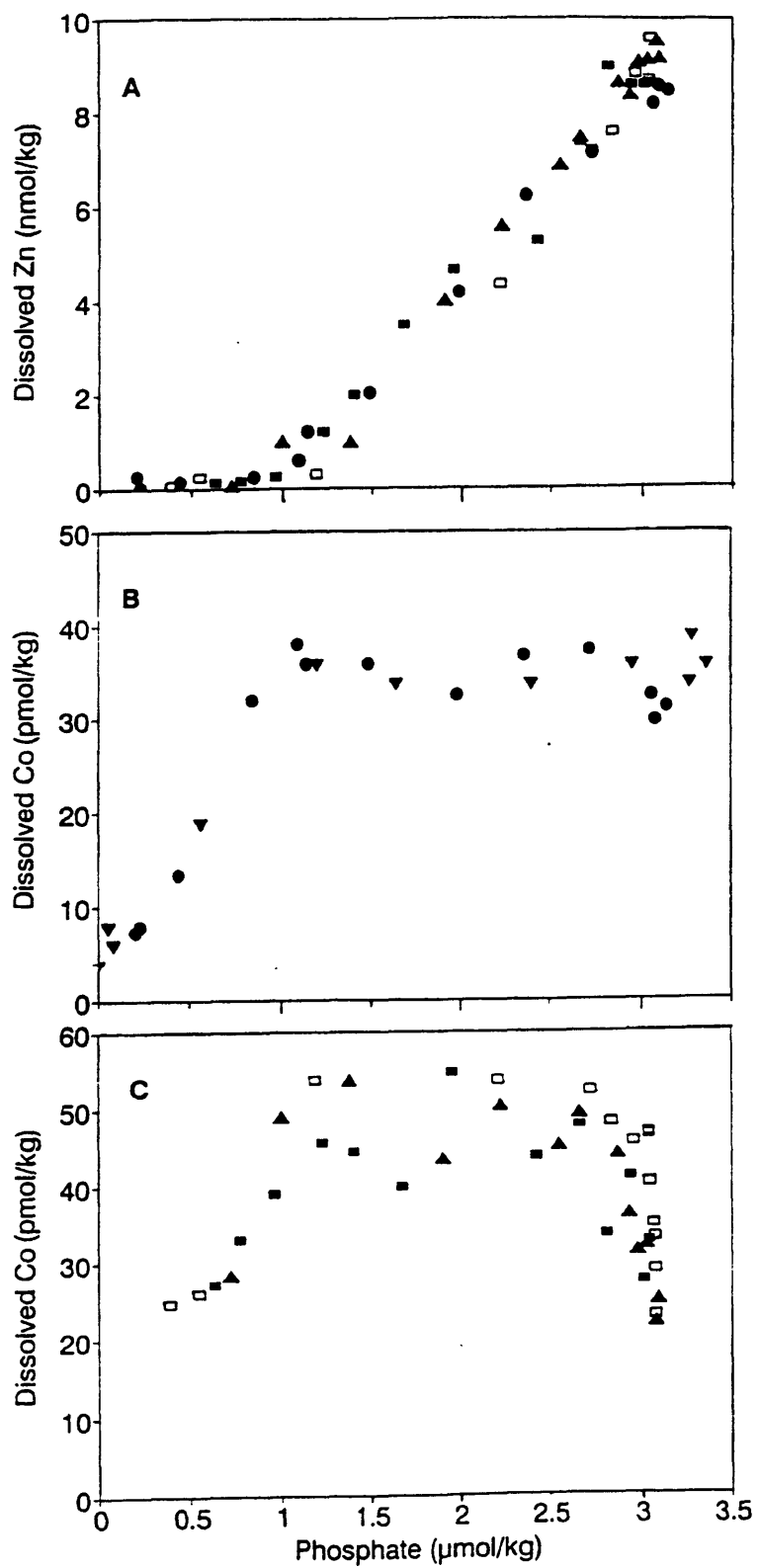
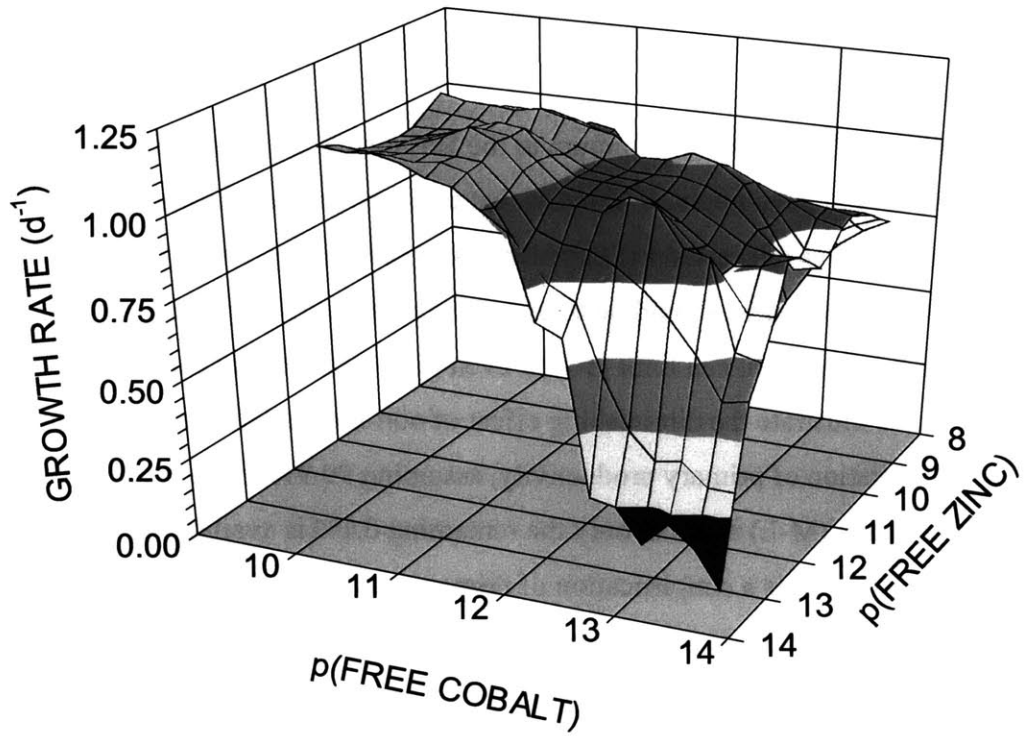


Figure 1-3

Growth rates of *Emiliana huxleyi* and *Synechococcus bacillarus* under cobalt and zinc limiting conditions. *E. huxleyi* can substitute cobalt for zinc and vice versa. In addition, growth rates are maximal under high cobalt conditions, rather than high zinc conditions, suggesting a preference for cobalt over zinc in this important phytoplankton species. *Synechococcus* shows no ability to substitute zinc for the absolute cobalt requirement shown here. It is important to note that under media conditions that are zinc limiting for *E. huxleyi*, *Synechococcus* displays no zinc limitation effects, indicating that the zinc requirement of *Synechococcus* is significantly less than that of the eukaryotic *E. huxleyi*. These plots were generated from data presented in Sunda and Huntsman (1995).

Emiliana huxleyi



Synechococcus

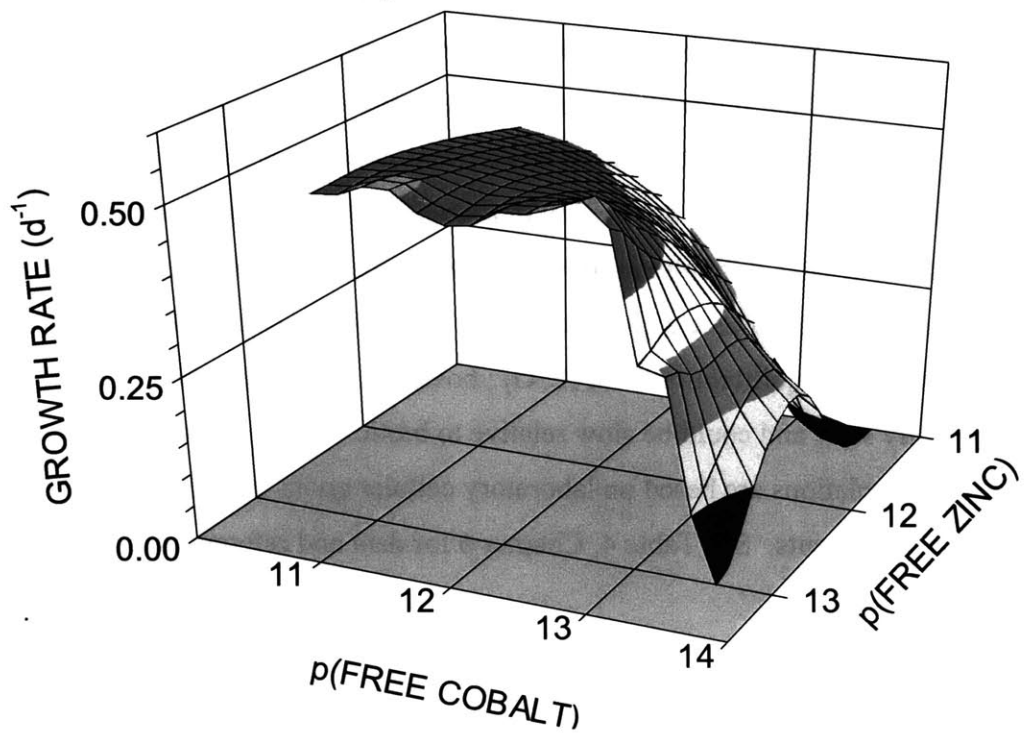


Figure 1-4

Application of Liebig's law of the minimum to the Sargasso Sea (A) and HNLC regions (B). Each bar refers to the amount of biomass that could be produced using the quantity of each element in a liter of seawater if that element were limiting. The lowest bar in each graph indicates which element should be limiting according to Liebig's law, which states that a single required element can limit growth even if all others are in excess (DeBaar, 1994). The circles illustrate the diminishing effect of non-bioavailable metal-ligand complexes on limitation of primary productivity, assuming 99.9% of the metal exists as a metal-ligand complex (M-L) and that only the remaining 0.1% is available to phytoplankton. This plot is a simplification of primary productivity in oceanic ecosystems since it does not account for regeneration, recycling, advective input, aeolian input, or numerous other biogeochemical processes. Variation in the cellular quotas for N and P are taken from the "revised Redfield ratio" study of Takahashi et al. (Takahashi et al., 1985). Variation in the cellular quotas for transition metals is caused by physiological adjustment of the biota rather than experimental variability. Organisms tend to reduce their cellular quotas for a metal if it becomes limiting. Instead of using variability in cellular carbon quotas, the concentrations of two inorganic carbon chemical species (bicarbonate and $\text{CO}_{2(\text{aq})}$) are used with a single cellular carbon quota ($\text{C:P} = 106:1$) to illustrate greater difficulty in utilizing $\text{CO}_{2(\text{aq})}$ relative to bicarbonate (high POC value corresponds to bicarbonate and the low POC value to $\text{CO}_{2(\text{aq})}$). $\text{CO}_{2(\text{aq})}$ drawdown will be replenished by equilibration with HCO_3^- ; however, the dehydration of carbonic acid is kinetically slow and could be slow relative to biotic carbon uptake rates (Riebesell et al., 1994). Calculations are based on laboratory cellular quota experiments and total trace metal measurements. See Table 4, Chapter 6 for data and references.

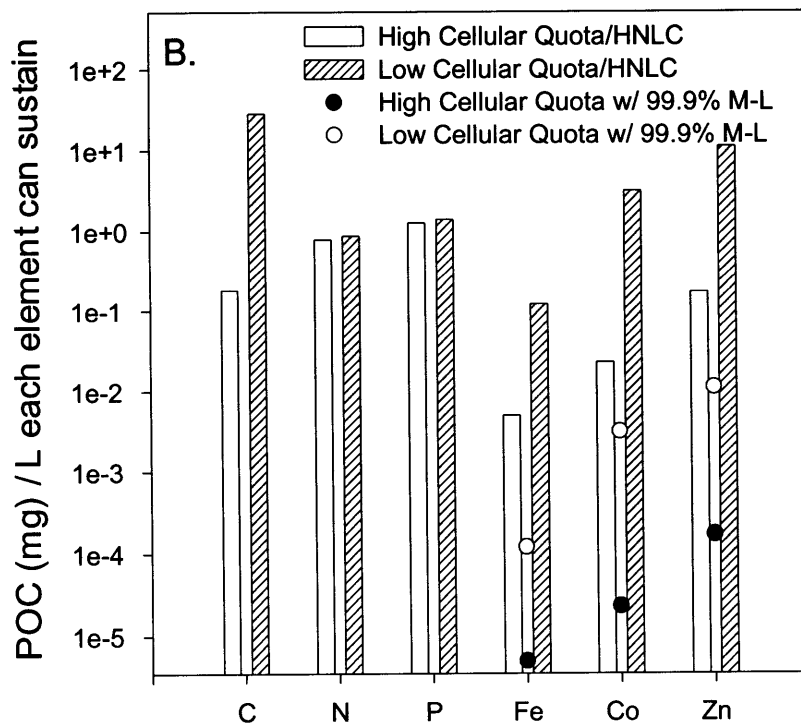
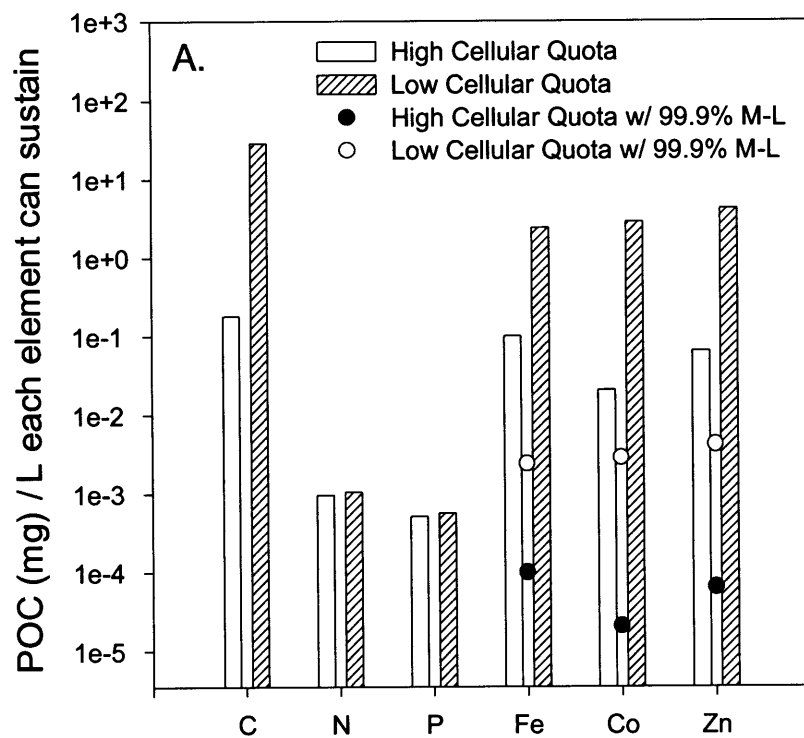
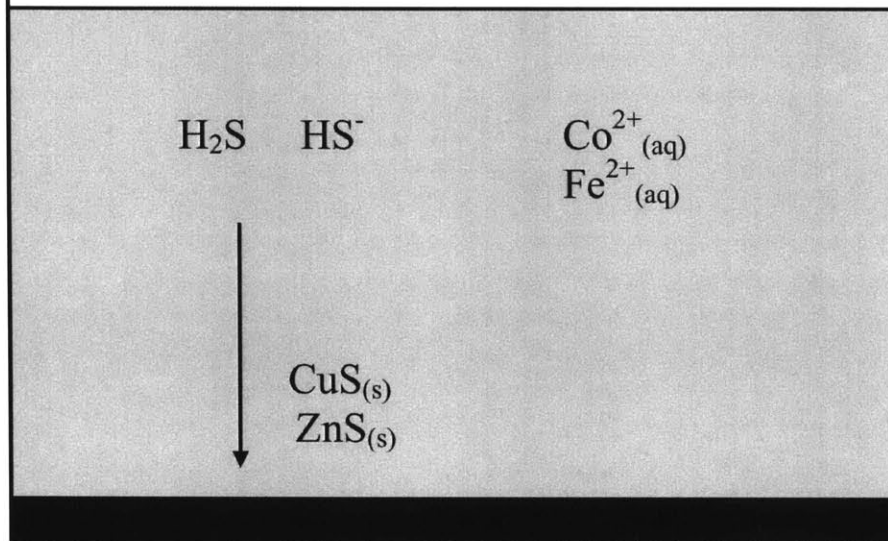


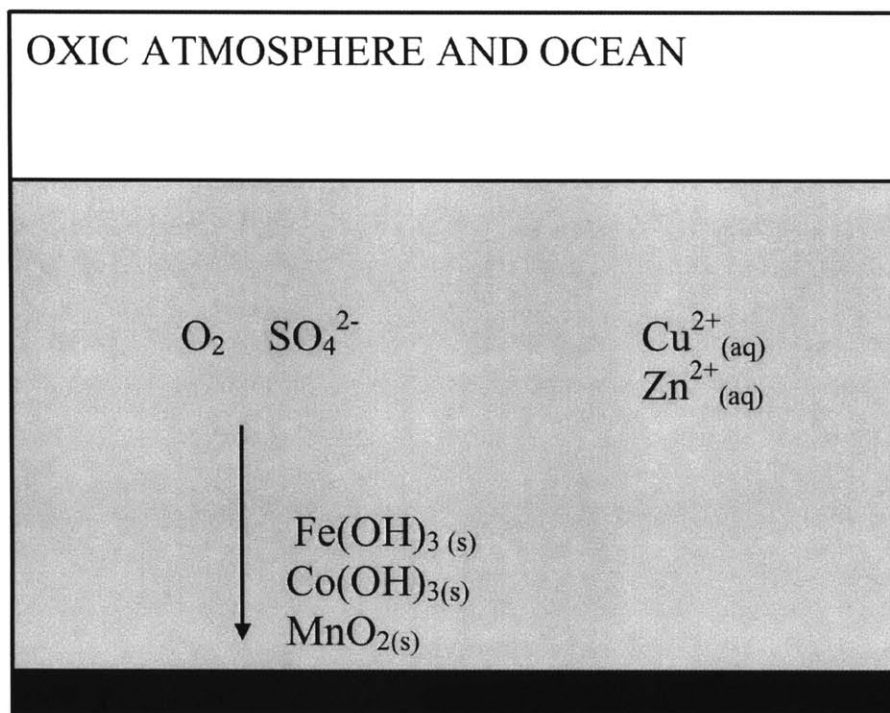
Figure 1-5

The effect of increasing oxygen concentrations on the trace metal chemistry of the early ocean. The ancient ocean is thought to have been a reducing, electron-rich, environment. Under these conditions sulfide (HS^-) would have been the abundant form of sulfur species in seawater, resulting in a scarcity of dissolved zinc and copper. In contrast, iron, cobalt, and manganese would have been abundant because they do not form precipitates with sulfide as readily as zinc and copper; moreover, the reducing conditions would prevent them from forming insoluble oxide species. Once the early photosynthetic cyanobacteria on Earth introduced sufficient oxygen in the atmosphere to make seawater an oxidizing environment, oxidation of sulfides to sulfate changed the metal chemistry drastically. As a result zinc and copper became soluble, and iron, cobalt and manganese were susceptible to precipitation as oxides.

PRE-OXIC
ATMOSPHERE AND OCEAN



OXIC ATMOSPHERE AND OCEAN



Chapter 2

Complexation of cobalt by natural organic ligands in the Sargasso Sea as determined by a new high-sensitivity electrochemical cobalt speciation method suitable for open ocean work

Mak A. Saito^{ψ,*} and James W. Moffett^{*}

^ψ MIT/WHOI Joint Program in Chemical Oceanography, mak@mit.edu

^{*} Marine Chemistry and Geochemistry Department, Woods Hole Oceanographic Institution, Woods Hole MA 02543, USA

Submitted to Marine Chemistry

Abstract

A high sensitivity cobalt speciation method was developed and applied to a profile in the N. Atlantic. Method development included examining the redox chemistry of the analytical system and calibrating the electroactive cobalt ligand dimethylglyoxime (DMG) using EDTA as a model ligand. The method was applied to a depth profile at the Bermuda Atlantic Time Series Station (BATS) during a September 1999 cruise. Total dissolved cobalt, measured using adsorptive cathodic stripping voltammetry (ACSV) on ultraviolet light irradiated samples, revealed a nutrient-like profile for cobalt. Co speciation, measured using CLE-ACSV (competitive ligand exchange), showed a cobalt binding ligand concentration that was similar to that of total cobalt throughout the profile. An excess of ligand was observed in the chlorophyll maximum where *Prochlorococcus* and *Synechococcus* numbers were highest. Conditional stability constants for CoHDMG₂ and CoTETA were $\log K_{CoHDMG_2}^{cond} = 11.5 \pm 0.3$ and $\log K_{CoTETA}^{cond} = 11.2 \pm 0.1$ at pH 8.0. A pH dependence for $K_{CoHDMG_2}^{cond}$ was observed and is consistent with model calculations based on the protonation constants for H₂DMG. The conditional stability constant for CoL was determined to be $\log K_{CoL}^{cond} = 16.3 \pm 0.9$ and total ligand concentrations varied from 9 to 83pM as calculated by a one-ligand non-linear fit using the Levenberg-Marquardt algorithm. Alternate interpretations of the data are discussed, including the possibility for an underestimation of ligand concentrations and stability constants caused by the existence of Co(III) ligands, and kinetic and thermodynamic competition for natural ligands by Ni and Co(II).

KEY WORDS: Cobalt, electrochemistry, Sargasso Sea, complexation, bioavailability, ligand

1. Introduction

Understanding the biogeochemistry of Co in seawater requires the ability to measure its oceanic chemical species. Zinc and cadmium have both been shown to be strongly complexed in seawater (Bruland, 1989; Bruland, 1992); however, due to the exceedingly low total dissolved cobalt concentrations in the picomolar range ($4\text{--}120 \times 10^{-12}\text{M}$) (Jickells and Burton, 1988; Martin and Gordon, 1988; Martin et al., 1989), open ocean cobalt speciation has never been rigorously studied. Strong complexation of cobalt has been measured in the Scheldt estuary (Zhang et al., 1990) at nanomolar total cobalt concentrations, and Donat and Bruland (Donat and Bruland, 1988) have reported data suggestive of strong complexation of cobalt in open ocean samples. Since then improvements in the analytical methodology for total cobalt measurements have lowered the detection limit by 1-2 orders of magnitude (Bobrowski, 1989; Bobrowski, 1990; Bobrowski and Bond, 1992; Herrera-Melian et al., 1994; Vega and van den Berg, 1997). With this added sensitivity, the 3pM detection limit for electrochemical methods is below open ocean cobalt concentrations; however, significant method development has been required to adapt this total cobalt measurement for speciation work. This included verifying that the reagents were not oxidizing Co(II) to Co(III), and calibrating the conditional stability constant for $\text{Co}(\text{HDMG})_2$ in seawater with this high sensitivity method.

The use of cobalt and nickel dioxime complexes in analytical electrochemistry has been an area of active research for more than 50 years (Baxter et al., 1998). Dioxime complexes, such as those with dimethylglyoxime (DMG), are characterized by the presence of oxime groups ($\text{C}=\text{N}-\text{OH}$) and have provided significant enhancement of cobalt(II) reduction signal relative to the reduction of Co^{2+} cations or other cobalt organic ligand complexes; and it is this enhancement of signal, coupled with other refinements in protocol such as computer assisted high speed scanning rates and nitrite catalytic activity (Bobrowski, 1989; Bobrowski and Bond, 1992) that have brought the detection limit and analysis time within the reach of the picomolar concentrations observed in oligotrophic

marine environments. However, a mechanistic explanation for the enhancement in signal provided by the complexation of cobalt and nickel by dioxime ligands has eluded researchers until only very recently. Baxter et al. (1998) and Ma et al., (1997) make a convincing case that the unusual signal enhancement found when using dioxime ligands is caused by the reduction of the two dioxime ligands (partial reduction of the 2 C=N per dioxime molecule) in addition to the reduction of the metal center. This mechanism provides 10 electrons per Co molecule as opposed to the typical 2 or 3 electrons from the metal ion obtained during most high sensitivity cathodic stripping voltammetry methods. It is a fortunate coincidence for environmental electrochemists that this cobalt dioxime reduction method is available since cobalt tends to be an order of magnitude lower in concentration than most other transition metals.

In order to make cobalt speciation measurements at oceanic concentrations it is necessary to consider the redox state of cobalt. We were concerned that the use of nitrite as an additional signal enhancer could inadvertently oxidize Co(II) to Co(III), which was hypothesized by Vega and van den Berg (1997). The resulting system could be experimentally intractable for cobalt speciation due to the presence of two redox states each with its own set of thermodynamic constants. We used spectrophotometric methods to show that nitrite cannot oxidize Co(II)-EDTA as a model for Co(II)HDMG₂ on time scales that are of experimental concern.

While the formation of Co(III)-HDMG₂⁺ complexes is possible (Costa et al., 1987), it is unknown if Co(III)-HDMG₂⁺ complexes are also electroactive at the low concentrations typical of seawater analyses. However, it is also well known that Co(III) chelates have much higher stability constants than their corresponding Co(II) complexes. It is often stated that such Co(III) chelates once formed are chemically inert to further reaction (Ogino and Ogino, 1982). Moreover, the oxidation of inorganic and many organic Co(II) species is often kinetically slow, despite being thermodynamically possible at ambient oxygen concentrations. However, Co(II) oxidation does occur in natural waters. In coastal waters Co(II) oxidation by Mn oxidizing bacteria appears to be the dominant removal pathway for dissolved Co (Moffett and Ho, 1996). In that study,

Co(II) oxidation was associated with precipitation on a manganese oxide. However, there is no evidence for Co redox cycling in the dissolved phase in seawater. Moffett and Ho (1996) showed that in the open ocean, Co uptake is probably non-oxidative and dominated by phytoplankton. Although there is little experimental evidence, it is presumed that open ocean cobalt exists as Co(II) except for a small fraction as cobalamin (vitamin B₁₂) (Menzel and Spaeth, 1962) which occurs as a Co(III) complex (Glusker, 1995).

The complexation of cobalt in the open ocean has been suggested in previous studies of open ocean total cobalt concentrations (Donat and Bruland, 1988; Vega and van den Berg, 1997). Cobalt is an essential micronutrient for many key phytoplankton species (Sunda and Huntsman, 1995; Saito, 2000). Given the exceedingly low total dissolved concentrations of cobalt in seawater, an understanding of the chemical species of cobalt present in seawater is crucial to improving our understanding of how phytoplankton acquire this necessary micronutrient.

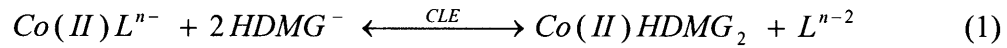
2. Theory

A variety of electrochemical techniques have been used to achieve the sensitivity needed for the determination of trace elements found in seawater, including adsorptive cathodic stripping voltammetry (ACSV) and anodic stripping voltammetry (ASV). In this study, we have used ACSV for total cobalt measurements, using the method of standard additions, and ACSV coupled with competitive ligand exchange equilibria for cobalt speciation determinations (CLE-ACSV).

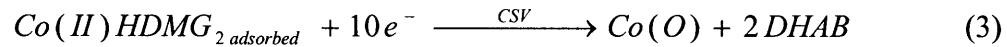
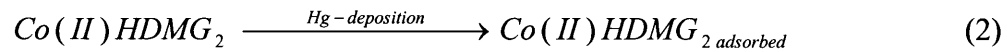
2.1 Competitive Ligand Exchange

Competitive ligand exchange methods determine the extent to which a metal is bound to natural organic complexes by competition between the electroactive synthetic reagent ligand and natural ligands (equations 1 and 2). Competitive ligand exchange refers to the equilibrium that is established between natural Co ligands (L) and the added

electroactive ligand (DMG in this study). Inherent in this method is the assumption that no oxidation or reduction of cobalt occurs during the time needed to achieve equilibrium.



This competitive ligand equilibrium is then measured using a hanging mercury drop, which accumulates CoHDMG₂ on the surface of the drop by applying a negative potential for a programmed deposition time. The accumulated CoHDMG₂ is reduced by scanning from the deposition potential to a more negative potential (equation 3). The resultant peak is proportional to the concentration of CoHDMG₂ in solution and to the deposition time. In addition to the reduction of the cobalt ion, the HDMG⁻ groups are also irreversibly reduced to 2,3-bishydroxylaminebutane (DHAB, Baxter et al., 1998). The reaction at the electrode surface is:



The competition between the natural and synthetic ligands is influenced by their stability constants and the concentrations of each ligand. Due to the unique analytical matrix of seawater and a lack of sufficient literature data, conditional stability constants that have been calibrated at seawater pH and ionic strength are used in lieu of literature thermodynamic stability constants (equations 4 and 5).

$$K_{DMG}^{cond} = \frac{[CoHDMG_2]}{[Co^{2+}][DMG']^2} \quad (4)$$

$$K_{CoL}^{cond} = \frac{[CoL]}{[Co^{2+}][L^{2-}]} \quad (5)$$

In this study, $[DMG'] = DMG_{TOT}$, since $CoHDMG_2$ and $NiHDMG_2 \ll DMG_{TOT}$. The thermodynamic stability constant for DMG with Co is not well characterized. The only reference we are aware of for $CoHDMG_2$ is a conditional stability constant

($\log K_{CoHDMG_2}^{cond}$) by Zhang and van den Berg (Zhang et al., 1990) of 12.85 ± 0.10 .

Moreover, this previous calibration was conducted in coastal waters with the traditional low speed scan protocol, much higher Co concentrations, and at a pH of 8.7. The recently developed high speed scan total cobalt protocols utilize high-speed scans (10 V sec^{-1}) and a catalytic reaction. The relative concentrations and thermodynamic stability constants of the natural ligands and the synthetic ligand (DMG) determine the partitioning of cobalt species in equation 1. With titration of a seawater sample with cobalt, the concentrations and strength of the natural ligands can be estimated.

2.2 Model Ligands - Calibration of speciation methodology

The non-electroactive synthetic ligand EDTA was used to determine a $K_{CoHDMG_2}^{cond}$ for DMG. Constant cobalt and DMG concentrations were titrated with increasing concentrations of EDTA. Mass law equations for $CoEDTA^{2-}$, $CaEDTA^{2-}$ and $MgEDTA^{2-}$ complexes were taken from Martell and Smith (Martell and Smith, 1993). The mass balance for cobalt in the EDTA calibration is:

$$[Co_{TOT}] = [Co'] + [CoHDMG_2] + [CoEDTA^{2-}] \quad (6)$$

Where Co' indicates the summation of the important inorganic cobalt species in seawater:

$$[Co'] = [Co^{2+}] + [CoCl_{(aq)}^+] + [CoOH_{(aq)}^+] + [Co(OH)_{2(aq)}] + [Co(OH)_{3(aq)}^-] \quad (7)$$

X is then assigned to be the fraction of cobalt masked by binding to the non-electroactive EDTA, where i is the CoHDMG₂ reduction peak current, measured by peak height and in the presence (*i*_{p,i}) and absence (*i*_{p,o}) of EDTA.

$$X = \frac{i_{p,i}}{i_{p,o}} \quad (8)$$

Peak height can be related to the concentration of the electroactive CoHDMG₂ complex by the sensitivity (S), derived from the slope of the cobalt addition plot. Using the cobalt mass balance equation, *i*_{p,i} (and *i*_{p,o} where [CoEDTA²⁻] = 0) is equal to:

$$i_{p,i} = S \cdot [CoHDMG_2] = S \cdot (Co_{TOT} - Co' - CoEDTA^{2-}) \quad (9)$$

$$\frac{i_{p,i}}{i_{p,o}} = \frac{S(CoHDMG_2)_{p,i}}{S(CoHDMG_2)_{p,o}} = \frac{S(Co_{TOT} - Co' - CoEDTA^{2-})}{S(Co_{TOT} - Co')} \quad (10)$$

Algebraic manipulations of equation 10 using mass law and mass balance equations yields:

$$X = \frac{K_{DMG}^{cond} \cdot [DMG']^2}{(K_{DMG}^{cond} \cdot [DMG']^2 + K_{EDTA}^{cond} \cdot [EDTA'])} \quad (11)$$

where DMG' = DMG_{TOTAL} because DMG' >> Co_{TOT}.

$$X = \frac{CoHDMG_2 - K_{EDTA}^{cond} \cdot Co' [EDTA']}{CoHDMG_2} \quad (12)$$

The conditional stability constant for CoHDMG₂ can then be calculated by fitting the equilibrated EDTA titration with:

$$K_{DMG}^{cond} = \frac{X \cdot K_{EDTA}^{cond} [EDTA']}{([DMG']^2 - X \cdot [DMG']^2)} \quad (13)$$

TETA (1,4,8,11-tetraazacyclotetradecane-1,4,8,11-tetraacetic acid hydrochloride hydrate) was used in this study as a model ligand for strong natural ligands. Unlike CoHDMG₂, TETA is not electroactive using the electrochemical parameters of our analytical system, so we calibrated CoTETA against DMG using the CoHDMG₂ conditional stability constant. This can be done using equation 13 after substituting K_{TETA}^{cond} for K_{EDTA}^{cond} and rearranging:

$$K_{TETA}^{cond} = \frac{K_{DMG}^{cond} ([DMG']^2 - X \cdot [DMG']^2)}{(X \cdot [TETA'])} \quad (14)$$

2.3 Calculation of CoL, L_T, and K_L^{cond}

The calculations of the concentrations and conditional stability constants for natural ligands in previous work have utilized Langmuir isotherms (also described as van den Berg/Ruzic plots), Scatchard plots, and non-linear fits (Gerringa et al., 1995; Moffett, 1995). All of these algorithms begin with a calculation of CoL, which is a simple mass balance:

$$[CoL] = [Co_{TOT}] - [CoHDMG_2] - [Co'] \quad (15)$$

where Co_{TOT} and CoHDMG₂ are measured in separate analyses and Co' is insignificant.

The equations for Langmuir isotherm calculations of L_T , and K_{CoL}^{cond} utilize a ligand mass balance equation (16) substituted into a conditional stability constant equation to produce a linearized equation (17):

$$[L_{TOT}] = [L'] + [CoL] \quad (16)$$

$$\frac{[Co^{2+}]}{[CoL]} = \frac{[Co^{2+}]}{[L_{TOT}]} + \frac{1}{K_{CoL}^{cond} \cdot [L_{TOT}]} \quad (17)$$

where $x = Co^{2+}$, $y = Co^{2+}/CoL$, the slope is equal to the inverse of L_{TOT} , and the y-intercept is equal to $1/(K_{CoL}^{cond} L_{TOT})$.

The calculations of K_{CoL}^{cond} are sensitive to the value of S in calculating Co^{2+} . In work with Fe-salicylaldoxime (Rue and Bruland, 1995) and Cu-bzac (Moffett, 1995) the slope of equilibrated titrations approached that of titrations in ultraviolet light irradiated seawater. However, in this study we noticed that S was substantially lower in surface waters of the Sargasso than in UV-irradiated samples. Such a decrease can reflect matrix effects on S caused by surfactants; alternatively, an apparent decrease in S may be caused by the presence of additional chelators in excess of the highest Co concentration in the titration. The latter effect does not influence the actual value of S , so to distinguish the two, we determined S from a special set of titrations with no equilibration time. The assumption was that Co(II) complexes would not have time to form, but matrix effects would be unchanged. This approach has worked well for Cu in previous reports (Lucia et al., 1994; Moffett and Brand, 1997). S determined in this way is hereafter described as non-equilibrated S . Calculations of ligand concentration and stability constants were made using the non-equilibrated S , determined at each depth, in equation 9. Because Langmuir isotherm fits of titration data can lead to an increase in errors at the high concentration range of titrations, non-linear fits of titration data have been invoked as a means to reduce the error on estimates of K and L and have been shown to yield similar

results to the traditional Langmuir isotherm algorithms (Gerringa et al., 1995). We utilized a single ligand non-linear fit in MATLAB using a Levenberg-Marquardt algorithm to solve for the parameters K and L using the titration data for CoL and Co²⁺ in the following equation:

$$\frac{[CoL]}{[Co^{2+}]} = \frac{[L] \cdot K_{CoL}^{cond}}{1 + K_{CoL}^{cond} \cdot [Co^{2+}]} \quad (18)$$

3. Materials and Methods

3.1 Instrumentation and Reagents

We used a high-speed scan protocol with a Metrohm 663 hanging mercury drop electrode stand with a teflon sample cup and an Eco-chemie μ Autolab computer interface. Dimethylglyoxime (DMG) from Aldrich was recrystallized in milli-Q (Millipore) water and 10⁻³M EDTA (Sigma Ultra) to remove impurities, dried and redissolved in HPLC grade methanol to a concentration of 0.1M. Final concentrations of DMG in the seawater samples were 0.000235M. Solutions of 1.5M sodium nitrite (Fluka Puriss) was equilibrated overnight with prepared Chelex-100 beads (Price et al., 1988/1989) to remove metal contaminants; 1.5mL of this nitrite solution was added to 8.50mL of seawater sample. A 0.5M EPPS buffer solution (Fisher) was cleaned by running through a column with 3mL of clean Chelex-100 beads (BioRad) and diluted in the sample to 0.0025M. Cobalt additions for standard additions and speciation titrations prepared from Fisher certified Co(NO₃)₂ stock solution were freshly diluted in polymethylpentene volumetric flasks of Milli-Q water every few days.

The μ Autolab analysis protocol involved a 3.25 minute purge with filtered 99.999% N₂, a 90 second deposition time at -0.6V, a 15 second equilibration period followed by a high-speed negative scan at 10V sec⁻¹ from -0.6V to -1.4V. The linear

sweep wave form was used, and stirrer speed 5, and drop size of 0.52mm^2 . Cobalt signal was measured as the peak height from the baseline. Titration samples were analyzed in order of increasing concentration and rinsed with 10% HCl then pH 3 HCl (Baker Ultrex II) at the completion of each titration. The teflon sample cup was preconditioned with filtered seawater before adding equilibrated samples.

3.2 Sample collection and handling

Seawater samples were collected from the Sargasso Sea using acid-cleaned 10L Go-Flo bottles, using kevlar wire and PVC-messengers. Seawater was pumped into a positive pressure clean van with $0.2\text{ }\mu\text{m}$ filtered N_2 gas and teflon tubing, and was immediately filtered through acid-cleaned $0.2\text{ }\mu\text{m}$ Nuclepore polycarbonate filters into teflon bottles for speciation samples and polyethylene bottles for total dissolved samples. Samples were refrigerated in darkness until analysis. All labware was soaked with the acidic detergent Citranox and Milli-Q water solution overnight, rinsed with copious Milli-Q water, heated for 36h with 1M HCl (Baker Instra-Analyzed Grade) at 60°C , then rinsed three times and soaked with pH 3 HCl (Baker Ultrex II).

3.3 Total cobalt measurements: analytical standards, reagent blank and field samples

To measure the analytical blank, cobalt-free seawater was created by ultraviolet light irradiating Sargasso seawater (UV-SSW), followed by equilibration with clean chelex-100 resin beads (Price et al., 1988/1989). This seawater was then UV-irradiated again to degrade any diamino-acid groups that were released from the chelex. This final irradiation step was important at these picomolar levels, despite the rigorous protocol used to prepare the chelex.

The accuracy and precision of our analytical methodology was verified using CASS-3 Coastal Seawater Reference material and NASS-5 (National Research Council Canada-Institute for National Measurements). The CASS-3 seawater was diluted with Milli-Q water from a cobalt concentration of $700\pm150\text{ pM}$ to $310\pm69\text{ pM}$, where the error

is standard deviation of four different analytical techniques used by the National Research Council Canada. The NASS-5 was analyzed without dilution. The reference materials were UV-irradiated for 3.0 hours in covered quartz vessels, then transferred to LDPE bottles and the pH was raised to between 7.5 and 9 using Gold Label NaOH (Johnson-Matthey).

Total samples were stored in darkness at 4°C after filtration until analysis immediately upon returning from sea. Total cobalt measurements on field samples were UV-irradiated at ambient pH for 3.0 ± 0.1 hours in quartz vials covered with plastic caps, parafilm, and aluminum foil to prevent exposure to dust and losses by evaporation. Analysis was carried out 2-24h after irradiation. This analytical protocol for total cobalt analysis with UV-irradiation without strong reducing agents was shown to be effective by Vega and van den Berg (1997).

3.4 Calibration of DMG and TETA

Determination of the conditional stability constant of DMG relative to EDTA was performed using Na₂EDTA (Sigma Ultra) and 150pM of Co(NO₃)₂ on three different occasions with separately prepared reagents. In all experiments the EDTA-DMG cobalt mixtures were allowed to equilibrate for between 12 and 24 hours in teflon bottles, and resulted in similar value for $K_{CoHDMG\ 2}^{cond}$. The pH was measured using an Orion pH electrode calibrated using pH 7 and pH 10 buffers. In the first of three calibration experiments, the nitrite and EPPS were added prior to the equilibration period, while in the other two experiments these reagents were added immediately before analysis.

TETA (1,4,8,11-tetraazacyclotetradecane-1,4,8,11-tetraacetic acid tetrahydrochloride hydrate, Aldrich) was calibrated against 0.5mM DMG by equilibration with 100pM CoCl₂, EPPS, and nitrite in UV-irradiated seawater.

3.5 *Co(II) oxidation experiments*

Spectrophotometry experiments used a Heward Packard UV-VIS spectrophotometer and acid cleaned 1 cm pathlength quartz cuvettes. Solutions of Na₄EDTA (Fisher Biotech electrophoresis grade), CoCl₂, and Fluka Puriss NaNO₂ were prepared and allowed to equilibrate overnight before addition of 0.61M Baker Ultrex H₂O₂ to cuvettes immediately before analysis.

3.6 *CLE –ACSV Co speciation titrations*

Equilibrations of seawater with cobalt and DMG were prepared in clean teflon bottles. 8.50mL of filtered seawater was equilibrated with 0-510pM of Co(NO₃)₂ for 1-2 hours, followed by an equilibration with 20μl of 0.1M DMG (0.000235M) for ≥12h. The teflon sample cup was preconditioned with filtered seawater from the same sample, and the EPPS and nitrite were added immediately before analysis (50μl 0.5M EPPS pH 8.0, and 1.50mL NO₂⁻). Titrations of irradiated Sargasso seawater (UV-SSW) were conducted with the same parameters and concentrations of reagents but without the equilibration periods. DMG kinetics in UV-SSW are extremely rapid due to the absence of natural ligands. Titrations were also conducted without equilibration time on filtered fresh Sargasso seawater samples by addition of reagents to the seawater sample in the electrochemical cup and direct additions of Co(NO₃)₂.

3.7 *Flow cytometry analysis of Prochlorococcus and Synechococcus*

Flow cytometry samples were collected by Niskin bottle and immediately analyzed at sea. 0.474μm beads were added as an internal standard immediately prior to analysis on a modified FACScan (Dusenberry and Frankel, 1994). A syringe pump was used (Harvard Apparatus) with a flow rate of 10μl/min, and 15000 counts were collected on all samples.

4. Results

4.1 Method Development: Accuracy, Precision, and Blank

The accuracy of our total cobalt measurement protocol was determined using CASS-3 and NASS-5 coastal and open ocean reference seawaters, respectively, from the National Research Council Canada (NRCC). Standard additions analysis to diluted CASS-3 seawater with Fisher certified 1000ppm $\text{Co}(\text{NO}_3)_2$, yielded a concentration of $249 \pm 7\text{pM}$. The error was based on propagation of uncertainty associated with least-squares linear fit of the standard additions. Standard addition analysis of NASS-5 standards yielded a concentration of $169 \pm 16\text{pM}$. The error here gives the standard deviation for three replicate analyses. These results showed excellent agreement with values reported by NRCC (Table 1): our results were within the NRCC error range and were slightly lower than their values, consistent with our low reagent blank measurements.

The analytical blank of our reagents and equipment determined using twice UV-irradiated chelexed SSW was close to or below detection limit (Fig.1A). Raw spectra were analyzed by both peak height and one-second scan baseline subtraction followed by peak height measurements; in most cases peak heights without baseline correction yielded better precision than those with baseline corrections due to slight baseline variations between samples. Due to the observation of a negative Co blank in some chelexed UV-SSW (Fig. 1B and 1C), a small Co blank in our reagents was left to assure ourselves that we were not inadvertently introducing synthetic cobalt ligands to our speciation measurements. This Co blank was determined for each batch of reagents and subtracted from titration results.

4.2 Calibration and pH effects

There are few published data for the stability constant of dimethylglyoxime with cobalt(II). A calibration performed by Zhang et al. (1990) with EDTA yielded a conditional stability constant of $\log K_{\text{CoHDMG}2}^{\text{cond}}$ of 12.85 ± 0.10 at pH 8.7 and 35‰

salinity. We conducted three calibration experiments with EDTA as a model ligand using UV-irradiated Sargasso seawater that showed a pH dependent conditional stability constant. $\log K_{CoHDMG_2}^{cond}$ at pH 8.0 in our experimental system was determined to be 11.5 ± 0.3 , where the error is calculated from the standard deviation of the three stability constants from these three separate calibration experiments each with freshly prepared reagents. A $\log K_{CoHDMG_2}^{cond}$ of 10.6 ± 0.01 at pH 7.6 was determined, representing a one log unit shift in conditional stability constant per half pH unit (Fig. 2A and Table 2). This pH dependence was predicted by calculations in which we modeled EDTA-DMG competition experiments as a function of pH (Fig. 2B). In these calculations we used protonation and binding constants for EDTA with Co^{2+} , Mg^{2+} , and Ca^{2+} from the Martell and Smith database at $\mu=0.5$ (1993), and protonation and a Co^{2+} conditional stability constant from Martell and Smith (1993) and this study, respectively. We were unable to find binding constants for DMG with major seawater divalent cations, calcium and magnesium; however, these ions tend to have a preferential affinity for carboxylic acid groups rather than the nitrogen ligands found in DMG. We assume that DMG does not participate in significant binding with Ca^{2+} and Mg^{2+} ; nevertheless, the conditional stability constants measured here would incorporate any effect of major ion binding.

The squared $HDMG^-$ term in the $CoHDMG_2$ stability constant equation (equation 4) creates the strong pH dependence, where a one unit decrease pH change causes a two order of magnitude change in the conditional stability constant of $CoHDMG_2$ ($K_{CoHDMG_2}^{cond}$). The difference in our conditional stability constant for $CoHDMG_2$ from that of Zhang et al. (1990) is explained by the differences in pH at which $CoHDMG_2$ was calibrated: our study was conducted at ambient seawater pH (8.0-8.1) with the addition of EPPS buffer immediately before analysis, while the Zhang et al. calibration was performed at pH 8.7 by equilibration with the triethanolamine (TEA)/ NH_4Cl buffer. According to our calculations this increase in pH would result in a conditional stability constant that is 1.4 log units higher, consistent with the difference between our value for $\log K_{CoHDMG_2}^{cond}$ of 11.5 ± 0.3 and Zhang et al.'s value of 12.85 ± 0.10 .

For Co(II)TETA, $\log K_{CoTETA}^{cond} = 11.1 \pm 0.2$ by calibration against DMG using the conditional stability constant measured in this study. CoTETA is a mono complex, while CoHDMG₂ is a bis complex; thus despite similar stability constants, the CoTETA complexes are significantly stronger than CoHDMG₂.

4.3 Method Development: Co(II) and Co(III) Redox Chemistry

The high-speed scan/catalytic reaction utilizes nitrite to catalytically increase the reduction current. The reaction mechanism for this catalytic activity is unknown (Bobrowski and Bond, 1992; Vega and van den Berg, 1997). There have been several mechanisms proposed that account for the unusually high electrochemical signal of Co-dioxime complexes. Ma et al. (1997) argued convincingly that in addition to the reduction of the Co²⁺, the dioxime ligand is itself also being reduced with 8e⁻ per 2 dioxime groups, for a total of 10e⁻ per CoHDMG₂ complex. However, the use of nitrite and its influence on the reaction mechanism have not been carefully explored yet. An important question that pertains to the development of a speciation method is whether the nitrite acts as a ligand for Co(II) or if it actually can oxidize cobalt(II) complexes to cobalt(III) complexes on experimental time scales.

A spectrophotometric study of Co redox chemistry was carried out using DMG and EDTA as ligands to explore the influence of nitrite on cobalt coordination and redox chemistry. At millimolar concentrations, CoHDMG₂, Co(II)EDTA²⁻, Co(III)EDTA⁻, and CoEDTA(NO₂)_x have distinct absorbance spectra. Initially, we examined the oxidation of Co(II)EDTA²⁻ to Co(III)EDTA⁻ by H₂O₂, a ubiquitous oxidant in marine surface waters. EDTA was selected because the reaction can be monitored using a broad Co(II)EDTA²⁻ peak at 472-520nm and a Gaussian peak at 535nm for Co(III)EDTA⁻ (Fig. 3A) and because there is a strong thermodynamic driving force for this reaction caused by the much higher stability constant of the Co(III) chelate ($\log K_{Co(II)EDTA} = 16.45$, $\log K_{Co(III)EDTA} = 41.4$ from Martell and Smith, 1977; Xue and Traina, 1996, respectively). This reaction was very slow, requiring several hours for completion at millimolar H₂O₂ levels. A Co(II)EDTA complex was equilibrated overnight with NO₂⁻ yielding a unique

spectra, suggesting coordination of nitrite had occurred (Fig. 3B). It is likely that the valence of Co in the new complex was still +2, since subsequent addition of H₂O₂ led to formation of the familiar Co(III)EDTA complex spectrum. Presumably, a mixed CoEDTA(NO₂⁻)_x complex was formed. These results suggest that nitrite probably does not induce a redox shift when added to a solution containing organically complexed Co(II), but may influence Co(II) speciation, even in the presence of a polydentate ligand like EDTA. It is possible that the addition of nitrite could influence the apparent stability constant of DMG or naturally occurring ligands through mixed complex formation. We think this is unlikely because conditional stability constants for CoHDMG₂ obtained here and by Zhang and coworkers (who did not use nitrite) are consistent when pH effects are accounted for (above), and our estimates of conditional stability constants for natural ligands are not substantially higher than those of Zhang et al.

4.4 Method Development: Wall Effects

Given the low concentration of total cobalt and potential natural ligands we used a small addition of ⁵⁷Co radiotracer to our teflon equilibration bottles to determine if there were losses of Co-complexes to the surface area of the bottles during the equilibration period. An equilibration bottle with fresh filtered 1500m Sargasso seawater was prepared in the same manner as those used for titrations. An aliquot of ⁵⁷Co (⁵⁷CoCl₂, Isotope Products) was added before adding DMG to make a final concentration of 100pM ⁵⁷Co. 0.10mL aliquots were withdrawn in triplicate at t=0 and after four days. Samples were counted by germanium gamma counter (Canberra). We measured 97.98 ± 2.1% recovery of added ⁵⁷Co after 5 days of equilibration (28.39 ± 0.60 counts per second n=3, 27.81 ± 0.34 counts per second n=4, for t₀ and t₁ respectively), indicating no wall effects in our equilibrations.

4.5 Sargasso Sea Field Titrations

Titration were conducted at sea and immediately upon returning to land. Filtered refrigerated samples were used instead of frozen samples to avoid any loss of ligands due to the freezing process and precipitation associated with the freeze/thaw cycle. Total cobalt measurements were conducted on a profile at BATS to 3000m from September 1999 (Fig. 4A) and showed a nutrient-like profile with a maximum of 73pM at 1500m and approximately a three-fold increase in total cobalt concentration with depth. Only limited resolution was possible at greater depths due to difficult "chinese-finger" wire extensions used to acquire the deep samples.

Total L and K_{CoL}^{cond} were calculated using non-linear fits of titration data, incorporating the surface variability in slope as discussed in section 2.3 (Fig. 4B). Total L shows a peak in total ligand concentration near the *Prochlorococcus* and *Synechococcus* maximum and a decrease in the surface waters (Fig. 5A). The calculation of K_{CoL}^{cond} is made relative to our calibration of CoHDMG₂ at ambient seawater pH. Log K_{CoL}^{cond} has a profile average of 16.3 ± 0.9 with the most variability occurring at or near the ligand maximum (Fig. 5B).

Each cobalt speciation measurement utilized two independent titrations to calculate final speciation results. In the first titration, subsamples were allowed to equilibrate for ≥ 12 h with added cobalt, natural ligands, and the synthetic DMG ligand (Fig. 6A). These titrations were remarkably linear and had consistently low x-axis intercepts, which when blank corrected resulted in labile cobalt values close to zero (Tables 3 and 4). A second titration was run without equilibration on replicate samples to determine the sensitivity slope for the Co(HDMG₂) chelate (S). These non-equilibrated cobalt titrations also resulted in linear responses but with a steeper slope than that of the equilibrated titrations (Fig. 6A). These non-equilibrated titrations were repeated for all titration depths and the ratios of non-equilibrated slopes to equilibrated slopes decreased with depth (Fig. 4B). In addition, standard addition analysis of UV-irradiated samples was conducted to measure total cobalt.

Estimates of CoL, total L and K_{CoL}^{cond} were calculated from these data. A representative non-linear fit is shown in Figure 6B. Concentrations of CoL with respect to depth are calculated by simple mass balance subtraction shown in equation 15, and resemble the total cobalt nutrient-like profile.

5. Discussion

5.1 Total Cobalt

The total dissolved cobalt profile at the Bermuda Atlantic Time Series Station (31 °79'N, 64 °26'W) shows a depletion of cobalt in surface waters consistent with nutrient-like behavior (Fig. 4A). This is the first observation of a nutrient-like profile for cobalt at BATS. Jickells and Burton (1988) saw no trends with depth for Co at BATS, but were at their limit of detection. Our profile is similar to a profile reported by Martin et al. (Martin, 1993) at an oligotrophic station in the North Atlantic at 59 °30'N, 20 ° 45'W, suggesting that the modest surface depletion we report may be a typical feature under oligotrophic conditions. Phytoplankton uptake is thought to be the dominant removal mechanism of cobalt in the euphotic zone of the Sargasso Sea (Moffett and Ho, 1996). The surface waters at BATS were dominated by *Prochlorococcus* and *Synechococcus* (Fig. 7), both of which are known to have an absolute cobalt requirement (Saito et al., 2000; Sunda and Huntsman, 1995, respectively), and which may have contributed to the surface depletion of total Co.

5.2 Cobalt Speciation

Results show that Co speciation is dominated by strong ligands at concentrations very similar to the total Co concentration (Fig. 8). Similar results have been reported for other metals, such as Cu and Fe, but Co titrations show two pronounced features. First, there is little or no DMG-exchangeable Co in the initial sample. Secondly, there is no evidence for an excess of strong ligand that is titrated by additional Co. If there were, the slope of the titration plot would show a progressive increase with increasing Co (i.e.

curvature). Instead, Co appears to be strongly complexed by a strong ligand in seawater, but there is no evidence for subsequent formation of this complex under the conditions of our titration. The observation of a lack of curvature and a near-zero cobalt intercept in equilibrated titrations was observed by John Donat in his thesis work; our findings over several years of work are consistent with this. Zhang et al. (1990) also did not observe any curvature in their titration plots of cobalt speciation work in estuarine waters.

The simplest explanation is provided by our calculations; a strong Co(II) ligand exists with concentrations very close to that of total Co. This explanation requires a mechanism by which metal and ligand concentrations should be similar. For instance, excess Co could be rapidly scavenged from the water column. However, there are alternative explanations that could account for the titration features even if ligand concentrations were higher.

First, it is possible that the natural Co complexes in the Sargasso are in fact Co(III) chelates. We are unable to remove significant amounts of cobalt from these natural ligands at the DMG concentration utilized, which is consistent with the properties of Co(III) complexes. Their stability constants tend to be much higher than the corresponding Co(II)-complexes (e.g. $\log K_{\text{Co(II)EDTA}}=16.45$, $\log K_{\text{Co(III)EDTA}}=41.4$ from Martell and Smith, 1977; Xue and Traina, 1996, respectively), indicating Co(III) complex dissociation should be slow. For instance, we found that Co(III)EDTA^- , prepared in Section 4.3 was exchangeable with DMG, but only fractionally (<5%). Dissolved cobalt in seawater may be found in the form of a biogenic molecule such as cobalamin (vitamin B₁₂) or degradation products of cobalamin or other strong cobalt ligands. Cobalt in cyano-cobalamin is known to be in the Co(III) redox state (Glusker, 1995) and hence would be kinetically inert to competitive ligand exchange reactions. Cobalamin is probably inaccessible to our speciation method, but the cobalt would be released in our total method by degradation of the corrin ring during UV-irradiation. Moreover, measurements of cobalamin in the Sargasso Sea by bioassay show subpicomolar concentrations, making them a small fraction of the total cobalt (Menzel and Spaeth, 1962).

A second explanation for the similarity between CoL and total dissolved cobalt is that any ligand in excess of Co is bound to Ni, which is present at much greater abundance. While the Co peak is virtually absent from equilibrated samples, indicating little or no free Co, the Ni peak is not saturated with strong natural ligands (Fig. 9). A database survey of strong synthetic Co ligands shown in Table 5 shows that most strong Co ligands have as strong an affinity for Ni as for Co, supporting the idea of an equilibrium in seawater involving both metals. Moreover, Ni has not been reported to be saturated by natural ligands. In previous work by van den Berg and Nimmo (1986), Ni in coastal Britain was found to be partially complexed by strong Ni ligands with a $\log K_{NiL}^{cond}$ between 17.3 and 18.7 using cathodic stripping voltammetry and dimethylglyoxime as the electroactive synthetic Ni ligand. It is interesting to note that these investigators did not observe any curvature in their titrations of nickel, due to the excess of nickel over organic complexes in all of their titrations. We explored the possibility of competition for Co and Ni by a single ligand using model ligand calculations with a range of thermodynamic binding constants for nickel and cobalt (Fig. 10). The modeling work for the Co/Ni equilibria is derived from the mass law equations described above and the following mass balance equations.

$$L_{TOT} = L_{Free} + CoL + NiL + \sum ML \quad (19)$$

$$TotCo = Co' + CoL \quad (20)$$

$$TotNi = Ni' + NiL \quad (21)$$

Given that many of the stronger cobalt and nickel ligands do not seem to have as much affinity for other metals and due to the lack experimental evidence, we assumed that $\sum ML$ was insignificant, allowing the simplified equation:

$$\frac{L_{Free}}{L_{TOT}} = \frac{1}{1 + K_{NiL}^{cond} \cdot [Ni^{2+}] + K_{CoL}^{cond} \cdot [Co^{2+}]} \quad (22)$$

Using K_{NiL}^{cond} and K_{CoL}^{cond} as parameters to study this system, we are left with an equation with L_{Free} as the only unknown:

$$\frac{L_{Free}}{L_{TOT}} = \frac{1}{1 + K_{NiL}^{cond} \cdot \frac{TotNi}{\alpha'_{Ni} + K_{NiL}^{cond} L_{Free}} + K_{CoL}^{cond} \cdot \frac{TotCo}{\alpha'_{Co} + K_{CoL}^{cond} L_{Free}}} \quad (23)$$

In addition to the potential competition of nickel for cobalt ligands, once bound, nickel ligands may appear recalcitrant to our speciation protocol due to kinetic factors. Nickel is known to have slow coordination kinetics because of its slow water-loss rate constants in the case of an disjunctive mechanism, or the stability of the partially dissociated complex for an adjunctive mechanism (Hudson et al., 1992). The water-loss rate constant for Ni^{2+} is two orders of magnitude slower than that of Co^{2+} , and adjunctive rate constants have been shown to correlate with water-loss rate constants in EDTA systems. The slow kinetics of nickel can be used to explain our speciation titration results: we would expect the metal exchange between NiL and CoL to be kinetically slow for both disjunctive and adjunctive mechanisms.

Figure 11 illustrates the effects of differing rates of Ni and Co exchange kinetics. An excess of TETA was added to a seawater solution containing CoHDMG₂ and NiHDMG₂ complexes. The Co peak decreases immediately reflecting formation of the non-electroactive TETA complex, but NiHDMG₂ is relatively unchanged. The relatively slow kinetics of Ni relative to Co are also apparent in the calibration of TETA where CoTETA complexes equilibrate with CoHDMG₂ in the 24h equilibration period, but NiTETA complexes have only partially formed (Fig. 12).

Any of these explanations for the titration features must be considered in the context of the other important feature of the titrations – the difference in slope between equilibrated and non-equilibrated samples (Fig. 4). We argued above that this reflects

cobalt complexation by weaker ligands at concentrations substantially higher than our highest Co addition. How important are these weak ligands? The α coefficient for the weaker ligands is related to S as follows:

$$\frac{\alpha_{DMG} + \alpha_{WL}}{\alpha_{DMG}} = \frac{S_{non-equil}}{S_{equil}} \quad (24)$$

From this equation α_{WL} (where $\alpha_{WL} = K_{CoL_2}^{cond} \cdot L^2$, L_2 is the weak ligand and α_{DMG} = side reaction coefficient for $CoHDMG_2$ complexes) ranges from 1.7×10^3 to 1.2×10^4 . By contrast the coefficient for the strong ligand, α_{SL} , calculated from K_{CoL}^{cond} and ligand concentrations, is 1.4×10^6 . However, the strong ligand is saturated at most depths, so the relative importance of the weaker ligands increases. It is possible that the strong and weak ligands are the same species, but the former is a Co(III) complex and the latter a Co(II) complex, with oxidation kinetics that are too slow on the timescale of these titration experiments. The weak ligand class requires further investigation. Our efforts to fit the titration data using a two-ligand model resulted in large errors associated with $K_{CoL_1}^{cond}$. It also removed the feature of the slight excess of strong cobalt ligands in the *Prochlorococcus* and *Synechococcus* maximum; this makes sense in the context of how these calculations have been performed, with the changes in S in surface waters forcing the increase in L at the *Prochlorococcus* and *Synechococcus* maximum. Although Co speciation is clearly dominated by the stronger ligand class, a small fraction complexed by the weaker ligands may constitute an important reactive and bioavailable class. Raw titration data is available in the thesis of M. Saito (Saito, 2000) in case future work warrants a revision of these interpretations.

The theoretical free Co^{2+} concentration is difficult to calculate from the data without large errors, since the strong ligand and Co concentrations are so similar. One approach is to simply divide the Co concentration that is in excess of the strong ligand by the α coefficient for the weak ligands. This would provide an upper limit on free Co^{2+}

with concentrations that range from 10^{-14} to 10^{-17} M. The various interpretations of our cobalt speciation data presented here are not mutually exclusive: Co(II) and Ni ligands may exist in our samples, which also might bind Co(III) but with a much higher binding constant. This latter scenario could lead to an underestimate of ligand concentrations and conditional stability constants relative to the one ligand non-linear fit model that we have described.

Conclusions

In this study we have begun to examine the difficult problem of cobalt speciation in oceanic environments. Our finding that cobalt is strongly bound by ligands of nearly equivalent concentration is intriguing and warrants further study to determine if these ligands are inert Co(III) molecules (e.g. B₁₂ degradation products) or if they are binding other metals like nickel. These findings have important implications for both the biological utility of cobalt and its geochemistry. With the predominant form of cobalt in the Sargasso as strongly bound CoL, the CoL is likely bioavailable since the resultant Co²⁺ concentrations would certainly limit growth of organisms with absolute cobalt requirements such as the photosynthetic cyanobacteria. Moreover, the strength of these ligands and their presence in deep Atlantic waters could result in a longer oceanic residence time than we would expect from a scavenged-type trace element.

Acknowledgements

We would like to thank the captain and crew of the R/V Oceanus for their invaluable assistance. We appreciated the flow cytometry data generated by Matthew Sullivan, and the chlorophyll profile collected by Jason Ritt and analyzed by Stephanie Shaw. Thanks to Katherine Barbeau and Christie Hauptert for their assistance with sampling at sea. We are indebted to Bettina Voelker and Ken Bruland for comments on this manuscript. Mak Saito was funded by an EPA STAR graduate fellowship and a NSF Coastal Traineeship. This work was funded by the NSF under grant OCE-9618729.

References

- Baxter, L., Bobrowski, A., Bond, A., Heath, G., Paul, R., Mrzljak, R., and Zarebski, J. 1998. Electrochemical and Spectroscopic Investigation of the Reduction of Dimethylglyoxime at Mercury Electrodes in the Presence of Cobalt and Nickel. *Anal. Chem.*, 70: 1312-1323.
- Bobrowski, A., 1989. Polarographic Methods for Ultratrace Cobalt Determination Based on Adsorption-Catalytic Effects in Cobalt(II)-Dioxime-Nitrite Systems. *Anal. Chem.*, 61: 2178-2184.
- Bobrowski, A. and Bond, A., 1992. Exploitation of the Nitrite Catalytic Effect to Enhance the Sensitivity and Selectivity of the Adsorptive Stripping Voltammetric Method for the Determination of Cobalt with Dimethylglyoxime. *Electroanal.*, 4: 975-979.
- Bruland, K.W., 1989. Complexation of zinc by natural organic ligands in the central North Pacific. *Limnol. Oceanogr.*, 34(2): 269-285.
- Bruland, K.W., 1992. Complexation of cadmium by natural organic ligands in the central North Pacific. *Limnol. Oceanogr.*, 37(5): 1008-1016.
- Costa, G., Tavagnacco, C., Puxeddu, A., Balducci, G. and Kumar, R., 1987. Electrochemistry of cobalt mixed Schiff base/oxime chelates. *J. of Organometallic Chem.*, 330: 185-199.
- Donat, J.R. and Bruland, K.W., 1988. Direct Determination of Dissolved Cobalt and Nickel in Seawater by differential Pulse Cathodic Stripping Voltammetry Preceded by Adsorptive Collection of Cyclohexane-1,2,-dione Dioxime Complexes. *Anal. Chem.*, 60: 240-244.
- Gerringa, L.J.A., Herman, P.M.J. and Poortvliet, T.C.W., 1995. Comparison of the linear van den Berg/Ruzic transformation and a non-linear fit of the Langmuir isotherm applied to Cu speciation in the estuarine environment. *Mar. Chem.*, 48: 131-142.
- Glusker, J.P., 1995. Vitamin B12 and the B12 Coenzymes. *Vitamins and Hormones*, 50: 1-76.
- Hudson, R.J.M., Covault, D.T. and Morel, F.M.M., 1992. Investigations of iron coordination and redox reactions in seawater using ^{59}Fe radiometry and ion-pair solvent extraction of amphiphilic iron complexes. *Mar. Chem.*, 38: 209-335.

- Jickells, T.D. and Burton., J.D., 1988. Cobalt, copper, manganese and nickel in the Sargasso Sea. *Mar. Chem.*, 23: 131-144.
- Lucia, M., Campos, A.M. and van den Berg, C.M.G., 1994. Determination of copper complexation in sea water by cathodic stripping voltammetry and ligand competition with salicylaldoxime. *Anal. Chim. Acta*, 284: 481-496.
- Ma, F., Jagner, D. and Renman, L., 1997. Mechanism for the Electrochemical Stripping Reduction of the Nickel and Cobalt Dimethylglyoxime Complexes. *Anal. Chem.*, 69: 1782-1784.
- Martell, A.E. and Smith, R.M., 1993. NIST Critical Stability Constants of Metal Complexes Database.
- Martin, J.F., SE; Gordon, RM; Hunter, CN; Tanner, SJ, 1993. Iron, primary production and carbon-nitrogen flux studies during the JGOFS North Atlantic Bloom Experiment. *Deep-Sea Res. II*. 40(1-2): 115-134.
- Martin, J.H. and Gordon, R.M., 1988. Northeast Pacific iron distribution in relation to phytoplankton productivity. *Deep-Sea Res*, 35: 177-196.
- Martin, J.H., Gordon, R.M., Fitzwater, S. and Broenkow, W.W., 1989. VERTEX: phytoplankton/iron studies in the Gulf of Alaska. *Deep-Sea Res.*, 36(5): 649-680.
- Menzel, D.W. and Spaeth, J.P., 1962. Occurrence of vitamin B12 in the Sargasso Sea. *Limnol. Oceanogr.*, 7: 151-154.
- Moffett, J.W., 1995. Temporal and spatial variability of copper complexation by strong chelators in the Sargasso Sea. *Deep-Sea Res. I.*, 42(8): 1273-1295.
- Moffett, J.W. and Brand, L.E., 1997. Production of strong, extracellular Cu chelators by marine cyanobacteria in response to Cu stress. *Limnol. Oceanogr.*, 41(3): 388-395.
- Moffett, J.W. and Ho, J., 1996. Oxidation of cobalt and manganese in seawater via a common microbially catalyzed pathway. *Geochim. Cosmo. Acta*, 60(18): 3415-3424.
- Nakani, B.S., Welsh, J.J.B. and Hancock, R.D., 1983. Formation Constants of Some Complexes of Tetramethylcyclam. *Inorg. Chem.*, 22: 2956-2958.
- Ogino, H. and Ogino, K., 1982. Redox Potentials and Related Paramaters of Cobalt(III/II) Complexes Containing Aminopolycarboxylates. *Inorg. Chem.*, 22: 2208-2211.

- Price, N.M. et al., 1988/1989. Preparation and chemistry of the artificial algal culture medium Aquil. *Biol. Oceanogr.*, 6: 443-461.
- Rue, E.L. and Bruland, K.W., 1995. Complexation of iron(III) by natural ligands in the Central North Pacific as determined by a new competitive ligand equilibration/asorptive cathodic stripping voltammetric method. *Mar. Chem.*, 50: 117-138.
- Saito, M.A., 2000. The Biogeochemistry of Cobalt in the Sargasso. Ph.D. Thesis, MIT-WHOI Joint Program in Chemical Oceanography, Massachusetts.
- van den Berg, C.M.G. and Nimmo, M., 1986. Determination of interactions of nickel with dissolved organic material in seawater using cathodic stripping voltammetry. *Sci. Total Environ.*, 60: 185-195.
- Zhang, H., van den Berg, C.M.G. and Wollast, R., 1990. The Determination of Interactions of Cobalt (II) with Organic Compounds in Seawater using Cathodic Stripping Voltammetry. *Mar. Chem.*, 28: 285-300.

Figure 2-1

(A) Blank determination: ACSV spectra of an UV-irradiated and chelexed Sargasso seawater sample with standard additions of 38.3pM $\text{Co}(\text{NO}_3)_2$. Nickel peaks at -1.05V are negligible, and cobalt peaks are at -1.17V . (B) Baseline subtraction of the same data set using one second deposition time scan as a baseline. (C) Peak heights of the standard addition showing no blank with all points (triangles), and a slight negative blank without the 0pM point (circles). The negative of the x-axis intercept is equal to the reagent blank indicating slight contamination with synthetic ligands from the chelex reagent clean-up methods.

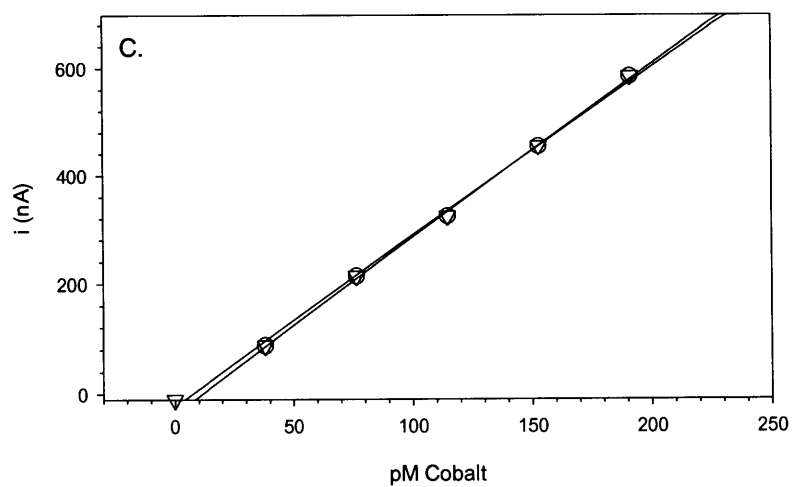
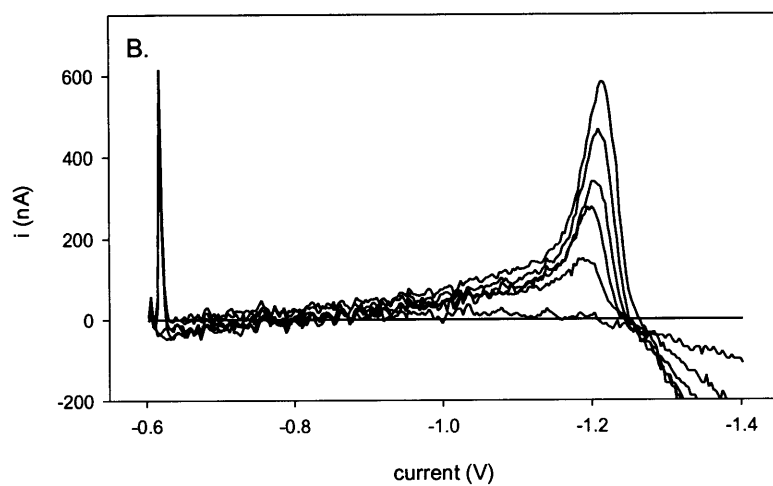
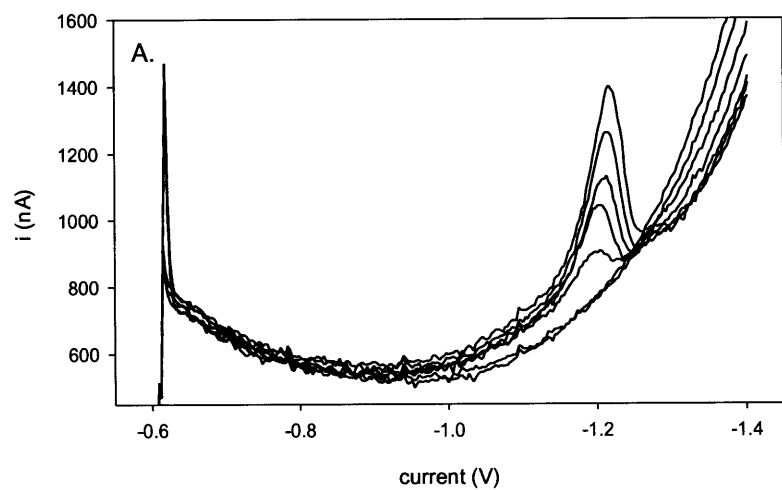


Figure 2-2

(A) Calibration of the conditional stability constant of CoHDMG₂ using EDTA as a model ligand. [DMG]= 0.0005M and Co_{TOT} = 191pM. The higher pH causes an increase in logK_{CoHDMG₂} and an increase in sensitivity. (B) Model cobalt speciation calculations showing the influence of protonation constants for H₂DMG on $K_{CoHDMG_2}^{cond}$. K_{a1} and K_{a2} for H₂DMG are 10^{10.45} and 10^{11.9} from Martell and Smith (1993) were used with the calibrated $K_{CoHDMG_2}^{cond}$ presented in Table 2. The application of protonation constants in these model calculations agrees well with our data in 2A, and explains the discrepancy between our $K_{CoHDMG_2}^{cond}$ constant and that of Zhang and van den Berg (1990) as described in the text.

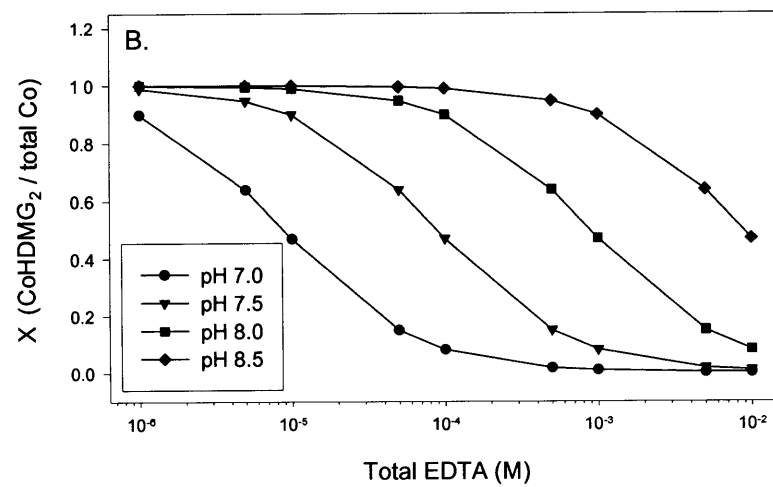
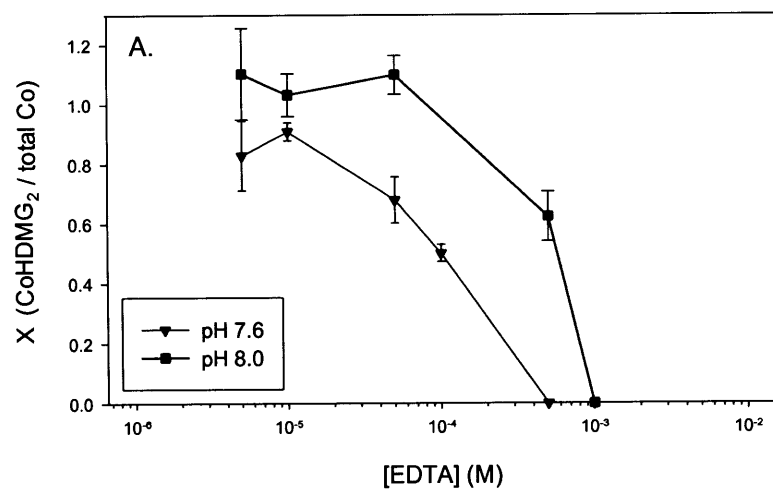


Figure 2-3

(A) Oxidation of Co(II)EDTA to Co(III)EDTA by H_2O_2 can be observed on a UV-VIS spectrophotometer. Spectra are shown from various times during the oxidation of Co(II)EDTA to illustrate the progression of reaction. Co(II)EDTA has a peak at 490nm and Co(III)EDTA has two distinct peaks at 380nm and 535nm. (B) Equilibration of nitrite with Co(II)EDTA produces a new spectra indicating a new complex has formed $\text{CoEDTA}-(\text{NO}_2)_x$, which can be oxidized to a Co(III)EDTA complex with the characteristic 535nm maxima. Free nitrite has a broad absorption peak at 360nm.

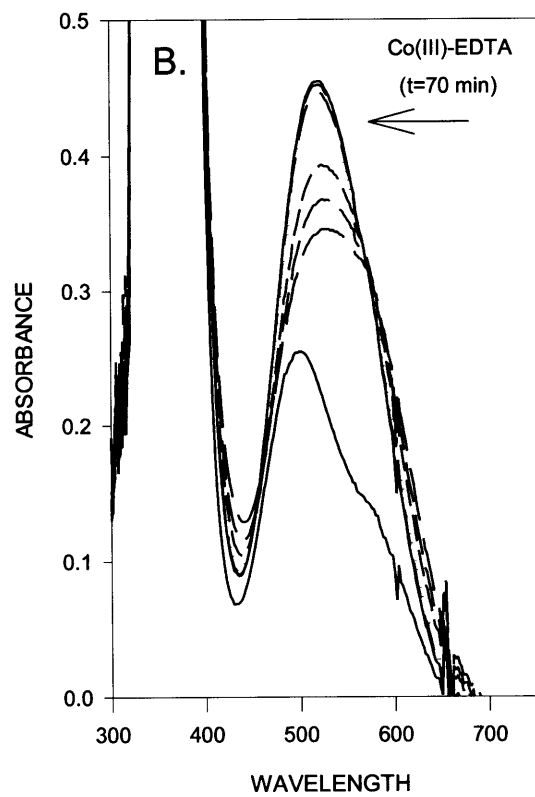
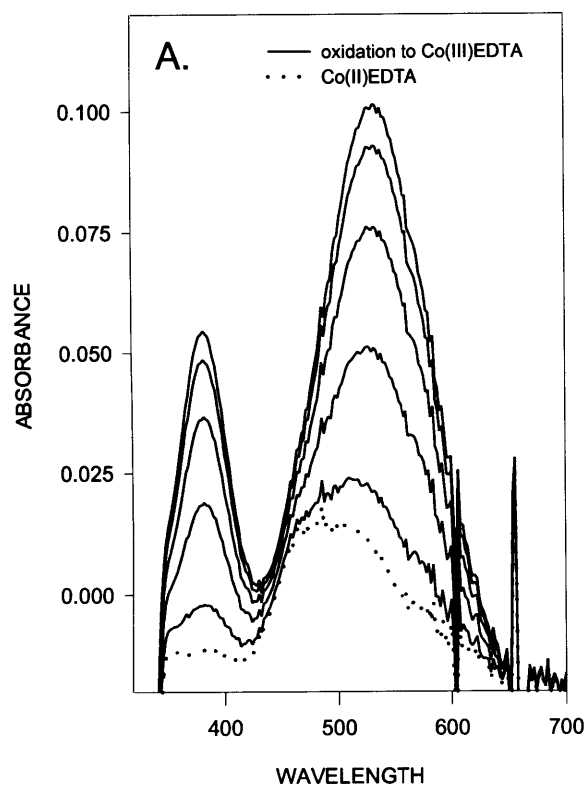


Figure 2-4

(A) Total dissolved cobalt at BATS in September of 1999. (B) Titration data presented as the ratio of non-equilibrated versus equilibrated slopes (S), showing a surface maximum.

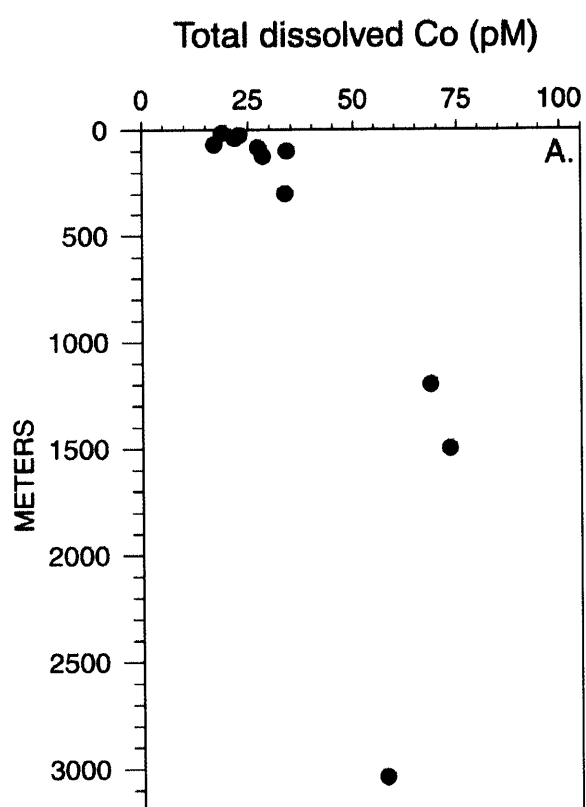


Figure 2-5

(A) Total ligand concentrations at BATS, September 1999. Total L is calculated by non-linear fitting of titration data. (B) Calculated stability constants for natural cobalt ligands.

$\text{Log } K_{CoL}^{cond}$ is also calculated by non-linear fitting of titration data.

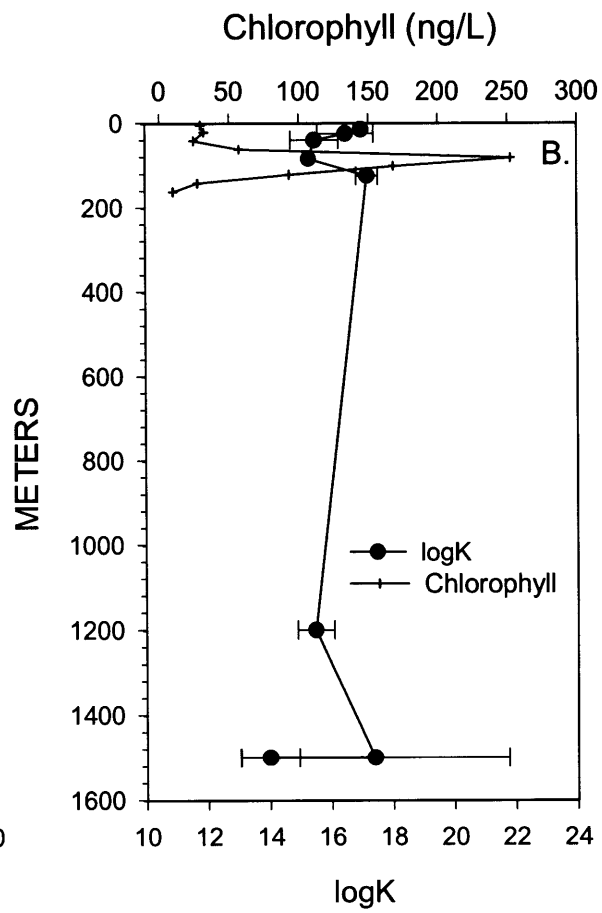
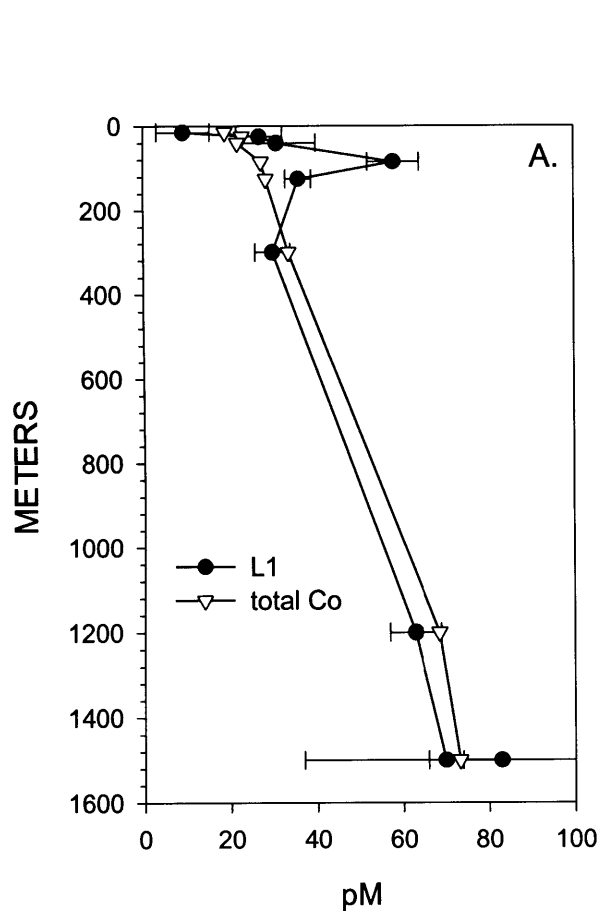


Figure 2-6

(A) A typical titration (*), showing linear response to cobalt additions with a y-intercept close to zero (before blank subtraction) and a non-equilibrated titration (+) with a higher slope. (B) Titration data fit with a non-linear least regression analysis using the Levenberg-Marquardt algorithm. Co free refers to Co^{2+} .

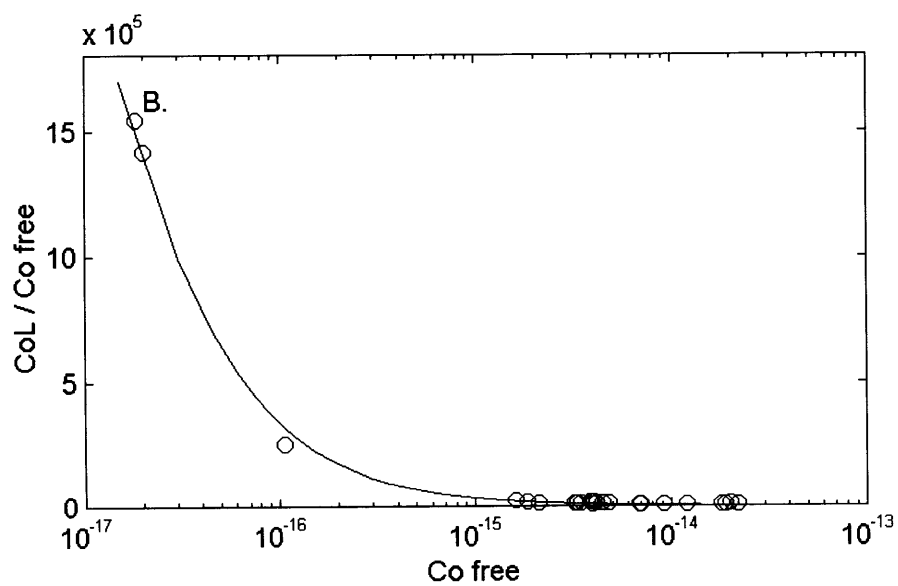
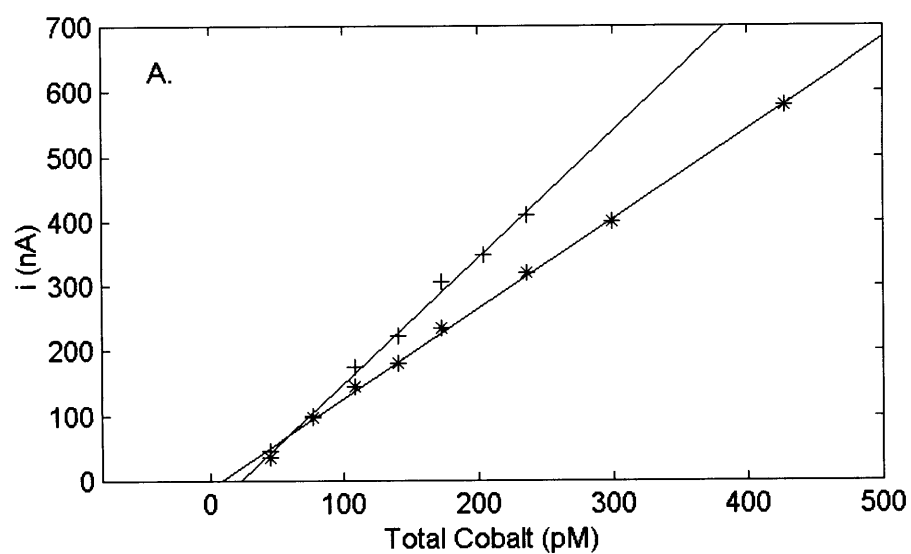


Figure 2-7

Hydrographic data and cell number abundances of *Synechococcus* and *Prochlorococcus* for BATS September 1999. Dashed lines in the temperature and salinity plots indicate the change in profiles during our occupation of the station. Cell numbers of *Synechococcus* and *Prochlorococcus* are given by star and cross symbol, respectively.

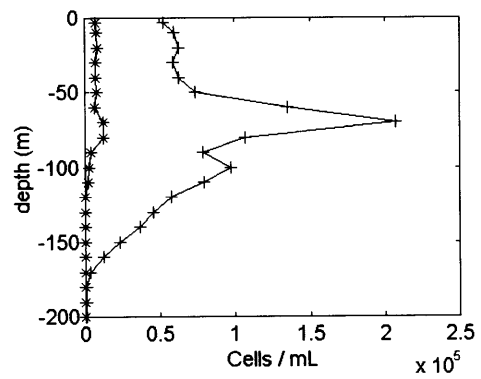
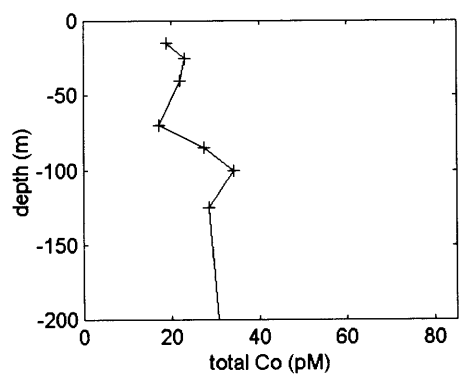
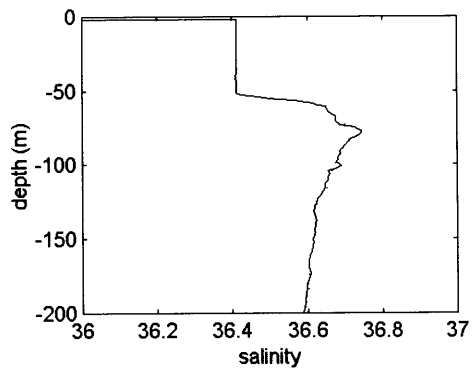
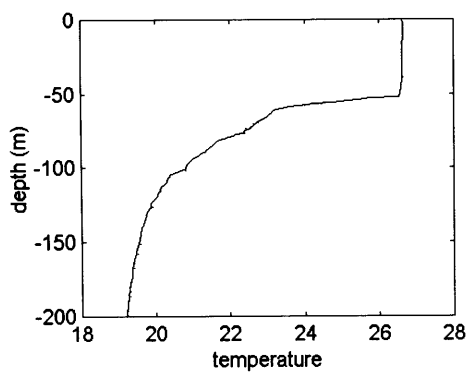


Figure 2-8

The linear relationship between total dissolved cobalt and CoL. Cobalt appears to be tightly bound with a ligand concentration close to the total cobalt concentration.

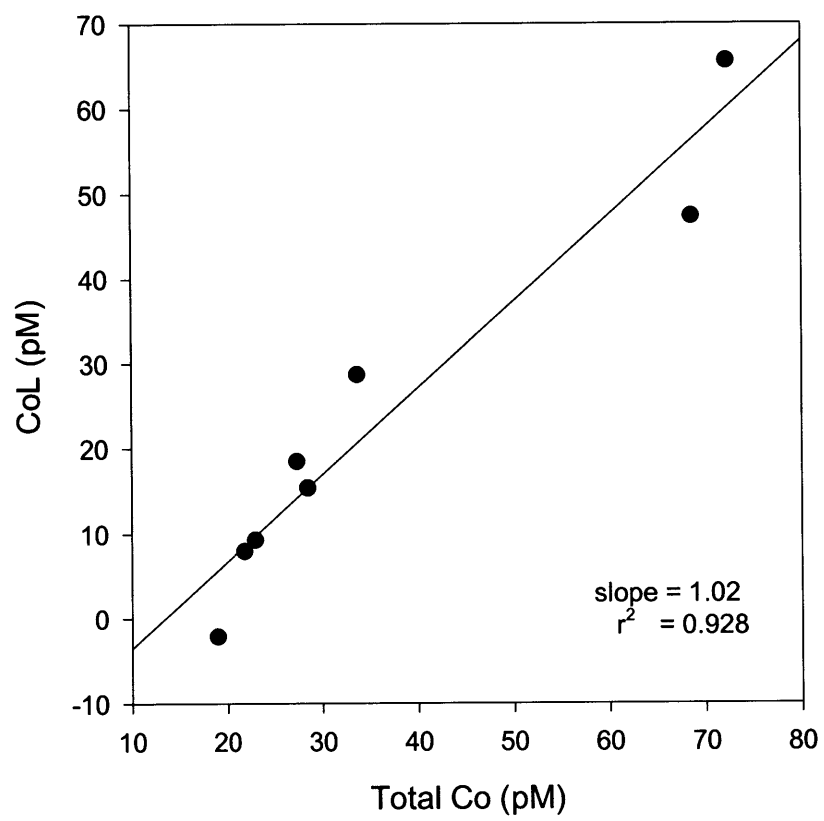


Figure 2-9

A comparison of raw ACSV spectra showing the lack of cobalt signal in filtered samples after equilibration (dotted line), relative to the larger cobalt peak (-1.19V) after UV-irradiation. By comparison the nickel peak (-1.05V) increases only slightly after UV-irradiation. In this figure total cobalt is ~50pM while total nickel is ~2nM.

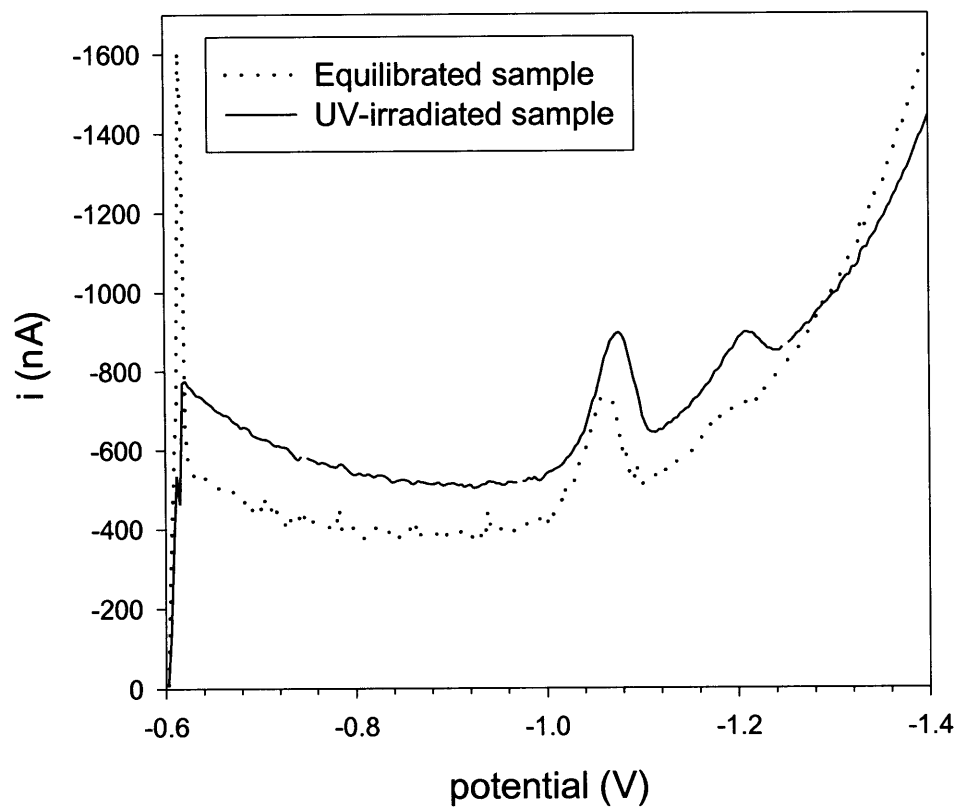


Figure 2-10

(A) Competition of natural ligands for cobalt and nickel is modeled in the absence of DMG. In order for partial binding of nickel and cobalt the conditional stability constant for CoL cannot be less than two orders of magnitude smaller than that of NiL. Since nickel is in excess of both natural ligands (the peaks are not saturated) and cobalt (2nM versus 40pM), there are no constraints on a conditional stability constant of CoL being greater than that of NiL. Total Co = 100pM, total Ni = 4nM, total L = 1nM, $\log K_{CoL}^{cond} = 16$. (B) Model calculations of a natural ligand and dimethylglyoxime electrochemical system where affinity of natural ligands to nickel is included. A loss of curvature in the titrations is observed as the conditional stability constant for cobalt is increased. Total Ni = 2nM, total L = 1nM, $\log K_{CoL}^{cond} = 16$, $\log K_{CoHDMG_2}^{cond} = 12.85$, $\log K_{NiHDMG_2}^{cond} = 17.2$, total DMG = 0.0002M.

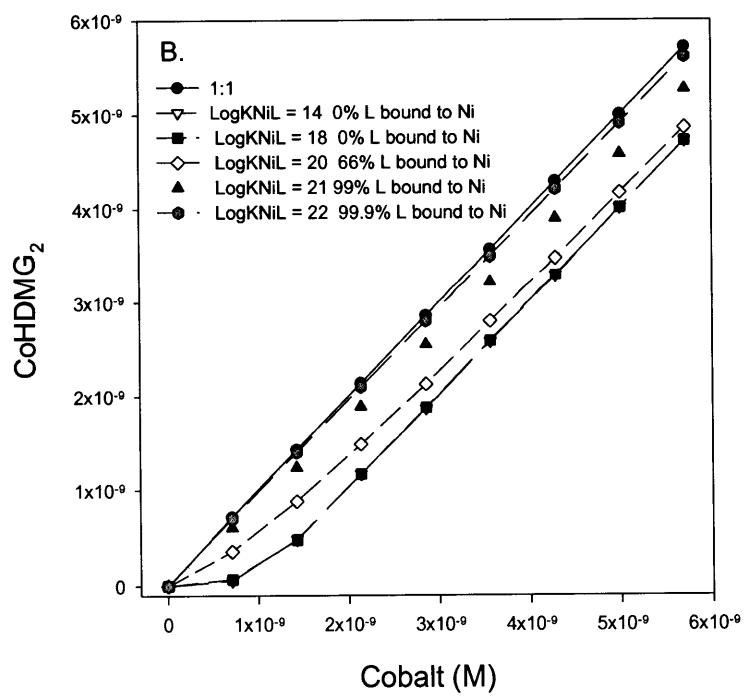
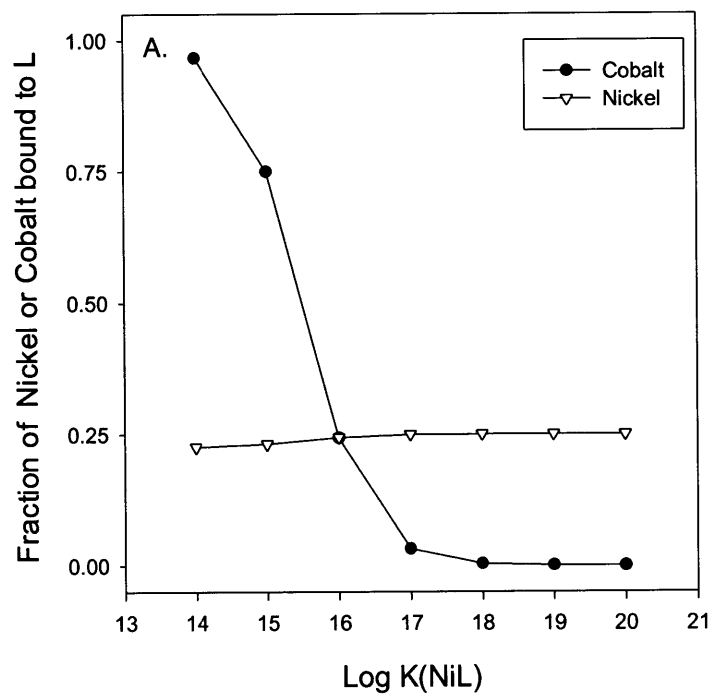


Figure 2-11

A kinetic study of the formation of cobalt and nickel TETA complexes. CoHDMG_2 was pre-equilibrated prior to a TETA addition. The cobalt peak disappears rapidly while the nickel peak is not significantly affected even after 24h.

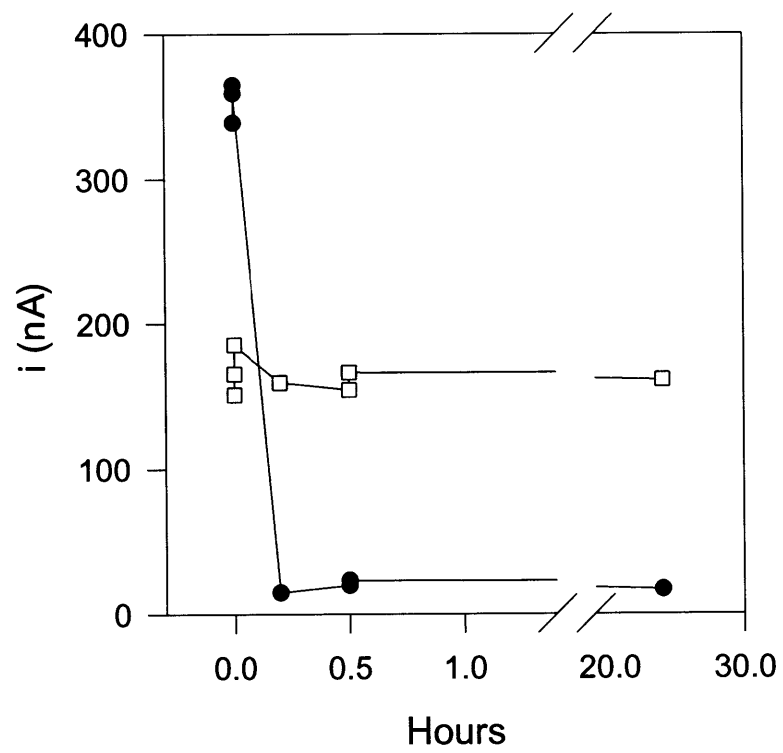


Figure 2-12

Calibration of TETA and DMG against EDTA. A) CoTETA forms significantly stronger complexes than CoEDTA. B) Nickel appears to be kinetically slow in reacting with TETA with the incomplete formation of NiTETA complexes within the overnight equilibration period. This phenomenon of slow nickel kinetics could have implications for cobalt speciation in our Sargasso Sea samples.

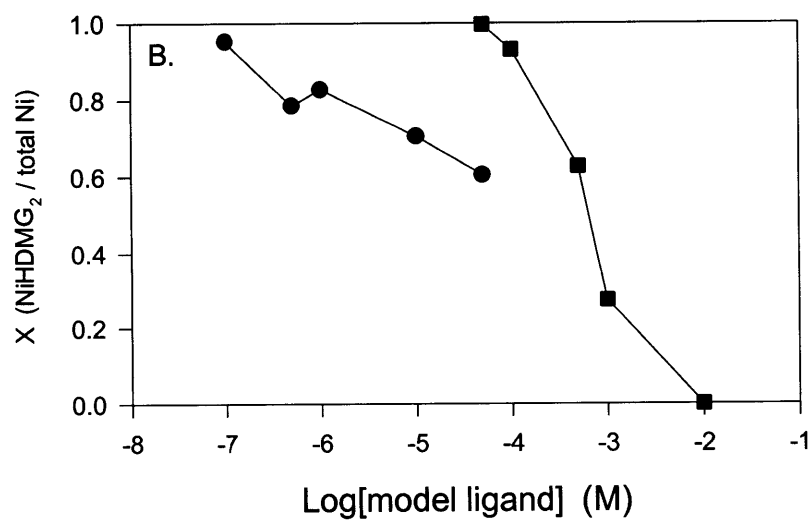
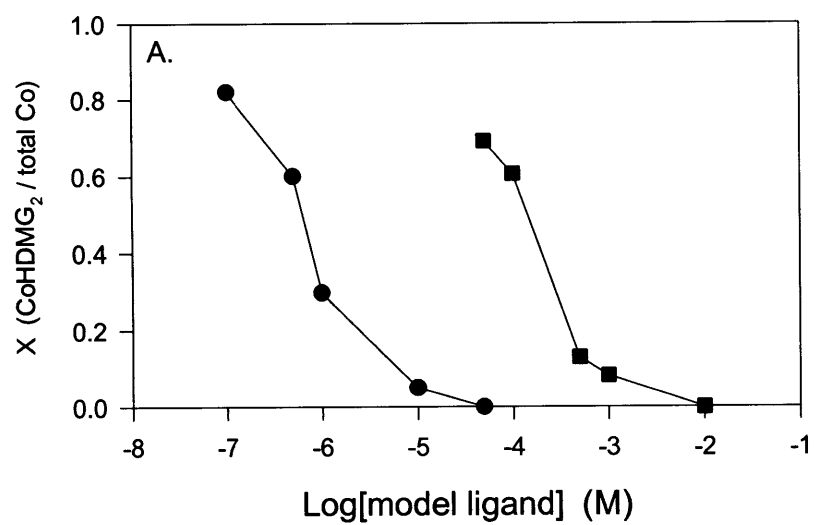


Table 2-1 The accuracy of total cobalt electrochemical measurements verified by standard additions of National Research Council of Canada reference seawater

Reference standard	NRCC value (picomoles/L)	Co by ACSV (picomoles/L)	number of analyses
CASS-4 coastal seawater (diluted)	$315 \pm 75^{\phi}$	$249 \pm 7^{\phi}$	2
NASS-5 open ocean seawater	187 ± 51	169 ± 16	3

^{ϕ} NRCC error is calculated from different analytical techniques, our errors are from the standard deviation from replicate samples or error propagation from the linear fit of titration data.

Table 2-2 Conditional Stability Constants for DMG and TETA calibrated using EDTA

Compound	Stoichiometry	$\log K^{cond}$
Co(II)Dimethylglyoxime (pH = 8.0)	$[ML_2]/[M][L]^2$	$11.5 \pm 0.3^+$
Co(II)Dimethylglyoxime (pH = 7.6)	$[ML_2]/[M][L]^2$	$10.6 \pm 0.01^*$
Co(II)TETA	$[ML]/[M][L]$	11.2 ± 0.1

⁺ error from standard deviation of mean results of three separate calibration curves.

^{*} error from standard deviation of individual points on titration curve $n \geq 3$.

Table 2-3 Co-Speciation incubations – BATS September and October 1999

titration #	date	depth	slope/r ² non-eq	slope/r ²	ratio	x-intercept (pM)*
1	9/25	125	0.284/0.961	0.194/0.976	1.46	25.0 ± 1.2; 20 ± 0.9
2	9/27	40	0.195/0.997	0.139/0.998	1.40	25.7
3	9/29	85	0.217/0.969	0.149/0.994	1.46	21.4 ± 4.6
4	9/29	15	0.203/0.995	0.159/0.996	1.28	31.8 ± 6.5
5	9/29	25	0.270/0.976	0.160/0.992	1.69	25.4 ± 1.9
6	10/1	1500	0.185/0.998	0.153/0.993	1.21	20.4 ± 5.8
8	10/5	300	0.262/0.999	0.229/0.999	1.14	18.1
9	10/11	1200	0.224/0.983	0.215/0.994	1.04	31.9 ± 1.8
10	10/11	1500	0.191/0.999	0.188/0.976	1.02	81.1 ± 4.1 (cont.)

* not dilution corrected – divide by 0.85 for reagent dilution correction

Table 2-4 Comparison of totals of equilibrated bottles to UV-Total Cobalt

Depth	Total equil	total equil w/dil. corr.	minus blank (corr tot Eq)	Total Cobalt (pM)	Error TotCo	[CoL] (totCo-TotEq)
15	31.8	37.4	21.1	19.0	4.690	-2.122 ⁺
25	25.4	29.9	13.7	23.0	0.03	9.3
40	25.7	30.2	13.9	21.9	--	8.0
85	21.4	25.1	8.9	27.4	0.500	18.474
125	25.0	29.4	13.1	28.5	--	15.378
300	18.1	21.2	5.0	33.7	1.170	28.666
1200	31.9	37.5	21.2	68.6	8.330	47.361
1500	81.1	95.4	79.1	73.3	2.100	-5.852 [*]
1500	20.4	24.0	7.7	73.3	2.100	65.560

+ this value is within the range of the error on the total cobalt measurement (4.7pM)

* this equilibration sample was contaminated by comparison with a replicate measurement.

Table 2-5 Stability Constants of strong synthetic cobalt and nickel ligands

Compound	Stoichiometry	LogK(Co(II))	LogK(Ni)	Reference
Dimethylglyoxime	$[ML_2]/[M][L]^2$	12.85	17.2	a
Nioxime	$[ML_2]/[M][L]^2$	15.62	21.5	a, b
TETA	$[ML]/[M][L]$	16.62	20.0	b
Cyclam	$[ML]/[M][L]$	12.71	22.2	b
Isocyclam	$[ML]/[M][L]$	10.9	-	b
Tetramethylcyclam	$[ML]/[M][L]$	7.58	8.65	c
Cyclen	$[ML]/[M][L]$	13.8	16.4	b, d
EDTA	$[ML]/[M][L]$	16.45	18.4	b
DTPA	$[ML]/[M][L]$	19.45	20.17	b

a. Zhang and van den Berg, 1990. Conditional stability constants

b. Martell and Smith, 1993. Thermodynamic stability constants

c. Nakani et al., 1983. Thermodynamic stability constants

d. cyclen is 1,4,7,10-tetraazacyclododecane ([12]aneN4)cyclen

Chapter 3

Total Cobalt in the Western North Atlantic and the Sargasso Sea

Abstract

A vertical profile of total dissolved cobalt at the Bermuda Atlantic Time Series (BATS) station ranged from 17-73pM and displayed surface depletion indicative of biological utilization. This profile when compared to a cobalt profile from the northeast Pacific shows no increase in deepwater concentrations with thermohaline circulation through the deep ocean basins. Moreover, the mid-depth maximum observed in northeast Pacific profiles is not present in the Sargasso Sea, perhaps due to the lack of cobalt scavenging by particulate manganese oxides in surface waters and due to the absence of a sub-oxic oxygen minimum zone in the Sargasso, which would dissolve the manganese oxides.

Total dissolved cobalt measurements were also made on a surface transect from the Sargasso Sea to coastal Massachusetts, U.S.A. and on time-series samples from MITESS, (Moored in-situ Trace Element Serial Sampler). Dissolved cobalt on this transect correlated strongly with salinity ($r^2=0.93$) and ranged from 19pM to 133pM, indicating mixing of cobalt from shelf waters into the Sargasso Sea.

Time-series samples from BATS did not show an obvious response to the summer maximum in aeolian dust deposition, with an annual average of $20\text{pM} \pm 10\text{pM}$ at 40-47m depth. Using this annual value and literature particulate cobalt data, we calculate 100m surface water residence times as low as 8.5-50d for cobalt. Several sharp decreases in cobalt were observed in the time series that occur simultaneously with a shallowing of the thermocline depth. These decreases could be caused by nutrient drawdown associated with higher productivity cold core eddy events (McGillicuddy and Robinson, 1997).

A west-east surface transect across the south Atlantic showed high cobalt concentrations at the boundaries of the transect and low concentrations in the center due to low salinity/high temperature waters of the Intertropical Convergence Zone. Low-level phosphate measurements showed the same trends as the total cobalt transect. A regression of cobalt versus phosphate reveals a slope that is an order of magnitude higher than that of the northeast Pacific and that is similar to the slopes observed for zinc versus phosphate in the Pacific.

Introduction

Cobalt is an important micronutrient for marine phytoplankton, in particular, the photosynthetic cyanobacteria (Chapter 4; Sunda and Huntsman, 1995), yet its surface water concentrations are very low based on the sparse available data. The factors controlling the distribution of cobalt in seawater are not well understood. The distribution of trace metals in seawater can be categorized into two broad classifications: metals that are cycled via biological uptake and regeneration (nutrient-type) or metals that are removed or cycled via particle adsorption or precipitation (scavenged-type) (Bruland, 1994). Nutrient-type metals, like the major nutrients nitrate and phosphate, show depletion in surface waters and remineralization with depth. Moreover, these metals show an increase in deep Pacific waters relative to deep Atlantic waters consistent with their transport with deepwater masses and long oceanic residence times. Cadmium, zinc, and nickel are examples of metals with nutrient-type behavior. Scavenged-type metals show net removal even in deep waters, and do not show an increase in concentration between deep ocean basins. Manganese, aluminum and lead are examples of scavenged-type metals, and iron and cobalt have intermediate behavior. A mechanistic explanation for these scavenged-type of profiles can be attributed to their chemistry: the tendency to precipitate as oxides, hydrolysis species, or to be associated with particles results in a low solubility in seawater. Furthermore, some of these metals such as Fe, Co, and Mn can be oxidized to highly insoluble redox states, from more soluble reduced states (Fe(II), Co(II), Mn(II)). There are both thermodynamic and biological factors that influence the rate of oxidation of these metals. With the oxygen-water redox couple dominating redox conditions in seawater, the oxidation state of the metals should be dictated by thermodynamic equilibria. However, some of these redox reactions like the oxidation of Co(II) and Mn(II) are kinetically slow, allowing biological processes to utilize the thermodynamic gradients for energy or other metabolic purposes (Tebo, 1997). In either case, the lower solubility of the oxidized forms of the metals is a likely cause of the scavenged-type profile of these metals. While it has been demonstrated that cobalt can

be oxidized by Mn oxidizing bacteria in coastal environments (Tebo et al., 1984), Co uptake in the surface waters of the Sargasso Sea appears to be dominated by phytoplankton uptake rather than Mn oxidation (Moffett and Ho, 1996).

With solubility influencing the distribution of scavenged-type metals, we would expect atmospheric deposition to be more important to the input function of these metals relative to the nutrient-type metals. This is because scavenged-type metals with their much shorter residence times would be preferentially removed as they are transported from shelf environments to the open ocean. However, the transect data in this work and in Bruland and Franks (1983), show cobalt and manganese correlating strongly with salinity on the slope/shelf of the western Atlantic, suggesting that advective transport from coastal waters is an important source to the open ocean. Duce et al. calculated that input of a variety of trace metals into oligotrophic oceanic regimes is primarily controlled by atmospheric deposition in the form of aeolian dust. This atmospheric deposition, which includes anthropogenic contributions, was the largest source of Pb, Cd, Cu, Zn, and Fe to the ocean.

There are relatively few measurements of cobalt in seawater available to us for use in explaining the cobalt's water column geochemical properties. Samples from 0.2-2350m off central California showed an inverse correlation with salinity suggestive of input from continental weathering (Knauer, 1982). Measurements of Cd, Zn, Ni, and Cu by Bruland and Franks (Bruland and Franks, 1983) and Boyle et al., (1984) led to the realization that the elevated metal values in the shelf and slope environments of the western Atlantic could not be explained by wind-induced coastal upwelling as on the eastern North Pacific Californian coast. A previous Co data set in the northwest Atlantic measured concentrations of 71-317pM and did not have an obvious relationship with salinity (Boyle et al., 1987). Profiles of cobalt in the open ocean, like iron, can be either nutrient-type or scavenged-type. Co and Fe profiles are similar to nutrient-type profiles in that they can display surface water depletion, yet they do not show deepwater enrichment in the Pacific and Indian Oceans as is observed for Zn, Ni, and Cd. This surface depletion in profiles has been observed for cobalt in the Pacific on several

occasions (Martin and Fitzwater, 1988; Martin et al., 1989) and in the North Atlantic (Martin, 1993). A previous profile of cobalt at near Bermuda showed neither surface depletion or surface enrichment; however the authors noted that their values were below the working precision range of their protocol (Jickells and Burton, 1988). Other cobalt profiles from the coastal northeast Pacific, the Mediterranean Sea, and the Philippine Sea have shown low concentrations with surface maxima from aeolian input (Knauer et al., 1982; Vega and Berg, 1997; Wong et al., 1995).

The purpose of this work was to address the sensitivity of cobalt concentrations in the Sargasso to atmospheric inputs relative to riverine and shelf inputs. Using both time series measurements from the Bermuda Atlantic Time Series station and transect data we discuss the importance of shelf and aeolian dust input functions and the residence time of cobalt in the western Atlantic Ocean. In addition, the possibility of upwelling as a source of cobalt is discussed in the context of a transect from the south Atlantic with cobalt, phosphate, salinity, and temperature data. Given the importance of cobalt and other trace metals like Fe, Cd, and Zn as micronutrients to marine phytoplankton, understanding the input function and residence times of these elements is important in understanding how these trace elements influence primary productivity in surface waters.

Methods

Sample collection and storage

Seawater samples were collected for a profile at the Bermuda Atlantic Time Series (BATS, 31.79°N, 64.26°W) and a surface transect (15m depth) between the Sargasso Sea and coastal waters off New England using acid-cleaned 10L Go-Flo bottles, kevlar hydrowire, and positive pressure clean-van. Seawater was pumped into the van with 0.2 μm filtered N_2 gas and teflon tubing, and was immediately filtered through acid-cleaned 0.2 μm nuclepore polycarbonate filters into teflon bottles. All labware was cleaned with overnight soaking in citranox detergent, a 2d 1M HCl (Baker Instra-analyzed grade) soak at 60°C, followed by rinsing and soaking at pH 2 in Ultrex II HCl

(Baker). Samples were kept at 4°C and in darkness until analysis within one month of collection. These samples were not acidified in order to minimize artifacts caused by acidification and subsequent neutralization. The strong correlation of samples with salinity suggests that substituting refrigeration for acidification in filtered samples was an effective means to avoid loss of cobalt due to wall loss or precipitation.

Seawater samples for time-series analysis were collected using the MITESS automated trace metal sampler (Moored *in-situ* Trace Element Serial Sampler) at the Bermuda Testbed Mooring³ near Bermuda in the Atlantic (31° 41.57' N, 64° 09.04' W). The MITESS sampler was deployed at a depth of 40-47m throughout 1999, and 10m samples were collected during retrieval of the mooring. These samples were collected unfiltered and were preserved at the time of collection with triple distilled HCl (distilled in a vycor still) to pH ~2.5.

Seawater samples from the south Atlantic transect were collected with a clean water pumping system, pumped into a clean hood and filtered through a 0.2µm filter prior to storage in polyethylene bottles. Samples were stored and analyzed at ambient seawater pH, except for four samples that were acidified to pH 2 (1M HCl, Baker Ultrex II) prior to UV-irradiation and neutralized to pH 8 (0.1M NaOH, Alfa Aesar metals basis) for analysis.

Analytical methodology

We utilized an electrochemical method known as cathodic stripping voltammetry (CSV) to make low-level cobalt analyses. Previous work has shown this method to be sufficiently sensitive for oceanic cobalt measurements (Bobrowski, 1989; Bobrowski, 1990; Bobrowski and Bond, 1992; Bond et al., 1978; Donat and Bruland, 1988; Herrera-Melian et al., 1994; Vega and Berg, 1997). An Eco-Chemie µAutolab system with a Metrohm 663 hanging mercury electrode was operated at 10V/sec scan rates in linear

³ For more information and data see the Bermuda Testbed Mooring website:

<http://www.opl.ucsb.edu/btm.html>

sweep mode between -0.6V to -1.4V. Prior to the scan a -0.6V deposition potential was applied to seawater sample for 90sec, followed by a 10sec equilibration period. All samples were purged for 3min with 99.999% filtered N₂ gas prior to analysis. Drop size was 0.52mm² and stirrer speed was set at 5. A sample size of 8.5mL was pipetted into the teflon sample cup to which reagents were then added.

Dimethylglyoxime (DMG) from Aldrich was recrystallized in 10⁻³M EDTA (Sigma Ultra) dissolved in Milli-Q water to remove impurities, dried and redissolved in HPLC grade methanol at a concentration of 0.1M. EPPS buffer reagent was prepared at 0.5M and pH 8.0. Sodium nitrite was prepared to 1.5M concentration by dissolution in Milli-Q water. The cobalt blank was greatly reduced in the EPPS buffer and nitrite reagent by treating with pretreated chelex-100 beads (Bio-Rad) as described by Price et al. (1988/1989) for a few minutes and overnight, respectively. Final concentrations of DMG, EPPS, and nitrite in the sample cup were 0.5mM, 2.5mM and 0.15M, respectively. Cobalt stock solutions for standard additions were prepared from a cobalt nitrite certified stock solution (Fisher) and diluted in polymethylpentene volumetric flasks for 25pM increment standard additions.

Samples were irradiated with ultraviolet light for 3.0 ± 0.1 h in quartz tubes to degrade organic complexes of metals. Irradiation times of this length have been shown to be sufficient to degrade organic complexes of cobalt without measurable losses of cobalt due to oxidation to Co(III) and subsequent precipitation (Vega and Berg, 1997). The acidified time series samples were pH adjusted to pH 7.5 to 8.5 between 2 and 24h after irradiation using 0.1M NaOH (Alfa Aesar metals basis). This dilute base concentration was utilized to prevent the precipitation of Mg(OH)_{2(s)} that appears upon addition of 1.0M NaOH. Blanks for HCl and NaOH were determined and subtracted from total metal calculations (not detectable and 9pM/mL respectively). MITESS samples were UV-irradiated while acidified, then neutralized to pH 8 prior to analysis. Four samples from the mooring were run in duplicate to determine precision.

To measure the analytical blank, cobalt-free seawater was created by UV-SSW, followed by equilibration with pre-treated chelex-100 resin beads (Bio-Rad) (Price et al.,

1988/1989). This seawater was then UV-irradiated again to degrade any diamino acid groups that were released from the chelex. We observed this last step to be important at these low picomolar Co levels, despite the rigorous protocol used to prepare the chelex.

Accuracy and Precision

The accuracy and precision of our analytical methodology was checked with CASS-3 Coastal Seawater Reference material and NASS-5 (National Research Council Canada-Institute for National Measurements). The CASS-3 seawater was diluted with Milli-Q water from 700 ± 150 pM to 310 ± 69 pM (error is standard deviation of four different analytical techniques), and NASS-5 was analyzed without dilution. The reference materials were UV irradiated for 3.0h in covered quartz vessels, then transferred to LDPE bottles and the pH was raised to between 7.5 and 9 using NaOH.

Cell numbers of *Prochlorococcus* and *Synechococcus* were determined using flow cytometry on modified FACScan (Dusenberry and Frankel, 1994). Samples were frozen and stored in liquid nitrogen after preservation in 0.125% glutaraldehyde. Samples were thawed at 35°C for 3min prior to analysis and run immediately thereafter.

Low-level phosphate measurements were made on samples from the south Atlantic transect using the method of Thomson-Bulldis and Karl (Thomson-Bulldis, 1998).

Results and Discussion

A pe-pH (Pourbaix) stability diagram (Figure 1) was calculated using constants from Table 1 (Martell and Smith, 1977; Stumm and Morgan, 1996). Sulfate and sulfide species were omitted for the purpose of exploring the geochemistry of cobalt in oxic seawater. At equilibrium with the O_2/H_2O redox couple, inorganic cobalt is close to the boundary line between $Co(II)Cl^-$ and $Co(III)(OH)_{3(s)}$. At the pe of 12.5 with 0.21 atm O_2 and a seawater pH of 8.1, the predominant inorganic cobalt species is $CoCl^-$. This is close to the pe value of 14.8 where the cobalt is equally distributed between $Co(OH)_{3(s)}$ and $CoCl^-$ at pH 8.1. These calculations define the species of cobalt that should exist in

seawater, assuming equilibrium between redox states. However, this is a simplified representation of cobalt in seawater: complexation chemistry with organic complexes or adsorption onto surfaces (e.g. MnO_2) would change the diagram significantly. For example, in a laboratory study with Co(III)-acacen complexes⁴, increasing the electron donating capacity of the axial ligands was shown to lower the energy required to reduce the Co(III) center (Bottcher et al., 1997). While we have electrochemical evidence showing the binding of cobalt to strong organic complexes (Chapter 2), we know little about the redox behavior of Co those complexes at this time.

We were concerned that addition of NaOH base to neutralize the acid preservative prior to analysis might reduce the recovery of cobalt due to scavenging by $\text{Mg}(\text{OH})_{2(s)}$ precipitates. Precipitates formed when neutralizing the pH 2.5 seawater samples with additions of 1M NaOH and disappeared after several hours. We decreased the concentration of base as a precaution to 0.1M NaOH to avoid this problem. A test of the recovery of cobalt during acidification and neutralization showed complete recovery of cobalt ($98.9\% \pm 3.2\%$) using this protocol (Figure 2).

BATS Profile

A profile of total dissolved cobalt at the BATS (Figure 3) station in September 1999 is shown in Figure 4. This profile exhibits nutrient-like behavior with surface depletion of cobalt. Of the few profiles of cobalt in the Atlantic, there has been only one previously reported nutrient-like profile (Martin et al., 1993). The rare observation of such phenomena could possibly be due to their sporadic occurrence, or to detection limit problems (Jickells and Burton, 1988). Comparing this profile with those generated by Martin et al. in the northeast Pacific (1988)(Figure 4), we do not see the large increase in deepwater concentrations between the Atlantic and Pacific that we do for other bioactive trace elements like cadmium and zinc. In these environments, cobalt's geochemistry is similar to that of iron with the potential for oxidation to an insoluble form and subsequent scavenging by particles. Martin argued that the mid-depth maximum in cobalt at this

⁴ acacen=N,N'-Ethylenebis(acetylacetylidenimine)

northeast Pacific station was due to regeneration of sinking material and advective transport through the oxygen minimum zone (Martin, 1985). With the co-precipitation of cobalt with manganese oxides in marine environments (Murray and Dillard, 1979; Tebo, 1984), scavenged cobalt could be released upon dissolution of those particles as they pass through the oxygen minimum zone. In contrast to the northeast Pacific, we do not see a mid-depth maximum of cobalt in the Sargasso Sea. Here, removal of cobalt by co-precipitation with manganese oxides is an insignificant process relative to phytoplankton uptake (Moffett and Ho, 1996); moreover, the low productivity of surface waters as well as the highly ventilated intermediate waters in the Sargasso Sea results in an oxygen minimum zone that does not reach the sub-oxic chemical conditions required to dissolve sinking manganese oxides. Under these conditions we might expect regeneration of cobalt from organic particles to dominate over manganese oxide dissolution, resulting in a more gradual regeneration of cobalt with depth in the profile.

BATS - Shelf transect

We collected samples from 15m depth along a transect from the BATS station to the Bermuda Rise and towards the shelf region off of Massachusetts (Figures 3 and 5). The total cobalt in these samples correlated tightly with salinity ($r^2=0.93$), similar to the measurements of Mn, Ni, Cu, Zn and Cd made by Bruland and Franks (1983) on a similar transect. Extrapolation of the slope of the salinity-metal regression to zero salinity provides an estimate of what river water concentration should be if mixing were completely conservative (Table 2). The calculated zero-salinity end member for cobalt had a value of 0.785nM. This value is close to or lower than what might be expected for river water. Moreover, the ratio between the zero-salinity end member and the open ocean is 41, significantly lower than the 270 and 550 values of Zn and Cd, respectively. Given the potential oxidation of cobalt to insoluble cobalt(III) phases it is surprising that these end member ratios, which are dependent on the slope of the regressions, are lower for cobalt than for Zn and Cd. With the longer residence times of Zn and Cd (Table 3) we might expect their decrease from coastal waters to be less than that of cobalt.

However, the high-end member ratios for Zn and Cd are likely related to the strong effect of biological drawdown in the surface waters.

Flow cytometry data of the picoplankton community showed a dominance of *Prochlorococcus* until slope waters (Figure 6). *Synechococcus* was found in the oligotrophic regions of the transect and increased in slope waters. There was a third population of picoeukaryotes that increased in cell number near slope waters. Both *Prochlorococcus* and *Synechococcus* are known to have absolute requirements for cobalt that zinc cannot substitute for (Chapter 4 and Sunda and Huntsman, 1995 respectively). However, the distribution of *Prochlorococcus* in the oceans is thought to be primarily controlled by temperature (Cavender-Bares et al., 1999).

MITESS - Total Cobalt Time Series

Time Series samples from the MITESS trace metal water sampler were measured with biweekly resolution for 1999 (Figure 7). All samples were less than 50pM in total cobalt with a mean of 20 ± 9.8 pM excluding duplicate analyses. The data do not show an obvious seasonal pattern that would be expected with atmospheric dust input. For comparison, Al in surface waters showed a 3-5 fold increase between June-August in 1981-1983 (Jickells et al., 1990) relative to the rest of the year. We do observe several fold oscillations in the data set that are analytically reproducible (replicate samples were analyzed for three of the low values, see Table 9). However, the pronounced seasonal effect that Jickells et al. observed with Al from aeolian input maybe not be apparent due to the mooring's location below a shallow thermocline.

Temperature data from the mooring at 14-15m and 34-35m shows the formation of a seasonal thermocline and significant warming of both depths through the summer (Figure 8). There was a decreasing trend in cobalt concentration between Julian day 150 and 267 which might be related to this thermocline formation, followed by a rapid increase with mixing of the surface waters after day 267. The thermocline structure separated the surface waters and their aeolian inputs from the mooring sampler at 43-

44m, resulting in a decrease when cobalt is not replenished from aeolian input.

Moreover, several of the sharp decreases in cobalt concentration occur during periods when the thermocline becomes shallower (days 138, 186, and 267). This could result from cold core eddies causing upwelling of nutrients followed by an enhanced biological drawdown of cobalt with the higher productivity (McGillicuddy and Robinson, 1997; McGillicuddy et al., 1998).

The notion that dust is an important source of trace elements to the oceans is based on the relative contribution of atmospheric input to dissolved riverine input. Estimated ratios of aeolian input to dissolved riverine input for Pb, Cd, Cu, Ni, Zn, As, and Fe are 40, 11, 4.5, 1, 28, 0.5, and 2.9, respectively (Duce et al., 1991). Interestingly, aeolian input consists of particulate and dissolved components, and the dissolved fraction exceeded that of the particulate fraction for all of these metals but iron in this study. The dissolved riverine value used to calculate these ratios is based on the assumption that no particulate matter from rivers would remain upon transport to the open ocean. Based on these ratios, the aeolian input is at most 1-2 orders of magnitude larger than to dissolved riverine input, and often can be comparable to the riverine flux (e.g., Ni). Unfortunately, Duce et al. did not include cobalt in their review of atmospheric deposition; however, we can use the crustal abundance of cobalt (0.0012%)(Taylor and McLennan, 1985). In comparison, the crustal abundance of Fe is 3.1% and the Fe:Co ratio in dust is 2600:1. With seawater abundances of Fe in the 0.4 - 2nM range the predicted cobalt concentration based solely on crustal abundance would be 0.12 to 0.8pM, far lower than the annual average 20pM measured at BATS. This suggests slower removal mechanisms than iron, increased solubility of cobalt from dust relative to iron, or the importance of other input sources such as shelf water input.

South Atlantic Transect

An west-east surface transect across the south Atlantic in November and December of 1998 (5m depth, Figure 9, Table 7) showed quite high cobalt concentrations on each end while the center of the transect had low cobalt, low salinity and high

temperature (Figure 10). This central part of the transect is thought to correspond to the Intertropical Convergence Zone where high precipitation and warm temperatures isolate the surface water masses (A. Fischer, pers. comm.). Interestingly, the pattern of total cobalt distribution on this transect corresponds to that of phosphate, and the correlation between these two elements suggests that as both are drawn down, cobalt will be depleted first in this region (Figure 11). Of note is the large cobalt and phosphate peak at transect point 2: cell number counts at this site also showed a high concentration of coccolithophores cells (M. Conte, pers. comm.).

An analysis of the data collected by Martin et al., (1988) by Sunda and Huntsman (1995) showed a strong correlation between zinc and phosphorus (see Figure 2, Chapter 1) until zinc was depleted, at which point cobalt and phosphate begin to correlate. This phenomenon is suggestive of substitution of cobalt for zinc in the northeast Pacific. In the south Atlantic, we can speculate that the biological demand for cobalt might be more intense relative to that of the Pacific due to the lack of zinc-rich deep waters, and hence a smaller zinc supply from vertical diffusion and advection processes. Following this logic, organisms that can substitute cobalt for zinc may need to make the switch more frequently as zinc becomes depleted. However, on the south Atlantic transect, the surface waters are oligotrophic unlike the high nutrient waters of the NE Pacific, with concentrations of phosphate in the low nanomolar range instead of micromolar. A comparison of the slope ($\Delta\text{Co}/\Delta\text{P}$) of the Co versus PO_4 plot with data from the northeast Pacific (Table 4) shows that south Atlantic cobalt uptake relative to phosphate uptake is more than an order of magnitude higher than of the northeast Pacific. This high value of $\Delta\text{Co}/\Delta\text{P}$ ($560 \mu\text{mol}/\text{mol}^{-1}$) in the south Atlantic is similar to that of $\Delta\text{Zn}/\Delta\text{P}$ in the northeast Pacific (251, 370 and $254 \mu\text{mol}/\text{mol}^{-1}$), suggestive of an increased biological importance of cobalt relative to zinc in this region⁵. However, the particulate Co, Cd, and

⁵ Cobalt and phosphate data from the North Atlantic (Martin et al., 1993) were examined to see if this relationship between two elements was apparent. No significant correlation was observed for Co and P; however, a correlation between Zn and P was observed in two profiles ($r^2=0.94, 0.67$) with $\Delta\text{Zn}/\Delta\text{P}$ values of 1950 and $1680 \mu\text{mol}/\text{mol}^{-1}$, compared with $\Delta\text{Zn}/\Delta\text{P}$ values of 251-370 $\mu\text{mol}/\text{mol}^{-1}$ in the Northeast Pacific. These calculations suggest the North Atlantic community is using zinc relative to cobalt, and that

Zn profiles by Sherrell and Boyle show a depletion in Co:C and Zn:C in surface waters (Figure 12). These values are similar to the surface particulate metal:carbon and metal:P ratios reported by Kuss and Kremling (1999) (Co:C 1.1 $\mu\text{mol/mol}$, Co:P 190 $\mu\text{mol/mol}$).

In addition, the south Atlantic Co:P ratio in seawater ($\sim 500 \mu\text{mol/mol}^{-1}$) is at the upper end of the range of Co:P ratios in phytoplankton (8.5 to 1200 $\mu\text{mol/mol}^{-1}$; Table 6-4, Sunda and Huntsman, 1995).

Residence Time Calculations

Residence times are calculated by dividing the seawater inventory by either the input or output to the ocean. Despite the simplicity of the equation, obtaining values for these global parameters is difficult. Several residence time calculations have been made for cobalt in the ocean. An early estimate of $\sim 1000\text{y}$ was proposed in 1977 (Bewers and Yeats, 1977). Knauer et al. calculated a whole ocean residence time estimate for cobalt of 52y using stream input data and 43y using sedimentation rate data (Knauer et al., 1982). Lacking any open ocean cobalt concentration data, these authors utilized a 17pM estimate of world cobalt concentrations based on a prediction using Mn:Co ratios in coastal waters. Taylor et al., also used a seawater estimate of 17pM and calculated a residence time of 40y based on cobalt abundance in pelagic clays and estimates of sedimentation rates (Taylor and McLennen, 1985). These seawater estimates of cobalt concentration are quite close to the 20pM annual average for BATS that we report here. Without further revision of the input or output flux terms of cobalt, our annual average cobalt concentration provides a minor correction of the Taylor et al. residence time to 47y.

Residence times in the upper 100m surface waters for dissolved scavenged-type metals Al and Fe have been calculated to be 1660-4750d and 214-291d, respectively (Jickells, 1999). These calculations were based on measured solubilities of Al and Fe in dust. While we are unaware of any dust solubility measurements for cobalt, we can

it is obtaining a higher Zn:P quota in the North Atlantic than the North Pacific. No zinc data are available from the South Atlantic transect for comparison.

calculate a surface water residence time using a range of possible values. Using the 2600 Fe:Co ratio in continental crust abundance ratio and atmospheric iron input estimates from Jickells (1999) we can estimate the Co flux by dust deposition to the Sargasso Sea to be $0.0016 \mu\text{M m}^{-2} \text{ d}^{-1}$, yielding a residence time of 3.4 to 34y using an estimated dust solubility range of 100% to 10%, respectively.

We can also calculate a surface residence time using the flux of carbon export as new production. With cobalt:carbon (Co:C) ratios in particulate matter calculated from Sherrell and Boyle (1992, see Table 5) and new production at BATS estimated at $0.7 - 4.2 \text{ mol C m}^{-2} \text{ y}^{-1}$ and assuming no preferential release of cobalt from the exported carbon, we can estimate the flux of cobalt from the water column. Using our 20pM inventory in the upper 100m of the water column yields an upper 100m residence time of 0.32-1.9y. This value uses the surface water Co:C ratio; however, the >300m depth Co:C ratio is ~10 fold higher than in surface waters (Table 5, Figure 12). If these deepwater Co:C values are used, the residence time would be significantly shorter (8.5 - 50d). One scenario that could explain this is that export is primarily associated with larger phytoplankton and has a higher cobalt quota, whereas the microbial loop community, not thought to contribute significantly to new production, subsists on a significantly smaller Co:C quota.

The discrepancy between the 100m surface residence time estimates using estimated dust input (3.4 to 34y) and the deep water particulate matter (8.5 - 50d) is significant. Even with the conservative range of solubilities for cobalt that we utilize (10-100%) the difference in residence times is 24 to 1400 fold. This disparity may be caused by an underestimate of the input fluxes to the surface waters. The residence time calculation above that is based on input flux assumes that aeolian dust input is the only significant input mechanism to the Sargasso Sea. However, if the flux of upwelled and horizontally advected dissolved cobalt is comparable to the dust flux, and this flux were included in the calculation, the residence time estimate would decrease significantly.

In laboratory experiments with phytoplankton species, Co cellular quotas have been measured that can span almost two orders of magnitude (from $0.3 - 11 \mu\text{mol Co /}$

mol C) depending on the Co concentration in the culture media (Sunda and Huntsman, 1995). These large cellular quota ranges for metals can often occur in a single phytoplankton species with the variability reflecting a physiological adjustment rather than experimental variability. The particulate Co:C ratios measured by Sherrell and Boyle are within the range of these laboratory cellular quotas. Upper water column residence time calculations for cobalt, now based on cellular quota data instead of particulate Co measurements suggest that the potential range of biological demand for cobalt would result in a 100m surface water residence time between 10y to as short as 16d.

These residence time estimates using either particulate Co values or laboratory cellular quota data show that the biological uptake and removal of Co from the Sargasso has the potential to cause a turnover of the Co reservoir in surface waters on timescales of less than a year. In order to avoid depleting the Co reservoir, a logical strategy for phytoplankton would be to reduce their cellular quota, and thereby adapt to the low Co environment.

Future directions

While these and other data sets allow us to comment and speculate on the nature of cobalt's oceanic biogeochemistry, we are clearly still data limited. Of particular priority for future studies will be high-quality data sets from the Atlantic that include Co, Zn, Cd, and coupled with the new methodology for low-level nutrient analyses needed for the vast oligotrophic regions of the Atlantic. Such data sets would help us gain an understanding of their relative importance of Co, Zn, and Cd in primary productivity.

Conclusions

Cobalt is a trace element that exhibits characteristics of both scavenged-type and nutrient-type categories of trace metals. Thermodynamic calculations suggest that it could be oxidized relatively easily to its insoluble Co(III) form, and indeed the microbial manganese oxidation pathway has been shown to oxidize cobalt in coastal waters but not

in the open ocean. As a result of these chemical properties, the few deepwater measurements of cobalt suggest that it does not accumulate in the deep ocean with thermohaline circulation as do non-scavenged nutrient-type elements. However, surface water depletion of cobalt has now been observed in the Pacific and Atlantic; suggesting that like iron, its biological utility can result in this nutrient-type feature. Calculations of the residence times of scavenged-type metals show very short residence times in the tens of years. Upper 100m water column residence time calculations for cobalt, based on the cobalt time series data and particulate cobalt from Sherrell and Boyle (1993), yield residence times as low as 8.5-50d. This result is suggestive of adaptation for a low cobalt environment by the biota.

Our transect and time-series data for cobalt in the Western North Atlantic show two surprising features. First, despite its typical characterization as a scavenged-type element, there is a strong correlation between salinity and cobalt in the slope/shelf waters implying that mixing from coastal waters is an important input mechanism for cobalt. Second, the biweekly time-series data do not show the type of atmospheric deposition induced increases that are apparent in elements such as aluminum and iron. With measurements of cobalt at the BTM mooring consistently less than 50pM and with an annual average of $20\text{pM} \pm 10\text{pM}$, our data suggests that unlike aluminum with its aeolian dust source, upwelling and coastal fluxes may also be important to the input flux of cobalt to the Sargasso Sea.

Acknowledgements

I would like to acknowledge Ed Boyle and Rick Kayser for the samples from the MITESS sampler and helpful discussions. Special thanks to J.C. Weber and Maureen Conte for collecting the S. Atlantic samples and analyzing the low-level phosphorus data. The Ocean Physics Lab at UCSB and the Bermuda Testbed Mooring Program were generous in sharing temperature data from their mooring. Also thanks to Kathy Barbeau and Christie Hauptert for assisting in the collection of the N. Atlantic transect and profile. The captain and crew of the R/V Oceanus were of great assistance in our seagoing work.

References

- Bewers, J.M. and Yeats, P.A., 1977. Oceanic residence times of trace metals. *Nature*, 268: 595-598.
- Bobrowski, A., 1989. Polarographic Methods for Ultratrace Cobalt Determination Based on Adsorption-Catalytic Effects in Cobalt(II)-Dioxime-Nitrite Systems. *Anal. Chem.*, 61: 2178-2184.
- Bobrowski, A., 1990. Determination of Cobalt by Adsorptive Stripping Voltammetry Using Cobalt(II)-nioxime-nitrite Catalytic System. *Anal. Let.*, 23: 1487-1503.
- Bobrowski, A. and Bond, A., 1992. Exploitation of the Nitrite Catalytic Effect to Enhance the Sensitivity and Selectivity of the Adsorptive Stripping Voltammetric Method for the Determination of Cobalt with Dimethylglyoxime. *Electroanal.*, 4: 975-979.
- Bond, A.M., Keene, F.R., Rumble, N.W., Searle, G.H. and Snow, M.R., 1978. Polarographic Studies of the Geometric Isomers of the Bis(diethylenetriamine)cobalt(III) and -cobalt(II) Cations in Acetone. *Inorg. Chem.*, 17: 2847-2853.
- Bottcher, A., Takeuchi, T., Hardcastle, K.J., Meade, T.J. and Gray, H.B., 1997. Spectroscopy and Electrochemistry of Cobalt(III) Schiff Base Complexes. *Inorg. Chem.*, 36(12): 2498-2504.
- Boyle, E.A., D.F. Reid, S.S. Husted, and J. Hering. 1984. Trace metals and radium in the Gulf of Mexico: an evaluation of river and continental shelf sources. *Earth Planet. Sci. Lett.* 69. 69-87.
- Boyle, E.A., B. Handy, and A. van Geen. 1987. Cobalt Determination in Natural Waters Using Cation-Exchange Liquid Chromatography with Luminol Chemiluminescence Detection. *Anal. Chem.* 59. 1499-1503.
- Bruland, K.W. and Franks, R.P. (Editors), 1983. Mn, Ni, Cu, Zn and Cd in the western north Atlantic. Trace metals in seawater NATO Conf. Ser.4, 9. Plenum.
- Cavender-Bares, K.K., Mann, E.L., Chisholm, S.W., Ondrusek, M.E. and Bidigare, R.R., 1999. Differential Response of equatorial Pacific phytoplankton to iron fertilization. *Limnol. Oceanogr.*, 44(2): 237-246.
- Donat, J.R. and Bruland, K.W., 1988. Direct Determination of Dissolved Cobalt and Nickel in Seawater by differential Pulse Cathodic Stripping Voltammetry

- Preceded by Adsorptive Collection of Cyclohexane-1,2,-dione Dioxime Complexes. *Anal. Chem.*, 60: 240-244.
- Duce, R.A. et al., 1991. The Atmospheric Input of Trace Species to the World Ocean. *Glob. Biogeochem. Cycles*, 5(3): 193-259.
- Dusenberry, J.A. and Frankel, S.L., 1994. Increasing the sensitivity of a FACScan flow cytometer to study oceanic picoplankton. *Limnol. and Oceanogr.*, 39(1): 206-209.
- Herrera-Melian, J., Hernandez-Brito, J., Gelado-Caballero, M. and Perez-Pena, J., 1994. Direct determination of cobalt in unpurged oceanic seawater by high speed adsorptive cathodic stripping voltammetry. *Anal. Chim. Acta*, 299: 59-67.
- Jickells, T.D., 1999. The inputs of dust derived elements to the Sargasso Sea; a synthesis. *Mar. Chem.*, 68: 5-14.
- Jickells, T.D. and Burton, J.D., 1988. Cobalt, copper, manganese and nickel in the Sargasso Sea. *Mar. Chem.*, 23: 131-144.
- Jickells, T.D., Deuser, W.G. and Belostock, R.A., 1990. Temporal Variations in the Concentrations of some Particulate Elements in the Surface of the Sargasso Sea and their Relationship to Deep-Sea Fluxes. *Mar. Chem.*, 29: 203-219.
- Knauer, G.A., Martin, J.H. and Gordon, R.M., 1982. Cobalt in north-east Pacific waters. *Nature*, 297: 49-51.
- Kuss, J. and K. Kremling. 1999. Spatial variability of particle associated trace elements in near-surface waters of the North Atlantic (30°N/60°W to 60°N/2°W), derived by large volume sampling. *Mar. Chem.* 68. 71-86.
- Martell, A.E. and Smith, R.M., 1977. Critical Stability Constants, 3. Plenum Press, New York, 495 pp.
- Martin, J.F., SE; Gordon, RM; Hunter, CN; Tanner, SJ, 1993. Iron, primary production and carbon-nitrogen flux studies during the JGOFS North Atlantic Bloom Experiment. *Deep-Sea Res.*, 40(1-2): 115-134.
- Martin, J.H., 1985. Iron and Cobalt in NE Pacific Waters. *EOS*, 66(51): 1291.
- Martin, J.H. and Fitzwater, S.E., 1988. Iron deficiency limits phytoplankton growth in the north-east Pacific subarctic. *Nature*, 331: 341-343.
- Martin, J.H. and Gordon, R.M., 1988. Northeast Pacific iron distribution in relation to phytoplankton productivity. *Deep-Sea Res*, 35: 177-196.

- Martin, J.H., Gordon, R.M., Fitzwater, S. and Broenkow, W.W., 1989. VERTEX: phytoplankton/iron studies in the Gulf of Alaska. *Deep-Sea Res.*, 36(5): 649-680.
- McGillicuddy, D.J. and Robinson, A.R., 1997. Eddy-induced nutrient supply and new production in the Sargasso Sea. *Deep-Sea Res*, 44(8): 1427-1450.
- McGillicuddy, D.J., A.R. Robinson, D.A. Siegel, H.W. Jannasch, R. Johnson, T.D. Dickey, J. McNeil, A.F. Michaels, and A.H. Knap. 1998. Influence of mesoscale eddies on new production in the Sargasso Sea. *Nature*. 394. 263-266.
- Moffett, J.W. and Ho, J., 1996. Oxidation of cobalt and manganese in seawater via a common microbially catalyzed pathway. *Geochim. Cosmo. Acta*, 60(18): 3415-3424.
- Murray, J. and Dillard, J., 1979. The oxidation of cobalt(II) adsorbed on manganese dioxide. *Geochim. et Cosm. Acta*, 43: 781-787.
- Price, N.M. et al., 1988/1989. Preparation and chemistry of the artificial algal culture medium Aquil. *Biol. Oceanogr.*, 6: 443-461.
- Saito, M.A. and Moffett, J.W., 2000. Complexation of cobalt by natural organic ligands in the Sargasso Sea as determined by a new high-sensitivity electrochemical cobalt speciation method suitable for open ocean work. submitted.
- Sherrell, R.M. and E.A. Boyle. 1992. The trace metal composition of suspended particles in the oceanic water column near Bermuda. *Earth Planet Sci. Lett.* 111. 155-174.
- Stumm, W. and Morgan, J.J., 1996. Aquatic Chemistry: Chemical Equilibria and Rates in Natural Waters. John Wiley & Sons, Inc., New York, 1022 pp.
- Sunda, W.G. and Huntsman, S.A., 1995. Cobalt and Zinc interreplacement in marine phytoplankton: biological and geochemical implications. *Limnol. Oceanogr.*, 40: 1404-1417.
- Taylor, S.R. and McLennen, S.M., 1985. The Continental Crust: its Composition and Evolution. Geoscience Texts. Blackwell Scientific Publications, Boston.
- Tebo, B., Nealson, K., Emerson, S. and Jacobs, L., 1984. Microbial mediation of Mn(II) and Co(II) precipitation at the O₂/H₂ interfaces in two anoxic fjords. *Limnol. and Oceanogr.*, 29: 1247-1258.

- Thomson-Bulldis, A.K., D, 1998. Application of a novel method for phosphorus determinations in the oligotrophic North Pacific Ocean. *Limnol. Oceanogr.*, 43(7): 1565-1577.
- Vega, M. and van den Berg, C.M.G., 1997. Determination of Cobalt in Seawater by Catalytic Adsorptive Cathodic Stripping Voltammetry. *Anal. Chem.*, 69: 874-881.
- Wong, G., Pai, S.-C. and Chung, S.-W., 1995. Cobalt in the Western Philippine Sea. *Oceanol. Acta*, 18: 631-638.

Figure 3-1

pe-pH diagram for Cobalt in seawater showing redox states and solid phases. Total cobalt concentration of 100pM and chloride concentration of 0.545M were used. Sulfate/sulfide chemistry was omitted to focus attention on the redox state of cobalt in oxic seawater. The '*' symbol indicates ambient seawater pe and pH. Inorganic cobalt in seawater at thermodynamic equilibrium should exist as soluble CoCl^+ , but this species is quite close to oxidation to the $\text{CoCl}^+/\text{Co(III)(OH)}_2$ line. Presumably regions of oxygen supersaturation and high concentrations of other oxidants could result in the inorganic oxidation of Co(II) to Co(III). This diagram is a simplified representation of seawater in the absence of organic ligands. Since we know little about the redox properties of natural organic Co ligands, it is not possible to include them in the calculation of a redox equilibrium.

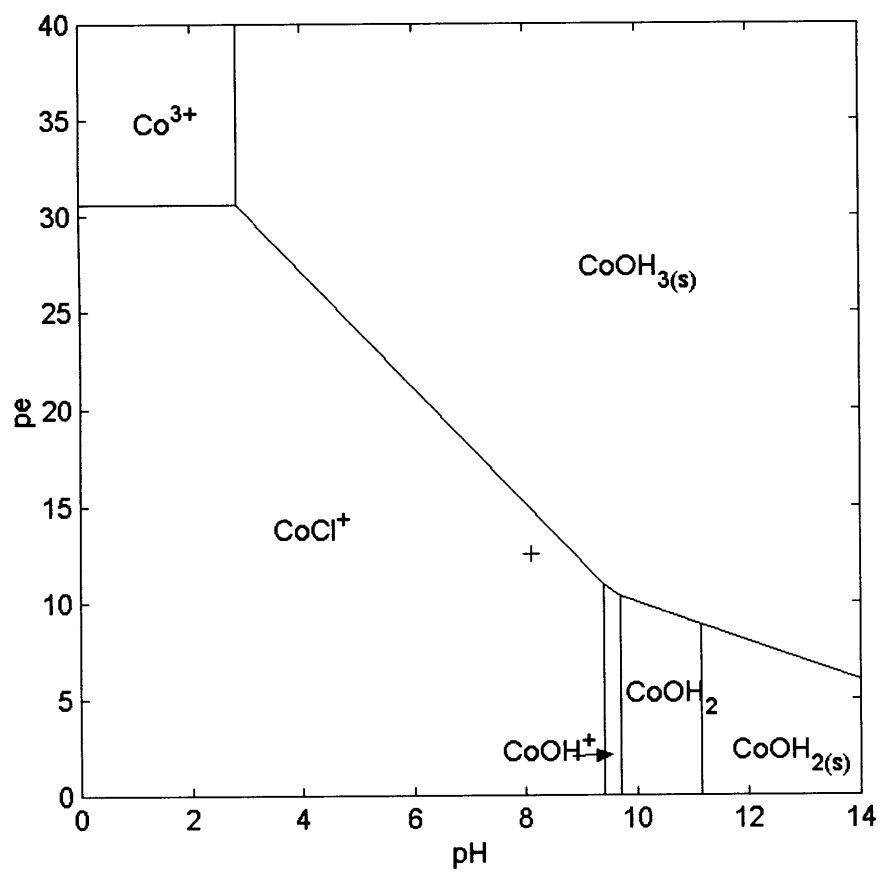


Figure 3-2

Method Development: Recovery with addition of base. Given the possibility of precipitation of carbonates and coprecipitation of cobalt with those phases during the addition of NaOH, we tested the recovery of cobalt from a sample where the pH was manipulated from pH 8 to 2 and back to 8 again using HCl and NaOH. The 0.1M NaOH used was dilute enough to avoid visible precipitation upon addition. Recovery was $98.9 \pm 3.2\%$ after subtraction of blank associated with the NaOH (6pM).

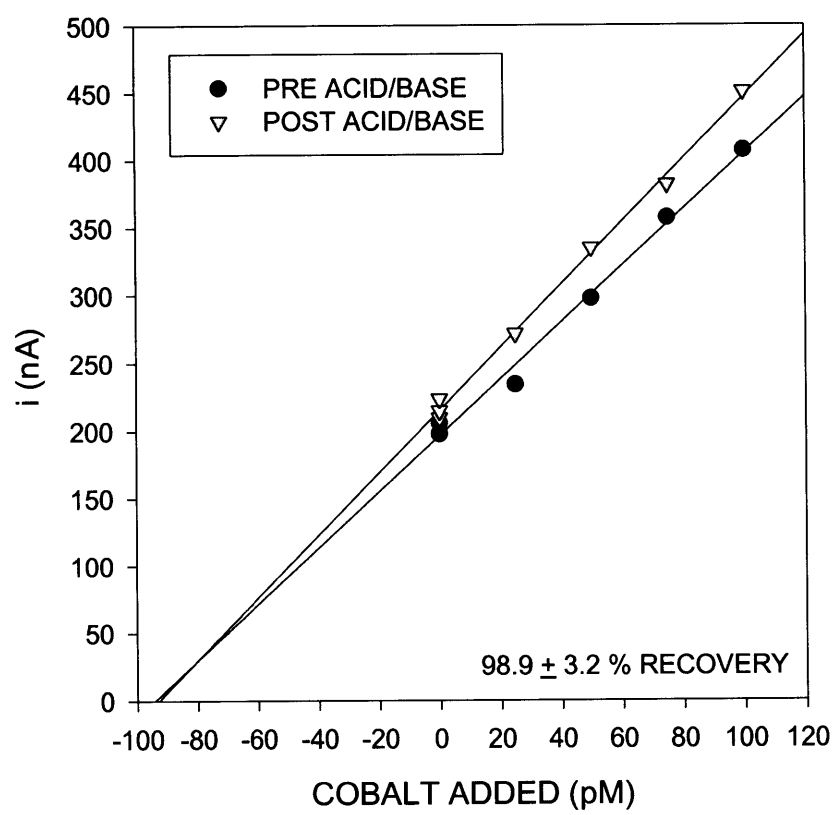


Figure 3-3

Cruise track of R/V Oceanus cruise 349 on a western North Atlantic transect in September-October 1999. Station (1) is the Bermuda Atlantic Time Series station.

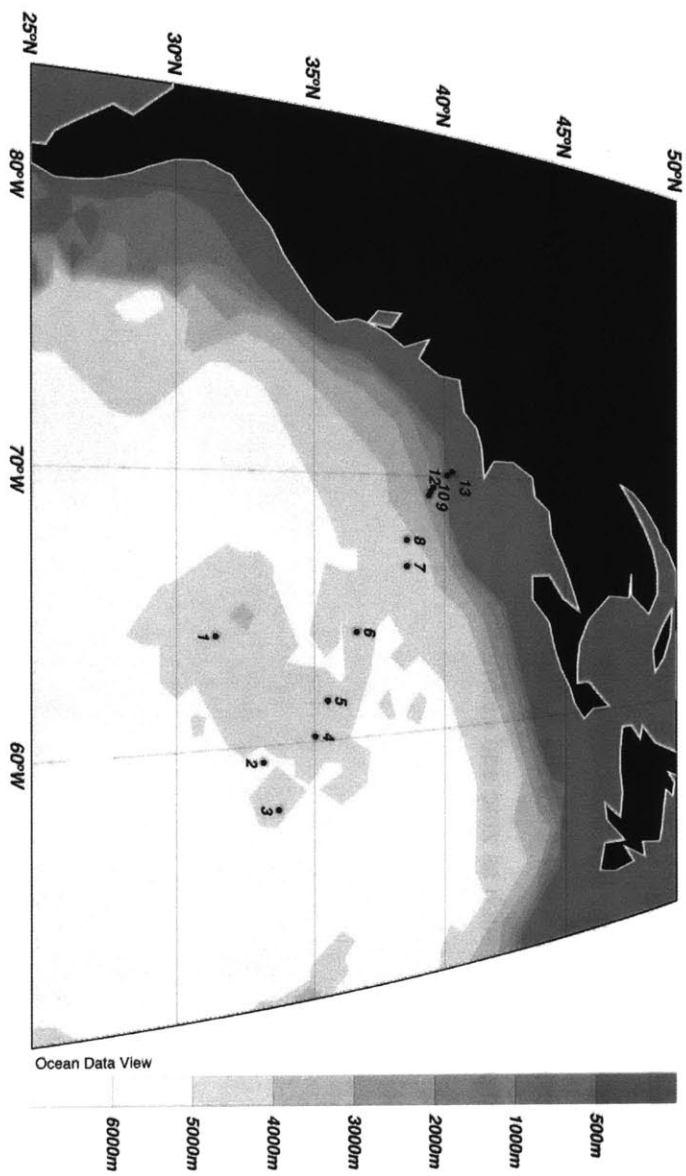


Figure 3-4

Comparison of total dissolved cobalt depth profiles from A) Sargasso Sea (BATS station September 1999, data from this study), B) the northeast Pacific from Martin et al. (Martin and Gordon, 1988), and C) the north Atlantic 47°N 20°W (Martin et al., 1993). All three profiles show nutrient-like behavior with surface depletion of cobalt, yet there is no enrichment in deep water from the Atlantic to the Pacific as is observed with non-scavenged metals such as zinc and cadmium.

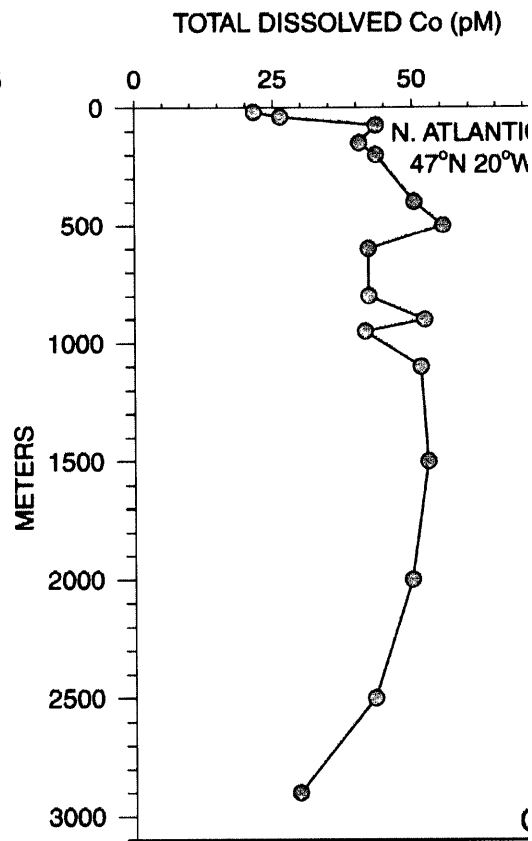
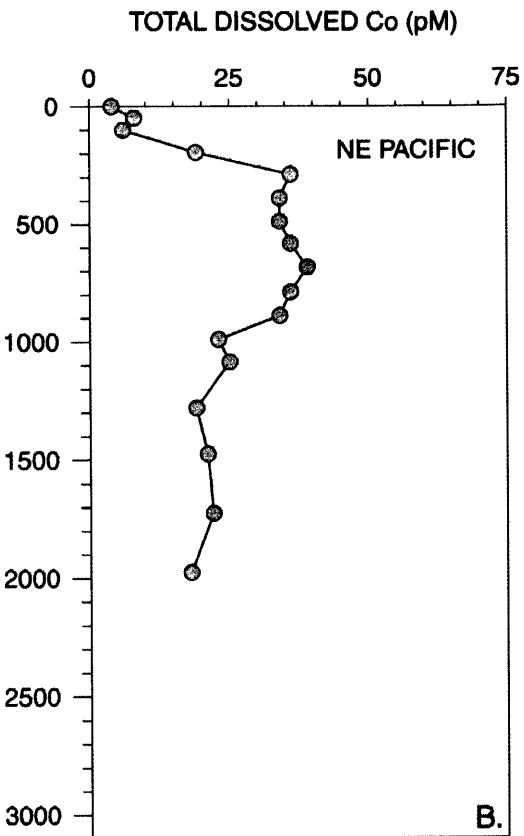
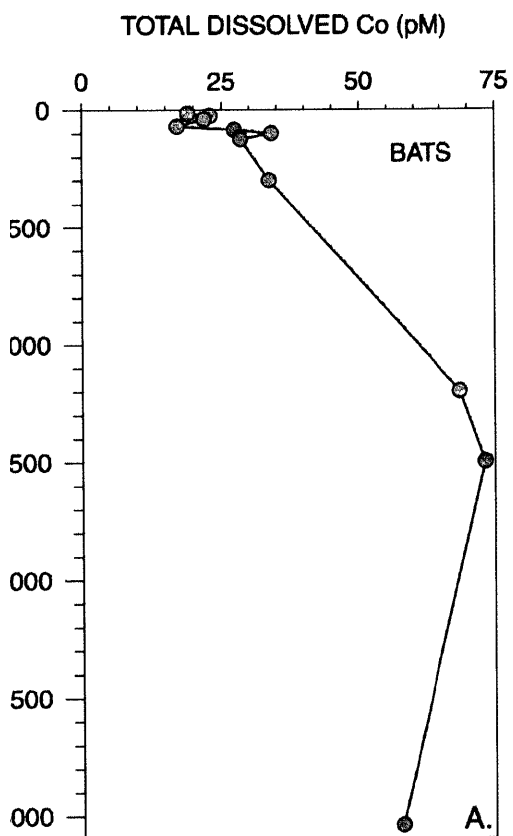


Figure 3-5

- A). Transect of Total Dissolved Cobalt from BATS to WHOI, via the Bermuda Rise (station 3) from the R/V Oceanus September, 1999. B). Temperature and Salinity data. C). An inverse correlation between salinity and cobalt was observed .

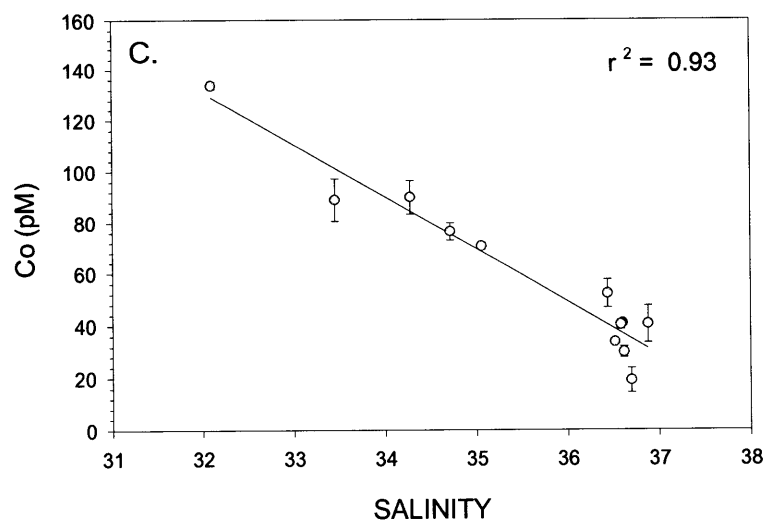
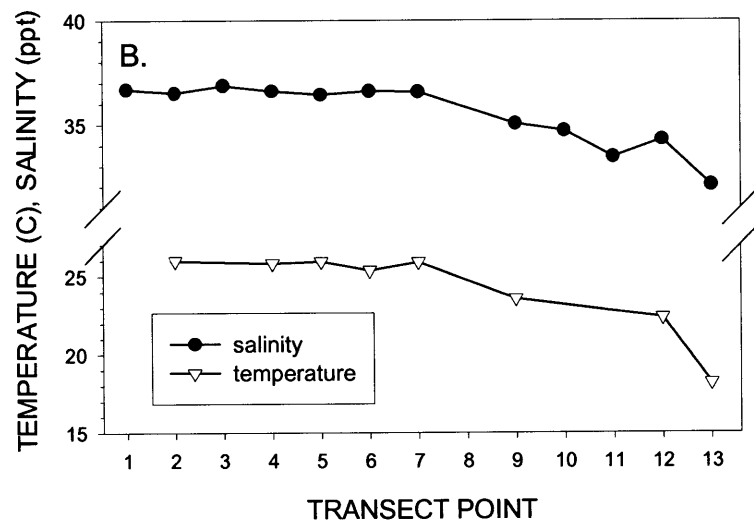
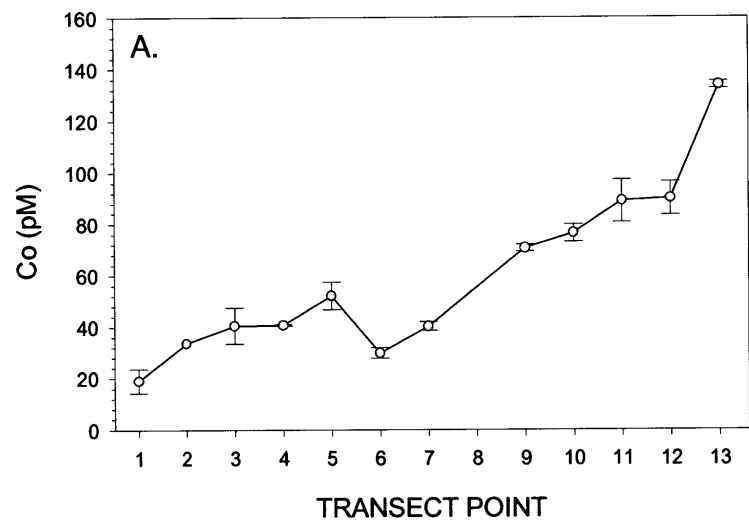


Figure 3-6

Distribution of *Prochlorococcus*, *Synechococcus*, and a population of larger cells (picoeukaryotes) along the western Atlantic transect, September-October 1999.

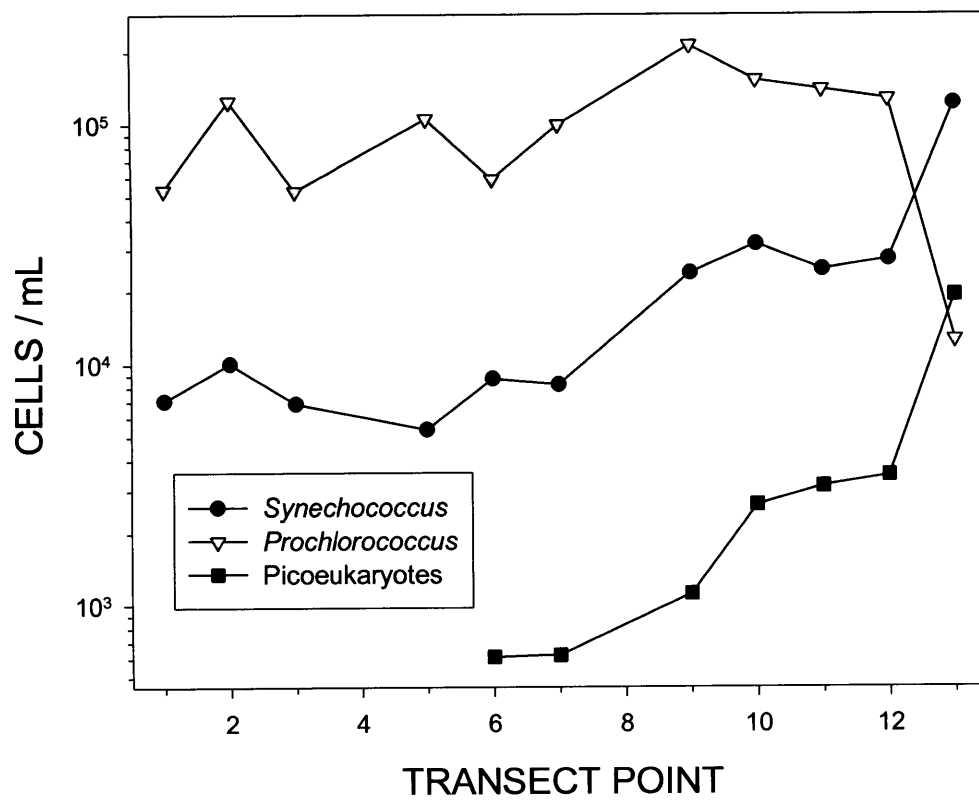


Figure 3-7

Time series cobalt data at the Bermuda Testbed Mooring. Samples were collected by automated trace metal sample collector (MITESS). Biweekly samples were analyzed from ~40m depth (see Table 9 for precise sample depth), and several 10m samples were collected upon retrieval of the mooring. Error bars represent the standard deviation of triplicate scans before standard additions on a sample. Several samples were analyzed twice (see Table 9), in which case both samples were plotted.

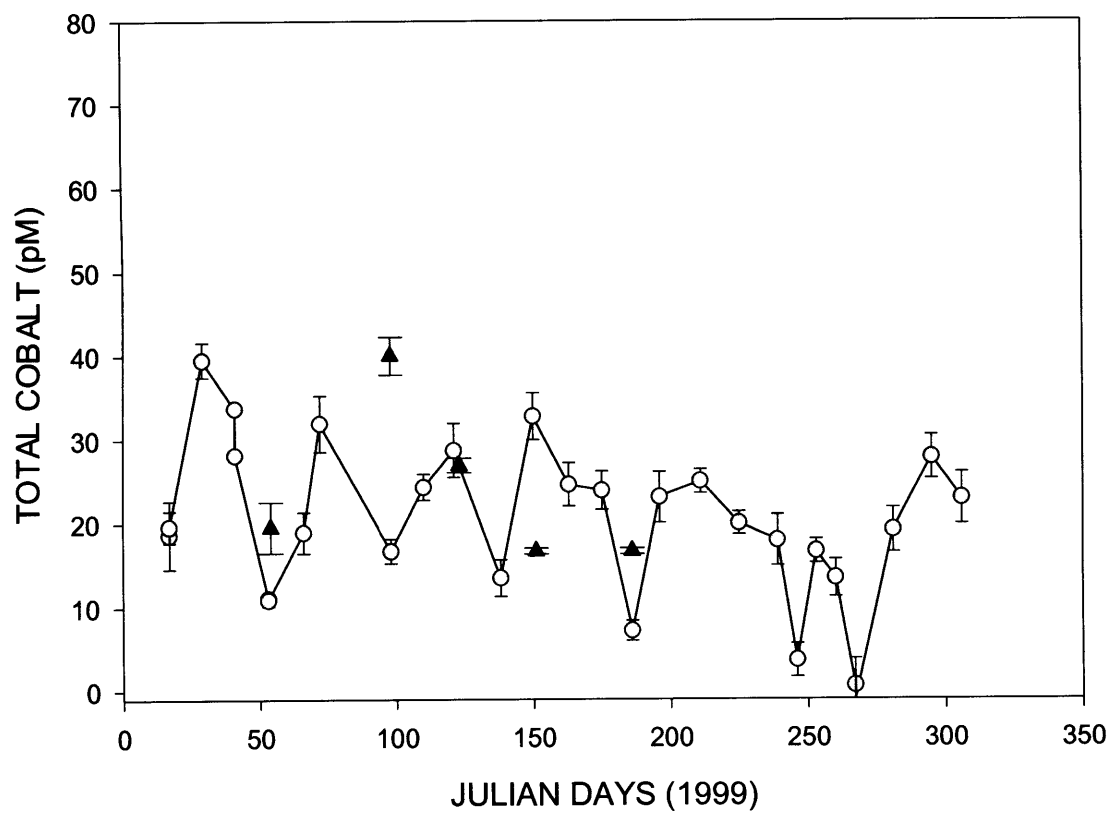


Figure 3-8

Water column stratification compared to the total cobalt data from 44-47m for (11/11/99 to 3/19/99) and 40-43m (remainder of 1999). Cobalt data is shown as open circles, except for several 10m samples shown as crosses. Temperature data at 14-15m (red line) and 34-35m depth (blue line) shows seasonal stratification with the 14-15m temperature measurements warming relative to the 34-35m. Vertical lines indicate simultaneous changes in cobalt concentration and temperature. We hypothesize that these sudden decreases in cobalt may be the result of higher productivity associated with nutrient input from mesoscale cold eddies or mixing events. Temperature data is from the Bermuda Testbed Mooring Project using TIDBIT instrumentation.

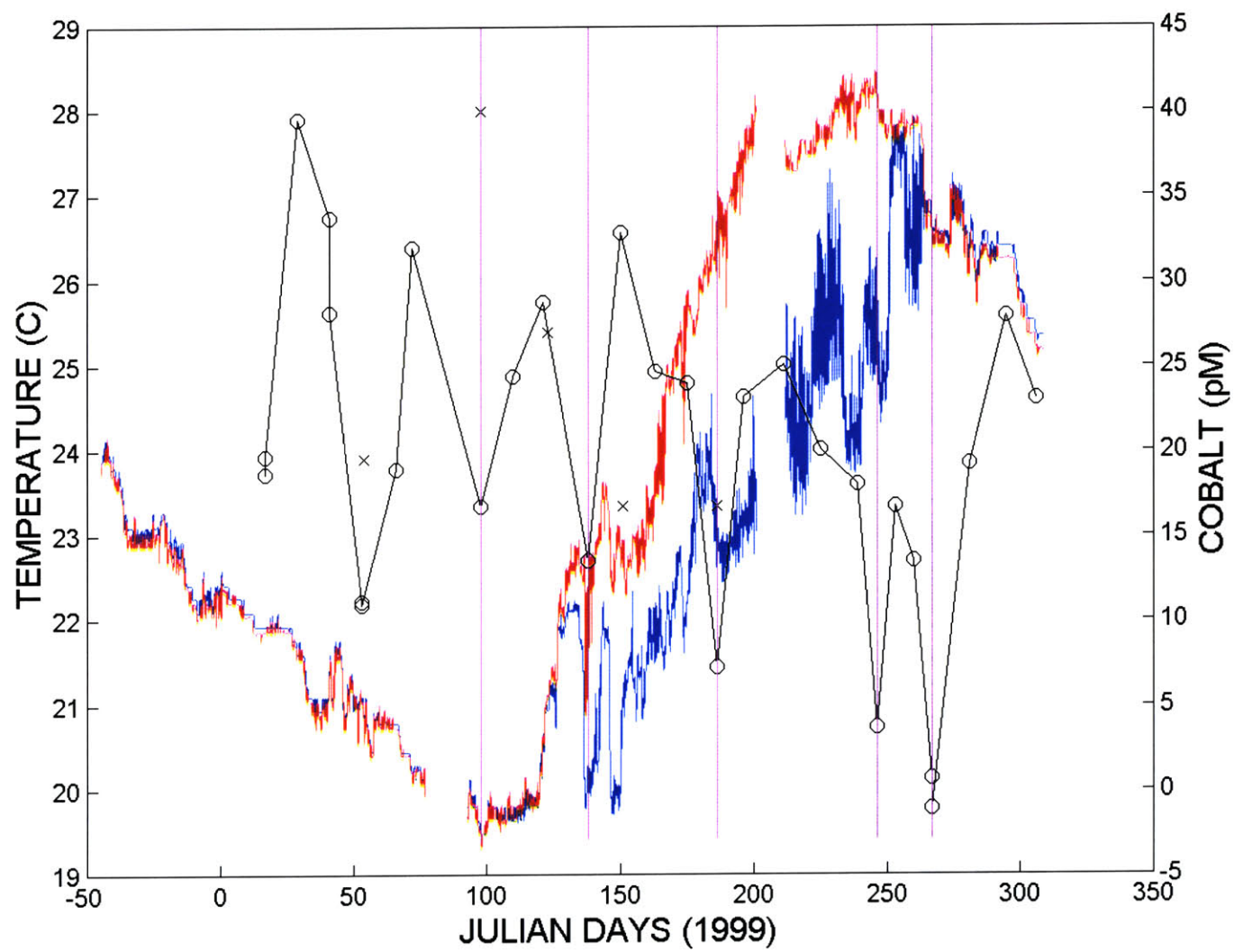


Figure 3-9

Map of south Atlantic transect aboard the R/V Knorr, November-December 1999. Trace metal samples, provided by M. Conte and J.C. Weber, were collected using a clean water pumping system and an in-line 0.2 μ m filtration system in a laminar flow hood.

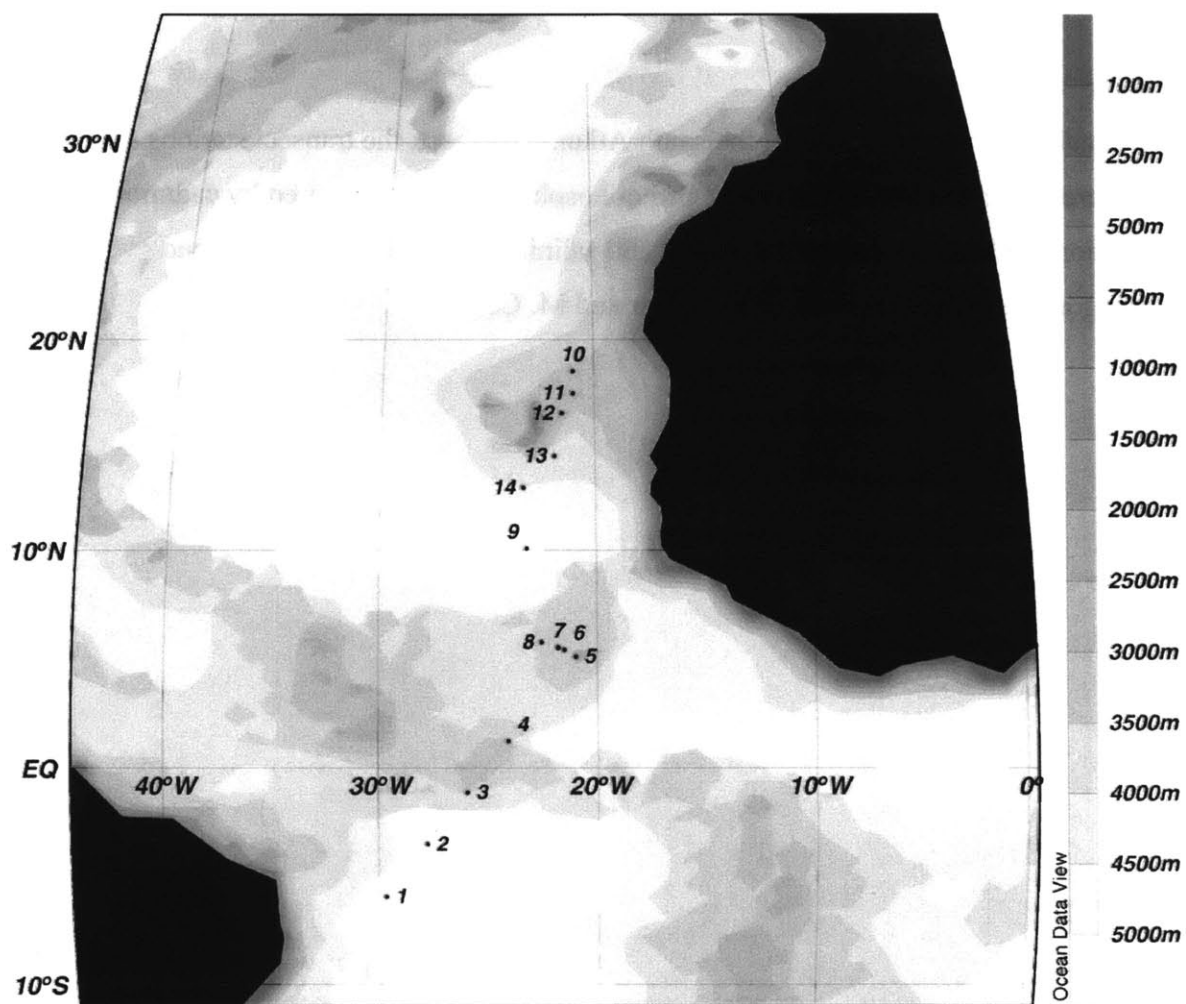


Figure 3-10

A) Total dissolved cobalt along the south Atlantic transect; the transect stations are numbered as shown on Figure 9. B) Orthophosphate data as measured by cadmium reduction method. C) Temperature (°C) and salinity (ppt) data. Phosphate and hydrographic data provided by J.C. Weber and M. Conte.

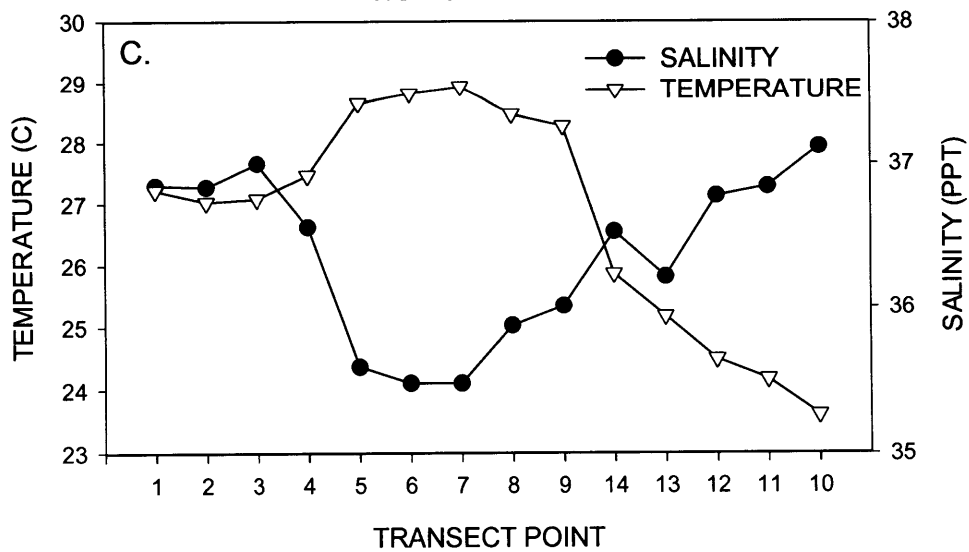
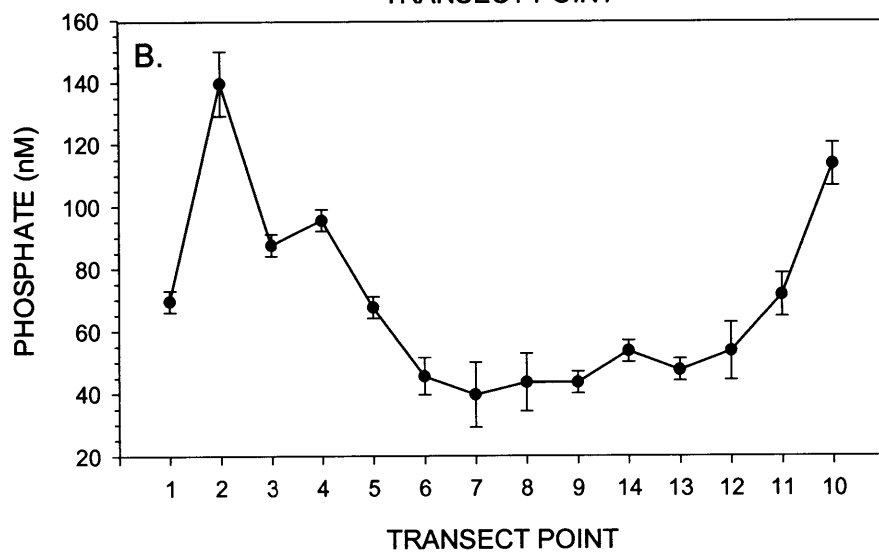
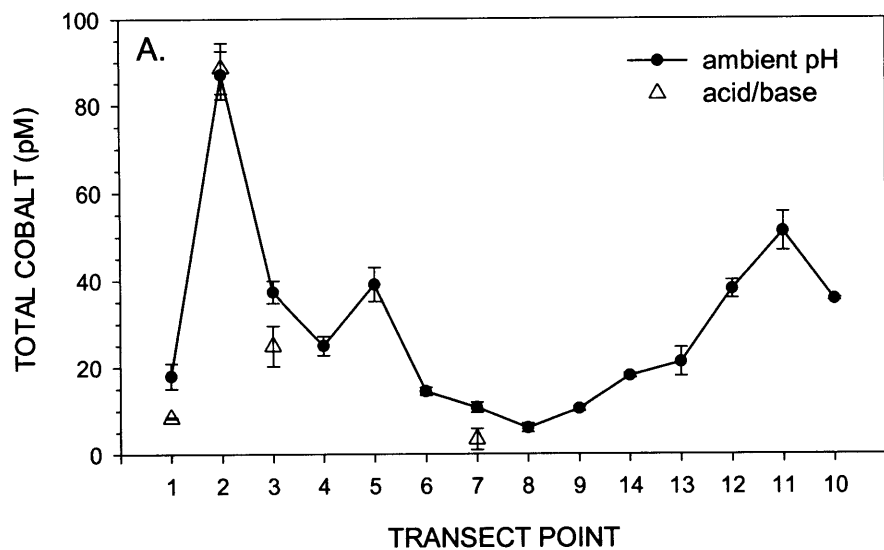


Figure 3-11

Positive correlation between total cobalt and phosphate on the 1999 south Atlantic transect. A linear regression of the data suggests that cobalt will be depleted before phosphate.

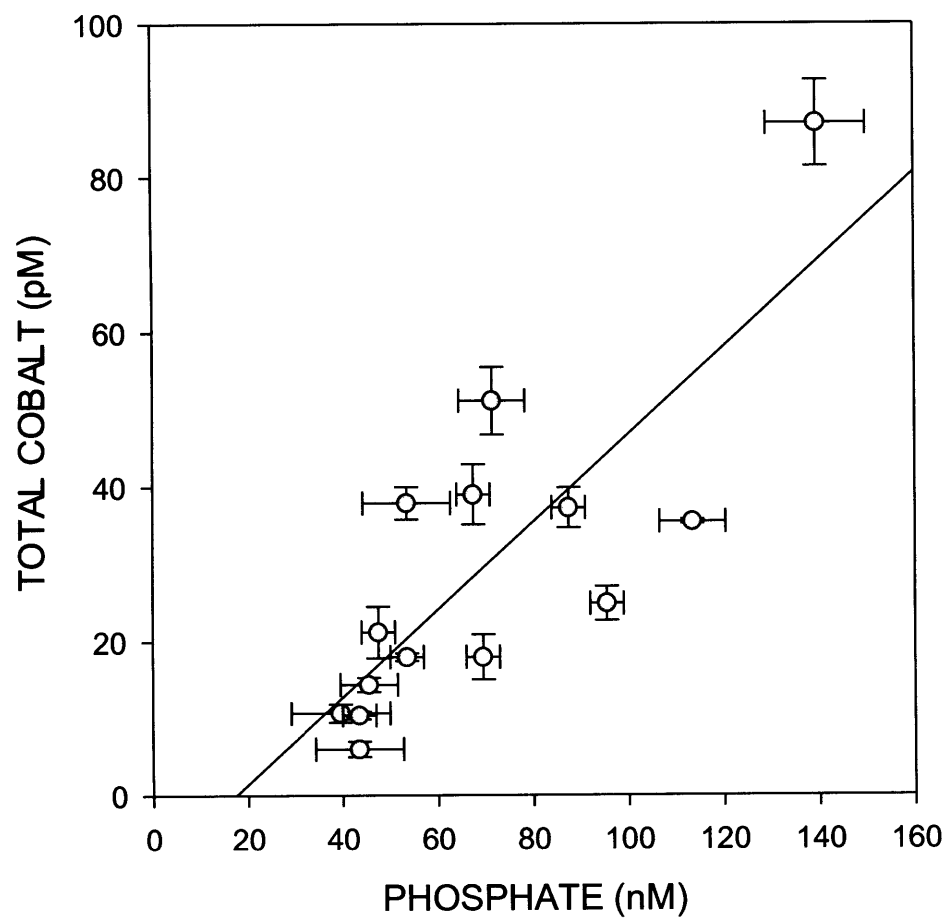
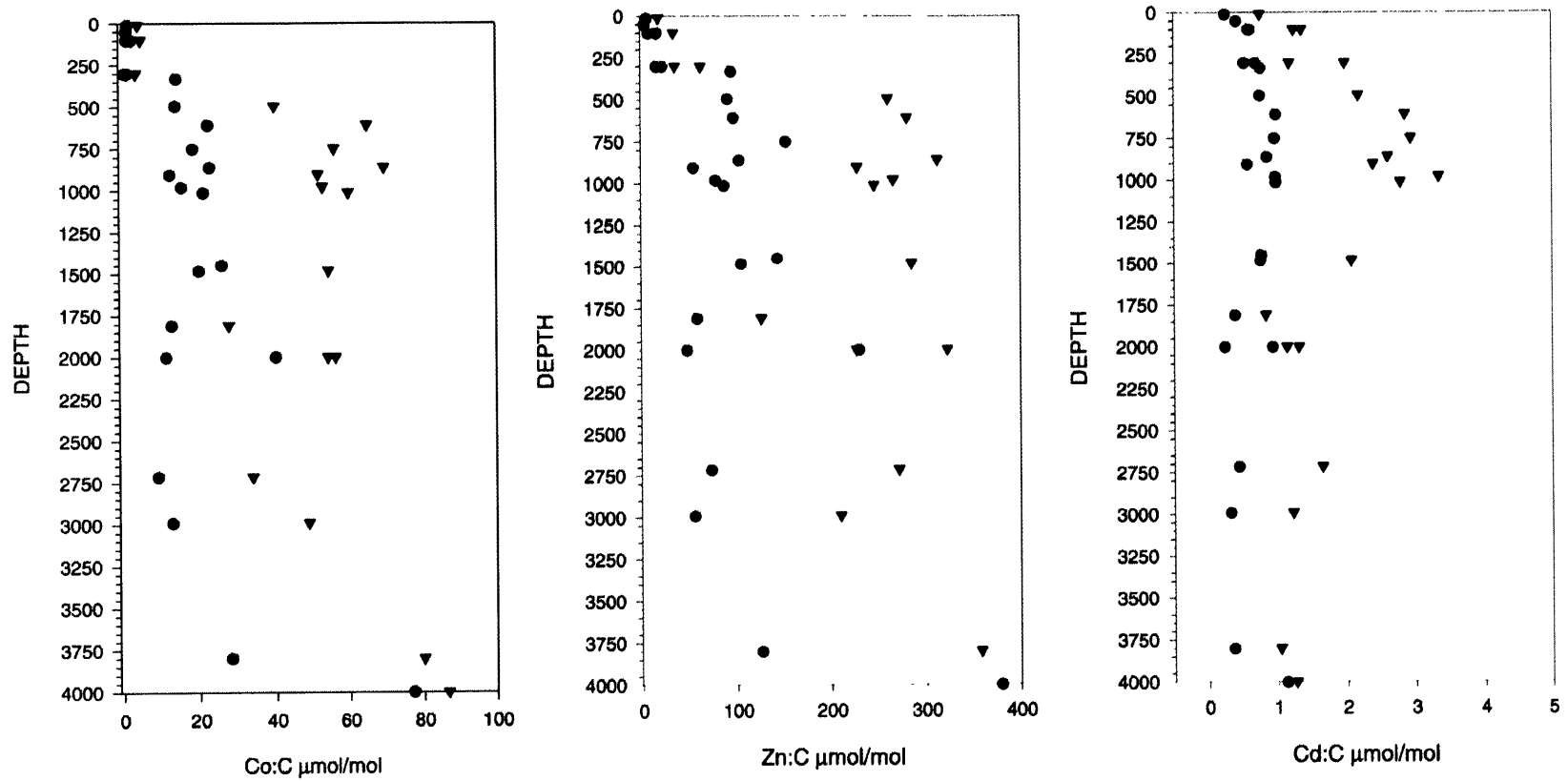


Figure 3-12

Ratios of Co, Zn and Cd to carbon near Bermuda. Surface water Co:C ratios were significantly less than that of deepwater, perhaps due to increased demand and resultant scarcity for cobalt in surface waters. Ratios were calculated from data by Sherrell and Boyle (1993).



● USING Corg estimates
▼ using Co:P and estimated C:P=106

Table 3-1 Selected Thermodynamic data for pe-pH diagram

Species	logK	Reference
CoCl ⁺	-0.14	a
CoOH ⁺	4.2	a
Co(OH) ₂	8.5	a
Co(OH) _{2(s)}	15.7	b
Co(OH) _{3(s)}	43.5	c
Co ³⁺ + e ⁻ ⇌ Co ²⁺	31	b

a. (Martell and Smith, 1977)

b. (Stumm and Morgan, 1996)

c. Derived from constants in table

Table 3-2 Sargasso Sea, Shelf Water and Extrapolated Zero Salinity Concentrations (nM)

Element*	Sargasso Sea End Member	Shelf Concentration	Extrapolated Zero Salinity End Member	Ratio of End Members
Mn	2.3	21	114	50
Ni	2.3	5.9	21	9
Cu	1.2	4.0	19	6
Zn	0.06	2.4	16	270
Cd	0.002	0.20	1.1	550
Co	0.02	0.13	0.79	41

* Mn, Ni, Cu, Zn and Cd transect data from Bruland and Franks, (1983)

Table 3-3 Crustal composition of transition elements (data from Taylor and McLennan, 1985)

Element	Crustal composition	$\log K_y^{SW}$
Iron	4.0 (FeO)	-8.9
Aluminum	14 (Al ₂ O ₃)	-8.0
Cobalt	0.0012	-6.7
Manganese	0.068	-6.3
Zinc	0.0052	-5.2
Nickel	0.0019	-4.6
Cadmium	no data	-3.1

Table 3-4 Regression slopes of Co vs PO₄ (μmol mol⁻¹)

Location	Depth (m)	Co (pM)	$\Delta\text{Co}/\Delta\text{P}$	r^2
S. Atlantic	5	6-87	560	0.63
NE. Pacific (T5)	50-150	7.9-32	39.8	0.981
NE. Pacific (T6)	50-150	28-40	35.5	0.994
NE. Pacific (T8)	8-50	25-55	38.4	0.977

* NE. Pacific data from Sunda and Huntsman (1995) and Martin et al., (1989)

Table 3-5 Particulate metal:carbon ratios near Bermuda ($\mu\text{mol/mol}$, calculated from Sherrell and Boyle, 1992)

	10-100m (n=4)	300-4000m (n=19)
Co:C	1.5 ± 0.6	20 ± 17
Zn:C	8.2 ± 5.6	106 ± 83
Cd:C	0.47 ± 0.17	0.71 ± 0.27

Table 3-6 Particulate metal:carbon ratios near Bermuda ($\mu\text{mol/mol}$, calculated from Sherrell and Boyle, 1992). These ratios were calculated using measured P concentrations, and converted to C using the an estimated 106:16 C:P ratio.

	10-100m (n=4)	300-4000m (n=19)
Co:C	3.8 ± 1.2	49 ± 23
Zn:C	22.7 ± 9.9	258 ± 111
Cd:C	1.12 ± 0.32	1.92 ± 0.79

Table 3-7 Particulate metal:phosphate ratios near Bermuda ($\mu\text{mol/mol}$, calculated from Sherrell and Boyle, 1992). These ratios were calculated using measured P concentrations.

	10-100m (n=3)	300-4000m (n=17)
Co:P	403 ± 128	5420 ± 2440
Zn:P	2410 ± 1050	27300 ± 11800
Cd:P	119 ± 33	205 ± 83

Table 3-8 Total Dissolved Cobalt Concentrations in the Sargasso Sea and northwest Atlantic Ocean, September 1999 (R/V Oceanus Cruise 349)

Station	Depth (m)	Total Dissolved Cobalt (pM)	Salinity (ppt)
BATS	15	19	
BATS	25	23	
BATS	40	22	
BATS	70	17	
BATS	85	27	
BATS	100	34	
BATS	125	28	
BATS	300	34	
BATS	1200	69	
BATS	1500	73	
BATS	3040	58	
1) 64.10W, 31.40N	15	19	36.7
2) 59.42W, 33.14N	15	34	36.5
3) 57.62W, 33.69N	15	41	36.9
4) 60.21W, 35.04N	15	41	36.6
5) 61.51W, 35.50N	15	52	36.4
6) 64.04W, 36.58N	15	30	36.6
7) 66.50W, 38.51N	15	40	36.6
9) 69.27W, 39.38N	15	71	35.1
10) 69.43W, 39.46N	15	76	34.7
11) 69.57W, 39.56N	15	89	33.5
12) 70.07W, 40.10N	15	90	34.3
13) 70.23W, 40.31N	15	134	32.1

Table 3-9 MITESS Time Series at the Bermuda Testbed Mooring (Moored in-situ Trace Element Serial Sampler)

Date	Depth (m)	Total Co (pM)
1/17/99	44	19
1/17/99	44	20
1/29/99	44	40
2/10/99	44	34
2/10/99	44	28
2/22/99	44	11
2/22/99	44	11
3/7/99	44	19
3/13/99	47	32
4/8/99	47	17
4/20/99	40	24
5/1/99	40	29
5/18/99	43	14
5/30/99	43	33
6/12/99	43	25
6/24/99	43	24
7/5/99	43	7
7/15/99	43	23
7/30/99	40	25
8/13/99	40	20
8/27/99	43	18
9/3/99	43	4
9/10/99	43	17
9/17/99	43	14
9/24/99	40	1
9/24/99	40	n.d.
10/8/99	43	19
10/22/99	43	28
11/2/99	40	23
2/23/99	10	20
4/8/99	10	40
4/20/99	10	27
5/3/99	10	25
5/31/99	10	17

*n.d. stands for not detectable

Table 3-10 Total Cobalt along a south Atlantic surface transect (5m)

Stn	Latitude	Longitude	Date	Temp (C)	Salinity	Co (pM)	Stddev
1	07° 09.80' S	31° 15.09' W	18-Nov-98	27.2186	36.848	18	2.9
2	03° 43.41' S	27° 57.74' W	19-Nov-98	27.0271	36.835	87	5.6
3	01° 08.42' S	25° 56.26' W	20-Nov-98	27.0776	37	37.3	2.6
4	01° 35.02' N	23° 47.97' W	21-Nov-98	27.4583	36.558	24.9	2.2
5	05° 07.12' N	21° 00.55' W	23-Nov-98	28.6488	35.591	39	3.9
6	05° 25.48' N	21° 31.39' W	25-Nov-98	28.8148	35.48	14.4	0.9
7	05° 31.87' N	21° 48.34' W	26-Nov-98	28.9278	35.479	10.7	1.2
8	05° 50.38' N	22° 48.37' W	27-Nov-98	28.4683	35.873	6	1
9	10° 04.63' N	23° 13.53' W	2-Dec-98	28.2679	36.007	10.4	0.5
10	18° 28.14' N	21° 01.76' W	6-Dec-98	23.6066	37.12	35.5	0.3
11	17° 24.67' N	21° 05.58' W	11-Dec-98	24.1738	36.841	51.1	4.4
12	16° 27.63' N	21° 32.28' W	13-Dec-98	24.4887	36.775	37.9	2.1
13	14° 25.81' N	21° 54.44' W	15-Dec-98	25.1718	36.214	21.2	3.3
14	12° 55.83' N	23° 20.90' W	16-Dec-98	25.8642	36.526	18	0.5
1	07° 09.80' S	31° 15.09' W	18-Nov-98	27.2186	36.848	8.3*	0.2
2	03° 43.41' S	27° 57.75' W	19-Nov-98	27.0271	36.835	88.5*	5.9
3	01° 08.42' S	25° 56.26' W	20-Nov-98	27.0776	37	24.8*	4.7
4	05° 31.87' N	21° 48.34' W	26-Nov-98	28.9278	35.479	3.4*	2.4

* These samples are duplicates which were acidified, UV-irradiated, then neutralized prior to analysis.

Chapter 4

Cobalt limitation, uptake, and metal substitution in *Prochlorococcus*

Mak A. Saito^{φ α}, James W. Moffett^α, Sallie W. Chisholm[‡], John Waterbury^ε.

^φ MIT/Woods Hole Oceanographic Institution Joint Program in Chemical Oceanography

^α Department of Marine Chemistry and Geochemistry, Woods Hole Oceanographic Institution

[‡] Depts. of Civil and Environmental Engineering and Biology, Massachusetts Institute of Technology

^ε Department of Marine Biology, Woods Hole Oceanographic Institution

Abstract

With the recognition that primary production in vast regions of the ocean are limited by iron input (Coale et al., 1996; Martin and Fitzwater, 1988), processes that enable marine phytoplankton to acquire trace metals are fundamental to our understanding of primary productivity and global carbon biogeochemical cycling. Uptake of iron by complexation and retrieval of strong specific iron ligands called siderophores occurs in marine heterotrophic and photosynthetic bacteria (Wilhelm et al., 1998; Wilhelm et al., 1996b). Like iron, cobalt concentrations in the open ocean are extremely low, ranging from 4-81 picomoles per liter range (Jickells and Burton, 1988; Martin and Gordon, 1988). Moreover, the photosynthetic eukaryotic *Emiliana huxleyi* and prokaryotes *Prochlorococcus* and *Synechococcus* show a requirement of cobalt for maximal growth and an absolute requirement for cobalt respectively (Sunda and Huntsman, 1995). Here, we show laboratory evidence that cobalt uptake by *Prochlorococcus* is not dependent on the concentration of free cobalt (Co^{2+}) ions; but rather, cobalt uptake behavior is consistent with production of strong cobalt ligands or “cobalophores” that increase the bioavailable fraction of cobalt. These cobalophores would be analogous in function to siderophores, and would facilitate cobalt uptake. Growth rate studies under varying cobalt and zinc concentrations showed an absolute requirement for cobalt that could not be replaced by zinc. Nickel inhibition of growth was observed in *Prochlorococcus* cultures with 88pM total cobalt, but not in cultures with 790pM total cobalt. This effect was not observed with comparable zinc. We also present field evidence from the Costa Rica Upwelling Dome in the Pacific showing the upwelling of cobalt to a *Synechococcus* bloom, where the cobalt is 42% labile at 90m and becomes 100% complexed by strong organic cobalt ligands in the bloom surface waters. Like iron (Rue and Bruland, 1997) and copper (Moffett and Brand, 1996), the speciation of cobalt in oceanic environments may be biologically controlled by the production of ligands.

Introduction

Trace metal analytical methods have improved significantly over the past two decades contributing to important advances in our understanding of oceanic biogeochemistry. Notably, the discovery of iron-limited regions of the oceans and the publication of the first nutrient-like profiles of iron have altered thinking about the role of trace metals in global carbon cycling. The development of electrochemical iron speciation methods (Rue and Bruland, 1995; van den Berg, 1995; Wu and Luther III, 1995) has led to the idea that biogenic ligands may in fact be controlling the residence time of iron in the surface ocean (Johnson et al., 1997). With the discovery that zinc, cobalt and cadmium can be the metal co-factors for the enzyme carbonic anhydrase in phytoplankton (Morel et al., 1994; Price and Morel, 1990), and that potentially growth limiting levels of Co and Zn can be found in the environment (Martin et al., 1989; Sunda and Huntsman, 1995) researchers have hypothesized that these metals can result in metal-carbon co-limitation and hence influence the size and composition of the biological carbon pump (Morel et al., 1994; Riebesell et al., 1994).

The influence of trace metals on oceanic primary productivity, requires an understanding of the speciation of biolimiting metals. This is because the strong organic complexes can account for a significant part of the total metal in seawater. The organic complexation of metals like Fe and Zn (Rue and Bruland, 1995; Bruland, 1989) has important but as yet poorly understood implications for their bioavailability. For cobalt, an important micronutrient, there is no published evidence of organic complexation in oceanic waters much less a recognized source of ligands.

Prochlorococcus is a marine photosynthetic cyanobacterium (oxygenic photoautotroph) that is ubiquitous in the tropical and sub-tropical surface oceans (Partensky et al., 1999). Previous to this study, its cobalt requirements were unknown. Sunda and Huntsman (1995) have showed that the related cyanobacterium *Synechococcus bacillarus* has an absolute requirement for cobalt that cannot be substituted for zinc. Moreover, Wilhelm et al. show evidence of iron binding siderophore production in *Synechococcus* strain PCC 7002 (1996a and 1998). With oceanic cobalt concentrations tending to be about an order of magnitude lower than that of iron, and

given the absolute cobalt requirement of *Synechococcus*, we hypothesized that *Prochlorococcus* would also have an absolute cobalt requirement and that the uptake of cobalt may be facilitated by cobalt ligands.

Strong cobalt ligands with a conditional stability constant of $10^{16.3 \pm 0.9}$ were measured in seawater at the Bermuda Atlantic Time Series station (see Chapter 2). These ligands correlated with total cobalt concentrations with a small excess of ligand at the chlorophyll and *Prochlorococcus* maxima (Figures 5 and 7, Chapter 2). Direct measurements of cobalt ligands in *Prochlorococcus* cultures are ambiguous due to masking by high concentrations of EDTA.

This chapter combines culture technique and radiotracer uptake methodologies to examine cobalt requirements, metal substitution, and uptake pathways in *Prochlorococcus*. In addition, field data from a *Synechococcus* bloom observed September, 2000 at the Costa Rica Upwelling Dome shows evidence for the production of strong cobalt ligands by the microbial community.

Materials and Methods

Culture work

Prochlorococcus cultures were grown in polycarbonate 28mL tubes or glass borosilicate tubes. All labware was rigorously washed in detergent overnight, rinsed in Milli-Q water, soaked in 10% HCl (Baker Instra-Analyzed), and rinsed and soaked in pH 2 HCl prior to use. Culture media consisted of filtered Sargasso seawater prepared using a modified K-media recipe (Chisholm et al., 1992): an 11.7 μ M EDTA (Sigma Ultra) trace metal mix (90nM MnCl₂, 3nM Na₂MoO₄, 10nM Na₂SeO₃, 1.17 μ M FeCl₃) without copper, cobalt, nickel, and zinc and with chelexed major nutrients (10 μ M H₃PO₄, 50 μ M NH₄Cl, 100 μ M urea) (Price et al., 1988/1989). 10nM NiCl₂ and 8nM ZnSO₄ were added independently of the trace metal mix. The filtered Sargasso Seawater was microwave sterilized (Keller et al., 1988) and all amendments were sterile filtered and rather than autoclaved. Isolates from the Sargasso Sea (SS120) and the Mediterranean Sea (MED4) were used for experiments. In the course of this study, we succeeded in isolating an

axenic strain of MED4, which will be described as MED4-Ax in this chapter (see Appendix I. for isolation protocol).

Cultures were grown in duplicate tubes and growth was monitored by *in vivo* fluorescence on both replicates and by intermittent flow cytometric measurements of one of each duplicate pair (using the unopened culture as an uncontaminated reference). Experiments in which opened and unopened treatments deviated, as determined by *in vivo* fluorescence, were considered metal contaminated and were repeated. *In vivo* fluorescence correlates strongly with flow cytometry cell number measurements during exponential growth and above the detection limit of the fluorometer⁶, and intermittent flow cytometry samples were analyzed to verify that *in vivo* measurements were not biased by changes in fluorescence per cell (see Appendix III. for extensive discussion, see Figure captions for fluorometer detection limits in each experiment). This correlation begins to degenerate in stationary phase when pigment per cell decreases rapidly, and under severe nutrient limitation. The use of experimental designs that examine qualitative differences between treatments (from a single inoculum culture) rather than differences in growth rate avoids the problem of interpreting *in vivo* fluorescence data. For example, an antagonistic effect of a treatment causes a decrease in *in vivo* fluorescence relative to the control treatments; in this case we cannot specify if the effect is due to a change in growth rate or decrease in fluorescence per cell, yet the antagonistic effect itself is unambiguous. Two types of culture transfers were used: 1) high volume inoculum transfers used 2.2% and were from cultures of equivalent cobalt concentrations, except when starting experiments or when the low cobalt treatments rendered insufficient biomass for transferring, in which case inocula from the next lowest cobalt concentration was used. 2) Low inoculum transfers were conducted with the aim of diluting out both cobalt and cobalt ligands for study over a single transfer. I utilized a 0.08% inoculum volume from a single low cobalt culture on the same day to make treatments comparable. Growth rates were calculated from the exponential portion of the growth curve, and error bars were calculated from the standard deviation of replicate growth curves (n=4 to 12 depending on cobalt concentration). Growth rates were

⁶ This is only true for experiments done at the same light intensity, since pigment per cell is highly dependent on light availability.

normalized to the maximum growth rate in an experiment to allow comparison between experiments run in different years under slightly different laboratory settings.

⁵⁷Co Uptake experiments

Axenic *Prochlorococcus*, strain MED4-Ax, was centrifuged at 10000rpm (11180 x g) in a Biofuge 22R (Heraeus) at 20°C for 47min and decanted with sterile and trace metal clean technique, resuspended into fresh media without added cobalt and returned to 23°C constant light incubator for 48h. The first supernatant was collected and filtered through a trace metal clean acid-rinsed 0.2µm syringe filter (all-plastic syringe). This filtrate was checked for sterility using a marine broth purity test, and was added by 10% volume to fresh media. These solutions were allowed to equilibrate for 24h with 940, 290, and 94pM ⁵⁷Co (Isotope Products Laboratories, carrier-free ⁵⁷CoCl₂).

Glutaraldehyde was added at 0.75% concentration as a dead control immediately before adding cells. After three cycles of centrifugation and resuspension into fresh media prepared without cobalt additions, the cells (2.8×10^7 cells/mL) were added in fresh media to the treatment flasks as 10% of the volume. This inocula was checked for heterotrophic contamination using a marine purity broth. Cells were collected for radioactive counting after filtration and a filtered seawater rinse onto 0.2µm polycarbonate filters. Filters were counted on a germanium gamma counter detector (Canberra) to $\pm 5\%$ counting error. The 10% conditioned media addition volume was chosen to minimize the influence of nutrient drawdown in the added conditioned media.

Cells were grown in 10^{-5} M EDTA and resuspended into medium made with 10^{-5} M NTA, EDTA, or DTPA metal-ion buffers and varying concentrations of cobalt as ⁵⁷CoCl₂ (Figure 1B). This experiment used the same inocula as 1A, and was run concurrently to make the cobalophore (1A) and free-ion results (1B) comparable. Uptake rates of cobalt are proportional to the free-ion concentration of cobalt (1C) rather than the total cobalt (1B). However, the dotted triangle on the plot corresponds to the addition of conditioned media uptake rate (slope) measured in 1A, illustrating how the conditioned media treatment has increased uptake of cobalt relative to washed (and therefore free-ion ‘abiding’) cells. The media used here was described above, but was modified with NTA and DTPA substitutions for EDTA.

Analytical Measurements

The measurements were made by competitive ligand exchange adsorptive cathodic stripping voltammetry (CLE-ACSV) using a Metrohm 663 hanging mercury drop electrode and a μ Autolab Eco-chemie computer interface. Dimethylglyoxime (DMG) from Aldrich was recrystallized in milli-Q (Millipore) water and 10^{-3} M EDTA (Sigma Ultra) to remove impurities, dried and redissolved in HPLC grade methanol to a concentration of 0.1 M. Final concentrations of DMG in the seawater samples were 0.000235 M. Solutions of 1.5 M sodium nitrite (Fluka Puriss) was equilibrated overnight with prepared Chelex-100 beads (Price et al., 1988/1989) to remove metal contaminants; 1.5 mL of this nitrite solution was added to 8.50 mL of seawater sample. A 0.5 M EPPS buffer solution (Fisher) was cleaned by running through a column with 3 mL of clean Chelex-100 beads (BioRad) and diluted in the sample to 0.0025 M.

The μ Autolab analysis protocol involved a 3.25 minute purge with filtered 99.999% N_2 , a 90 second deposition time at -0.6 V, a 15 second equilibration period followed by a high-speed negative scan at 10 V sec^{-1} from -0.6 V to -1.4 V. The linear sweep wave form was used, and stirrer speed 5, and drop size of 0.52 mm^2 . Cobalt signal was measured as the peak height from the baseline. Titration samples were analyzed in order of increasing concentration and rinsed with 10% HCl then pH 3 HCl (Baker Ultrex II) at the completion of each titration. The Co detection limit was 3 pM and significant efforts were taken to minimize the reagent blank. The method development and calibration for this technique is described in detail in Chapter 2.

Bottle Incubations

Surface seawater was collected via a clean water pumping system, homogenized in a trace metal clean 50 L carboy, and distributed between triplicate 1 L polycarbonate bottles in a filtered air clean bubble. 1 nM FeSO_4 and 500 pM CoCl_2 were added to experimental treatments using clean technique. The bottles were placed in heat-sealed bags and incubated in an on-deck incubator covered with blue film and plumbed with flow-through seawater until analysis.

Free Metal Calculations

Free metal ion calculations were calculated using stability constants from Martell and Smith (Martell and Smith, 1993) for calcium and magnesium interactions with NTA, EDTA, and DTPA. Inorganic complexes with cobalt were also taken into account with the CoCl^+ as the major inorganic species. For our cobalt limiting media with an EDTA concentration of $11.7\mu\text{M}$, the ratio of free Co^{2+} to total cobalt was calculated to be $10^{-2.94}$. The ratio of free Zn^{2+} to total zinc is calculated to be $10^{-2.88}$, using Sunda and Huntsman's empirically derived conditional stability constant and correcting for the difference in EDTA concentration (Sunda and Huntsman, 1992).

Results

We present four lines of laboratory evidence that support the hypothesis that the dominant phytoplankter in the subtropical and tropical ocean, *Prochlorococcus*, produces a cobalt ligand or “cobalophore” that assists in cobalt uptake. First, ^{57}Co uptake rates were measured for in cobalt-limited *Prochlorococcus* MED4-Ax. Three metal ion buffers and three total ^{57}Co concentrations were used with rinsed cells to measure free-ion uptake rates (Figure 1A, B, and C). ^{57}Co uptake in the 94pM and 290pM cobalt concentrations of the DTPA experiment were below detection limit. When all of these uptake rate studies are plotted together, uptake rates are not proportional to total cobalt in the three types of metal ion buffers (Figure 2B). Instead, uptake is proportional to the free-ion form of cobalt ($^{57}\text{Co}^{2+}$, Figure 2C). If uptake were proportional to total cobalt the strength of the metal-ion buffer ligand would not affect the uptake rate and all of the points would fall upon a single line in Figure 2B. Yet because the metal ion buffers have different affinities for cobalt ($K_{\text{NTA}} = 10.38$, $K_{\text{EDTA}} = 16.45$, $K_{\text{DTPA}} = 19.15$) (Martell and Smith, 1993), they set different free Co^{2+} concentrations at equivalent total cobalt concentrations. Figure 2C shows that when all of the rinsed-cell uptake rates are plotted against the free Co^{2+} concentrations, all of the points fall upon a single line indicating that uptake rate is proportional to free Co^{2+} . For comparison, the uptake rate of ^{57}Co to a culture with a 10% addition of conditioned media (media from a late log phase culture

which has been sterile filtered under trace metal clean conditions) resulted in a doubling of cobalt uptake rates relative to fresh media (Figure 2A). This addition of conditioned media from axenic *Prochlorococcus* cultures is suggestive of the presence of organic cobalt compounds and an uptake system for those compounds. The increase in cobalt uptake rates observed with the addition of conditioned media (Figure 2A) is best explained by a cobalt ligand that has coordinated some of the cobalt away from the $^{57}\text{CoEDTA}^{2-}$ buffer, creating a bioavailable cobalt ligand fraction.

Second, long-term culture studies were performed in EDTA and NTA buffers to measure changes in growth rate under decreasing cobalt concentrations. In contrast to the free-ion model, growth rates of batch cultures grown over several months (see Appendix IV. for raw data) were proportional to the total cobalt concentration (Figure 3B) rather than the free cobalt (Figure 3A). This outcome is consistent with the idea of cobalt ligands that have accumulated in the media and are facilitating cobalt uptake by coordinating cobalt from the metal ion buffer.

Third, additions of conditioned media (5% by volume) to cultures inoculated with small volumes (0.08%) showed significant improvement in growth rates relative to low cobalt controls (Figure 4). Total cobalt in the conditioned media was 82pM, a concentration less than the media blank of 119pM; this shows that the increase in growth rate was not a result of cobalt contamination. This experiment also supports the idea that a secreted strong cobalt ligand was produced that increased the bioavailability of cobalt by accessing the cobalt in the metal-ion buffer.

Fourth, when cultures were grown with small inoculum volumes of 0.08%, nickel inhibition of growth was observed under low cobalt conditions of 0.1pM free Co, but not at 0.9pM free cobalt (Figure 5). This effect was not observed at comparable 6.4nM of zinc. These results are significant because most strong cobalt ligands are also strong nickel ligands (Chapter 2, Table 5); these results suggest that the uptake system for cobalt in *Prochlorococcus* involves a site that has a ligand with high cobalt and nickel specificity. While this experiment does not differentiate between strong cell surface ligands and free cobalt ligands excreted into the surrounding seawater, both of these possibilities are novel mechanisms of cobalt acquisition. It is notable that this 8nM nickel addition in EDTA is small relative to typical surface water values (~2nM); given

that this is a total nickel addition, once nickel complexation by EDTA is taken into account the nickel addition should result in a free nickel perturbation that is sub-nanomolar. In contrast, nickel in seawater tends to be only partially complexed by strong organic ligands (van den Berg and Nimmo, 1986; Saito and Moffett, unpublished data). These results have implications for the ability of biota to acquire cobalt in various oceanic environments where nickel concentrations may increase with upwelling of nickel-rich deep waters.

In addition to the laboratory evidence for cobalt ligands described above, we also present field evidence for the production of cobalt ligands in a bloom of the marine cyanobacterium *Synechococcus*. A phycoerythrin-rich *Synechococcus* bloom with cell densities of 10^6 cells mL⁻¹ was observed at the Costa Rica Upwelling Dome (8.59 N, -90.58 E) in the Pacific (flow cytometry analysis by C. Trick, pers. comm.)⁷. High concentrations of labile cobalt were measured in the upwelled deepwater using CLE-ACSV (see methods section in this chapter and Chapter 2 for protocols), and as that water reached the *Synechococcus* bloom in surface waters, the total cobalt was depleted (Figure 6A) and the remaining cobalt was complexed by strong cobalt ligands (Figure 6B and 6C). Additions of 500pM cobalt and 1nM iron in triplicate bottle incubations resulted in an increase in chlorophyll after two days, while each element alone did not (Figure 7A). Moreover, the 500pM of cobalt that was added became $\geq 85\%$ complexed by strong organic ligands after 4d of interaction with the biota (Figure 7B). Filtered controls did not show this effect indicating that the ligands were being released by the microbial community or from particulate matter. Together, these field results provide strong evidence that a bloom dominated by *Synechococcus* was a source of cobalt ligands to this oceanic environment.

⁷ Due to the recent date of the cruise (September, 2000) samples for flow cytometry samples for *Prochlorococcus* enumeration have not yet returned from Chile at the time of this writing. *Synechococcus* cell counts were performed at sea on a Becton-Dickinson FACScaliber flow cytometer (C. Trick, pers. comm.) and verified by epi-fluorescent microscopy (D. Kirchman, pers. comm.). Visual inspection of filters from this station showed the orange-pink color typical of *Synechococcus*. Detailed pigment analyses by G. DiTullio are being processed.

Metal Substitution Experiments

The ability of *Prochlorococcus* to substitute zinc and cadmium was explored using these culture techniques. Zinc limitation studies showed that cobalt and zinc do not substitute for each other in *Prochlorococcus* strain MED4-Ax (Figure 8). However, slight zinc limitation was possible, a trait not shown in the Sunda and Huntsman (1995) study of *Synechococcus bacillus* but which their unpublished results did show (Sunda, pers. comm.) and which we have observed here for *Prochlorococcus*. A low-inoculum experiment (0.08%) with the Sargasso strain SS120 showed that cadmium could alleviate cobalt limitation (Figure 9). However, these experiments were repeated with MED4-Ax and were not conclusive.

Discussion

There are important biogeochemical implications for biogenic cobalophore production in seawater. As has been proposed for iron in seawater (Johnson et al., 1997), the solubility of cobalt may be enhanced by complexation by strong and specific organic cobalt ligands. These ligands would serve to protect cobalt from scavenging by particles and from oxidants like hydrogen peroxide and the subsequent precipitation of insoluble inorganic Co(III) species. Using these electrochemical techniques, it is not currently possible to distinguish between Co(II) and Co(III) ligands in seawater. It is possible that the ligands we have measured are apo-cobalamin or B₁₂ degradation products. Historically, B₁₂ was also explored as a potentially limiting micronutrient for marine phytoplankton (Guillard and Cassie, 1963; Menzel and Spaeth, 1962; Swift, 1992; Swift and Taylor, 1972). Calculations of B₁₂ quotas and cobalt quotas in *Synechococcus* suggest that B₁₂ is only a minor component of both the cobalt requirement (Appendix II.).

The biochemical use for cobalt in *Prochlorococcus* and *Synechococcus* is unknown at this time, although given the high carbonic anhydrase activity observed (Tchernov et al., 1997) and low zinc requirement in *Prochlorococcus* and *Synechococcus* (Sunda and Huntsman, 1995), it is plausible that a large fraction of the cobalt requirement is for this enzyme. Zinc, cadmium and cobalt have been shown to influence carbon uptake in marine phytoplankton by limiting the synthesis of the enzyme carbonic

anhydrase (Morel et al., 1994; Yee and Morel, 1996). Hence, production of cobalophores may be important in affecting the ability of marine cyanobacteria to fix CO₂. Given the global importance of these organisms (Partensky et al., 1999; Waterbury et al., 1979; Waterbury et al., 1986) and their potential POC and DOC contributions to the marine biological carbon pump, understanding the influence of cobalt ligands on productivity and carbon uptake is an important future area of global carbon cycling research.

The trends observed in the cellular requirements of cobalt are distinct from those of iron: while all marine phytoplankton are known to require iron to survive, an absolute requirement for cobalt has only been observed for *Synechococcus bacillus* (Sunda and Huntsman, 1995) and *Prochlorococcus marinus* (Figure 3). Cobalt is required for optimal growth of the coccolithophore *E. huxleyi* (Sunda and Huntsman, 1995; see Chapter 1, Figure 3). Cobalt substitution for zinc and cadmium has been observed for several eukaryotic species (Price and Morel, 1990; Sunda and Huntsman, 1995; Yee and Morel, 1996). Since the oxygenic photosynthetic bacteria are evolutionarily older than eukaryotic algae, it is conceivable that the absolute requirement for cobalt is vestigial from a time period when the Earth's atmosphere and oceans were still anoxic (Sunda and Huntsman, 1995) making cobalt abundant and zinc scarce. Cobalophores may have evolved as a means to obtain cobalt in a newly oxic environment where cobalt was rapidly scavenged. Given this scarce cobalt, eukaryotic organisms evolving later in an oxic ocean may have evolved to utilize zinc as a substitute for cobalt (Sunda and Huntsman, 1995). Similar arguments exist for the evolution of the cobalt center in B₁₂ (Scott, 1990). The inability of zinc to substitute for cobalt we observed in Figure 8 and Table 1 is consistent with this ancient ocean hypothesis. Besides increasing cobalt solubility, another possible function of cobalophores may be to restrict other species' access to a limiting resource. In this sense, the oxygenic photosynthetic bacteria (e.g. *Prochlorococcus* and *Synechococcus*), which dominate many oligotrophic regimes, may have evolved the strategy of producing cobalophores and siderophores to increase the availability of cobalt and iron and while restricting access of these metals to non-siderophore/cobalophore synthesizing organisms.

The term cobalophore was chosen to describe a hypothesized strong organic ligand that is involved in facilitating cobalt uptake into the cell. Siderophores are ligands

that not only facilitate iron uptake, but also are inducible under conditions of iron stress. While we show evidence for facilitated cobalt uptake by the hypothesized cobalophore, we do not show evidence for induction of ligand production with cobalt stress. The reason for this is that the control treatment in uptake experiments cannot reasonably distinguish between free-ion uptake and cobalt-ligand uptake when cobalt concentrations are high. Moreover, it is not clear that production of siderophores by marine organisms is actually induced under only low iron conditions: the opposite was observed for production of iron binding ligands upon iron fertilization in the equatorial Pacific (Rue and Bruland, 1997).

There have been reports that iron reductases may have evolved to allow eukaryotic algae to obtain iron from non-specific organic complexes (Maldonado-Pareja, 1999). This strategy relies on the reduction of the Fe(III) center to Fe(II), which has a significantly lower stability constant than Fe(III) for many strong iron complexes. It is uncertain at this time whether or not Co ligands in seawater are Co(II) or Co(III) ligands (Saito and Moffett, 1999). If cobalt ligands in seawater bind Co(II), the cell surface reductase strategy utilized by eukaryotic organisms would not be a viable mechanism for obtaining cobalt from those organic complexes. This could have been a selection pressure for the ability to substitute zinc for cobalt in many eukaryotic alga.

We have presented a hypothesis and supporting evidence for a cobalophore uptake mechanism in laboratory studies with *Prochlorococcus* and for cobalt ligand generation from a natural population dominated by *Synechococcus*. We have also discussed some of the important ecological and biogeochemical implications for the existence of an abundant marine cobalt ligand. While conclusive proof of this hypothesis will require the chemical structure of the ligand and the knowledge of the genes that regulate its production, it has taken several decades to reach this level of understanding with iron siderophores. We present these data as an introduction to the inquiry of cobalophores.

References

- Anderson, M.A. and Morel, F.M.M., 1982. The influence of aqueous iron chemistry on the uptake of iron by the coastal diatom *Thalassiosira weissflogii*. *Limnol. Oceanogr.*, 27(5): 789-813.
- Chisholm, S.W. et al., 1992. *Prochlorococcus marinus* nov. gen. nov. sp.: An oxyphototrophic marine prokaryote containing divinyl chlorophyll a and b. *Arch. Microbiol.*, 157: 297-300.
- Coale, K.H., Fitzwater, S.E., Gordon, R.M., Johnson, K.S. and Barber, R.T., 1996. Control of community growth and export production by upwelled iron in the equatorial Pacific Ocean. *Nature*, 379: 621-624.
- Guillard, R.L. and Cassie, V., 1963. Minimum cyanocobalamin requirements of some marine centric diatoms. *Limnol. Oceanogr.*, 8: 161-5.
- Jickells, T.D. and Burton, J.D., 1988. Cobalt, copper, manganese and nickel in the Sargasso Sea. *Mar. Chem.*, 23: 131-144.
- Johnson, K.S., Gordon, R.M. and Coale, K.H., 1997. What controls dissolved iron in the world ocean? *Mar. Chem.*, 57: 137-161.
- Keller, M.D., Bellows, W.K. and Guillard, R.L., 1988. Microwave treatment for sterilization of phytoplankton culture media. *J. Exp. Mar. Biol. Ecol.*, 117: 279-283.
- Maldonado-Pareja, M.T., 1999. Iron Acquisition by Marine Phytoplankton. Ph.D. Thesis. McGill University, Montreal, 201 pp.
- Martell, A.E. and Smith, R.M., 1993. NIST Critical Stability Constants of Metal Complexes Database.
- Martin, J.H. and Fitzwater, S.E., 1988. Iron deficiency limits phytoplankton growth in the north-east Pacific subarctic. *Nature*, 331: 341-343.
- Martin, J.H. and Gordon, R.M., 1988. Northeast Pacific iron distribution in relation to phytoplankton productivity. *Deep-Sea Res.*, 35: 177-196.
- Martin, J.H., Gordon, R.M., Fitzwater, S. and Broenkow, W.W., 1989. VERTEX: phytoplankton/iron studies in the Gulf of Alaska. *Deep-Sea Res.*, 36(5): 649-680.
- Menzel, D.W. and Spaeth, J.P., 1962. Occurrence of vitamin B12 in the Sargasso Sea. *Limnol. Oceanogr.*, 7: 151-154.

- Moffett, J.W. and Brand, L.E., 1996. Production of strong, extracellular Cu chelators by marine cyanobacteria in response to Cu stress. *Limnol. Oceanogr.*, 41(3): 388-395.
- Morel, F.M.M. et al., 1994. Zinc and carbon co-limitation of marine phytoplankton. *Nature*, 369: 740-742.
- Partensky, F., Hess, W.R. and Vault, D., 1999. *Prochlorococcus*, a Marine Photosynthetic Prokaryote of Global Significance. *Microbiol. Mol. Biol. Rev.*, 63(1): 106-127.
- Price, N.M. et al., 1988/1989. Preparation and chemistry of the artificial algal culture medium Aquil. *Biol. Oceanogr.*, 6: 443-461.
- Price, N.M. and Morel, F.M.M., 1990. Cadmium and cobalt substitution for zinc in a marine diatom. *Nature*, 344: 658-660.
- Riebesell, U., Wolf-Gladrow, D.A. and Smetacek, V., 1994. Carbon dioxide limitation of marine phytoplankton growth rates. *Nature*, 361: 249-251.
- Rue, E.L. and Bruland, K.W., 1995. Complexation of iron(III) by natural ligands in the Central North Pacific as determined by a new competitive ligand equilibration/asorptive cathodic stripping voltammetric method. *Mar. Chem.*, 50: 117-138.
- Rue, E.L. and Bruland, K.W., 1997. The role of organic complexation on ambient iron chemistry in the equatorial Pacific Ocean and the response of a mesocale iron addition experiment. *Limnol. Oceanogr.*, 42(5): 901-910.
- Saito, M.A. and Moffett, J.W., 1999. Organic complexation of cobalt in the Sargasso Sea, American Society for Limnology and Oceanography Meeting Proceedings, Santa Fe, NM.
- Scott, A.I., 1990. Mechanistic and Evolutionary Aspects of Vitamin B12 Biosynthesis. *Acc. Chem. Res.*, 23: 308-317.
- Sunda, W.G. and Huntsman, S.A., 1992. Feedback interactions between zinc and phytoplankton in seawater. *Limnol. Oceanogr.*, 37: 25-40.
- Sunda, W.G. and Huntsman, S.A., 1995. Cobalt and Zinc interreplacement in marine phytoplankton: biological and geochemical implications. *Limnol. Oceanogr.*, 40: 1404-1417.
- Swift, D.G., 1992. Multiple micronutrient effects in phytoplankton enrichment experiments: Influence of vitamin B12, cobalt, and nitrate on responses to iron or

- aerosol addition. In: A.F.S. Jr. (Editor), AGU 1992 Fall Meeting Proceedings, San Francisco CA., pp. 83.
- Swift, D.G. and Taylor, W.R., 1972. Growth of vitamin B12 - limited cultures: *Thalassiorira pseudonana*, *Monochrysis lutheri*, and *Isochrysis galbana*. J. Phycol., 10: 385-391.
- Tchernov, D. et al., 1997. Sustained net CO₂ evolution during photosynthesis by marine microorganisms. Curr. Biol., 7: 723-728.
- van den Berg, C.M.G., 1995. Evidence for organic complexation of iron in seawater. Mar. Chem., 50: 139-157.
- van den Berg, C.M.G. and Nimmo, M., 1986. Determination of interactions of nickel with dissolved organic material in seawater using cathodic stripping voltammetry. Sci. Total Environ., 60: 185-195.
- Waterbury, J.B., S.W. Watson, R.R.L. Guillard and Brand, L.E., 1979. Widespread occurrence of a unicellular, marine, planktonic, cyanobacterium. Nature, 277: 293-294.
- Waterbury, J.B., Watson, S.W., Valois, F.W. and Franks, D.G. (Editors), 1986. Biological and Ecological Characterization of the Marine Unicellular Cyanobacterium *Synechococcus*. Photosynthetic Picoplankton. Can. Bull. Fish. Aquat. Sci., 583 pp.
- Wilhelm, S., Maxwell, D. and Trick, C., 1996a. Growth, iron requirements, and siderophore production in iron-limited *Synechococcus* PCC 7002. Limnol. and Oceanogr., 41: 89-97.
- Wilhelm, S.W., MacAuley, K. and Trick, C.G., 1998. Evidence for the importance of catechol-type siderophores in the iron limited growth of a cyanobacterium. Limnol. Oceanogr., 43(5): 992-997.
- Wilhelm, S.W., Maxwell, D.P. and Trick, C.G., 1996b. Growth, iron requirements, and siderophore production in iron-limited *Synechococcus* PCC 7002. Limnol. Oceanogr., 41(1): 89-97.
- Witter, A.E. and III, G.W.L., 1998. Variation in Fe-organic complexation with depth in the Northwestern Atlantic Ocean as determined using a kinetic approach. Mar. Chem., 62: 241-258.
- Wu, J. and Luther III, G., 1995. Complexation of Fe(III) by natural organic ligands in the Northwest Atlantic Ocean by a competitive ligand equilibration method and a kinetic approach. Mar. Chem., 50: 159-177.

Yee, D. and Morel, F.M.M., 1996. In vivo substitution of zinc by cobalt in carbonic anhydrase of a marine diatom. *Limnol. Oceanogr.*, 41(3): 573-577.

Zhang, H., Van den Berg, C.M.G. and Wollast, R., 1990. The Determination of Interactions of Cobalt (II) with Organic Compounds in Seawater using Cathodic Stripping Voltammetry. *Mar. Chem.*, 28: 285-300.

Figure 4-1

⁵⁷Co uptake in *Prochlorococcus* strain MED4-Ax (axenic) under varying metal buffer conditions and ⁵⁷Co concentrations. As ⁵⁷Co concentrations are increased, more ⁵⁷Co is taken into cells. Yet as the metal-ion buffer strength increases (K_{Co} for NTA<EDTA<DTPA) uptake of cobalt into the cell decreases. 10⁻⁵M NTA, EDTA, and DTPA were allowed to equilibrate overnight with ⁵⁷Co prior to addition of cells (2.8 x 10⁷ cells/mL for all treatments)

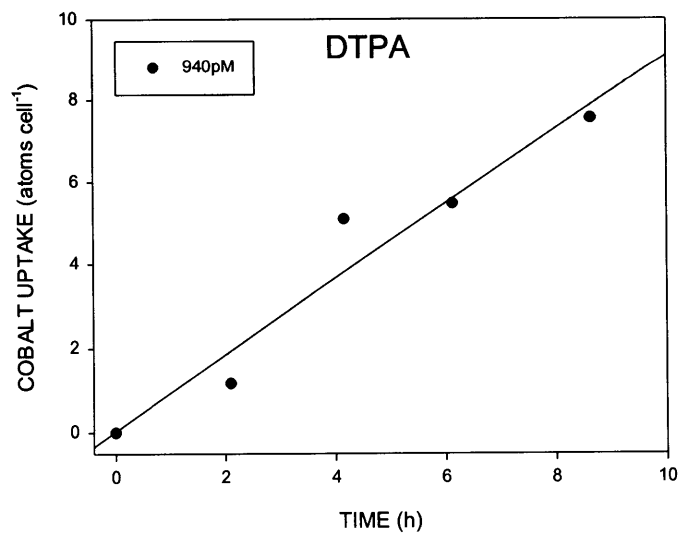
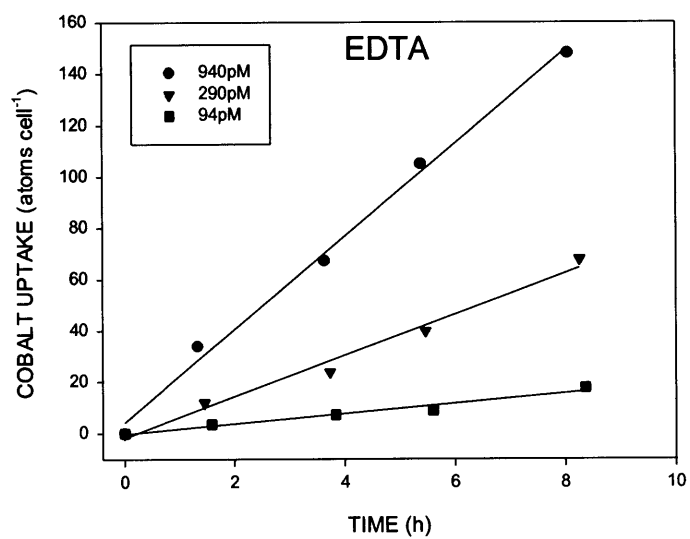
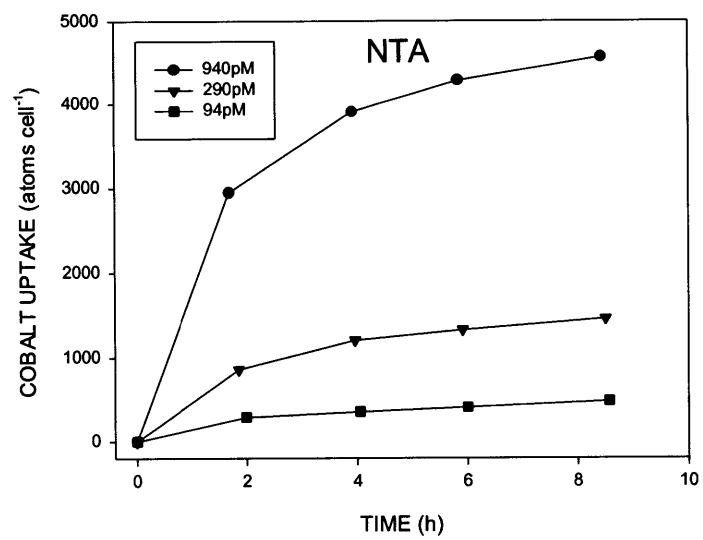


Figure 4-2

A) The effect of adding conditioned media, which contains the putative cobalophore, on cobalt uptake in *Prochlorococcus* strain MED4-Ax (2.8×10^7 cells/mL in all treatments). The conditioned media must contain strong ligands capable of removing some of the ^{57}Co from the large CoEDTA reservoir (99.88% of total cobalt before adding conditioned media) during the 12h equilibration period in order to increase uptake rates by 108% relative to the fresh media control. Glutaraldehyde killed cells are shown as an additional control with no significant ^{57}Co uptake. 2B and 2C) The rate of uptake calculated from data in Figure 1A, 1B, 1C, and 2A (slope of ^{57}Co uptake versus time) are plotted with respect to total and free cobalt concentration. For cells in fresh media (all solid symbols) uptake rates are significantly different between the three metal-ion buffers at a constant total cobalt concentration (2B), indicating that uptake is not proportional to total cobalt. However, when the binding affinities of those the metal-ion buffers are taken into account, uptake rates correlate with the resulting free cobalt (Co^{2+}) concentrations (2C). This indicates that when cells are rinsed and placed in fresh media uptake rates are governed by the free metal concentration rather than the total metal concentration. This free cobalt uptake is additional to the hypothesized enhanced uptake of organically complexed cobalt observed with conditioned media additions (2A) and plotted as a rate (2B). Based on these results, the free-ion uptake system and a cobalophore uptake system do not seem to be mutually exclusive. This experiment is modeled after the classic free-ion model iron experiment of Anderson and Morel (1982), using Co(II) instead of Fe(III) and adding the “cobalophore” experiment (2A) for comparison.

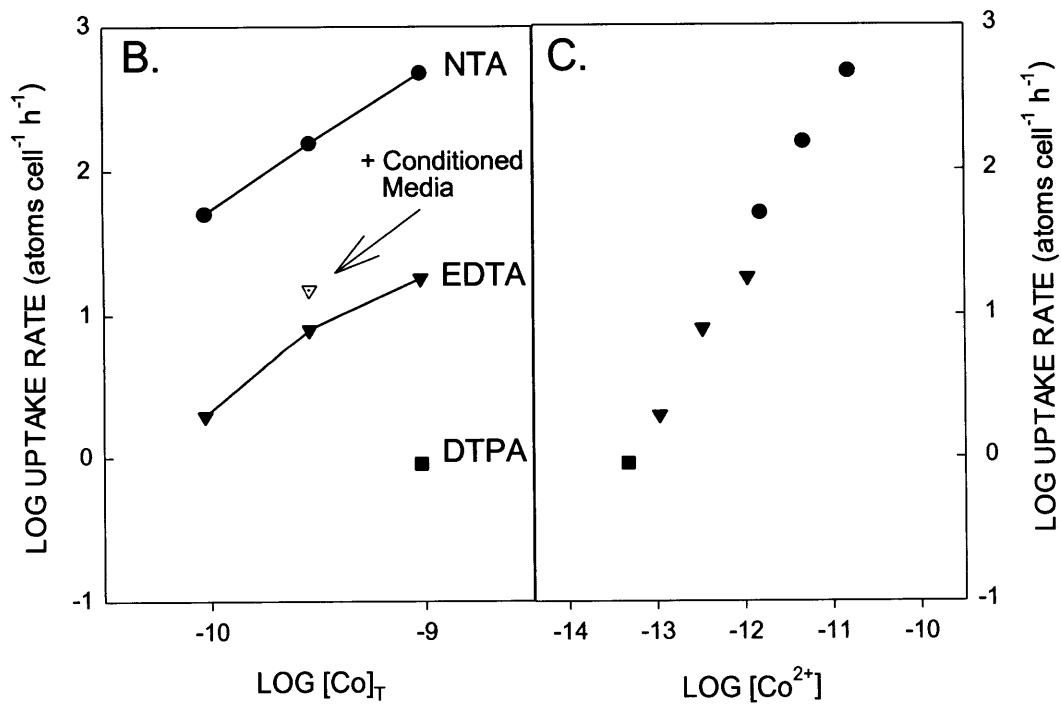
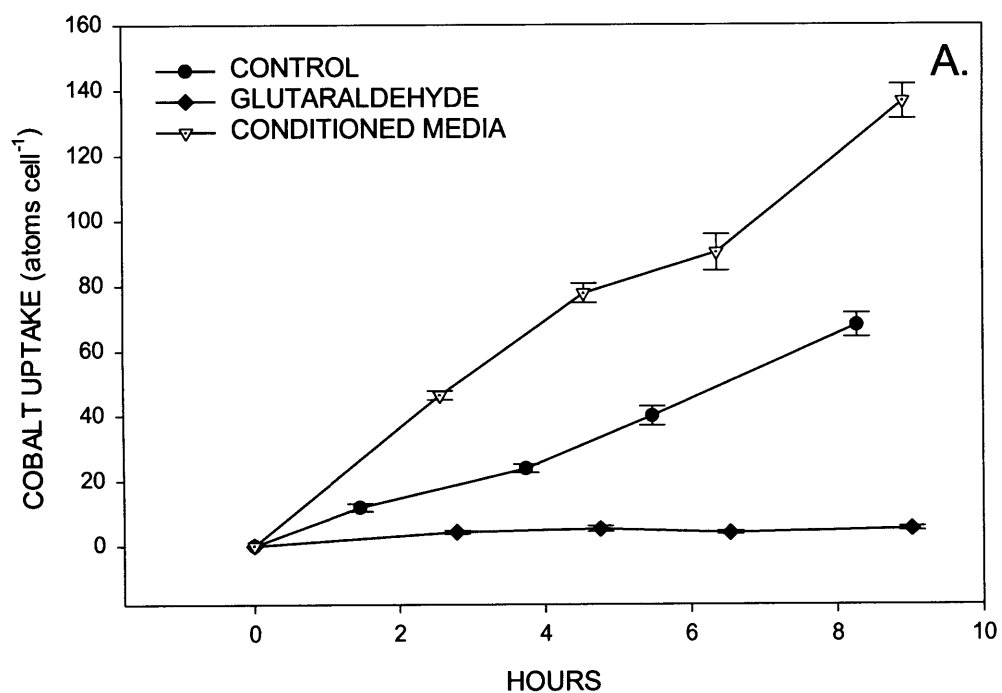


Figure 4-3

Relative growth rates of *Prochlorococcus* MED4 as a function of free (A) and total (B) cobalt in two different metal ion buffers: one EDTA as the synthetic ligand and one with NTA. Note that when plotted against the Co^{2+} concentration growth curves differ significantly, whereas when plotted against the total cobalt concentration the curves align, indicating that given both time and sufficient inoculum volume (2.2%) to condition their media these cultures are able to compete for cobalt by competition with the synthetic metal buffer. Long-term culturing studies were conducted with *Prochlorococcus* isolate MED4 and axenic strain MED4-Ax in NTA and EDTA medium (100 μM and 11.7 μM), respectively, for several months in batch culture using sterile and trace metal clean technique. Growth rates normalized to the growth rate of the highest cobalt concentration in each experiment.

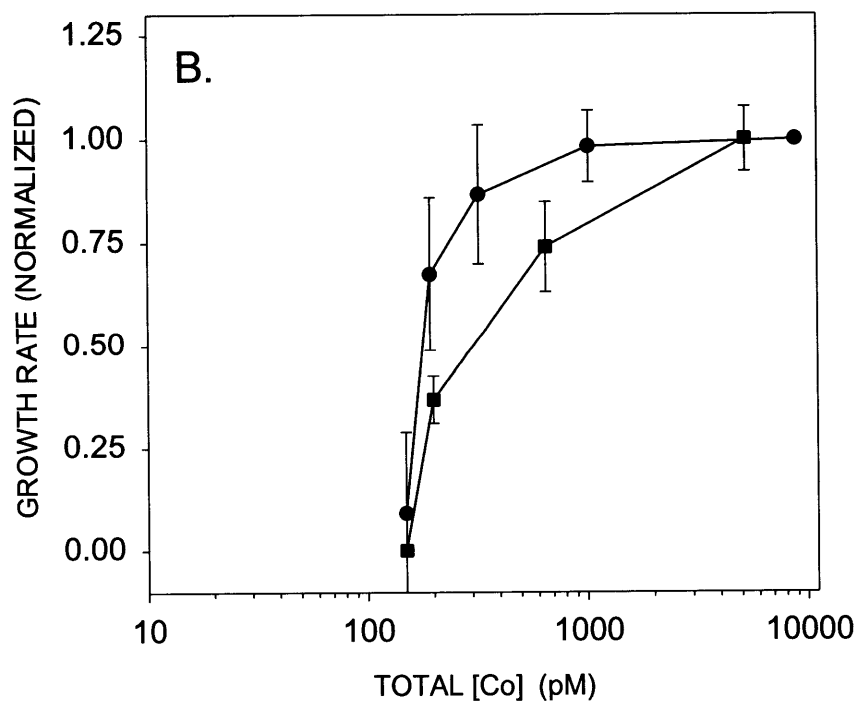
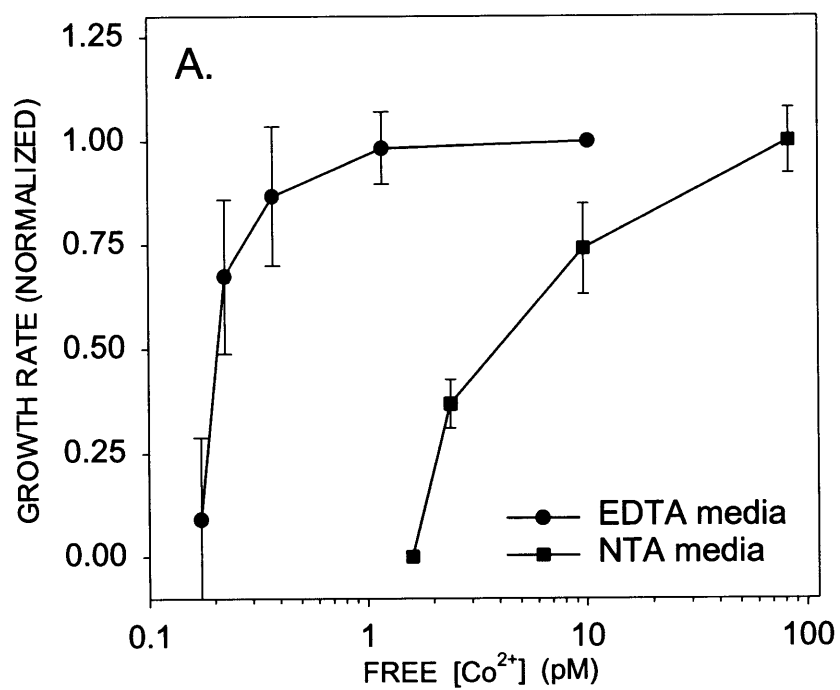


Figure 4-4

The influence of conditioned media additions on the growth of *Prochlorococcus* cultures. Additions of conditioned media (5% by volume, added on day 4) show an increase in growth of *Prochlorococcus* (isolate SS120) relative to a low cobalt control. The cobalt blank in the media before adding cobalt was equal to 119pM and in the conditioned media after filtering was 82pM. All treatments were inoculated from a single low cobalt culture with a 0.08% inoculum volume to dilute out any biogenic cobalt ligands present. Due to this low inoculum volume, the experiment begins below the detection limit of this fluorometer (-0.9) as shown by the horizontal line. While variability in fluorescence per cell can obfuscate attempts to convert *in vivo* fluorescence to cell number, this experiment is qualitatively comparing growth of treatments started from the same inoculum and hence is not subject to such interpretive problems (see Appendix III. for extensive discussion).

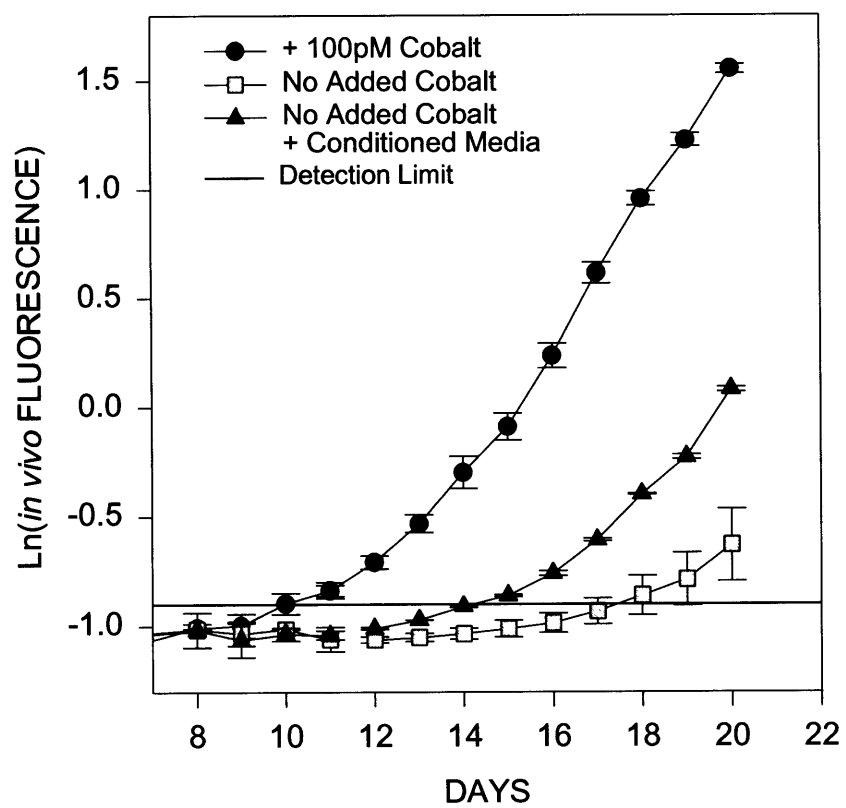


Figure 4-5

Nickel inhibition of cobalt-limited cultures. *Prochlorococcus* cultures grown with 8nM nickel addition were significantly delayed in growth relative to no nickel added controls. For comparison additions of 6.4nM zinc did not create the same delay. These results are consistent with the thermodynamic databases that show most strong cobalt ligands are also strong nickel ligands. A small inoculum volume of 0.08% was utilized to minimize the influence of biogenic ligands that may be carried over in the inoculum, and the equal volumes of inoculum given to treatments allow intercomparison of growth curves. Due to this small inoculum volume, measurements begin below the detection limit of the fluorometer (-1.7), datapoints below the detection limit are not shown here.

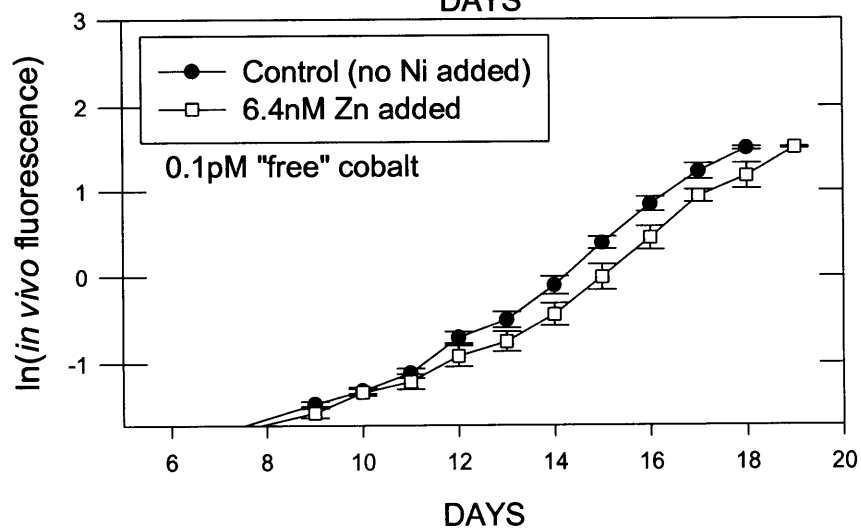
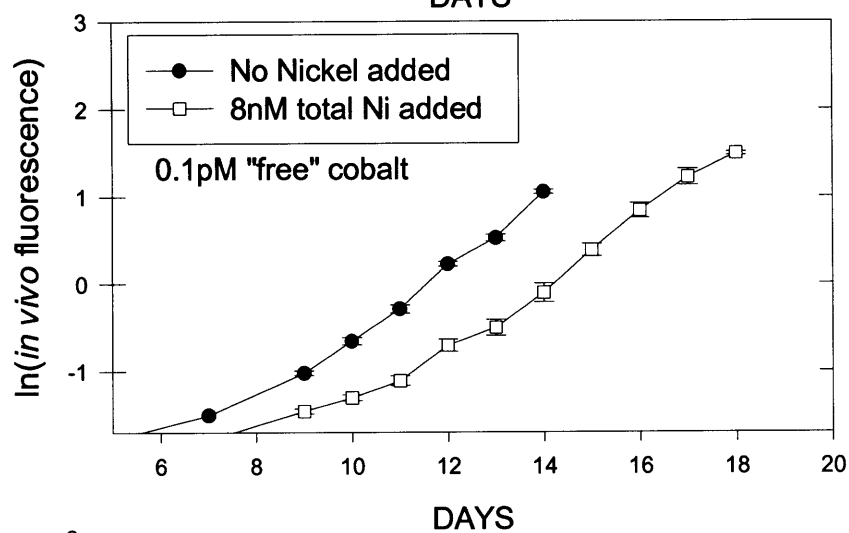
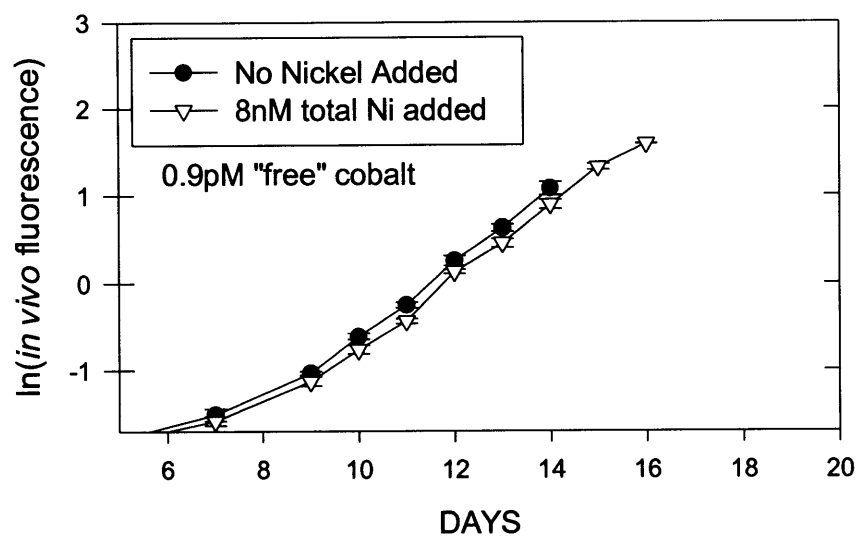


Figure 4-6

Total cobalt and cobalt speciation at the Costa Rica Upwelling Dome. A) High deepwater concentrations of total cobalt were depleted upon upwelling to surface waters. This nutrient-like profile is likely the result of biological drawdown by the *Synechococcus* bloom. B) Cobalt speciation indicated that the upwelling waters contained significant amounts of labile (inorganic) cobalt and as the waters approached the surface waters cobalt became increasingly complexed by strong cobalt ligands in the *Synechococcus* bloom.

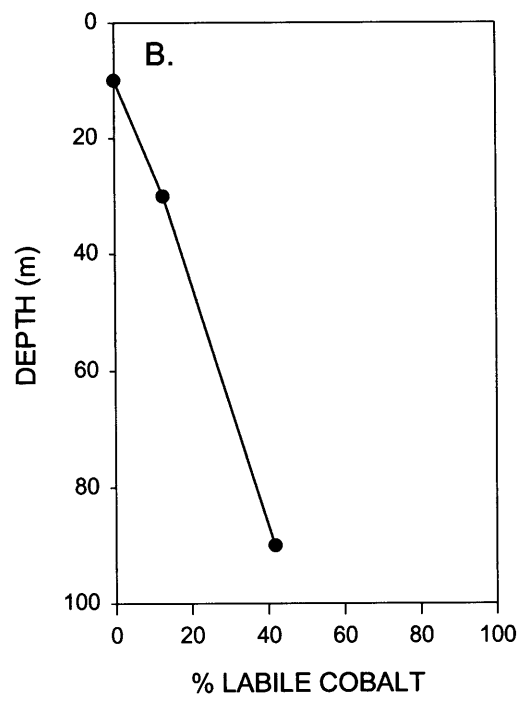
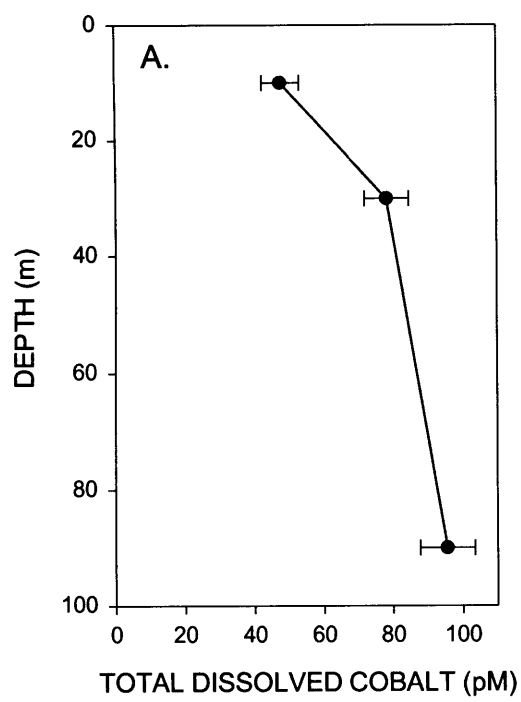


Figure 4-7

A) The effects of added cobalt and iron on the total chlorophyll in a 2d bottle incubation. Surface waters of the Costa Rica Upwelling Dome were incubated with 1nM FeSO₄ and/or 500pM CoCl₂. The addition of Fe and Co alone did not result in a significant increase in chlorophyll after two days, but together they caused an ~30% increase in chlorophyll relative to chlorophyll at the start of the experiment. B) Changes in cobalt speciation in a bottle incubation with added cobalt and iron. Cobalt added to bottle incubation experiments became completely complexed by strong organic ligands after 4 days of incubation relative to a filtered control, which was also incubated for 4 days after filtration and addition of cobalt. These speciation results, as measured by CLE-ACSV, indicate that the microbial community or the particulate matter was responsible for production of these cobalt ligands. C) Percent of the total cobalt bound to strong organic ligands.

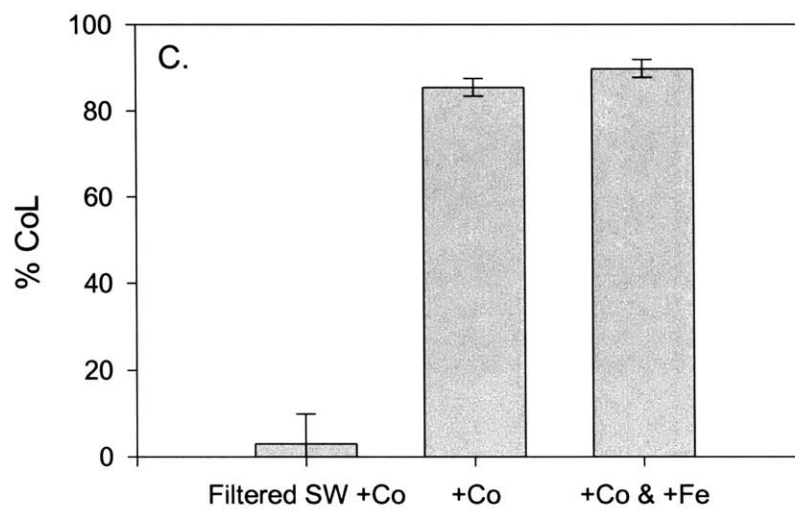
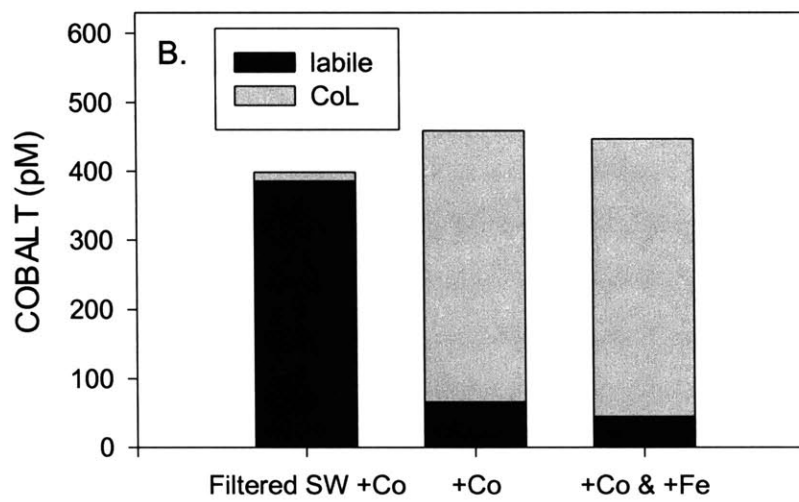
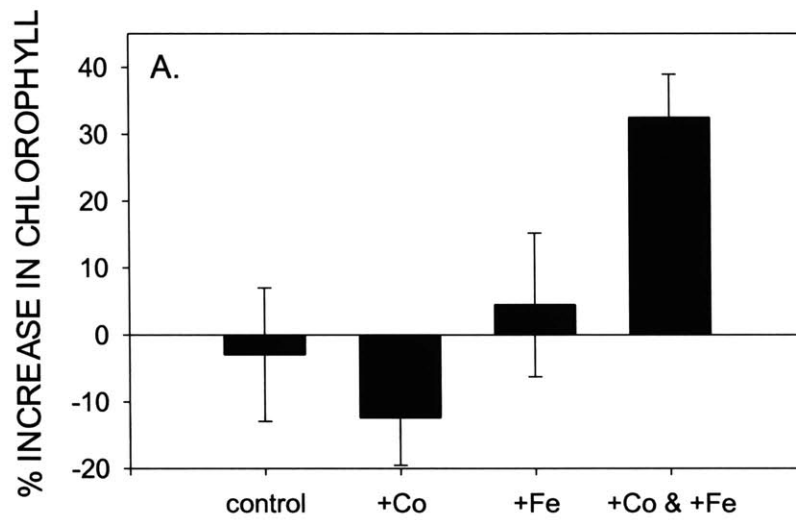


Figure 4-8

Cobalt and zinc non-substitutability in *Prochlorococcus*. The absolute requirement for cobalt in *Prochlorococcus* is not affected by modulations in zinc concentration.

However, slight zinc limitation is observed in this experiment. Sunda and Huntsman also found a small zinc requirement in *Synechococcus* at zinc concentrations that were severely limiting to eukaryotic phytoplankton (pers. comm. and 1995, see Figure 3 of Chapter 1).

This data set is given with standard deviations calculations and total cobalt and zinc values in Table 1.

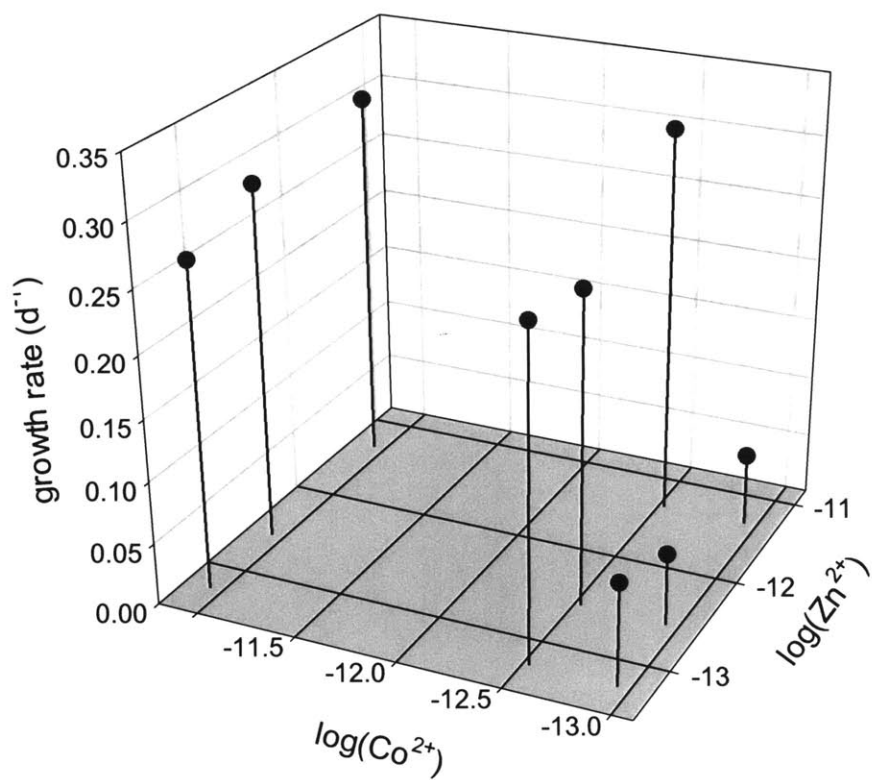


Figure 4-9

Cobalt and cadmium substitution in *Prochlorococcus* strain SS120. All culture tubes were started from the same inoculum on the same day allowing treatments to be compared. Due to the small inoculum volumes (0.08%) used to dilute out any influence from biogenic ligands, the cultures began below the detection limit of the fluorometer (-0.9, data below detection limit not shown).

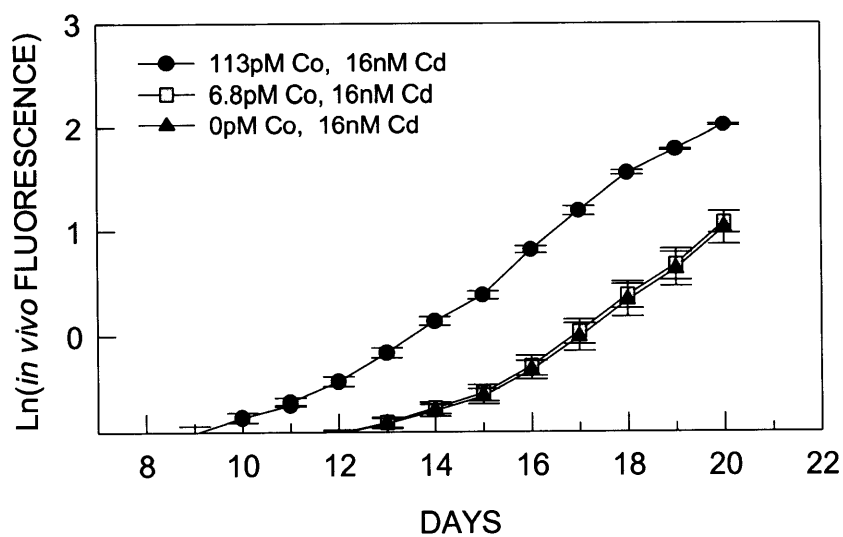
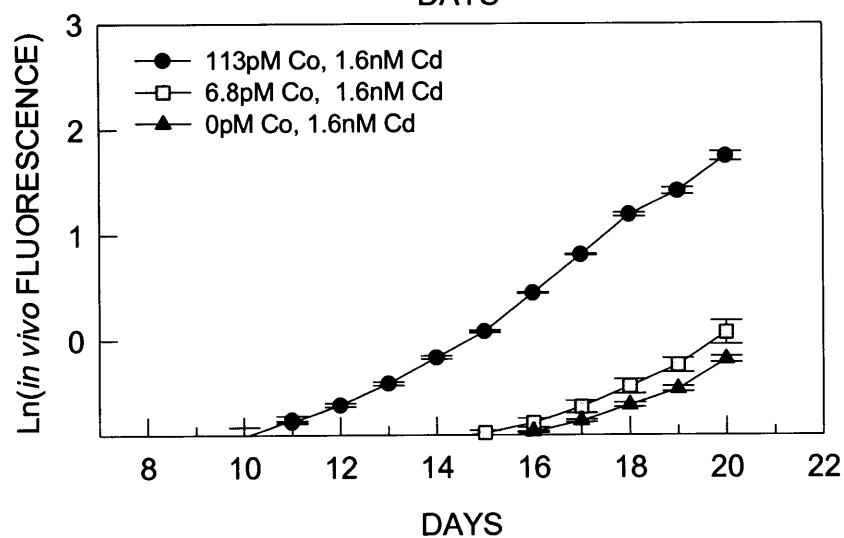
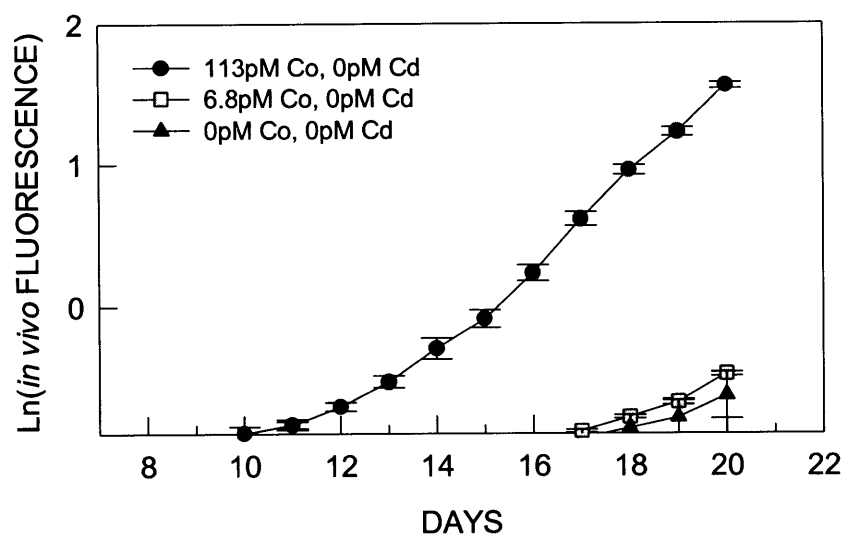


Table 4-1 Growth rates of *Prochlorococcus* zinc and cobalt limitation experiment shown in Figure 8.

Total Cobalt Log(Co) (M)	Total Zinc Log(Zn) (M)	μ (d ⁻¹)	Standard Deviation
-8.0	-8.1	0.32	0.0064
-8.0	-9.3	0.29	0.0042
-8.0	-10	0.28	0.014
-9.6	-8.1	0.32	0.0079
-9.6	-9.3	0.25	0.020
-9.6	-10	0.26	0.010
-10	-8.1	0.06	0.015
-10	-9.3	0.06	0.013
-10	-10	0.08	0.020

Chapter 5

The Influence of Cobalt Limitation on the Cell Cycle of *Prochlorococcus*

Mak A. Saito

*Massachusetts Institute of Technology/Woods Hole Oceanographic Institution Joint
Program in Chemical Oceanography, Woods Hole, Massachusetts 02543, USA,
msaito@whoi.edu*

Sallie W. Chisholm

*Department of Civil and Environmental Engineering and Department of Biology, 48-425,
Massachusetts Institute of Technology, Cambridge MA 01239, USA, chisholm@mit.edu*

William G. Sunda

*Beaufort Laboratory, NOAA, 101 Pivers Island Rd., Beaufort, North Carolina 28516
bill.sunda@noaa.gov*

James W. Moffett

*Department of Marine Chemistry and Geochemistry, Woods Hole Oceanographic Institution,
Woods Hole MA 02543, USA, jmoffett@whoi.edu*

Abstract

Little is known about the biochemical function of cobalt in the photosynthetic cyanobacteria. The physiological effects of cobalt limitation on the cell cycle of *Prochlorococcus marinus* strain MED4-Ax were studied using DNA stains and flow cytometric analyses. Cultures were grown in batch culture at constant light and low growth rates in order to adhere to the slow-growth model for the prokaryotic cell cycle. Cobalt limited cells showed an increase in the proportion of cells in G2 relative to cobalt replete cultures during both exponential growth and stationary phase, indicating an increase in duration of G2 as growth rate decreased. Iron, phosphorus, and nitrogen limited batch cultures were grown for comparison with these cobalt studies. Iron limitation did not shift the proportion of cells in each cell cycle stage as the batch culture moved from exponential growth to stationary phase. Under nitrogen limitation, cells arrested in G1, S and G2 at the onset of stationary phase. Phosphorus limitation caused a significant build-up of cells in S phase, consistent with previous findings. The increase in duration of G2 is consistent with our hypothesis about the possible existence of cobalt DNA transcription factor proteins, and it is similar to the cell cycle results of zinc limited *Euglena* cells, which are known to have numerous zinc containing DNA transcription factors. In addition, the observation that the proportion of cell cycle stages changes in exponential growth under severe cobalt limitation raises questions about the applicability of the free-ion model in cobalt-limiting *Prochlorococcus*. Moreover, these results suggest that *in situ* *Prochlorococcus* growth rate measurements using cell cycle analysis would not be subject to artifacts from N, P, Co, or Fe limitation.

Introduction

For decades oceanographers have explored the possibility that individual chemical elements or molecules might limit the biological productivity of the surface ocean. Nitrogen (Cullen, 1999) and iron (Martin and Fitzwater, 1988) are thought to be the major limiting nutrients in the surface oceans. Other elements such as phosphorus, carbon, zinc, and cobalt have been measured in such low concentrations that workers have hypothesized that they may also be limiting productivity (Karl, 1999; Morel et al., 1994; Riebesell et al., 1994; Sunda and Huntsman, 1995b). Under nutrient limitation, phytoplankton undergo physiological changes in response to the shifting chemical conditions eventually resulting in retardation or cessation of growth, as occurs in the stationary phase of batch cultures. Studies of the impact of nutrient limitation on population assemblages in the field have been numerous; however, while these studies are invaluable in understanding the ecology of natural environments, they are composite averages of the behavior of populations of species. The adoption of cell cycle analyses using DNA stains and flow cytometry has enabled *in situ* species specific measurements of growth rates independent of grazing and mortality terms (Liu et al., 1997; Mann and Chisholm, 2000; Vaultot et al., 1995; Vaultot and Marie, 1999). Workers in cell biology and biological oceanography are interested in the basic biological questions regarding cellular controls on cell cycle regulation; however, those in the latter field are also interested in how environmental parameters might bias *in situ* growth measurements that rely upon cell cycle analysis (Carpenter and Chang, 1988; McDuff and Chisholm, 1982). One inherent assumption in the use of cell cycle methods is that nutrient limitation by different nutrients does not alter the cell cycle in ways that could confound the *in situ* growth rate method.

The study of the cell cycles in photosynthetic prokaryotes is a young field: the cell cycle of the freshwater autotroph *Anacystis nidulans*, and the marine cyanobacteria *Synechococcus* and *Prochlorococcus* have begun to be explored (Armbrust et al., 1989; Binder and Chisholm, 1995; Chisholm et al., 1986; Parpais et al., 1996; Shalapyonok et al., 1998; Vaultot, 1995). The prokaryotic cell cycle is fundamentally different from that of eukaryotes due to differences in cellular ultrastructure, with a singular circular

chromosome and the absence of centrioles and nuclear membranes that are integral to the description of the eukaryotic phenomenon of mitosis. Nevertheless, the modes of the prokaryotic cell cycle can be observationally similar to those of eukaryotic cells: prokaryotic cells can also be described as existing in one of three stages: G1, S, and G2 when growing at slow growth rates. However, when prokaryotic cells are growing rapidly (e.g. *E. coli*), multiple replication forks appear on the chromosome due to a replication period that exceeds the length of the cell cycle itself. In contrast, an ultradian cell cycle has been observed in *Prochlorococcus*, where a cell undergoes more than one division per day with a second round of DNA replication occurring immediately after division (Mann and Chisholm, 2000; Shalapyonok et al., 1998). Moreover, *Synechococcus* has been observed with multiple DNA peaks at low growth rates in a laboratory study (Binder and Chisholm, 1995). The cell cycle of *Prochlorococcus* has been observed to be tightly entrained with regards to the diel light cycle (Vaulot et al., 1995).

Olson et al. (Olson, 1986) discussed two approaches to examining the influence of nutrient limitation on the cell cycle. The first approach involves completely depriving the culture of the nutrient of interest and examining which cell cycle stages the cells arrest in when population growth ceases (the starvation approach). This would help to identify cell cycle checkpoints, which are cellular control mechanisms that prevent the cell from progressing to the next cell cycle stage. The second approach involves calculating the duration of time spent in each cell cycle stage across a range of growth rates. This variation in growth rate is induced by varying the limiting nutrient of interest in a batch culture (Slater et al., 1977; Vaulot et al., 1987; Parpais et al., 1996) or chemostat (Olson et al., 1996; Armbrust et al., 1989; Binder, 2000). An increase of a cell cycle stage's duration in response to a decrease in growth rate is thought to indicate that stage's sensitivity to the limiting nutrient. These two approaches differ in that the first looks at the cells in stationary phase while the second observes cells in exponential growth. Using metal-buffered media, it is theoretically possible to mimic a chemostat system in a batch culture because of the presence of a large reservoir of biologically unavailable metal (e.g. CoEDTA^{2-}) that is in equilibrium with free metal ions (Co^{2+}). It has been shown that phytoplankton cultures respond to the free-ion concentrations of metals

(Anderson and Morel, 1982), unless uptake ligands with high affinities for specific metals, such as iron-siderophores, are present (Wilhelm et al., 1996).

In this study, we have explored the influence of nutrient limitation on the cell cycle of axenic *Prochlorococcus* strain MED4-Ax, utilizing both starvation studies and cell cycle stage duration studies for cobalt, and the latter approach for ammonia, phosphorus, and iron under identical light, temperature, and culture media conditions.

Methods

Axenic *Prochlorococcus marinus* was grown in Pro-1 K-Media (Chisholm et al., 1992) as described in Table 1. All media was made with filtered Sargasso Seawater in a Class-100 cleanroom environment and microwave sterilized (Keller et al., 1988). All plasticware was cleaned with acidic detergent (CitranoX) in Milli-Q water overnight, followed by 10% HCl soak for 48h at 60°C, a pH 2 Ultrex II HCl (Baker) rinse and soak, and microwave sterilization. Major nutrients were combined and run through a pretreated chelex-100 (Bio-Rad) column at pH 8 (Price et al., 1988/1989), then filtered sterilized through 10% HCl acid (Baker Instra-analyzed) and pH 2 Milli-Q water rinsed 0.2µm acrodisks and all-plastic syringes, with the exception of N and P limitation studies where sterile solutions of ammonia and phosphoric acid were added independently and were not treated with chelex-100.

Cultures were grown under $17\mu\text{E m}^{-2}\text{s}^{-1}$ constant light in a 23°C incubator in 28mL polycarbonate tubes, and had been acclimated to constant light for several months. *In vivo* fluorescence and flow cytometry samples were taken every two days from inoculation until late stationary phase. Each nutrient limitation treatment was carried out in duplicate with non-invasive *in vivo* fluorescence measured on both replicates and invasive 0.6mL aliquots taken on one replicate and placed in 0.125% glutaraldehyde and frozen in liquid nitrogen until flow cytometry analysis. Trace metal certified pipette tips were rinsed with concentrated Ultrex II HCl (Baker) and thrice with pH 2 Ultrex II HCl immediately before use to remove metal contamination and for sterilization. Using this sampling scheme, metal contamination caused by invasive sampling was easy to detect by discrepancies in *in vivo* fluorescence between replicates, and experiments were repeated when this occurred. *In vivo* fluorescence was measured on a Turner AU-10

fluorometer. Growth rates were calculated using the slope from linear regressions of exponential phase culture data.

Flow cytometric analysis was carried out on a FACScan Becton Dickinson flow cytometry (Dusenberry and Frankel, 1994), modified to use a syringe pump (Harvard Apparatus, Model 22) with a constant flow rate of 10 μ L/min. Cells were thawed for three minutes in a 35°C water bath and vortexed briefly. Aliquots were diluted into sterile filtered Sargasso Seawater, incubated with RNAase A (Sigma-Aldrich R-4875) for 30m at 37°C at a final concentration of 1 μ g/mL and cooled on ice for 5m. Cells were stained with a 1:10⁻⁴ final dilution of Sybr Green I (Molecular Probes) and 30 μ M of citrate buffer for 15m in the dark prior to analysis. Working stock solutions of Sybr Green were prepared in DMSO (Marie et al., 1997). Output from the green photomultiplier tube (PMT) was collected in linear mode with the voltage set to optimize measurements DNA stained cells. The coefficients of variation (% CV) on the green fluorescence PMT in linear mode were typically ~4%. The G2 peak is expected to appear at two times the value of the G1 peak, corresponding to twice the DNA content per cell. The ratio of green fluorescence intensity of cells in G2 to cells in G1 was 2.002 \pm 0.026, indicating a high degree of precision in our analyses. 20000 to 40000 events were counted for each sample analysis, and the green PMT histograms were analyzed in ModFit (Verity Software House, Inc.) for the percentage of cells in each cell cycle stage. Plots of histograms were generated by exporting raw data to MATLAB, normalizing each histogram to the total number of events, and plotting on axes of equal scale.

Duration of cell cycle stages were calculated using the percent age of cells in each cell cycle stage and growth rates (calculated from changes in cell number over time during exponential growth) using the Homogeneous Daughter Model from Slater et al. (Slater et al., 1977):

$$T(G1) = - (t_d/\ln 2)(\ln(1-[P(G1)/2])) \quad (1)$$

$$T(G2) = (t_d/\ln 2)\ln(1+[P(G2)]) \quad (2)$$

$$T(S) = (t_d/\ln 2)\ln(1 + P(S)/[1+P(G2)]) \quad (3)$$

where T is the length of time the cells spend in a particular cell cycle stage, t_d is the doubling time of the population, and P refers to the percentage of cells in cell cycle stages G1, G2, and S. These equations assume simple binary fission, with a constant cycle time for all cells. This is in contrast to the Mixed Mother-Daughter Model where cell division yields two unequal offspring, a "mother" and "daughter" cell, typical of the budding-style of cell division found in *Saccharomyces cerevisiae* (Slater et al., 1977). In this case, the mother cell has no G1 stage and gives rise to a new bud immediately. As a result, the mother has a significantly shorter life cycle than the daughter cell, which must complete G1 before entering S and G2 (Slater et al., 1977). The application of the Homogeneous Daughter Model to batch cultures of photosynthetic cyanobacteria is appropriate, given that these Homogeneous Daughter equations were derived for use with batch cultures of *Saccharomyces cerevisiae*, and has been applied in several studies of phytoplankton cultures (Olson et al., 1986; Vaultot et al., 1987, Armbrust et al., 1989; Brzezinski et al., 1990; Binder and Chisholm, 1995; Parpais et al., 1996, Binder, 2000).

There are two assumptions in the Homogeneous Daughter Model: 1) a constant cycle time for all cells (equal to the doubling time), and 2) the times for the various phases are assumed constant over all the cells and whose sum is the doubling time (Slater et al., 1977):

$$T(G_1) + T(S) + T(G_2) = t_d \quad (4)$$

The estimation of the doubling time of a microbial population involves measuring the rate of change in cell number (or a proxy for cell number such as radiocarbon uptake or increases in chlorophyll) with respect to time. Hence, this measurement is an aggregate of the doubling times of cells in the population, effectively averaging any variability in the growth rates of individual cells in the population. The two assumptions for the Homogeneous Daughter Model are not valid when subpopulations exist that are distinct beyond this natural variability of the doubling time of cells in a population. Two examples of this are: 1) when a cell divides into 'mother' and 'daughter' cells, and 2) when there is a subpopulation of dying cells. The former example is typical of the budding cell division of *Saccharomyces cerevisiae*, in which the mother cell skips the G1

phase and progresses immediately to S phase after cell division, while the smaller daughter cell buds must grow during a G1 phase. This type of cell cycle results in subpopulations of mother and daughter cells with distinct doubling times, and can be modeled using the Mixed Mother-Daughter Cell Model in Slater et al. (1977). The latter example can be observed in phytoplankton cultures as decreases in chlorophyll per cell, measured as red fluorescence by flow cytometry. No systematic increases in dying cells, as measured by decreases in red fluorescence per cell, were observed during the batch cultures in this study until late stationary phase.

Cell cycle phase duration experiments typically calculate one estimate of phase durations per experimental treatment (e.g. Olson et al., 1986; Brzezinski et al., 1990). In addition to this type of calculation, we have also utilized a three-point moving average growth rate in conjunction with the Homogenous Daughter Model to illustrate how phase durations might vary depending on what portion of the growth curve they are calculated from. This approach to calculating durations does not violate the two assumptions described above as long as subpopulations of dying cells do not become significant⁸.

Results

Cobalt limitation studies

Cobalt limited cultures were grown at four cobalt concentrations: 8800pM, 174pM, 44pM, and 0pM (picomolar) added as sterile CoCl_2 (Figure 1). The culture media cobalt blank of 140 ± 13 pM was measured by cathodic stripping voltammetry of

⁸ It is also conceivable that a range of growth rates might occur because of concomitant asynchronous growth (associated with constant light) and the gradual depletion of a limiting nutrient. This type of phenomenon could increase the spread of growth rates of individual cells in the population, depending on the rate of nutrient drawdown. Yet this effect is characteristically similar to that of the Gaussian-type variability for individual cells in growth rate measurements, as described above. Moreover, it is also clearly distinct from the bimodal subpopulations of mother/daughter cells or growing/dying cells. The Homogeneous Growth Model could be incorporated into a time-stepping model to precisely calculate cell durations during nutrient depletion in batch culture. This model would calculate instantaneous growth rate as a function of Michaelis-Menten kinetics for each individual cell in the population as the limiting nutrient becomes depleted. Given the large increase in durations that must occur in stationary phase, results from such a model would probably not be significantly different from those calculated using the three-point moving average in this chapter.

ultraviolet light irradiated samples as described in Chapter 2. Growth curves for these cultures were measured using both flow cytometric cell numbers and *in vivo* fluorescence. In addition to changes in growth rate, large differences in cell yield were observed, with a 33-fold decrease in cell number yield with 140pM cobalt relative to the 8940pM replete treatments (Figure 1B). A regression of cell number versus *in vivo* fluorescence is shown in Figure 1C.

Sybr Green stained cells are shown in Figure 2 for both cobalt replete and 0pM Co added cells on day 11. Each of these treatments gives rise to DNA-histograms with small and large G2 peaks respectively.

Cell cycle analysis of cobalt limited cells showed an unusual effect where the percentage of cells in G2 begins to increase while the cells were still in mid-log phase in the lowest cobalt treatments (Figure 3E). This increase of cells in G2 continues into stationary phase. This increase in the percentage of cells in G2 was also observed to a lesser extent in the other cobalt treatments (Figure 3B-D), where even the 8940pM cobalt treatment appears to have been cobalt limited (based on comparison with phosphate cell cycle data and the P-limited media composition, see below) due to numerous transfers under stringent trace metal conditions. An examination of the raw histogram data for 8940pM and 140pM cobalt also shows an increase in percentage of cells in G2 (Figure 4).

Cell cycle stage durations are calculated from either batch cultures (Slater et al., 1977; Vaultot et al., 1987, Parpais et al., 1996) or from chemostat cultures in balanced growth (Olson et al., 1986; Armbrust et al., 1989; Binder, 2000). Batch cultures that use metal-ion buffers such as EDTA should operate as chemostats, since free metal ions removed by phytoplankton uptake should be replenished by re-equilibration with metal bound to EDTA. Figures 5A and 5B show the durations of the cell cycle stages calculated in mid-exponential and late-exponential growth. The corresponding relationship between growth rate (presented as doubling times) and cobalt concentrations is shown in Figure 5C. There was a significant increase in the duration of the G2 portion of the cycle, with a smaller increase in the duration of S and no change in the duration of the G1 stage.

Iron Limited Batch Cultures

Iron limited cultures were grown in two treatments, with and without ferric iron additions. A slight decrease in growth rate and an 11-fold reduction in cell yield were observed between these two treatments (Figure 7A). The iron replete control cultures maintained a constant ratio of cells in each cell cycle stage until the beginning of stationary phase, where the percentage of cells in S began to increase (Figure 7B). This response was similar to that of the phosphorus limited culture (Figure 8C) where cells in S stage increased at the onset of stationary phase. Modfit analysis of these two stationary phase cultures looked characteristically similar. The media has an N:P ratio of 25:1 when ammonia (NH_4^+) and urea ($\text{CH}_4\text{N}_2\text{O}$) are summed, resulting in a phosphorus limited media (assuming *Prochlorococcus* has a Redfield N:P stoichiometry of 16:1). The iron limited culture did not change its proportions of cell cycle stages upon entering stationary phase (Figure 7C).

Nitrogen and Phosphorus Limited Batch Cultures

Nitrogen and phosphorus limited cultures were grown for comparison with our cobalt limited experiments. The culture media was prepared without ammonia or phosphorus and the cultures were verified to be limited by these substrates by additions of ammonia or phosphorus to one of the replicates. This addition resulted in a recovery of the population after several days (Figure 8A). The cell cycle analysis results for ammonia and phosphorus limitation are shown in Figure 8B and 8C. During exponential growth a majority of cells were in G1 at a relatively constant percentage, with a slight increase in the number of cells in G1 as the culture neared stationary phase. As the cells began to enter stationary phase, the relative amounts of cells in G1, G2, and S varied dramatically. In the ammonia limited cultures, the percentage of cells in G1 dropped rapidly and the numbers of cells in S and G2 increased correspondingly. The percentage of cells in G1 in the phosphorus limited cultures also dropped rapidly upon entering stationary phase; however, there was an increase in the number of cells in S stage rather than both S and G2 as observed for ammonia limitation. Interestingly, the S peak in the phosphorus limitation study shifted to have an increased amount of DNA upon arrival into stationary phase with an S:G1 DNA ratio of 1.546 ± 0.039 (n=8), relative to the

points in the exponential growth phase (1.456 ± 0.046 , $n=12$). This effect may be caused by the S phase arrest, leaving a fraction of the cells with partial complements of DNA, and thereby increasing the average S:G1 ratio.

Cell Size Data

Forward light scatter (FLS) information was collected as a measurement of cell size for nitrogen and phosphorus limited cultures. FLS data was normalized relative to $0.474\mu\text{m}$ fluorescent beads to adjust to day-to-day variability in flow cytometer sensitivity. FLS for ammonia and phosphorus limited cultures showed a rapid increase in both parameters at the onset of stationary phase (Figure 9A), and a modest decrease in both parameters during exponential growth. When this data is gated to examine the cell size of the cells in G1 and G2 stages, two phenomena are observed (Figure 9B). First, the cells in G2 are significantly larger than those in G1. Second, both cells in G1 and G2 increase in cell size at the onset of stationary phase.

Discussion

Previous cell cycle work in eukaryotic and prokaryotic phytoplankton suggests that cell cycle controls are either not tightly regulated or regulated with multiple checkpoints in the cell cycle (Table 2), as manifested by the observation of populations with significant numbers of cells arrested in their cell cycle stages S and G2. While nitrogen limitation experiments with the eukaryotic phytoplankton species *Thalassiosira weissflogii* and *Hymenomonas carterae* showed that nitrogen starvation caused cells to arrest in the G1 stage of the cell cycle, light limitation experiments with *T. weissflogii* showed that it has two light dependent segments in the cell cycle at both G1 and G2 (Vaulot et al., 1986). These researchers speculated that this was caused by two different light requiring processes in the cell, resulting in cells arresting in both G1 and G2. S phase arrest has been observed before in phosphate limited *Prochlorococcus*, leading to the conclusion that cell cycle controls are not very tight (Parpais et al., 1996), which we also observe in this study. Finally, arrest in G2 has been observed for both silica limitation in *T. weissflogii* and *C. fusiformis* (Brzezinski et al., 1990) and zinc limitation

in *Euglena* (Falchuk et al., 1975a). If cell cycle control is not tightly regulated under nutrient limitation, we should be able to couple these observations of physiological responses with specific biochemical systems requiring that nutrient. Conversely, if the cell cycle were tightly controlled, the influence of phosphorus limitation, for example, would cause strict arrest in G1 since the cell would shut down DNA replication when it determined phosphate was scarce. Some workers have speculated on connections between biochemistry and the cell cycle, such as phosphate's involvement in nucleic acid synthesis and silica's involvement in diatom frustule development, which would result in S and G2 arrest points, respectively (Brzezinski et al., 1990; Parpais et al., 1996). One difficulty in tying these physiological cell cycle observations to specific cellular functions is that a plurality of functions for a major element such as nitrogen or phosphorus may result in multiple arrest points. Trace micronutrients, such as cobalt and zinc, may give more specific cell cycle effects due to potentially fewer, albeit often unknown, biochemical functions. Moreover, the slow growth of our phytoplankton cultures (relative to *E. coli*) may result in the asynchronously dividing populations experiencing different chemical conditions, such as the depletion of cobalt with time, leading to the arrest of cells in different cell cycle stages.

Our results span the range of possible cell cycle arrest points: cobalt causes arrest in all three stages with an increase in the fraction of cells in G2, iron in all three stages but without increase in the fraction of cells in S or G2, ammonia in all three stages, and phosphate in S with many cells still in G1. However, cobalt limitation is unique in that there is a significant increase in the fraction of cells in G2 relative to the other stages, which begins during exponential growth (Figure 3E). Our finding that cobalt limitation causes cells to arrest in G2 is intriguing. Rarely have processes been found that induce cell cycle arrest in G2 (Parpais et al., 1996; Vaultot et al., 1995): two previous observations of a G2 cell cycle effect include silica and zinc limitation in *Thalassiosira weissflogii* and *Euglena*, respectively (Brzezinski et al., 1990; Falchuk et al., 1975a; Falchuk et al., 1975b).

At first comparison, Brzezinski et al.'s silica limited G2 arrest observations in eukaryotic phytoplankton appear similar to the cobalt effect we have observed in *Prochlorococcus*, with approximately an equal number of cells arresting in G2 as in G1.

However, there is a distinct difference: the increase in the proportion of cells in G2 caused by silica limitation begins at the onset of stationary phase, whereas the increase in cells in G2 that we observe begins during exponential growth and continues into stationary phase (Figure 3E, 5A, and 5B). Hence, silica starvation causes cells to arrest in G2, while cobalt limitation causes an increase in the duration of the G2 stage and cobalt starvation causes cells to arrest in G2, as evidenced by the continued increase of cells in G2 after the onset of stationary phase in Figure 3E. The duration of the G2 phase increases throughout the exponential growth portion of the growth curve, as shown in Figure 6. How *Prochlorococcus* is able to continue exponential growth while adjusting the duration of their cell cycle phases is an intriguing problem. Sunda and Huntsman observed that the cellular quota for cobalt can vary by several orders of magnitude in a coastal *Synechococcus* strain in response to limiting conditions (1995b). Hence, *Prochlorococcus* could be adjusting its biochemical operations in order to decrease its cellular quota in response to cobalt limitation, which then manifests itself in an increase in the duration of G2 stage and a shortening of the other stages.

The eukaryotic organism *Euglena gracilis* also arrests in G2 under zinc limitation (Falchuk et al., 1975a; Falchuk et al., 1975b). The authors of this study were perplexed by this observation: they compiled a table of the enzymatic functions of zinc and hypothesized on the likely component of the cell cycle which a lack of that enzyme would affect, but were not able to come up with a zinc containing protein that could induce cell cycle arrest in G2. With the discovery of zinc fingers in 1985 (Miller et al., 1985) this physiological cell cycle observation makes sense: zinc finger proteins are most often involved in the transcription of DNA. By zinc-limiting *Euglena*, the cells moved normally through G1 and S, but once the second set of DNA was completed the cells were not able to transcribe them into proteins due to a lack of the zinc-containing transcription factors. In other words, we speculate that zinc limitation might cause a G2 arrest because the cells would have an insufficient number of zinc transcription proteins to transcribe a doubled quantity of DNA. The net result would be cells that lack the protein-synthesis ability needed to complete cell division.

Our finding that cobalt causes this same rare G2 arrest point is fascinating: is it possible that there are cobalt proteins involved in gene transcription? Are these cobalt

proteins the ancestors to the zinc finger motif now known to be ubiquitous in eukaryotic cells? Given the difficulty in inducing zinc limitation in *Prochlorococcus* (Figure 8, Chapter 4) and our observation of a build-up of cells in G2 under cobalt limitation, our cell cycle data is consistent with the existence of a cobalt finger transcription factors in prokaryotic organisms. However, conclusive proof of this hypothesis awaits the application of molecular and genomic methodologies.

The observation that cobalt limited cells change physiologically during exponential growth and that the biomass yield is proportional to the cobalt concentration has important implications for the application of the free-ion model for cobalt limited cultures. The free-ion model is an important tool for physiological trace metal experiments with phytoplankton cultures and is based on the use of synthetic metal-binding ligands such as EDTA or NTA (Anderson and Morel, 1982). This ligand is added in excess of the total aggregate concentration of metals and binds ~99.9% of the dissolved cobalt in a non-biologically available form (Co-EDTA²⁻). The fact that we observe different cell yields for the cobalt concentrations (Figure 1) suggests that this Co-EDTA²⁻ reservoir is either becoming depleted as cells consume all of the Co²⁺ and cause re-equilibration with Co-EDTA²⁻, or that dissociation of cobalt from Co-EDTA²⁻ is kinetically slower than phytoplankton uptake. The assumption that metal limited batch cultures behave like continuous cultures because of these metal-ion buffers does not seem to hold given these results. If this assumption did hold we should be able to reduce growth rates significantly without depleting the Co-EDTA reservoir. Alternatively, these results are consistent with a strong-ligand cobalt uptake system, where the Co-EDTA²⁻ reservoir is depleted by equilibration with biogenic ligands analogous to iron binding siderophores (Chapter 4). Both the differences in cell yields and the physiological changes in the cell cycle before stationary phase could be caused by the depletion of the entire cobalt reservoir via cobalt ligands.

The array of cell cycle responses we have observed in this paper can also be used to discuss the robustness of the *Prochlorococcus in situ* growth rate method utilizing the cell cycle analysis method. While this is perhaps the most powerful and accurate methodology oceanographers currently have to estimate intrinsic specific growth rates of primary producers independent of viral lysis and grazing, we must be cautious because it

builds on the scarce knowledge we have of cell cycles in marine phytoplankton. The data in this paper and elsewhere (Parpais et al., 1996) indicate that there is not a strong G1 checkpoint for N, P, Co and Fe limitation. If in the natural environment the cell cycle were arrested in S or G2 by nutrient limitation, we should observe the persistence of those stages throughout the diel cycle. In recent field studies, ~95% of the cells are in G1 during the morning hours and then progress into S and G2 stages in the late afternoon (Mann and Chisholm, 2000; Vaultot, 1995) implying that none of those cells are in fact arrested in stationary phase due to nutrient limitation. We would have reason for concern if 1) we observed a type of severe nutrient limitation that causes cells to arrest strictly in G1 (as the eukaryotic cell cycle model does), and 2) and we measure field populations with growth rates of less than a doubling per day. If both of these conditions we observed, it would be difficult to differentiate between cells in stationary phase and cells merely growing slowly and not dividing during the diel study. However, this survey of N, P, Fe, and Co shows that none of these nutrients causes *Prochlorococcus* to arrest solely in G1 upon arrival in stationary phase. In other words, without a “strong” checkpoint in G1 some cells will arrest in S and/or G2 at stationary phase; and hence we should see a significant S and/or G2 peak in the morning if there are *Prochlorococcus* cells in stationary phase in the field.

The Mann and Chisholm (2000) and Vaultot et al. (1995) studies were performed in the iron limited equatorial Pacific. Initial results showed what were then believed to be high growth rates of 0.51-0.63 d⁻¹ for *Prochlorococcus* in the equatorial Pacific (Vaultot et al., 1995) leading to the conclusion that *Prochlorococcus* is not iron limited in this region. The observation that these growth rates can increase significantly upon iron fertilization to ultradian growth rates of 1.1 d⁻¹ (Mann and Chisholm, 2000) has changed this conclusion. The results of this laboratory study showing no change in the proportion of cell cycle stages under iron limitation is curious: the cells seem to freeze in the stage they are in upon arrival into stationary phase. In the Iron Ex II study, the iron limitation was not severe enough to cause any of the *Prochlorococcus* cells to arrest in their cell cycle, as evidenced by no cells arrested in S or G2 (>95% cells were in G1 prior to the synchronized replication time in the afternoon). In fact, even with slower growth rates in the Sargasso of 0.1 to 0.5d⁻¹, no cells are observed arrested in S or G2 throughout the diel

cycle (Mann, 2000). Hence, because there is no strong G1 checkpoint when severely limited by N, P, Co or Fe, these types of limitation should not interfere with the use of DNA cell cycle growth rate techniques. In addition, we can also conclude that *Prochlorococcus* cells in the natural environments examined thus far do not behave like stationary phase cells in culture.

Severe iron limitation appears to cause a general debilitation that affects the progression through all cell cycle stages, resulting in cells frozen in the cell cycle stage they were in previous to limitation. Given the large iron requirement in photosystem I and the numerous other iron containing components of the electron transport chain (Raven, 1990), iron limitation under our continuous light conditions could completely shut down the ability to both photosynthesize and respire carbon for energy. It is known that iron cellular quotas, like cobalt quotas, can vary by several orders of magnitude in marine phytoplankton (Sunda and Huntsman, 1995a). We speculate that since the iron required by the electron transport chain is fundamental to growth and energy production, that iron requirement might be prioritized highest and would be the last portion of the iron quota to be sacrificed under severe iron limitation. Once deprived of this last portion of iron, these components of the electron transport chain would then be lacking, resulting in an energetic paralysis and freezing cells in the cell cycle stage at which they were in at the onset of severe iron limitation. Clearly, more work is necessary to revisit this intriguing iron data set and our speculations as to their cause.

Factors controlling the coupling of cell size and cell cycle in marine phytoplankton appear characteristically different from the *E. coli* model. In *E. coli* there appears to be a simple cell length threshold, which upon exceeding the cell is committed to divide (Donnachie and Begg, 1989). In *Prochlorococcus*, cells entering stationary phase due to N and P limitation increase in cell size but do not divide (Figure 9A). Furthermore, an analysis of the size of individual cells in G1 and G2 under nitrogen limitation showed that while cells in G2 are significantly larger than cells in G1, both types of cells increase in size at the onset of stationary phase (Figure 9B). Hence, *Prochlorococcus* does not seem to have the threshold switch for cell division that is characteristic of *E. coli*: the increase in cell size should trigger division. The observation of large cell size under cobalt and zinc limitation has also been observed with eukaryotic

phytoplankton, especially Co limitation *Emiliania huxleyi* (Sunda and Huntsman, 1995b). Interestingly iron limitation is the exception to this pattern of large cell size with nutrient limitation (Cavender-Bares et al., 1999; Sunda and Huntsman, 1995a), perhaps for the same reasons that we have speculated it to have a unique cell cycle response. It is generally thought that nitrogen limited phytoplankton cells might increase in cell size as a means to store extra carbon materials in anticipation of better nutrient conditions. Hence, a rigid size threshold would not be advantageous for an organism that exists in a low nutrient environment, such as the open ocean. Binder (2000) measured a relatively constant initiation mass (the average cell volume at the time of DNA replication) of $0.41\mu\text{m}^3$ for nitrogen or light limited *Synechococcus* (WH8101) in chemostat cultures. However, Binder noted that this initiation mass increased at growth rates of less than 0.7d^{-1} . Similar results have also been reported for *E. coli* (Wold et al., as cited in Binder, 2000) and are consistent with the results of this study. A mechanism for this deviation from a size or volume related threshold of cell cycle regulation remains to be explained (Herrick et al., as cited in Binder, 2000).

Conclusions

In this work, we have explored the influence of cobalt limitation on the cell cycle of *Prochlorococcus* in comparison to iron, ammonia and phosphorus limitation. Our primary conclusions are that upon entering stationary phase, nutrient limitation can cause unique effects upon the proportion of cells in each cell cycle stage, with cobalt causing an increase in G2 stage, iron freezing the cells in the stage that were in before the onset of stationary phase, nitrogen causing a non-specific arrest in all three stages, and phosphorus causing an increase in S phase. More detailed work with cobalt limitation showed that the increase of the fraction of cells in G2 begins before stationary phase, and that the durations of G2 increased with slower growth rates. This study also shows that Co, Fe, N, and P limitation should not affect the robustness of *in situ* cell cycle growth rate measurements because none of these elements induces a strong G1 arrest in stationary phase. In addition, even slow growing field populations do not behave like stationary

phase cultures with respect to their cell cycle dynamics. Finally, we speculate that an inability to synthesize metal-containing transcription proteins might induce this G2 arrest. Future work should focus on more detailed experiments with each of these and other nutrients, such as combining cell cycle analysis with other molecular and biochemical measurements to test hypotheses of the causes cell cycle arrest points.

References

- Anderson, M.A. and Morel, F.M.M., 1982. The influence of aqueous iron chemistry on the uptake of iron by the coastal diatom *Thalassiosira weissflogii*. *Limnol. Oceanogr.*, 27(5): 789-813.
- Armbrust, E.V., Bowen, J.D., Olson, R.J. and Chisholm, S.W., 1989. Effect of Light on the Cell Cycle of a Marine *Synechococcus*. *Appl. Environ. Microbiol.*, 55(2): 425-432.
- Binder, B. 2000. Cell Cycle Regulation and the Timing of Chromosome Replication in a Marine *Synechococcus* (Cyanobacteria) During Light- and Nitrogen-Limited Growth. *J. Phycol.* 36. 120-126.
- Binder, B.J. and Chisholm, S.W., 1995. Cell Cycle Regulation in Marine *Synechococcus* sp. Strains. *Appl. Environ. Microbiol.*, 61(2): 708-717.
- Brzezinski, M.A., Olson, R.J. and S.W.Chisholm, 1990. Silicon availability and cell-cycle progression in marine diatoms. *Mar. Ecol. Prog. Ser.*, 67: 83-96.
- Carpenter, E.J. and Chang, J., 1988. Species-specific phytoplankton growth rates via diel DNA synthesis cycles. I. Concept of the method. *Mar. Ecol. Prog. Ser.*, 32: 139-148.
- Cavender-Bares, K.K., Mann, E.L., Chisholm, S.W., Ondrusek, M.E. and Bidigare, R.R., 1999. Differential Response of equatorial Pacific phytoplankton to iron fertilization. *Limnol. Oceanogr.*, 44(2): 237-246.
- Chisholm, S., Armbrust, E.V. and Olson, R., 1986. The Individual Cell in Phytoplankton Ecology: in Cell Cycles and Applications of Flow Cytometry. : 343-369.
- Chisholm, S.W. et al., 1992. *Prochlorococcus marinus* nov. gen. nov. sp.: An oxyphototrophic marine prokaryote containing divinyl chlorophyll a and b. *Arch. Microbiol.*, 157: 297-300.
- Cullen, J.J., 1999. Iron, nitrogen, and phosphorus in the ocean. *Nature*, 402(6760): 372.
- Donnachie, W. and Begg, W.J., 1989. Cell Length, Nucleoid Separation, and Cell Division of Rod-Shaped and Spherical Cells of *Escherichia coli*. *J. Bacteriol.*, 171(9): 4633-4639.
- Dusenberry, J.A. and Frankel, S.L., 1994. Increasing the sensitivity of a FACScan flow cytometer to study oceanic picoplankton. *Limnol. and Oceanogr.*, 39(1): 206-209.
- Falchuk, K.H., Fawcett, D.W. and Vallee, B.L., 1975a. DNA Distribution in the Cell Cycle of *Euglena gracilis*. *J. Cell Sci.*, 17.: 57-78.

- Falchuk, K.H., Krishan, A. and Vallee, B.L., 1975b. DNA Distribution in the Cell Cycle of *Eugena gracilis*. Cytofluorometry of Zinc Deficient Cells. *Biochem.*, 14(15): 3439-3444.
- Karl, D.M., 1999. A Sea of Change: Biogeochemical Variability in the North Pacific Subtropical Gyre. *Ecosystems*, 2: 181-214.
- Keller, M.D., Bellows, W.K. and Guillard, R.L., 1988. Microwave treatment for sterilization of phytoplankton culture media. *J. Exp. Mar. Biol. Ecol.*, 117: 279-283.
- Liu, H., Nolla, H.A. and Campbell, L., 1997. *Prochlorococcus* growth rate and contribution to primary production in the Equatorial and Subtropical North Pacific Ocean. *Aquat. Microb. Ecol.*, 12(1): 39-47.
- Mann, E.L., 2000. Trace Metals and the Ecology of Marine Cyanobacteria, Ph.D. Thesis. MIT/WHOI, Massachusetts, 176 pp.
- Mann, E.L. and Chisholm, S.W., 2000. Iron limits the cell division rate of *Prochlorococcus* in the Eastern Equatorial Pacific. *Limnol. Oceanogr.* 45:5. 1067-1076.
- Marie, D., Partensky, F., Jacquet, S. and Vaulot, D., 1997. Enumeration and cell cycle analysis of natural populations of marine picoplankton by flow cytometry using the nucleic acid stain SYBER Green I. *Appl. Environ. Microbiol.*, 63: 186-193.
- Martin, J.H. and Fitzwater, S.E., 1988. Iron deficiency limits phytoplankton growth in the north-east Pacific subarctic. *Nature*, 331: 341-343.
- McDuff, R.E. and Chisholm, S.W., 1982. The calculation of *in situ* growth rates of phytoplankton populations from fractions of cells undergoing mitosis: A clarification. *Limnol. Oceanogr.*, 27.: 783-788.
- Miller, J., McLachlan, A.D. and Klug, A., 1985. Repetitive zinc-binding domains in the protein transcription factor IIIA from *Xenopus* oocytes. *EMBO* , 4(6): 1609-1614.
- Morel, F.M.M. et al., 1994. Zinc and carbon co-limitation of marine phytoplankton. *Nature*, 369: 740-742.
- Olson, R.J., 1986. Effects of Environmental Stresses on the Cell Cycle of Two Marine Phytoplankton Species. *Plant Physiol.*, 80: 918-925.
- Parpais, J., Marie, D., Partensky, F., Morin, P. and Vaulot, D., 1996. Effect of phosphorus starvation on the cell cycle of the photosynthetic prokaryote *Prochlorococcus spp.* *Mar. Ecol. Prog. Ser.*, 132: 265-274.

- Price, N.M. et al., 1988/1989. Preparation and chemistry of the artificial algal culture medium Aquil. *Biol. Oceanogr.*, 6: 443-461.
- Raven, J.A., 1990. Predications of Mn and Fe use efficiencies of phototrophic growth as a function of light availability for growth and of C assimilation pathway. *New Phytol.*, 116: 1-18.
- Riebesell, U., Wolf-Gladrow, D.A. and Smetacek, V., 1994. Carbon dioxide limiation of marine phytoplankton growth rates. *Nature*, 361: 249-251.
- Shalapyonok, A., Olson, R.J. and Shalapyonok, L.S., 1998. Ultradian Growth in *Prochlorococcus* spp. *Appl. Environ. Microbiol.*, 64(3): 1066-1069.
- Slater, M.L., Sharrow, S.O. and Gart, J.C., 1977. Cell cycle of *Saccharomyces cerevisiae* in populations growing at different rates. *Proc. Natl. Acad. Sci.*, 74: 3850-3854.
- Sunda, W. and Huntsman, S., 1995a. Iron uptake and growth limitation in oceanic and coastal phytoplankton. *Mar. Chem.* 50. 189-206.
- Sunda, W.G. and Huntsman, S.A., 1995b. Cobalt and Zinc interreplacement in marine phytoplankton: biological and geochemical implications. *Limnol. Oceanogr.*, 40: 1404-1417.
- Vaulot, D., 1995. The Cell Cycle of Phytoplankton: Coupling Cell Growth to Population Growth. In: I. Joint (Editor), *Molecular Ecology of Aquatic Microbes*. NATO ASI Series, Berlin, pp. 303-322.
- Vaulot, D., D.Marie, Olson, R.J. and Chisholm, S.W., 1995. Growth of *Prochlorococcus*, a Photosynthetic Prokaryote, in the Equatorial Pacific Ocean. *Science*, 268: 1480-1482.
- Vaulot, D. and Marie, D., 1999. Diel variability of photosynthetic picoplankton in the equatorial Pacific. *J. Geophys. Res.*, 104(C2): 3297-3310.
- Vaulot, D., Olson, R.J. and Chisholm, S.W., 1986. Light and Dark Control of the Cell Cycle in Two Marine Phytoplankton Species. *Exp.Cell Res.*, 167: 38-52.
- Vaulot, D., Olson, R.J., Merkel, S. and Chisholm, S.W., 1987. Cell-cycle response to nutrient starvation in two phytoplankton species, *Thalassiosira weissflogii* and *Hymenomonas carterae*. *Mar. Biol.*, 95: 625-630.
- Wilhelm, S., Maxwell, D. and Trick, C., 1996. Growth, iron requirements, and siderophore production in iron-limited *Synechococcus* PCC 7002. *Limnol. Oceanogr.*, 41: 89-97.

Figure 5-1

Growth curves of cobalt-limited cultures. A) *In vivo* fluorescence for the four cobalt treatments. B) Cell number data as measured by flow cytometry. Comparisons of sampled and unsampled replicates by *in vivo* fluorescence was excellent indicating that the sampling for flow cytometry did not contaminate cultures with cobalt. C) Regression of fluorescence to cell number data. Not every *in vivo* fluorescence data point has a corresponding flow cytometry data point.

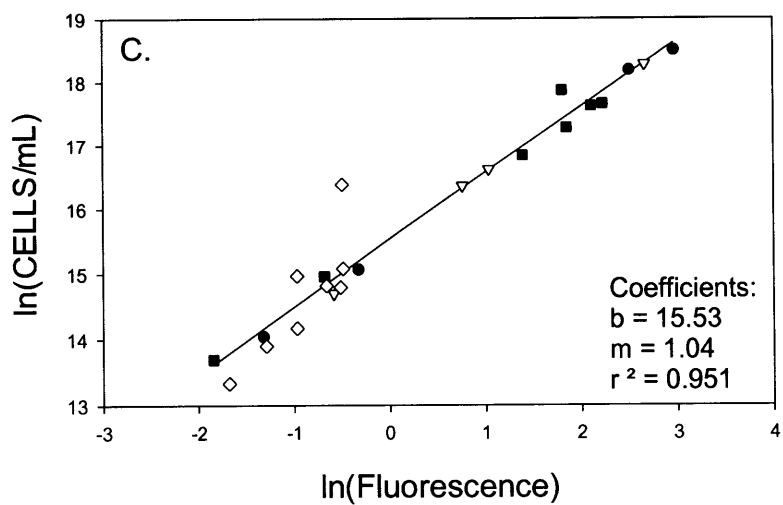
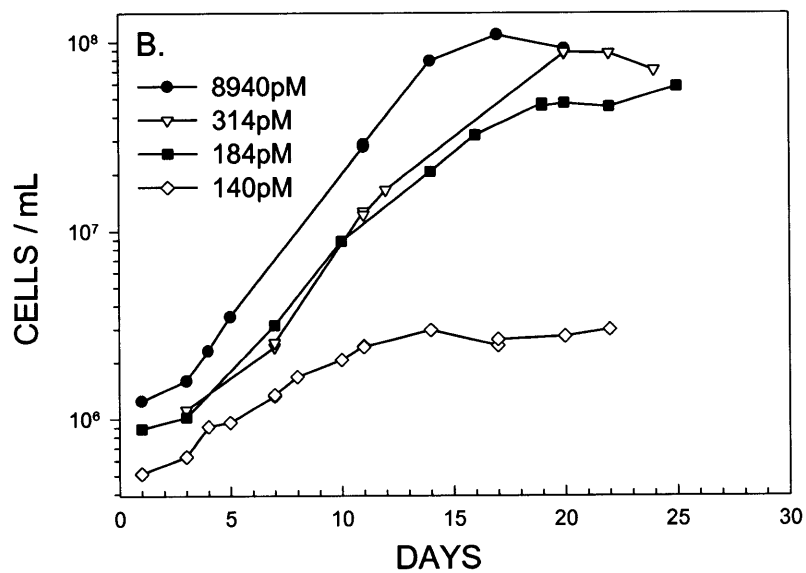
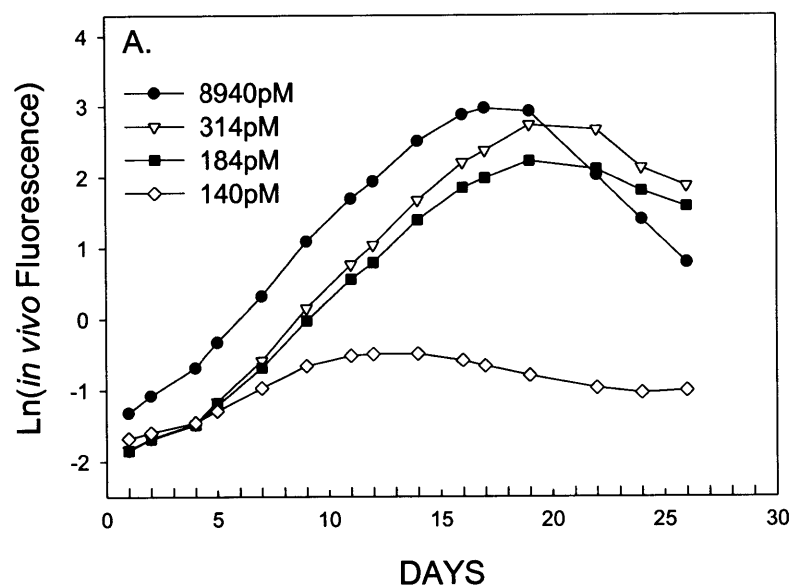


Figure 5-2

Flow cytometry scatter plots of cobalt replete and limited cells stained with Sybr Green. Panels A, B, and C are cobalt limited (140pM total cobalt) from day 11, and D, E, and F are cobalt replete (8940pM total cobalt) also from day 11. Red fluorescence is proportional to chlorophyll per cell, while green fluorescence is proportional to DNA per cell. Cells in cell cycle stage G1 and G2 are grouped into two populations in panels B and E. Histograms of green fluorescence show two distinct peaks associated with G1 and G2 stages in panels C and F. 0.474 μ m beads are added as a standard and to verify precision.

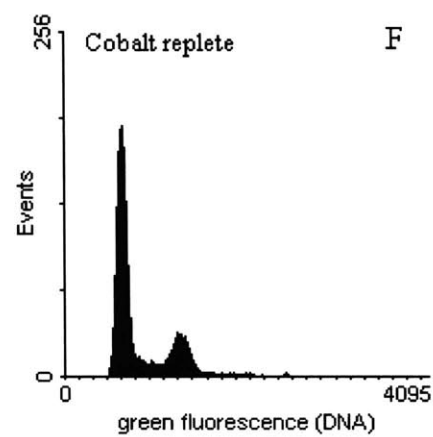
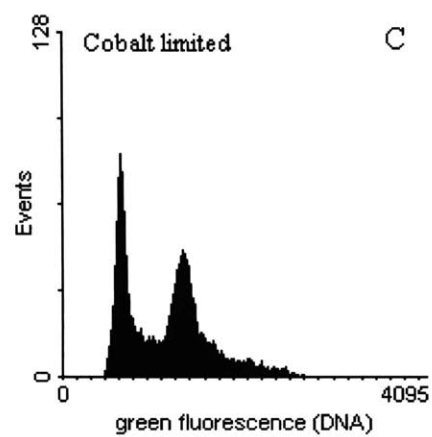
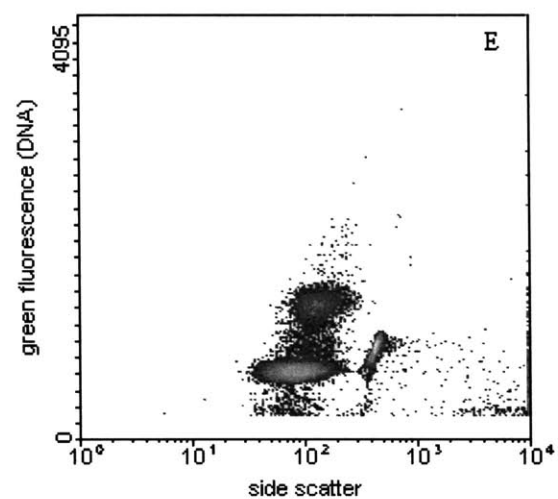
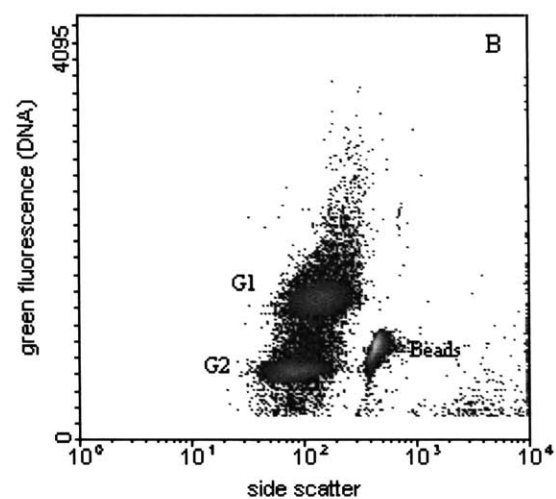
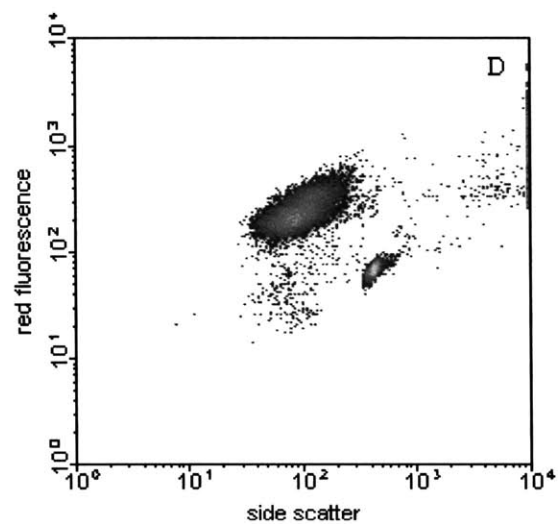
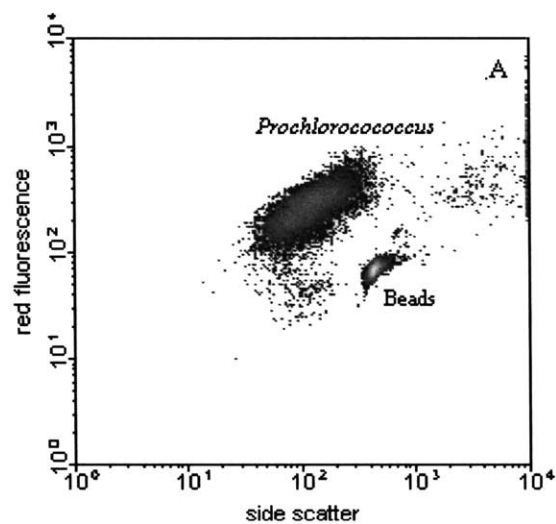


Figure 5-3

DNA analysis of cobalt limited cultures for the four cobalt treatments (A. 8940pM, B. 314pM, C. 184pM, and D. 140pM total cobalt). Due to multiple transfers in this rigorously trace metal clean media it is likely that even the 8940pM cobalt treatment is slightly cobalt limited rather than phosphorus limited. In the 140pM cobalt treatment, the proportion of cells begins to shift from G1 to G2 early in the exponential growth (day 4) and continues into stationary phase. Some data points have replicate analyses plotted as an indication of measurement precision.

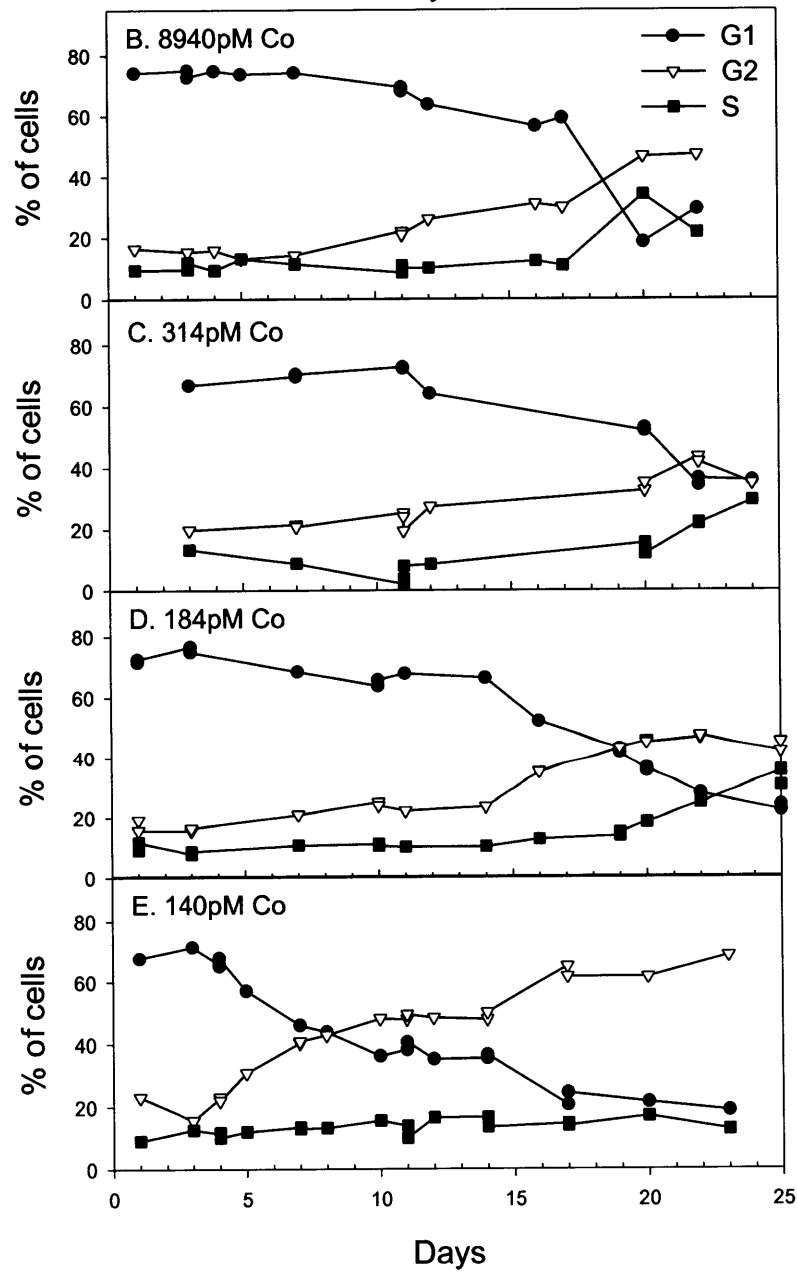
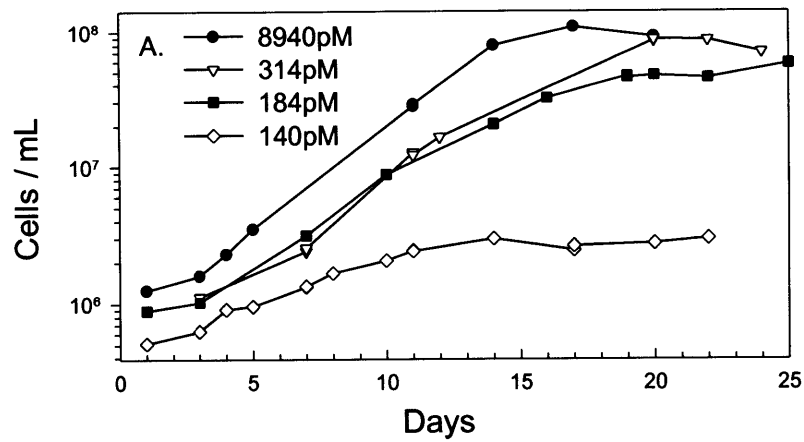


Figure 5-4

Histograms of DNA (green fluorescence versus cell number) as measured by flow cytometry during the exponential and stationary phases for 8940pM and 140pM total cobalt cultures (top and bottom rows, respectively). An increase in the G2 peak is evident during exponential growth 140pM cobalt treatment. In stationary phase (day 17), S peaks are evident on both the G1 and G2 peaks, suggesting that even cells with two sets of DNA are replicating but are unable to divide. Raw data is presented as histograms by normalizing to total cells measured in the sample to make histograms comparable.

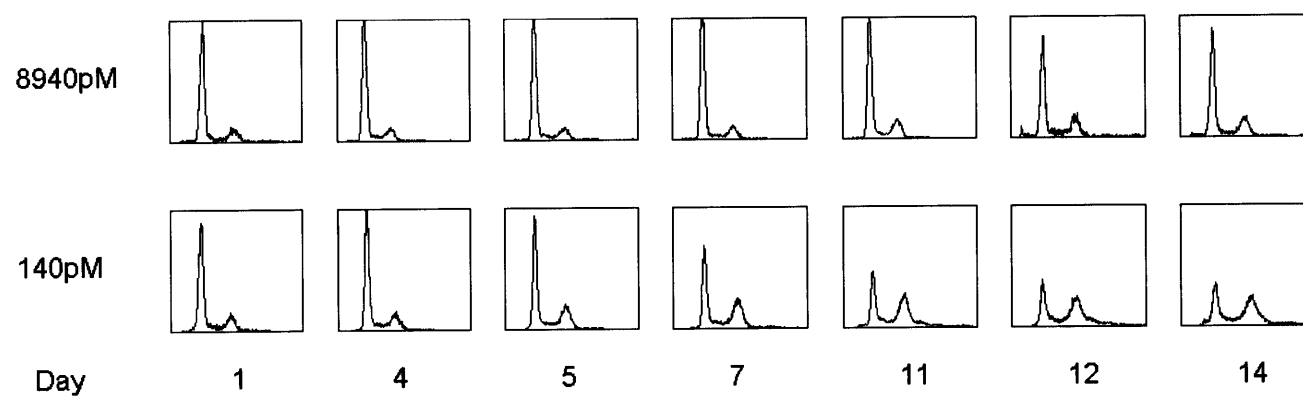


Figure 5-5

Duration of the cell cycle stages for the cobalt limitation experiments. A and B) Duration of stages as calculated using percentage data from mid-exponential growth and late-exponential growth. Data are calculated from day 11, 11, 11, and 7 (mid-exponential); and day 16, 20, 19, and 14 (late-exponential) for 8940, 314, 184, and 140pM total cobalt, respectively. C) Increases in doubling time of cobalt limited *Prochlorococcus* cultures with decreasing cobalt concentrations, calculated from data in Figure 3. Despite the use of metal-buffered media, the cultures were not in balanced growth (see discussion section), as a result duration results are dynamic with time as shown in Figure 6.

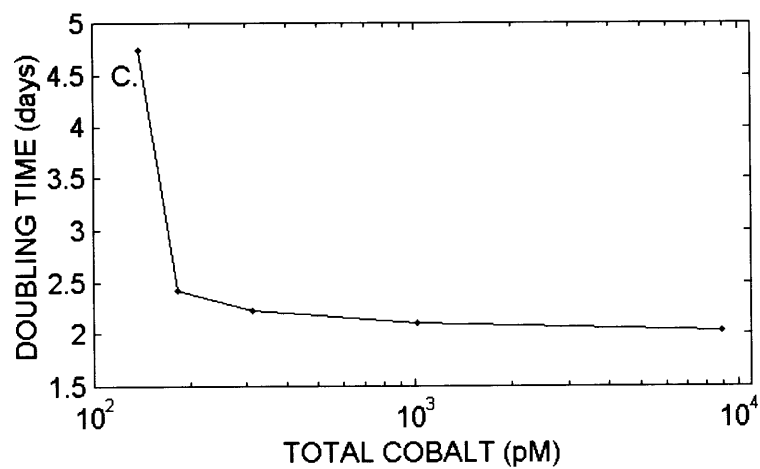
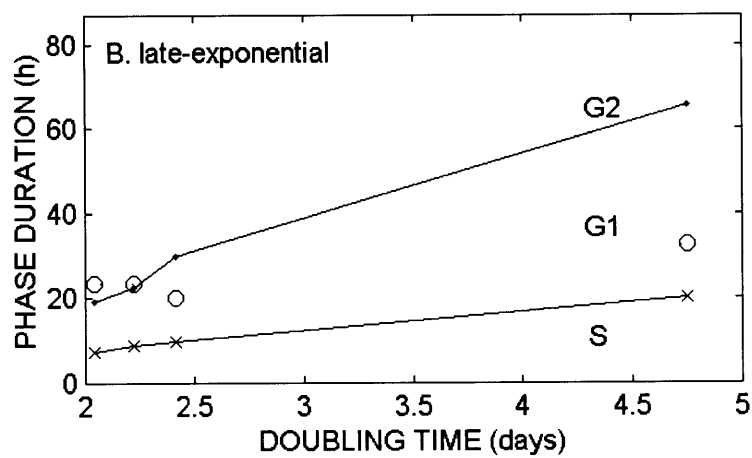
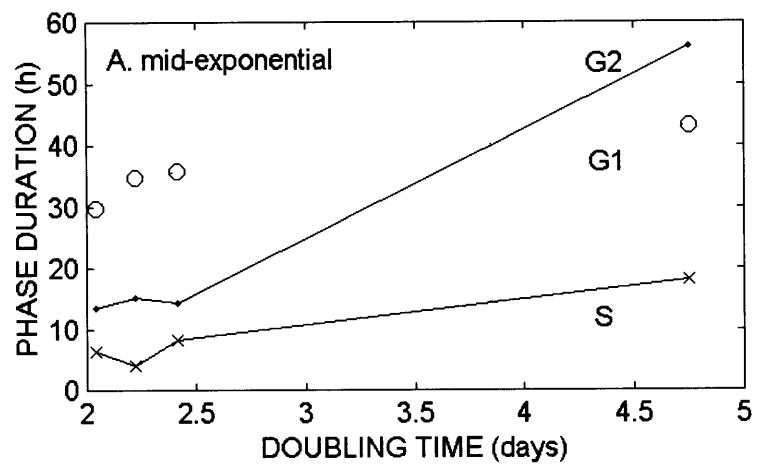


Figure 5-6

Cell cycle stage durations calculated as a function of growth rate in the 140pM cobalt culture (no added cobalt). A) Growth rate (d^{-1}) of the *Prochlorococcus* culture was calculated using a three-point moving average, approaching zero at the onset of stationary phase. B) The percentage of cells in each cell cycle phase, as calculated using ModFit software analysis is shown for each timepoint. C) The durations of those cell cycle phases is shown for at each time point, using the three-point moving average growth rate. The G2 duration increases significantly throughout the exponential growth phase, while G1 decreases correspondingly, and S is relatively unchanged. At the onset of stationary phase, all stages increase in duration as necessitated by the decrease of growth rate to zero.

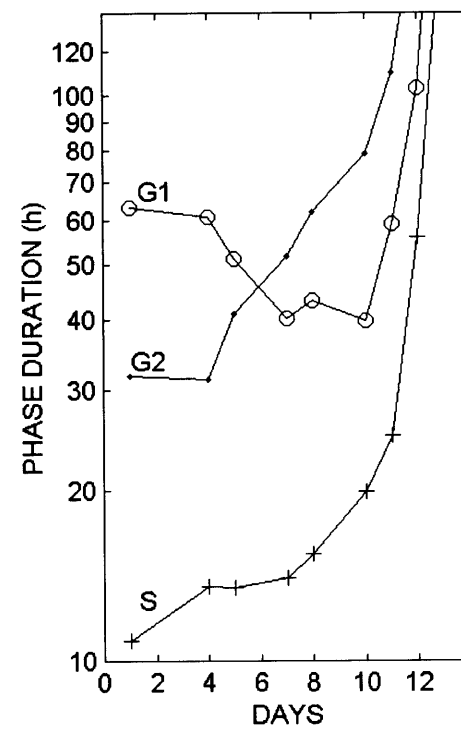
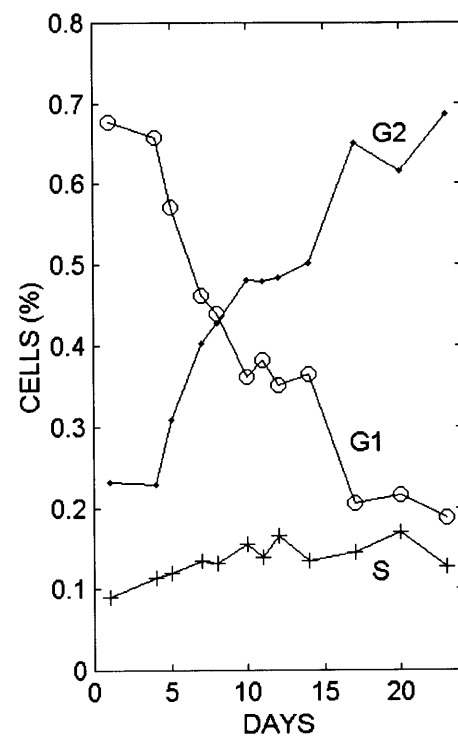
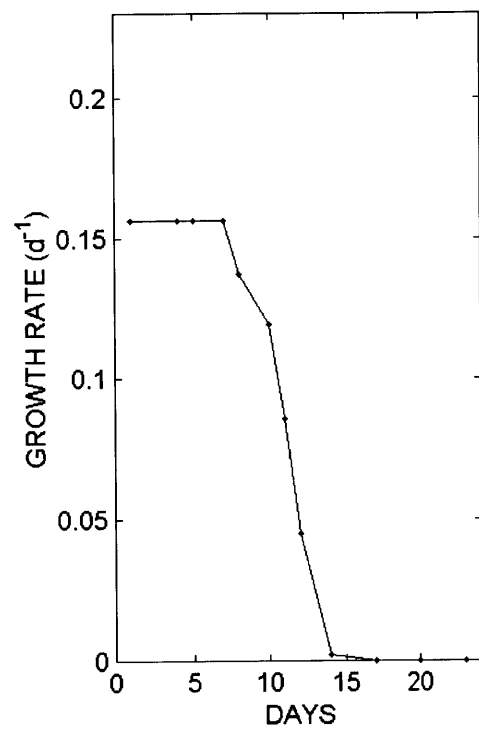


Figure 5-7

DNA analysis of iron-limited *Prochlorococcus* batch cultures. A) Cell number data. B) Cell cycle analysis of iron-replete control. The proportion of cells in each cell cycle stage remained constant until the onset of stationary phase at which point the amount of cells in S and G2 increased and decreased respectively. This result is similar to the phosphorus limitation results in Figure 8C and is consistent with the media N:P that is higher than the Redfield ratio. C) Cell cycle analysis of iron-limited cells showed no changes in the proportion of cells in each cell cycle phase upon entering stationary phase.

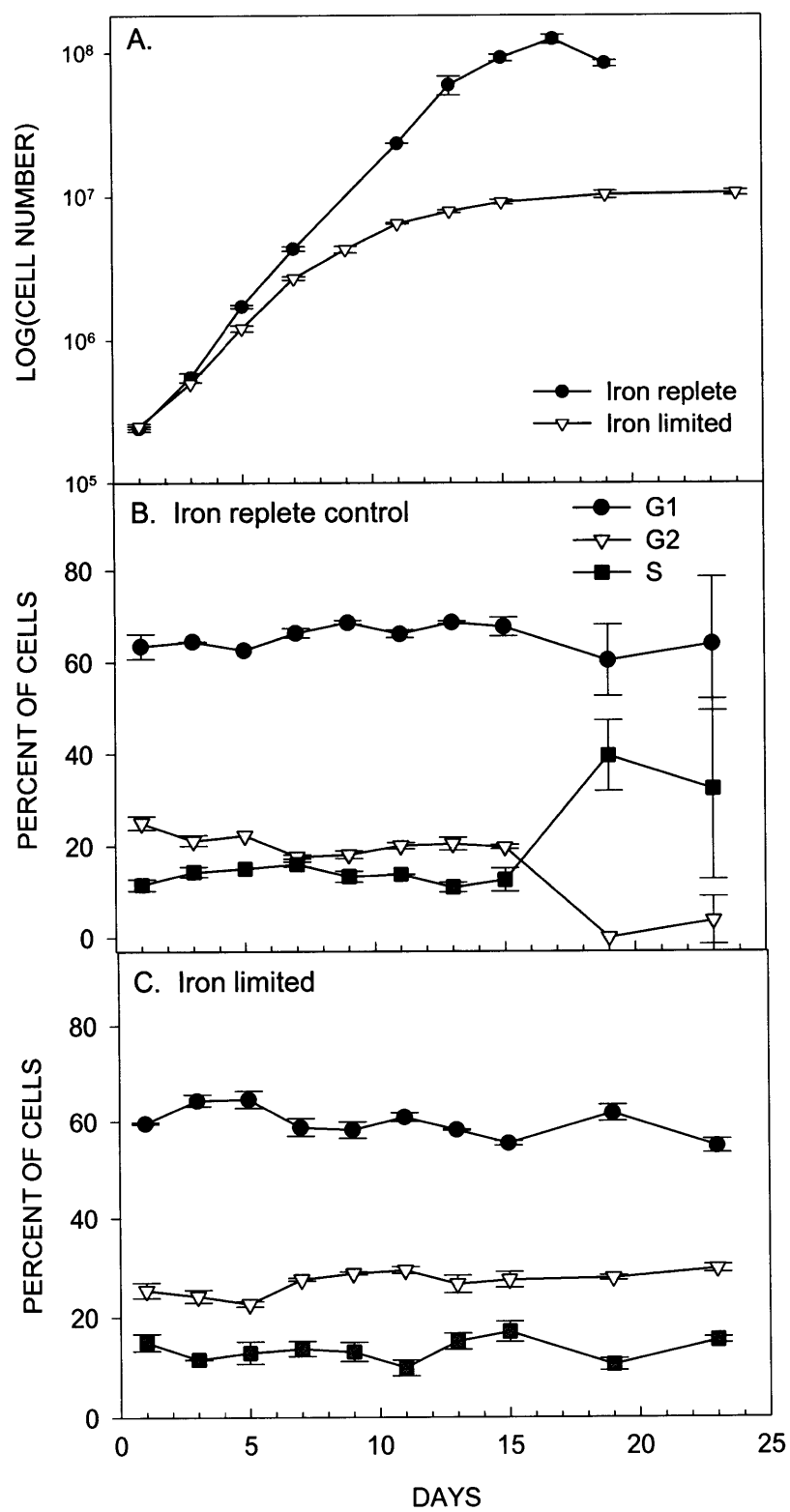


Figure 5-8

DNA analysis of nitrogen and phosphorus limited *Prochlorococcus* batch cultures. A) Growth curves of replicate cultures as measured by *in vivo* fluorescence. One replicate of each treatment was amended with its respective limiting nutrient (ammonia or phosphoric acid) on day 15 to verify that the cultures were limited as intended. These enrichments revived growth after several days. B) Cell cycle analysis results of nitrogen limited cultures. No ammonia or urea were added to the media. The proportion of cells in each cell cycle stage remained relatively constant until the onset of stationary phase on day 10 at which point the percentage of cells in G1 decreased rapidly and G2 and S increased. C) Cell cycle analysis results of phosphorus limited cultures. The proportion of cells in each cell cycle stage remained relatively constant until the onset of stationary phase on day 10 at which point the percentage of cells in G1 and S decreased and increased respectively.

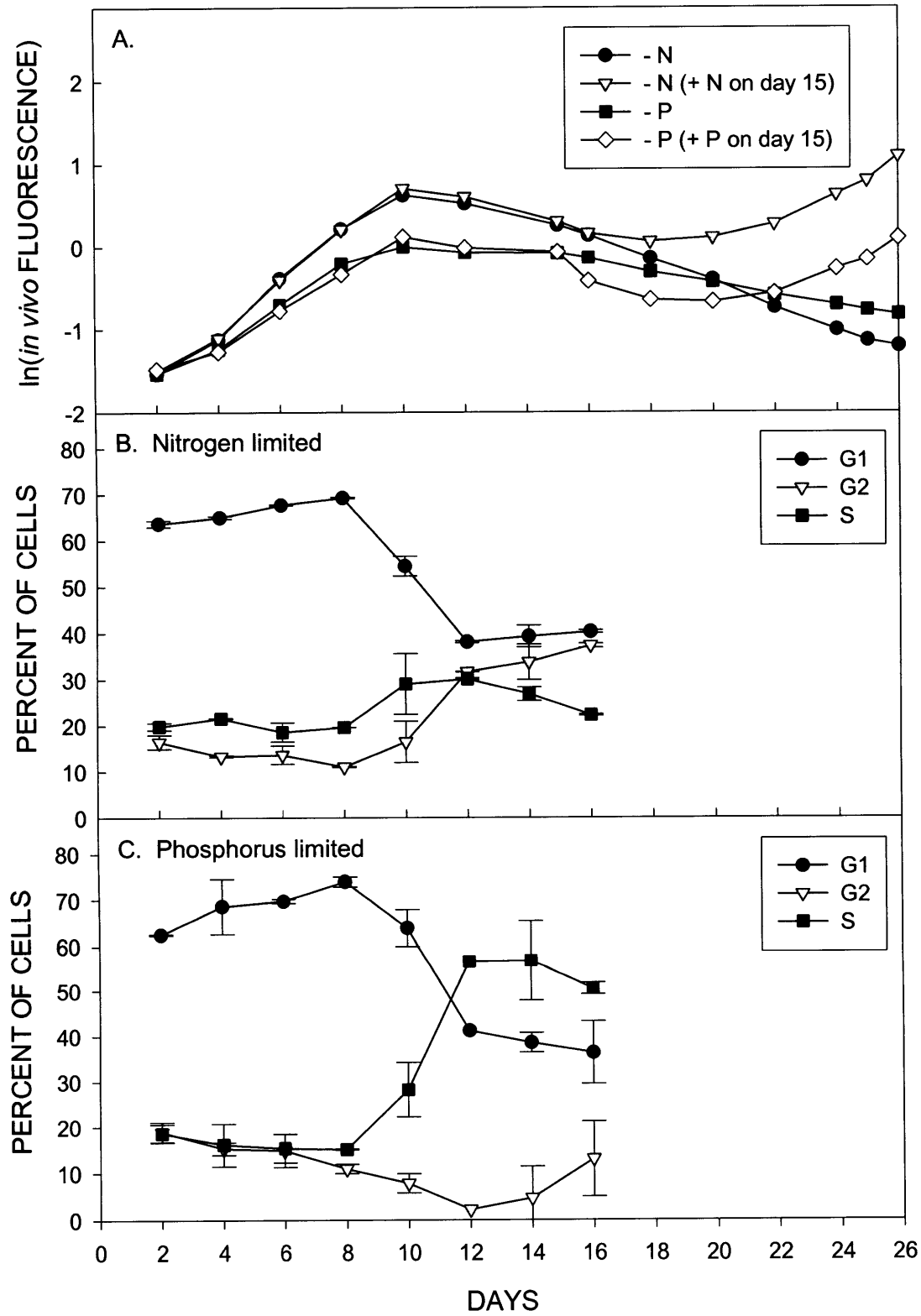


Figure 5-9

A) Cell size during nitrogen and phosphorus limitation as measured by forward light scatter, showing a large increase in cell size at the onset of stationary phase. B) Comparison of size of cells in G1 versus cells in G2 for nitrogen limited cells. Forward light scatter is significantly greater for cells in G2 than G1; however, at the onset of stationary phase the size of cells in both G1 and G2 increases significantly. Forward light scatter signal is normalized to 0.474 μ m beads.

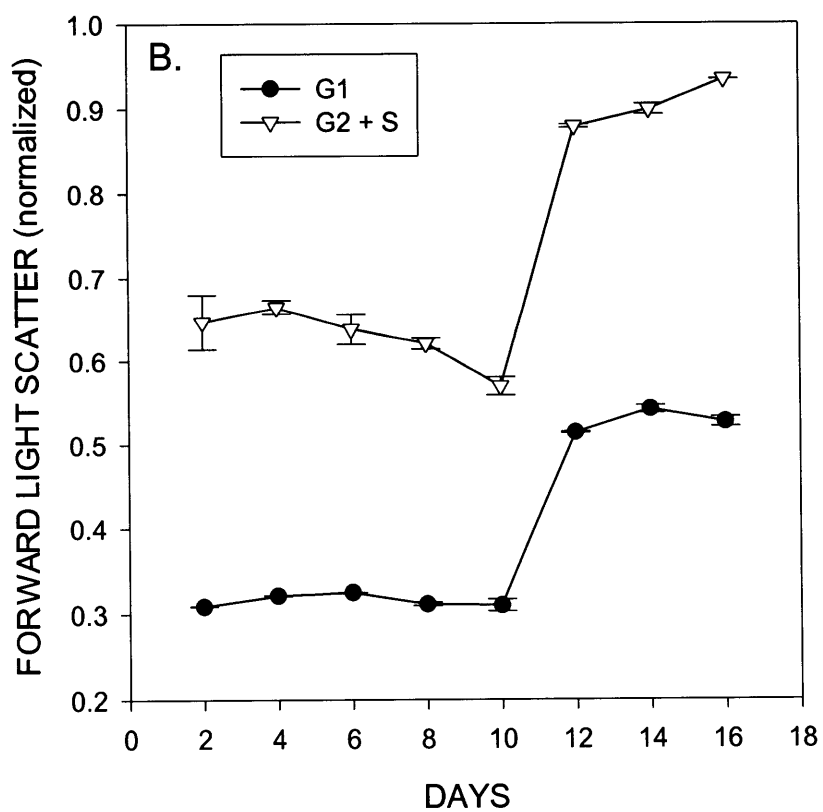
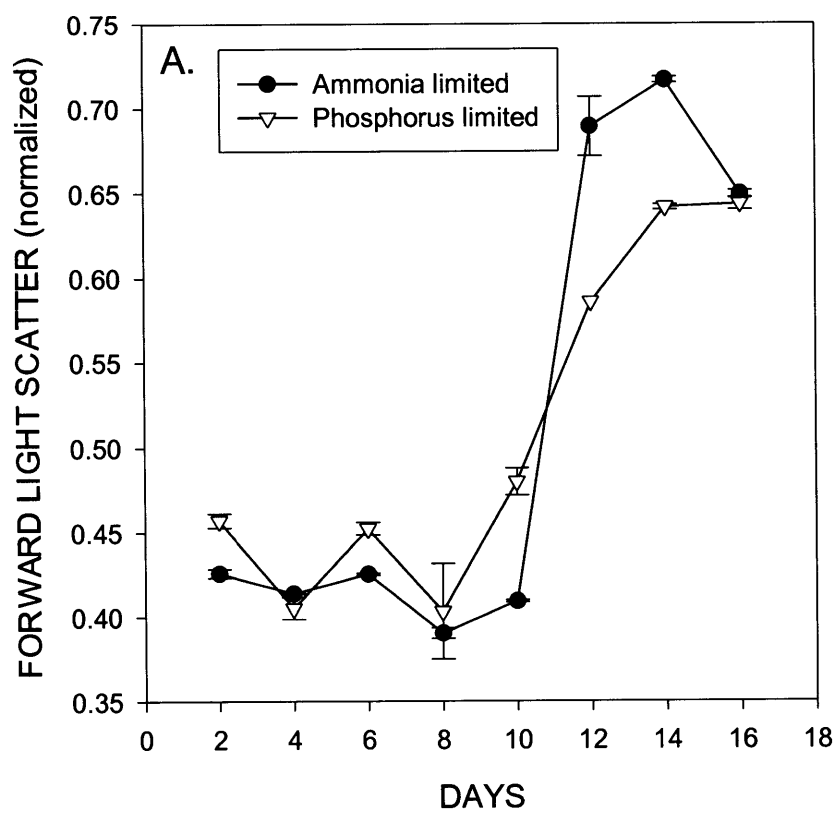


Table 5-1 Pro-1 media composition for trace metal limitation made with Sargasso Seawater

	Concentration
H ₃ PO ₄ ⁻	10 µM
Ammonia	50 µM
Urea	100 µM
Na ₂ EDTA (Sigma Ultra)	11.7 µM
Fe(III)Cl ₃	1.17 µM
Co(II)Cl ₂	8.8 nM*
NiCl ₂	10 nM
ZnCl ₂	8.0 nM
MoO ₄	3.0 nM
Mn	90 nM
Se	10 nM

* The cobalt concentration was increased from 5 nM to 8.8 nM for this study.

Table 5-2 The influence of environmental factors on the cell cycle of phytoplankton

Limiting nutrient	Organism	Duration	Stationary phase	References
Light	<i>T. weissflogii</i>	G1, G2 increase	G1>G2	a,b
Light	<i>H. carterae</i>	G1 increases	G1	a,b
Light	<i>Synechococcus</i>	G1, G2 increase	no data	c
Nitrogen	<i>Prochlorococcus</i>	no data	G1> S~G2	this study
Nitrogen	<i>T. weissflogii</i>	no data	G1	d
Nitrogen	<i>H. carterae</i>	no data	G1	d
Phosphorus	<i>Prochlorococcus</i>	no data	S>G1>G2	this study
Phosphorus	<i>Prochlorococcus</i>	no data	S	e
Silica	<i>T. weissflogii</i>	G2 increases	G2>G1>S	f
Iron	<i>Prochlorococcus</i>	no data	G1>G2>S	this study
Cobalt	<i>Prochlorococcus</i>	G2 increases	G2>G1>S	this study
Zinc	<i>Euglena</i>	no data	G2>G1,S	g

a. (Olson, 1986), b.(Vaulot et al., 1986), c. (Armbrust et al., 1989), d. (Vaulot et al., 1987), e. (Parpais et al., 1996), f. (Brzezinski et al., 1990), g. (Falchuk et al., 1975a; Falchuk et al., 1975b).

Chapter 6

The Effects of the Cobalt Ligand Teta on *Prochlorococcus* in Culture and in the Sargasso Sea

Abstract

The mechanism of cobalt uptake in oceanic microbial assemblages is unknown. Cobalt speciation in the Sargasso Sea is dominated by strong organic cobalt complexes (Saito and Moffett, 2000a). In this study we test the hypothesis that these natural cobalt ligands are involved in cobalt uptake by examining the effects of additions of the strong synthetic cobalt ligand called Teta on laboratory cultures and field populations of *Prochlorococcus*. This synthetic ligand has a high affinity for cobalt, making it a suitable chelate to attempt to perturb the equilibrium between natural cobalt ligands and inorganic cobalt in seawater, similar to the use of the terrestrial fungal siderophore desferrioxamine B (DFOB) to induce iron limitation in bottle incubations in the field. Kinetic studies with Teta showed that the CoTeta complex was labile by exchange with another strong cobalt ligand dimethylglyoxime (DMG). Laboratory experiments showed that the CoTeta complex was not bioavailable: additions of Teta and to a lesser extent DMG caused a reduction in growth rates of *Prochlorococcus* cultures, consistent with their relative strength conditional stability constants for cobalt. Moreover, short-term (12h) field experiments with ^{57}Co uptake experiments in bottle incubations from the Sargasso Sea also showed that $^{57}\text{CoTeta}$ complexes were not biologically available to the natural microbial assemblage. However, cobalt from $^{57}\text{CoTeta}$ was taken up into particulate matter in long-term experiments (3d) indicating either degradation of the $^{57}\text{CoTeta}$ molecule, or equilibration of the ^{57}Co bound to Teta with other complexes in seawater. Finally, additions of 50nM and 500nM Teta to bottle incubations from the Sargasso Sea did not decrease the net growth rate of *Prochlorococcus* by inducing cobalt limitation; on the contrary, we observed significant stimulation of the Teta addition treatments relative to controls. Given that Teta is not as strong a cobalt ligand as natural cobalt ligands measured in seawater, the experiments presented in this study are consistent with a strong cobalt ligand uptake system existing in the natural surface waters of the Sargasso Sea.

Introduction

Cobalt is an essential micronutrient for the photosynthetic cyanobacteria (Chapter 4, Sunda and Huntsman, 1995b) and can substitute for zinc in eukaryotic marine phytoplankton (Morel et al., 1994; Price and Morel, 1990; Sunda and Huntsman, 1995b; Yee and Morel, 1996) in the enzyme carbonic anhydrase (Table 1). However, concentrations of cobalt in the open ocean are exceptionally low, in the picomolar range, and often display a nutrient like profile (Martin and Gordon, 1988; Martin et al., 1989; Saito and Moffett, 2000a). It has been hypothesized that cobalt concentrations may be so low that it may control the growth or species composition of certain marine photosynthetic communities (Sunda and Huntsman, 1995). Additions of cobalt to seawater samples have not resulted in increased biomass, except when added with Fe (Hutchins, pers. comm.).

Oceanographers have struggled with questions of what limits the primary productivity for decades. The concept of nutrient limitation in oceanography has its origins in the application of Liebig's Law of the minimum (DeBaar, 1994). This concept, originally borrowed from soil science, states that the nutrient that is first depleted is the nutrient that limits growth. Only in recent years have we acquired data on the true concentrations of nitrate, orthophosphate, and transition metals in seawater (Martin and Gordon, 1988; Martin et al., 1989; Thomson-Bulldis and Karl, 1998; Wu et al., 2000). Using these seawater concentrations and cellular quotas, we can examine which nutrient should be limiting in environments like the oligotrophic Sargasso Sea and Equatorial Pacific (Figure 1A and 1B). Moreover, we can look at which nutrient would be next in line to limit productivity and thus how close the system is to co-limitation by multiple nutrients. Using this approach, one would predict the Sargasso Sea to be phosphorus limited with nitrogen limitation so closely next in line that co-limitation for N and P seems likely (Figure 1A). The recognition that phosphorus is also low enough to be limiting in the Sargasso Sea due to supply of nitrogen by nitrogen fixing organisms has been discussed Falkowski (Falkowski, 1997) and analytical determined by Wu et al. (2000). The Equatorial Pacific, on the other hand, is clearly iron limited with possible iron-cobalt co-limitation once iron is partially utilized (Figure 1B). However, the

potential for trace metal limitation is greatly exacerbated by the presence of organic ligands if the resultant metal ligand complexes are not bioavailable (circle symbols Figure 1A and 1B)⁹. In this case, the majority of the metal would exist as organic ligand complexes, and the bioavailable fraction of metal would be several orders of magnitude lower in concentration. Hence, the question of whether or not organically complexed cobalt in seawater is bioavailable is fundamental to our understanding of whether or not this nutrient could be limiting primary productivity in the oceans. With iron complexes in seawater, this is a difficult question that is only beginning to be addressed (Hutchins et al., 1999b). In this study, we utilize the synthetic ligand Teta (see Figure 2 for structure) with a high affinity for cobalt as a means to explore cobalt utilization. By perturbing natural systems with this ligand in a variety of experiments we can try to determine if cobalt uptake in the natural environments is dominated by inorganic Co or organic CoL uptake. For example, if additions of Teta did not cause any limitation of growth, we could speculate that inorganic cobalt uptake was not important because the addition of Teta would decrease the concentration of any inorganic cobalt by several orders of magnitude. Moreover, if Co limitation can be induced using Teta, experiments could be devised to probe how close marine environments are to being cobalt limited relative to other nutrients.

Researchers studying the importance of iron nutrition have done these types of exogenous ligand additions in an attempt to induce iron limitation in coastal waters (Hutchins et al., 1999a; Wells, 1999). In these experiments, additions of an exogenous fungal siderophore called desferrioxamine B (DFOB) in seawater incubations were monitored in the presence of radiotracers to explore the impact of this ligand on iron and carbon uptake. While uptake of iron and carbon were significantly lower upon additions of 100nM DFOB, cobalt, zinc and manganese uptake were unaffected by DFOB during short-term 6h studies (Wells, 1999). However, long-term 5d studies showed a significant

⁹ The question of whether or not natural metal ligand complexes in seawater are bioavailable is a major area of research in bioinorganic oceanographers today. Analytically this is an exceptionally difficult problem because these iron ligands in seawater, for example, exist in the nanomolar concentration range, making them extremely difficult to extract from the 70μM dissolved organic carbon that is already present. We know that in culture organisms can make siderophores that are metal chelates that are bioavailable (can be accessed by organisms), yet it is still unclear the extent to which Fe-L in natural environments is comprised of siderophores. This thought experiment shown in Figure 1 assumes the worse case scenario of all metal ligand chelates being unavailable for direct uptake by the biota to show the potential for limitation.

decrease in cobalt, zinc, and manganese uptake which Wells showed was concurrent with a decrease in biomass caused by DFOB induced iron limitation. Another study of the bioavailability of a range of iron ligands structures conducted in the open ocean revealed a preference amongst the smaller and predominantly prokaryotic size fraction for fungal and bacterial siderophores, while the larger eukaryotic size fraction was better suited to accessing iron within porphyrin ring structures (Hutchins et al., 1999b). This eukaryotic preference for tetradentate porphyrin complexes is consistent with the presence of an iron reductase uptake system in eukaryotic algae (Maldonado-Pareja, 1999).

Cobalt speciation measurements at the Bermuda Atlantic Time Series Station (BATS) showed that most of the cobalt appears to be bound to strong organic ligands ($\log K = 16.3 \pm 0.9$, Table 2), with concentrations that are similar to that of the total metal concentrations (Saito and Moffett, 2000a). These natural organic ligands were calibrated with respect to synthetic Co(II) ligands; however, the cathodic stripping voltammetry methodology cannot distinguish between Co(II) and Co(III) complexes with natural ligands. As a result, it is possible that natural cobalt ligands in seawater are Co(III) ligands with higher stability constants. It is possible that these organic ligands binding cobalt at BATS are cobalamin (vitamin B₁₂). However, Menzel and Spaeth (Menzel and Spaeth, 1962) measured B₁₂ in the Sargasso Sea using a sensitive bioassay and found that values did not exceed 0.1 ng/L or 0.2 pM - an insignificant fraction of the total cobalt. While the hypothesis put forward by Menzel and Spaeth (1962) that changes in B₁₂ are likely to influence the predominant species of algae, the experiments in this study are designed to explore cobalt uptake separate from any ecological influences of B₁₂. B₁₂ is generally found in the Co(III) oxidation state and as a result it would likely be inert to equilibration with our additions of Teta.

Materials and Methods

Bottle preparations

All labware was soaked with an acidic detergent (Citranox) overnight, rinsed in Milli-Q water, soaked in 10% HCl (Baker Instra-analyzed) overnight at 60°C, rinsed and soaked in 0.01M HCl (Baker Ultrex II) until use. The cleaning preparations were conducted in a clean room environment using clean technique.

Teta Solutions and Cobalt Blank

Teta solutions were prepared by dissolving 1,4,8,11 tetraazacyclotetradecane-1,4,8,11 tetraacetic acid hydrochloride hydrate (Aldrich) into Milli-Q water at a concentration of 0.5mM. A cobalt blank measured in our Teta stock solution showed a $\leq 0.0039\%$ cobalt blank, resulting in a 2pM addition of cobalt for a 50nM Teta addition. This blank was measured by dilution of Teta into a Sargasso seawater matrix and ultraviolet light digestion in quartz tubes, followed by analysis using cathodic stripping voltammetry for low level cobalt analyses as described in Chapter 2. This level of contamination should be unimportant given the large excess of exogenous ligand we are adding to the incubation bottles. The blank is an upper estimate of cobalt because the Sargasso seawater matrix itself contributed slightly to the cobalt blank.

Kinetic experiments with CoTeta

The kinetics of the disassociation rate of CoTeta were explored using electrochemical experiments were conducted using a Metrohm 663 hanging mercury drop electrode and a Ecochemie μ Autolab computer interface. A 100pM CoCl_2 addition was added to a pre-equilibrated sample of 10 μ M Teta, 50mM DMG, and 475pM CoCl_2 , 0.025M EPPS buffer (pH 8.1), and 0.225M NaNO_2 dissolved in UV-irradiated Sargasso seawater. The electrode parameters were set at 10V/s scan rate, scan range from -0.6 to -1.4V, deposition time of 90s, drop size of 0.52mm² and stirrer speed rate of 5. Using these parameters the electrode only measures the CoHDMG_2 species.

Culture experiments with Prochlorococcus

Experiments were designed to see whether additions of Teta or dimethylglyoxime would depress growth rates of *Prochlorococcus* (axenic strain MED4) by inducing Co limitation. Culture media were prepared from Sargasso seawater filtered through acid washed 0.2 μ m polycarbonate filters, and sterilized by microwaving for 10 minutes (Keller et al., 1988). After cooling trace metal mix was added to make 11.7 μ M EDTA (SigmaUltra grade), 1.17 μ M FeCl_3 , 5uM Na_2CO_3 , 8nM ZnSO_4 , 90nM MnCl_2 , 3nM

Na₂MoO₄, 10nM Na₂SeO₃, and 10nM NiCl₂. 500pM CoCl₂ was added separately after addition of the EDTA trace metal mix. H₃PO₄, NH₄OH and urea were combined and run through a pretreated chelex column at pH 8 (Price et al., 1988/1989). Final concentrations of orthophosphate, ammonia, and urea were 10μM, 50μM, and 100μM, respectively. All nutrient and trace metal solutions were sterilized by filtration using all-plastic syringes and 0.2 μM acrodisk rinsed with 1M HCl (Baker Instra-analyzed) and 0.01M HCl. Dimethylglyoxime (Aldrich, recrystallized as described in Saito and Moffett (2000a)) and Teta (1,4,8,11- Tetraazacyclotetradecane, Sigma) stock solutions were also sterile filtered separately and added to uninoculated 30mL polycarbonate culture tubes (Nalgene). Culture media was allowed to equilibrate for 24h prior to addition of a 2% inoculation by volume. A marine broth purity test showed that the inoculum culture was free from heterotrophic bacteria contamination (Waterbury et al., 1986).

Each experimental treatment was grown in duplicate at 17 μmol Q m⁻²s⁻¹ constant light and monitored by *in vivo* fluorescence measurements using a Turner AU-10 fluorometer. One of the replicates was sampled for flow cytometric analysis every two days by removing 0.6mL of the culture with a trace metal clean pipette tip (Fisher) that was rinsed with concentrated HCl (Baker Ultrex II) and three times with pH 2 Milli-Q water immediately before use to ensure sterility and remove metal contamination. The other replicate in each treatment was left unopened during the experiment to verify that sampling for flow cytometry was not contaminating the media with metals; comparison of non-invasive *in vivo* fluorescence measurements showed no contamination effects on the growth physiology of *Prochlorococcus*. Flow cytometry samples were preserved in 0.125% glutaraldehyde and stored in liquid nitrogen after 10 minutes dark fixation at room temperature.

Flow cytometric analyses of incubations with Teta in the Sargasso

Flow cytometry samples were thawed at 35°C for 3 minutes, vortexed, and subsampled. Culture samples were diluted with filtered Sargasso Seawater. 0.474μm beads were added as an internal standard immediately prior to analysis on a modified FACScan (Dusenberry and Frankel, 1994). A syringe pump was used (Harvard Apparatus) with a flow rate of 10μl/min, and 15000 counts were collected on all samples.

Short-term Co^{57} incubation in the Sargasso

A short-term radiotracer experiment was performed in the Sargasso to examine the influence of Teta on cobalt uptake on a 12h time span. Sargasso seawater was collected from 100m depth in an acid cleaned Go-Flo bottle on kevlar wire and pumped under N_2 into a positive pressure clean van through light shielded acid-cleaned teflon tubing at 9:00am. 1L of unfiltered seawater was gently added to four polycarbonate bottles. On the previous day, four 25mL spike solutions with 20pM ^{57}Co (carrier-free CoCl_2 , Isotope Products Laboratories) were pre-equilibrated with filtered Go-Flo seawater and Teta was added in excess (2 μM) to two of these bottles. At the start of the experiment, the pre-equilibrated spike solutions were added to the 1L incubation bottles, and an additional Teta spike of 50nM was added the experimental replicates, resulting in a final concentration of 100nM Teta in the experimental replicates and 0.5 pM ^{57}Co in both experimental and control replicates. At each timepoint 25mL aliquots were filtered through 0.2 μm nucleopore polycarbonate filters and rinsed once with artificial seawater made from NaCl dissolved in Milli-Q water. Bottles were incubated in a temperature regulated water bath at 20°C with 33 $\mu\text{mol Q m}^{-2}\text{s}^{-1}$ from cool white fluorescent lamps. Total samples were taken at the t=0 and t=24h by adding 0.1mL to adsorbent paper in petri-dishes.

Bottle Incubation with Teta in Sargasso seawater

Seawater used for this experiment was from the same Go-Flo bottle cast as the short-term ^{57}Co incubation described above. 270mL was added to polycarbonate bottles and the bottles were incubated at 2.7% of the on-deck light level in a Percival incubator programmed for 14:10 L/D cycle and 25 °C. All sampling was conducted in a laminar flow hood using clean technique.

Long-term $^{57}\text{CoTeta}$ incubation with Sargasso Sea microbial assemblages

An experiment was conducted to examine cobalt uptake from $^{57}\text{CoTeta}$ in Sargasso seawater over a 3d incubation period in two size fractions. 50mL of fresh

filtered seawater was incubated with 10pM ^{57}Co and allowed to equilibrate overnight. The following day, 50mL of unfiltered seawater was added to seven 60mL Nalgene polycarbonate bottles with 0-10nM Teta ligand and placed in a Percival incubator as described above. 4h after filling bottles and 24h after the ^{57}Co solution had equilibrated, 2mL of the ^{57}Co filtered seawater spike solution was added to each bottle to achieve a spike concentration of 0.3pM Co^{57} . Total cobalt in both the spike solution (before adding Co^{57}) and the experiment bottles was measured to be $40.5 \pm 7.0\text{pM}$ and $40.7 \pm 0.25\text{pM}$ respectively. After 68h (5:00pm) the samples were filtered through 0.2 μm and 3.0 μm Nucleopore polycarbonate 25mm filters and rinsed with artificial seawater to wash any dissolved ^{57}Co in the experimental seawater. Totals were taken at the end of the experiment by pipetting 0.1 mL of seawater onto absorbent paper lined petri dishes; in all cases $\leq 1.5\%$ of the total ^{57}Co was incorporated into particulate material.

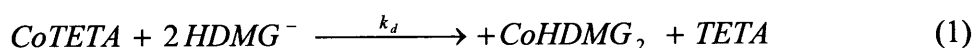
*^{57}Co uptake by *Prochlorococcus* in UV-light exposed seawater*

Filtered Sargasso seawater collected from surface waters was divided, with half added to quartz tubes and the other half stored in darkness as a control. The quartz tubes were capped with acid cleaned caps, sealed with parafilm, and left on-deck for 3d for exposure to sunlight. Control and sunlight-exposed seawater aliquots were added to polycarbonate tubes and allowed to equilibrate with tracer quantities of $^{57}\text{CoCl}_2$ (<1pM) overnight in darkness. Axenic *Prochlorococcus* cells were spun down, washed, and resuspended in clean filtered seawater and then added to triplicate experimental and control treatments. ^{14}C as HCO_3^- was (Amersham Life Sciences) added to sample bottles in tracer concentrations (<1 μM) immediately before the addition of cells. After 5h of incubation at 17 $\mu\text{mol Q m}^{-2}\text{s}^{-1}$ of fluorescent light the samples were filtered through 0.2 μm polycarbonate filters, vented of dissolved inorganic carbon by enclosure in a box with a vial of concentrated acid, and counted.

Results

Before examining the influence of Teta on field populations of *Prochlorococcus*, we first conducted a variety of culture, field, and chemical experiments with the Teta

molecule in order to answer questions regarding chemical reactivity and the bioavailability of the CoTeta complex. There were two primary questions that needed to be systematically answered prior to using the Teta ligand. First, we were concerned about the possibility of oxidation of Co(II)Teta to Co(III)Teta and the resultant inert Co(III) complex. Second, given the dearth of literature on the bioavailability of organic cobalt complexes, we needed to know if CoTeta could be taken up directly by marine biota. The former problem was important because uncertainties about the redox state of the chelate would confound interpretations of experiments with biota. The CoTeta complexes used in this study were prepared using Co(II); nevertheless, we were concerned about inadvertent oxidation to Co(III)Teta, which would likely have a much higher conditional stability constant (to our knowledge no data exists for a Co(III)Teta conditional stability constant). An experiment using cathodic stripping voltammetry showed that the Co(II)HDMG₂ complex equilibrates rapidly with CoTeta (Figure 3) in the following reaction:



In this experiment, 100pM CoCl₂ was added and rapidly formed CoTeta complexes, before dissociating and equilibrating with HDMG⁻. Due to the excess of HDMG⁻, this experiment yields a pseudo-first order dissociation constant (*k_d*) for CoTeta of 0.064h⁻¹. Co(III) chelates, with their octahedral coordination and their strong field d⁶ configuration, have notoriously slow kinetics and are often described as inert (Shriver et al., 1990). With its axial acetic acid ligands groups, CoTeta can also adopt a octahedral configuration, yet the results in Figure 3 show a labile CoTeta complex, suggesting that it is has not been oxidized to a more stable Co(III) form.

Testing the bioavailability of the CoTeta molecule was also of critical importance before utilizing the molecule in field studies. If CoTeta could be directly accessed by the biota, as some iron organic complexes are thought to be by eukaryotic phytoplankton (Maldonado-Pareja, 1999), its utility as a means to perturb the equilibria of natural cobalt complexes would be decreased since it would not be possible to differentiate between uptake of inorganic cobalt, CoTeta, and cobalt bound to natural organic ligands. Two

experiments were conducted to test this question: first, a culture experiment was conducted with axenic *Prochlorococcus* strain MED4-Ax, in which sterile Teta was added to EDTA buffered media (Figure 4A). Growth rates decreased with increasing Teta concentrations, suggestive of cobalt limitation (Figure 4B). A control experiment with 50nM Teta and 100nM cobalt concentrations showed that the Teta itself was not toxic to *Prochlorococcus* and that limitation was relieved by addition of cobalt (Figure 4B). Comparable experiments with DMG showed a lesser response, consistent with the weaker binding strength of DMG with cobalt (correcting for stoichiometry) (Figure 4B and Table 2). Second, a 12h bottle incubation experiment was conducted that showed little uptake of the $^{57}\text{CoTeta}$ complex by the microbial assemblage in the Sargasso Sea relative to controls without Teta (Figure 5). Together, these results indicate that the CoTeta complex is not bioavailable to either *Prochlorococcus* MED4-Ax or to the microbial community in the Sargasso Sea on short time scales.

Given that CoTeta is not bioavailable to *Prochlorococcus*, and that it is not readily oxidized to an inert Co(III) form under ambient seawater conditions, we conducted bottle incubations with Teta additions without added cobalt to see whether we could induce Co limitation of the *Prochlorococcus* community at BATS. 50 and 500nM additions of Teta did not induce cobalt limitation, but rather resulted in a significant increase in *Prochlorococcus* cell numbers (Figure 6). The cell densities in the 0nM and 500nM treatments are significantly different by t-test to >90% confidence level. We believe this result implies that the CoTeta ligand was not strong enough to compete with natural cobalt ligands in seawater, at least so as to induce biological limitation. In addition, *Prochlorococcus* was clearly stimulated by the addition of Teta. This result surprised us and we hypothesize that this response may have been caused by nitrogen fertilization using the nitrogen atoms found in the Teta molecule itself. Calculations show that only 2.3% of the 2 μM N added in 500nM Teta is needed to supply the 70000 *Prochlorococcus* cell increase we observe (Table 3; based on Redfield ratios and the 53fg C/cell (Campbell et al., 1994)). This hypothesis should be tested in laboratory cultures of *Prochlorococcus* and ^{15}N labeled Teta to determine if this type organic nitrogen acquisition is possible. There are three other possible explanations for the increase in *Prochlorococcus* growth observed with the addition of Teta. First, the *Prochlorococcus*

community may have been relieved from copper toxicity by the addition of Teta; however, this does not seem likely based on previous studies that showed copper tends to be completely bound to strong organic ligands at 100m where the water for the incubation was collected (Moffett, 1995), and hence free copper concentrations would already be below levels known to be toxic to *Prochlorococcus* (Mann, 2000). Second, chelation of nickel by Teta could have alleviated reduced cobalt uptake rates associated with competitive inhibition, as observed in culture studies in Chapter 4. This explanation does not seem as plausible as the nitrogen fertilization hypothesis described above since the Sargasso Sea is known to be nitrogen limited at times, whereas there are no published reports of cobalt limitation there. Alternatively, it is also possible that Teta acts as an inhibitor of cyanobacterial grazers. However, eukaryotic inhibitors typically require much higher concentrations (e.g. 0.2mM) than the concentrations of Teta we are using here, and they can be problematic in their ability to target grazers but not bacteria (Tremaine and Mills, 1987).

Long-term bottle incubation experiments (3d) at BATS conducted with ^{57}Co Teta showed that the microbial assemblage at BATS incorporated significant amounts of the ^{57}Co atoms relative to controls with ^{57}Co but without Teta up to 50nM (Figure 7). At 500nM uptake is significantly less than the no Teta control, suggestive of toxic effects of Teta to the microbial community. Given that the complexes were not bioavailable in the short-term uptake experiment, these results suggest re-equilibration with natural ligands and/or degradation of ^{57}Co Teta complexes with time. The former of these two possibilities, re-equilibration, was shown to occur in the laboratory with synthetic ligands as described above (Figure 3). Moreover, the biological stimulation observed in the Teta addition experiment (Figure 6) is also apparent in this experiment where an increasing percentage uptake of ^{57}Co occurs with increasing additions of Teta between 5nM and 50nM (Figure 7).

The influence of ultraviolet light on the uptake of cobalt by the natural microbial assemblage at BATS was performed using natural ligands without any Teta additions. It has been shown that copper ligands and iron ligands can be degraded by ultraviolet irradiation associated with sunlight (Moffett et al., 1990; Barbeau, pers. comm.). There are no data available for the stability of cobalt complexes with respect to UV-light. We

performed a preliminary experiment where filtered seawater was exposed to sunlight for 3d before adding ^{57}Co and measuring uptake rates into cells. Exposure of filtered seawater to direct sunlight on-deck resulted in a significant decrease in subsequent ^{57}Co uptake into axenic *Prochlorococcus* cells (incubated at moderate light intensities) relative to uptake in untreated control seawater (Figure 8). ^{14}C uptake in this experiment was not significantly different between the two treatments. Two interpretations of these results are possible: 1) inorganic cobalt uptake membrane proteins were flooded with other transition metals due to the degradation of a variety of metal ligand complexes; 2) the UV-degradation of cobalt organic complexes resulted in a decrease in cobalt uptake due to an inability of the cells to recognize bioavailable forms of cobalt. The latter interpretation could reduce uptake rates by competitive inhibition at the cobalt uptake site, or by toxicity associated with photodegradation of Cu-chelates. However, this mechanism is not consistent with the short time scale (5h) of this experiment relative to the longer time scale observed for Cu toxicity and *Prochlorococcus* in the Sargasso Sea (Mann, 2000).

Discussion

The question of whether or not organically complexed cobalt in seawater is bioavailable is fundamental to our understanding of whether or not this nutrient could be limiting primary productivity. Estimates based on the cellular quotas of major and trace elements show that cobalt (and iron and possibly zinc) would be limiting if the complexed forms were not accessible to the biota (Figure 1). Moreover, calculations using the residence time of cobalt (based on cobalt totals from a time-series at BATS) and cellular cobalt quotas suggest that marine phytoplankton in the Sargasso are at lower than optimal cobalt quotas (Saito and Moffett, 2000b). These calculations coupled with the lack of published evidence for cobalt limitation, suggest that organically bound cobalt in the oceans must be bioavailable for organisms that have an absolute cobalt

requirement¹⁰. The data in this study shows that Teta, a ligand that is not toxic in nanomolar concentrations (Figure 4B), does not cause decreases in the net growth rate of *Prochlorococcus* in the Sargasso Sea (Figure 6). This result is consistent with electrochemical measurements that show that cobalt is strongly bound to organic ligands. The conditional stability constant of Teta is five orders of magnitude weaker than that of natural organic ligands measured in the Sargasso (Table 2). By using a range of Teta concentrations it should be possible to shift equilibrium from natural CoL chelates to CoTeta, assuming the natural CoL chelates are not kinetically inert. Ideally we should use a stronger ligand that could compete with natural cobalt ligands instead of Teta; however, we are unaware of a synthetic ligand with a high enough conditional stability constant for Co(II).

We can compare our results to studies using the exogenous iron siderophore desferrioxamine B (DFOB). Additions of DFOB induced iron limitation in the eukaryotic size classes in natural environments (Hutchins et al., 1999a; Wells, 1999). However, this phenomenon was not observed in the picoplankton size class (0.2 - 1.0 μm) where the ⁵⁵Fe-DFOB molecules themselves are bioavailable, despite their non-marine origins (Hutchins et al., 1999b). In the same study, ⁵⁵Fe-porphyrin molecules were not available to the picoplankton size class. In contrast to FeDFOB, ⁵⁷CoTeta is not bioavailable to any size classes in short-term experiments (Figure 5). Yet in long term studies with Teta (without cobalt), no limitation of *Prochlorococcus* is observed (Figure 6). Moreover, in long term incubations with ⁵⁷CoTeta, the ⁵⁷Co is taken into both small and large size classes (Figure 7). Hence in the case of Co and Fe, the picoplankton size class is not metal limited by additions of an exogenous ligand (DFOB or Teta). Yet this inability to limit the picoplankton comes from different mechanisms: FeDFOB was bioavailable and hence did not prevent iron uptake, while CoTeta is not bioavailable but does not appear capable of exchanging cobalt with natural organic ligands that are already binding it. This is based on comparison of their conditional stability constants (Table 2) and the inability of Teta to limit growth in the Sargasso (Figure 6).

¹⁰ In this context bioavailable refers to a chelate that is directly available to the organism, either via uptake or cell surface reduction and removal of the metal center.

The chemical structures and kinetics of DFOB and Teta have implications for the bioavailability of the metals they chelate. As an hydroxymate ligand, DFOB has slow kinetics relative to catechol siderophores in iron exchange reactions with transferrin (Moffett, 2000), yet it has been used successfully in inducing iron limitation in field populations of phytoplankton (Wells, 1999; Hutchins et al. 1999a). In contrast, Teta has rapid kinetics for CoTeta formation (see Figure 11, Chapter 2), yet is unable to limit *Prochlorococcus* in Sargasso Sea bottle incubations (Figure 6) or Equatorial Pacific stations (Saito and Moffett, unpublished data). DFOB's efficacy in limiting primary productivity suggests that the iron in those studies was relatively labile, while the cobalt in our Sargasso studies appears to be inert to equilibration with Teta. This suggests that the natural CoL complex, while not accessible to Teta, is still bioavailable since we were unable to induce limitation. Teta has four co-planar N ligands that can bind Co as well as carboxylic acid groups that can bind axially. In chapter 2, we discuss the possibility of four co-planar nitrogen ligands as a potential structure for the natural cobalt ligands given their high stability constants for cobalt complexes. In this study, it is evident that CoTeta is not susceptible to direct uptake on short time scales (Figure 5). This implies that the natural microbial assemblage does not have a uniform mechanism to acquire cobalt from co-planar nitrogen ligands, as many eukaryotic phytoplankton appear to have for Fe-porphyrin structures (Hutchins et al., 1999b).

There is an emerging story that marine photosynthetic cyanobacteria are sources of strong iron, copper, and cobalt ligands (Wilhelm et al., 1998; Wilhelm et al., 1996; Saito, 2000; Moffett and Brand, 1997). The inability of both Teta and DFOB to limit the picoplankton, of which the photosynthetic cyanobacteria are a major component, could be explained by iron and cobalt ligand uptake systems that are resistant to perturbations by additions of exogenous ligands. However, the cyanobacteria may be the predominant users of cobalt in the open ocean: they have an absolute requirement for cobalt, while the eukaryotic algae can at least partially substitute zinc and cadmium for cobalt (Table 1). Hence, the addition of Teta may not cause the decreases in cell abundance observed with DFOB additions since the eukaryotic phytoplankton may not be affected appreciably. The observation that ^{57}Co enters the larger size fractions in our long-term study could

reflect incorporation of CoTeta into picoplankton followed by grazing, remineralization, and incorporation into larger eukaryotic phytoplankters.

In hindsight, the choice of BATS as a site for this study proved to be interesting, yet complicated. The observation that *Prochlorococcus* is stimulated by additions of Teta in these oligotrophic waters was unexpected. In addition to the stimulation observed in the *Prochlorococcus* population (Figure 6), the long-term ^{57}Co Teta experiment also shows stimulation of ^{57}Co uptake with 10^{-7}M and 10^{-8}M Teta additions (Figure 7). At the higher Teta concentrations, reduction in ^{57}Co uptake may have been caused by limitation by cobalt or another metal, or by Teta toxicity. While utilization of dissolved protein and amino acids in the Sargasso Sea has been shown to be important in supporting a significant fraction of the bacterial nitrogen demand (Keil and Kirchman, 1999; McCarthy et al., 1997), the ability to utilize other dissolved organic nitrogen species like Teta is an area that has not been significantly explored (D.Repeta, pers. comm.). While enzymes such as urease function to assimilate nitrogenous species from the surrounding milieu, it is not apparent whether this or other microbial enzymes might deaminate Teta. In preliminary experiments, the addition of small concentrations of nitrate (5-100nM N as $\text{Co}(\text{NO}_3)_2$) resulted in stimulation of *Synechococcus* and to a lesser extent *Prochlorococcus* in the Sargasso Sea, indicating that the biota has the potential to respond to small additions of nitrogen as Teta if a mechanism exists to liberate the nitrogen atoms from the ligand.

Future work could also apply the use of Teta to high nutrient low chlorophyll regions (HNLC), where nitrogen and phosphorus are abundant relative to iron and other trace elements. It should be noted that while cell numbers of *Prochlorococcus* did not increase in the Iron Ex-II experiment, intrinsic growth rates did increase upon iron additions (Mann and Chisholm, 2000), indicating a rapid response of grazing pressure to increased growth rates. As a result detecting the influence of Teta on *Prochlorococcus* may be difficult without sophisticated cell-cycle growth rate methods. In our Sargasso Sea experiments this is not an issue since we see a net increase in cell numbers with the Teta addition, indicating the cells were able to outpace grazing pressure or that grazers were inhibited (Figure 6).

Variability in the structures of natural ligands influences their specificity for certain metals and perhaps also their bioavailability. Both Fe-porphyrin and CoTeta have nitrogen ring structures and are biologically unavailable to picoplankton (Hutchins et al., 1999b; and this study). Instead of the porphyrin ring center, the CoTeta has a corrin ring similar to that of porphyrin in that there are four nitrogen ligands that ligate to a metal center. However, porphyrin rings and corrin rings (including vitamin B₁₂) have distinct chemistries: while the porphyrin ring is a highly unsaturated molecule yielding a rigid structure, the corrin ring is an saturated flexible ring which can flex in a manner that creates a steric effect that influences the bond disassociation energies of an axial organometallic cobalt-carbon bond (Geno and Halpern, 1986). These characteristics make these molecules suited for their specific biochemical purposes in photosynthesis and methylation for Fe and Co, respectively. For iron, marine siderophores have conditional stability constants that are ~1.5 log units higher than that of protoporphyrin IX (Witter et al., 2000), which suggests the picoplankton have evolved to use siderophore ligands for iron acquisition since they are superior in binding strength to porphyrin ligands. Given the large discrepancy between conditional stability constants for CoTeta and the natural CoL (Table 2), a parallel story may also be true for cobalt where the corrin ring was too weak a ligand for Co(II) uptake, and another as yet unknown ligand evolved. Alternatively, the natural cobalt ligands may be Co(III) corrin ligands, which might have much higher stability constants. It is interesting to note that the Fe-porphyrin rings are accessible to eukaryotic phytoplankters by non-specific cell surface reductases (Maldonado-Pareja, 1999), leading to the hypothesis that this is an opportunistic evolutionary adaptation of eukaryotic phytoplankton to the abundance of Fe-porphyrin molecules released by grazing and lysis (Hutchins et al., 1999b).

Future work could also utilize stronger synthetic cobalt ligands as a means to probe cobalt uptake in natural marine environments. While ligands with higher thermodynamic stability constants do exist, the difficulty is in finding one that is relatively specific for cobalt, like the dioxime ligands (e.g. DMG and nioxime) and the nitrogen ring macrocycles (e.g. Teta). This specificity is important because virtually every other first row transition metal has a higher seawater concentration than cobalt does, with the divalent cations of calcium and magnesium at concentrations of 0.0102M

and 0.0532M, respectively, 9 orders of magnitude higher in concentration than cobalt. Given these ligand design constraints, it is difficult to predict how the seawater matrix will modify the thermodynamic stability constant of a ligand to a conditional stability constant without time-consuming experimental calibrations, as we have done with Teta in this study. Nakani et al. found that Teta and 1,4,7,10-tetraazadecane (trien) have significantly higher Co formation constants than tetramethylcyclam (TMC) (Nakani et al., 1983), which is sterically hindered from the more stable isomer of the macrocycle by the presence of the methyl groups. Moreover, Teta (called CTA in Nakani et al), has been suggested to bind cobalt not with its four nitrogen donors, but rather with two of the ring nitrogens and two acetate groups (Nakani, et al., 1983). However, equimolar CoTeta chelates are significantly more stable than CoCyclam in seawater (data not shown). Perhaps two of the acetate groups and the four nitrogen ligands of Teta allow a six coordinate binding of the cobalt metal center and a high conditional stability constant for cobalt.

In conclusion, CoTeta does not appear to be bioavailable to marine microorganisms on short-term time scales or in *Prochlorococcus* cultures. However, when utilized in long-term incubations in the oligotrophic Sargasso Sea, ^{57}Co bound to Teta becomes incorporated into biota, and the biota is stimulated by additions of the Teta ligand. The inability of the Teta ligand to induce cobalt limitation in the Sargasso Sea is consistent with electrochemical measurements of strong organic cobalt ligands in seawater and with the hypothesis that organically bound cobalt can be directly taken up by phytoplankton.

Acknowledgements

This study was the work aided by Jordan Watson, who came to WHOI as a summer student fellow and stayed on into September to go on our cruise to BATS. He was responsible for the short-term cobalt uptake study. In addition, Jason T. Rex Ritt, whom also volunteered to come to sea, was invaluable in a variety of tasks and was involved in sampling the bottle incubations.

References

- Campbell, L., Nolla, H.A. and Vault, D., 1994. The importance of *Prochlorococcus* to community structure in the central North Pacific Ocean. *Limnol. Oceanogr.*, 39(4): 954-961.
- DeBaar, H.J.W., 1994. von Liebig's Law of the Minimum and Plankton Ecology (1899-1991). *Prog. Oceanog.*, 33: 347-386.
- Dusenberry, J.A. and Frankel, S.L., 1994. Increasing the sensitivity of a FACScan flow cytometer to study oceanic picoplankton. *Limnology and Oceanography*, 39(1): 206-209.
- Falkowski, P.G., 1997. Evolution of the nitrogen cycle and its influence on the biological sequestration of CO₂ in the ocean. *Nature*, 387: 272-274.
- Geno, M. and Halpern, J., 1986. Why Does Nature Not Use the Porphyrin Ligand in Vitamin B12. *Journal of the American Chemical Society*, 109: 1238-1240.
- Gordon, R.M., Johnson, K.S. and Coale, K.H., 1998. The behavior of iron and other trace elements during the IronEx-I and PlumEx experiments in the Equatorial Pacific. *Deep-Sea Res. II.*, 45: 995-1041.
- Hutchins, D.A., Franck, M., Brezezinski, M.A. and Bruland, K.W., 1999a. Inducing phytoplankton iron limitation in iron-replete coastal waters with a strong chelating ligand. *Limnol. Oceanogr.*, 44(4): 1009-1018.
- Hutchins, D.A., Witter, A.E., Butler, A. and Luther, G.W., 1999b. Competition among marine phytoplankton for different chelated iron species. *Nature*, 400: 858-861.
- Keil, R.G. and Kirchman, D.L., 1999. Utilization of dissolved protein and amino acids in the northern Sargasso Sea. *Aquatic Microbial Ecology*, 18(3): 293-300.
- Keller, M.D., Bellows, W.K. and Guillard, R.L., 1988. Microwave treatment for sterilization of phytoplankton culture media. *J. Exp. Mar. Biol. Ecol.*, 117: 279-283.
- Maldonado-Pareja, M.T., 1999. *Iron Acquisition by Marine Phytoplankton*, McGill University, Montreal, 201 pp.
- Mann, E.L., 2000. *Trace Metals and the Ecology of Marine Cyanobacteria*, MIT/WHOI, Massachusetts, 176 pp.
- Mann, E.L. and Chisholm, S.W., 2000. Iron limits the cell division rate of *Prochlorococcus* in the Eastern Equatorial Pacific. *Limnology and Oceanography*, in press.

- Martin, J.H. and Gordon, R.M., 1988. Northeast Pacific iron distribution in relation to phytoplankton productivity. *Deep-Sea Res.*, 35: 177-196.
- Martin, J.H., Gordon, R.M., Fitzwater, S. and Broenkow, W.W., 1989. VERTEX: phytoplankton/iron studies in the Gulf of Alaska. *Deep-Sea Res.*, 36(5): 649-680.
- McCarthy, M., T., P., Hedges, J. and Benner, R., 1997. Chemical composition of dissolved organic nitrogen in the ocean. *Nature*, 390(6656): 150-154.
- Menzel, D.W. and Spaeth, J.P., 1962. Occurrence of vitamin B12 in the Sargasso Sea. *Limnol. Oceanogr.*, 7: 151-154.
- Moffett, J.W. 2000. Transformations Among Different Forms of Iron in the Ocean. *Proceedings SCOR-IUPAC Symposium on Iron Biogeochemistry.* eds. D. Turner and K. Hunter.
- Moffett, J.W., R.G. Zika, L. Brand. 1990. Distribution and potential sources and sinks of copper chelators in the Sargasso Sea. *Deep-Sea Res.* 37. 1405-1427.
- Moffett, J.W., 1995. Temporal and spatial variability of copper complexation by strong chelators in the Sargasso Sea. *Deep-Sea Research I.*, 42(8): 1273-1295.
- Moffett, J.W. and Brand, L.E., 1997. Production of strong, extracellular Cu chelators by marine cyanobacteria in response to Cu stress. *Limnol. Oceanogr.*, 41(3): 388-395.
- Morel, F.M.M. et al., 1994. Zinc and carbon co-limitation of marine phytoplankton. *Nature*, 369: 740-742.
- Nakani, B.S., Welsh, J.J.B. and Hancock, R.D., 1983. Formation Constants of Some Complexes of Tetramethylcyclam. *Inorg. Chem.*, 22: 2956-2958.
- Partensky, F., Hess, W.R. and Vault, D., 1999. *Prochlorococcus*, a Marine Photosynthetic Prokaryote of Global Significance. *Microbiology and Molecular Biology Reviews*, 63(1): 106-127.
- Price, N.M. et al., 1988/1989. Preparation and chemistry of the artificial algal culture medium Aquil. *Biol. Oceanogr.*, 6: 443-461.
- Price, N.M. and Morel, F.M.M., 1990. Cadmium and cobalt substitution for zinc in a marine diatom. *Nature*, 344: 658-660.
- Riebesell, U., Wolf-Gladrow, D.A. and Smetacek, V., 1994. Carbon dioxide limitation of marine phytoplankton growth rates. *Nature*, 361: 249-251.

- Saito, M.A., 2000. The Biogeochemistry of Cobalt in the Sargasso. Ph.D. Thesis, MIT-WHOI Joint Program in Chemical Oceanography, Massachusetts.
- Saito, M.A. and Moffett, J.W., 2000a. Complexation of cobalt by natural organic ligands in the Sargasso Sea as determined by a new high-sensitivity electrochemical cobalt speciation method suitable for open ocean work. submitted.
- Saito, M.A. and Moffett, J.W., 2000b. Total Cobalt in the North Atlantic and Sargasso Sea. submitted.
- Shriver, D.F., P.W. Adkins and Langford, C.H., 1990. Inorganic Chemistry. Freeman and Company., New York., 706 pp.
- Sunda, W. and Huntsman, S., 1995a. Iron uptake and growth limitation in oceanic and coastal phytoplankton, NMFS, NOAA, Beaufort, NC, 44 pp.
- Sunda, W.G. and Huntsman, S.A., 1995b. Cobalt and Zinc interreplacement in marine phytoplankton: biological and geochemical implications. *Limnol. Oceanogr.*, 40: 1404-1417.
- Thomson-Bulldis, A. and Karl, D., 1998. Application of a novel method for phosphorus determinations in the oligotrophic North Pacific Ocean. *Limnol. Oceanogr.*, 43(7): 1565-1577.
- Tremaine, S. and Mills, A., 1987. Inadequacy of the eucaryote inhibitor cycloheximide in studies of protozoan grazing on bacteria at the freshwater-sediment interface. *Appl. Environ. Microbiol.*, 53(8): 1969-1972.
- Waterbury, J.B., Watson, S.W., Valois, F.W. and Franks, D.G. (Editors), 1986. Biological and Ecological Characterization of the Marine Unicellular Cyanobacterium *Synechococcus*. Photosynthetic Picoplankton. Can. Bull. Fish. Aquat. Sci., 583 pp.
- Wells, M.L., 1999. Manipulating iron availability in nearshore waters. *Limnol. Oceanogr.*, 44(4): 1002-1008.
- Wilhelm, S.W., MacAuley, K. and Trick, C.G., 1998. Evidence for the importance of catechol-type siderophores in the iron limited growth of a cyanobacterium. *Limnol. Oceanogr.*, 43(5): 992-997.
- Wilhelm, S.W., Maxwell, D.P. and Trick, C.G., 1996. Growth, iron requirements, and siderophore production in iron-limited *Synechococcus* PCC 7002. *Limnol. Oceanogr.*, 41(1): 89-97.

- Witter, A.E., Hutchins, D.A., Butler, A. and III, G.W.L., 2000. Determination of conditional stability constants and kinetic constants for strong model Fe-binding ligands in seawater. *Marine Chemistry*, 69(1-2): 1-17.
- Wu, J., Sunda, W., Boyle, E.A. and Karl, D.M., 2000. Phosphate Depletion in the Western North Atlantic Ocean. *Science*, 289(5480): 752-762.
- Yee, D., 1997. Cobalt Substitution for Zinc in Marine Phytoplankton. PhD. Thesis, Massachusetts Institute of Technology, Cambridge.
- Yee, D. and Morel, F.M.M., 1996. In vivo substitution of zinc by cobalt in carbonic anhydrase of a marine diatom. *Limnol. Oceanogr.*, 41(3): 573-577.

Figure 6-1

Application of Liebig's law of the minimum to the Sargasso Sea (A) and HNLC regions (B). Each bar refers to the amount of biomass that could be produced using the quantity of each element in a liter of seawater if that element was limiting. The lowest bar in each graph indicates which element should be limiting according to Liebig's law. The circles illustrate the diminishing effect of non-bioavailable metal ligand complexes on limitation of primary productivity. This plot is a simplification of primary productivity in oceanic ecosystems since it does not account for regeneration, recycling, advective input, aeolian input, or numerous other biogeochemical processes. Variation in the cellular quotas of transition metals are caused by physiological adjustment of the biota rather than experimental variability. Organisms tend to reduce their cellular quotas for a metal if it becomes limiting. Instead of using variability in cellular carbon quotas, the variability in concentration of inorganic carbon species is used with a single cellular carbon quota to illustrate greater difficulty in utilizing $\text{CO}_{2(\text{aq})}$ relative to bicarbonate. $\text{CO}_{2(\text{aq})}$ drawdown will be replenished by equilibration with HCO_3^- ; however, the dehydration of carbonic acid is kinetically slow and could be slow relative to biotic carbon uptake rates (Riebesell et al., 1994). Calculations are based on laboratory cellular quota experiments and total trace metal measurements. See Table 4 for data and references.

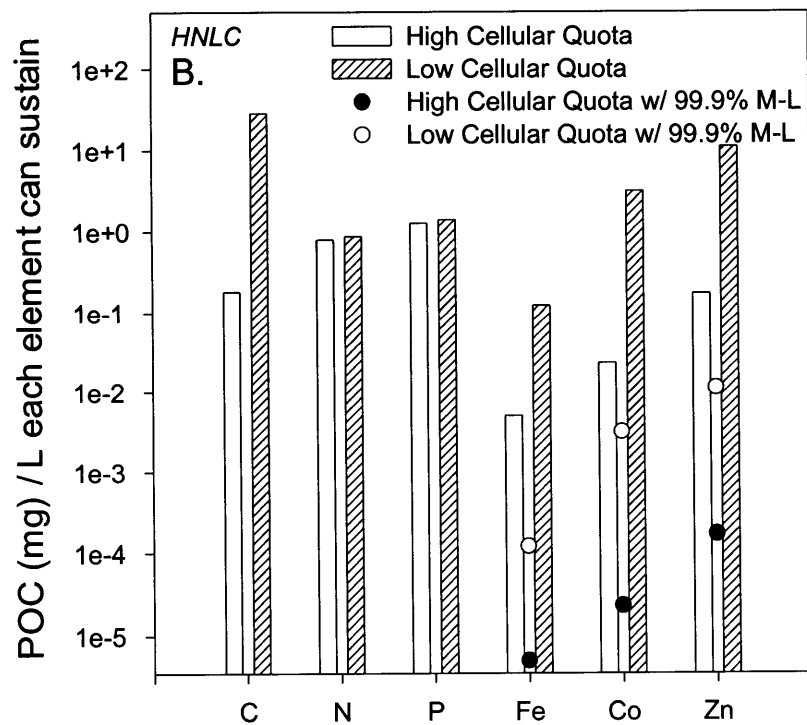
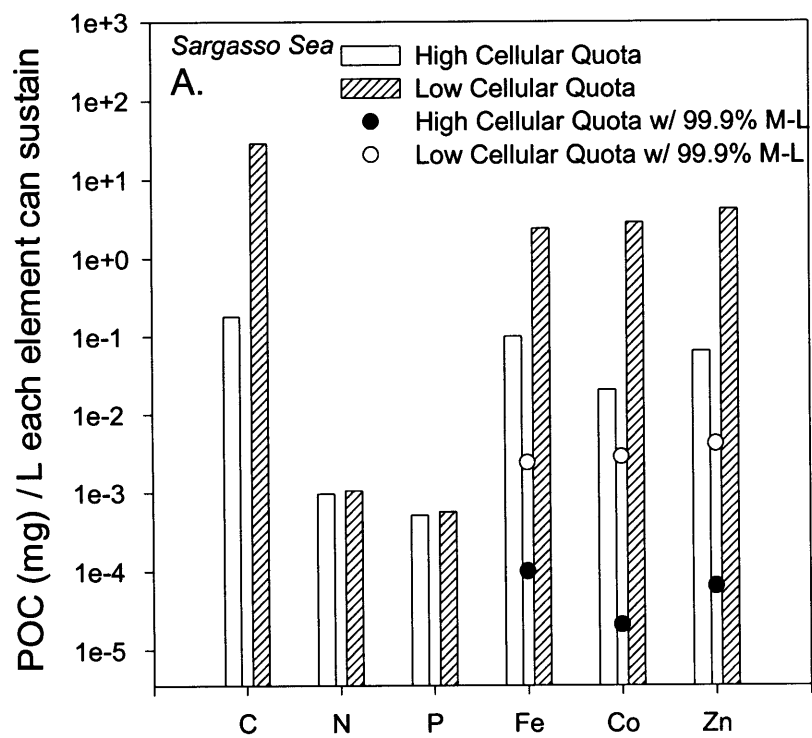
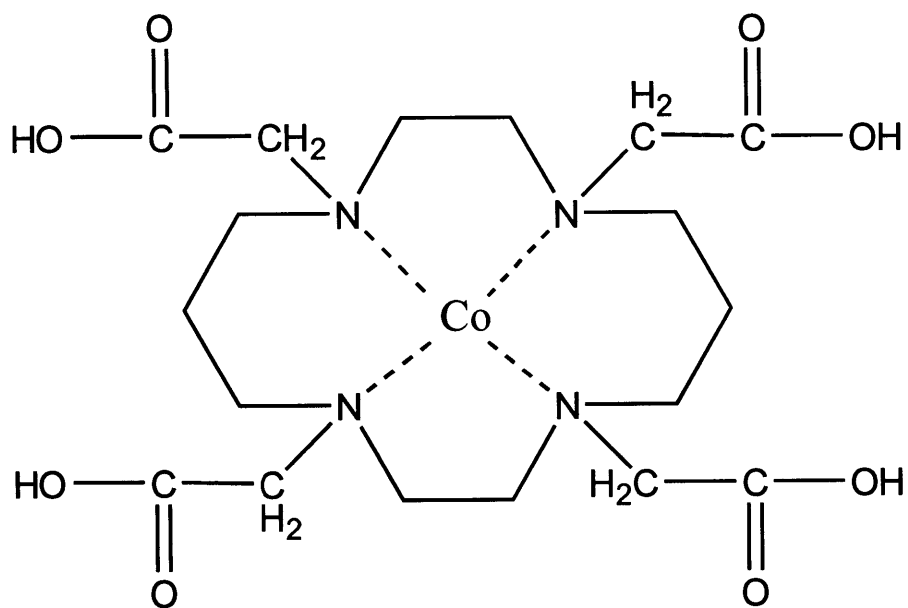
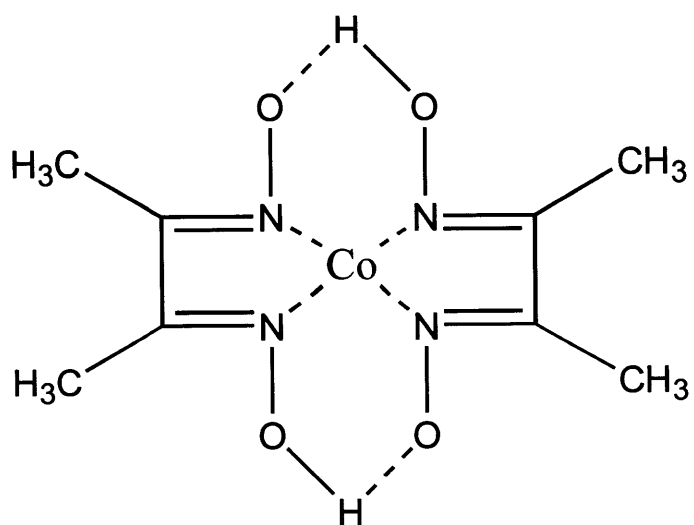


Figure 6-2

Structures of CoTeta (1,4,8,11 tetraazacyclotetradecane 1,4,8,11 tetraacetic acid hydrochloride hydrate) and CoDimethylglyoxime (CoHDMG₂).



Cobalt Teta



Cobalt Dimethylglyoxime

Figure 6-3

An electrochemical kinetic experiment with the Teta ligand illustrating how Co(II)Teta is not inert to chemical equilibria reactions. 100pM CoCl₂ was added to a 10μM Teta 50mM DMG UV-SSW matrix. The gradual increase in CoHDMG₂ as measured by peak height indicates 1) that CoTeta formation is fast and that a significant portion of the added CoCl₂ became CoTeta, and 2) that CoTeta is labile: we can observe its dissociation and the formation of CoHDMG₂ on a time scale of minutes.

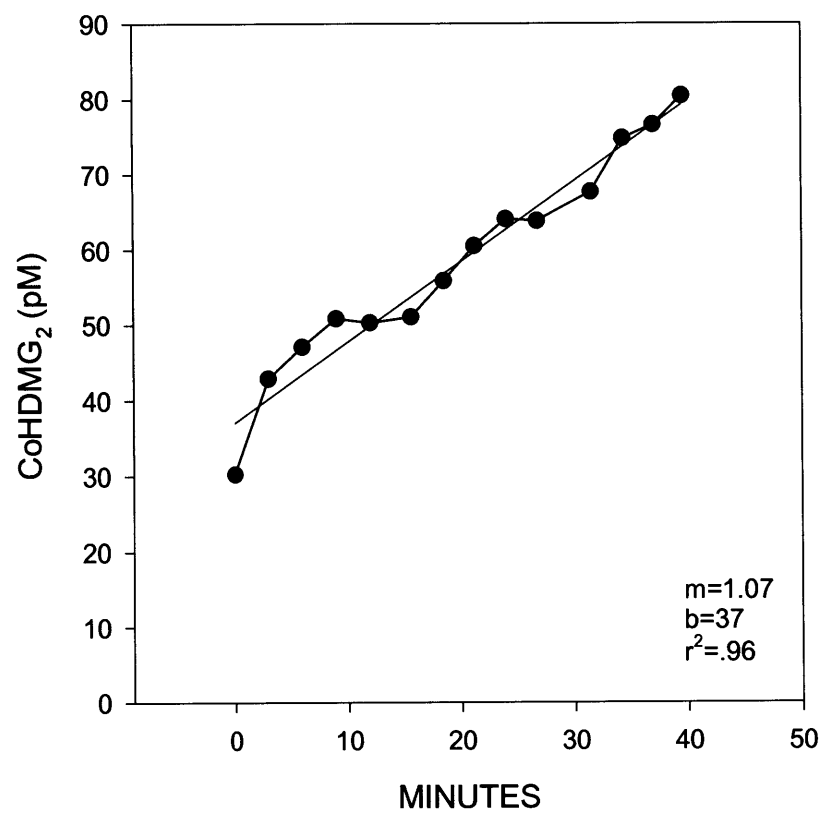


Figure 6-4

A) Effect of Teta and DMG on cobalt limitation of *Prochlorococcus* strain MED4-Ax in culture media containing 500pM Co and 11.7μM EDTA. Flow cytometry data shows how Teta limited growth by reduction in growth rate and in biomass yield with increasing Teta concentrations. B) A comparison of growth rates with Teta and DMG treatments. A control treatment with 100nM cobalt and 50nM cyclam verified that the cultures were cobalt limited.

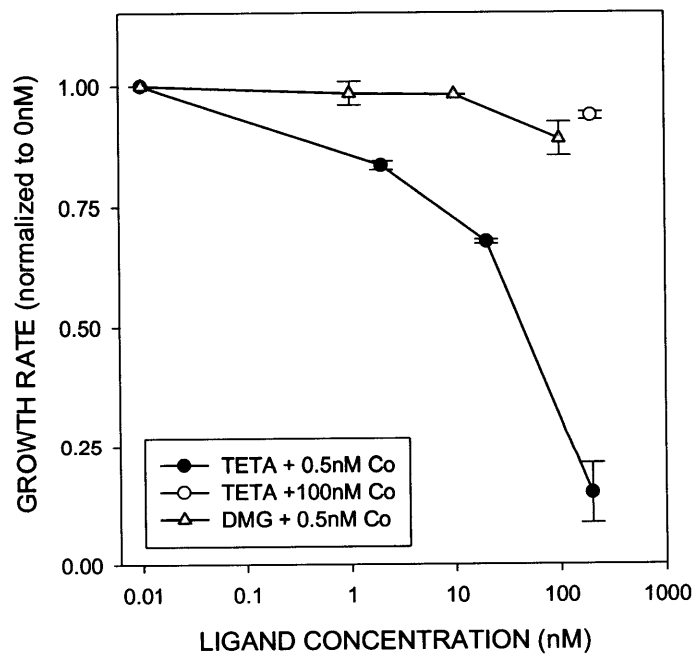
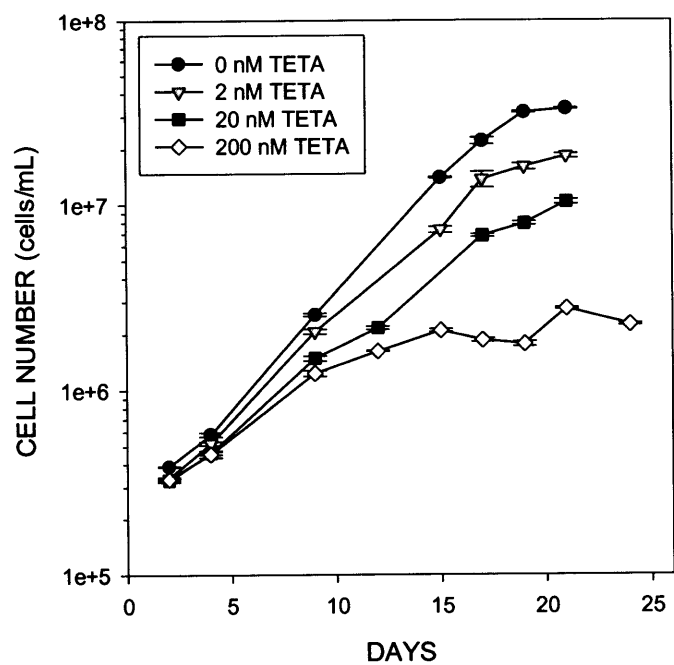


Figure 6-5

Short-term $^{57}\text{CoTeta}$ uptake experiment in a Sargasso seawater incubation. The addition of pre-equilibrated $^{57}\text{CoTeta}$ resulted in little cobalt uptake over a 12h period relative to control treatments where Teta was not added. A final concentration of 0.5 pM ^{57}Co and 100nM Teta was added to both treatments and the Teta treatment, respectively. This data set implies that the $^{57}\text{CoTeta}$ chelate itself is not bioavailable to the biota in seawater. Each of the replicates for each treatment is shown, and error bars are from detector counting statistics. Samples were filtered through 0.2 μm filters.

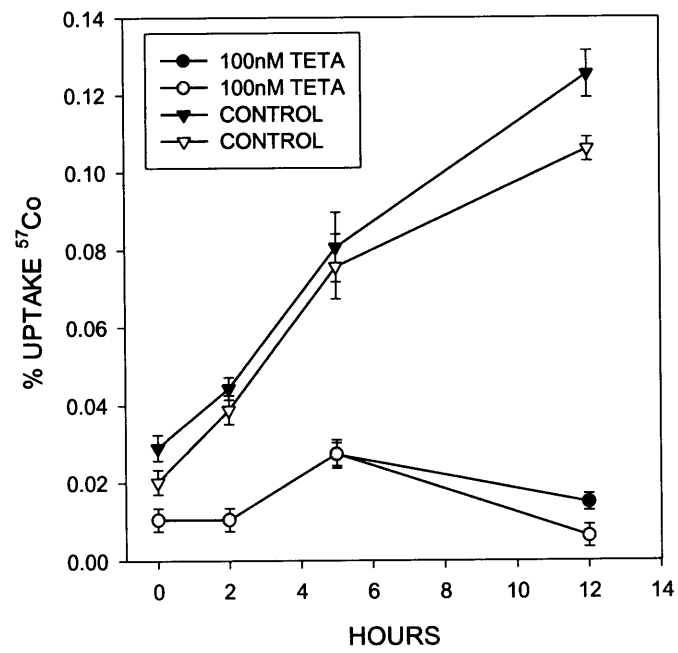


Figure 6-6

The effects of Teta on net growth of *Prochlorococcus* in Sargasso Sea bottle incubations. Teta additions showed an increase in *Prochlorococcus* cell numbers within 2d of the addition. *Prochlorococcus* did not appear to become cobalt limited with the addition of Teta, on the contrary we hypothesize that the stimulation observed may be related to alleviation of nitrogen limitation from the nitrogen present in Teta. Incubations were done in replicate and the differences between control and +500nM are significant to a confidence level greater than 90%. No cobalt was added with the Teta in this experiment.

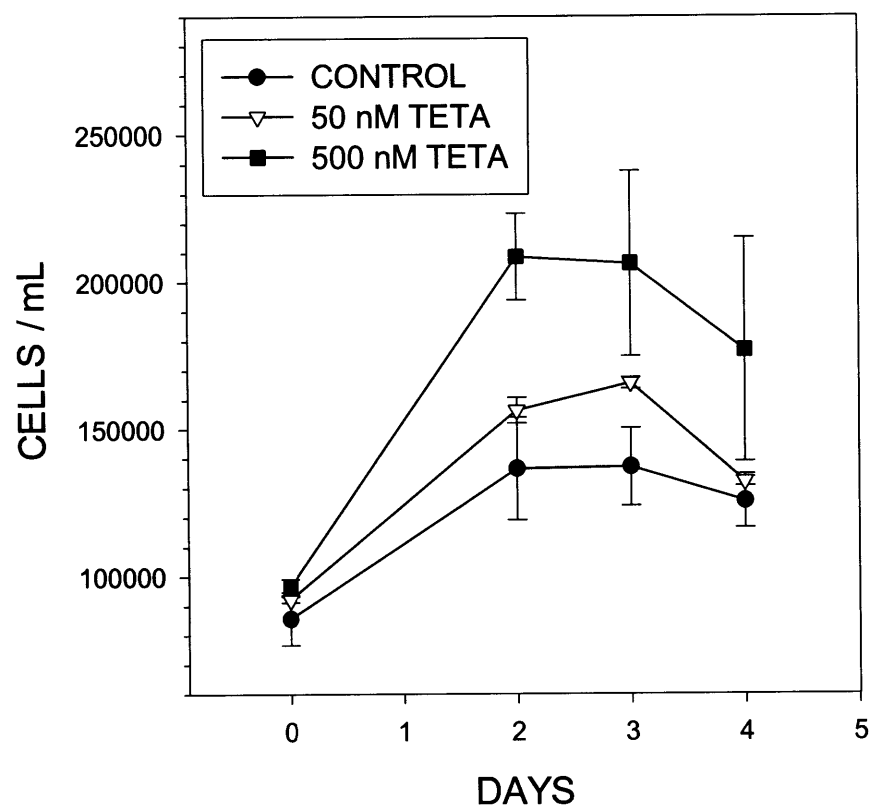


Figure 6-7

Effect of Teta on long-term (3d) ^{57}Co uptake by the microbial community from 100m.

Two particulate size ranges were examined by filter fractionation. After 3d of incubation with Teta and ^{57}Co an increase in uptake was observed with low concentration of Teta (0.5nM - 50nM) and a decrease in ^{57}Co uptake was observed in the 500nM and 5000nM treatments. These results suggest a lack of cobalt limitation and instead stimulation by Teta before Teta toxicity or cobalt limitation at higher concentrations.

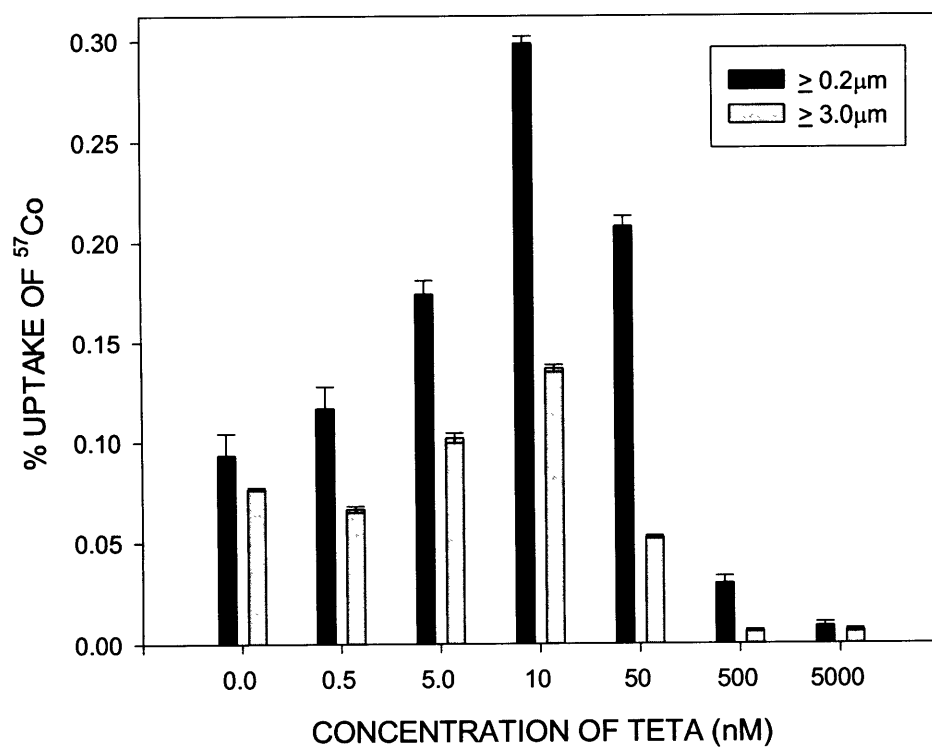


Figure 6-8

The influence of UV-light on the uptake of ^{57}Co equilibrated with filtered seawater. Axenic *Prochlorococcus* cells were added after the 3d sunlight exposure treatment and incubated for 5h with 3.3% of on-deck light level. Decreases in cobalt uptake rate suggest either degradation of cobalt uptake ligands or flooding of inorganic uptake channels by other metals released by ligand degradation.

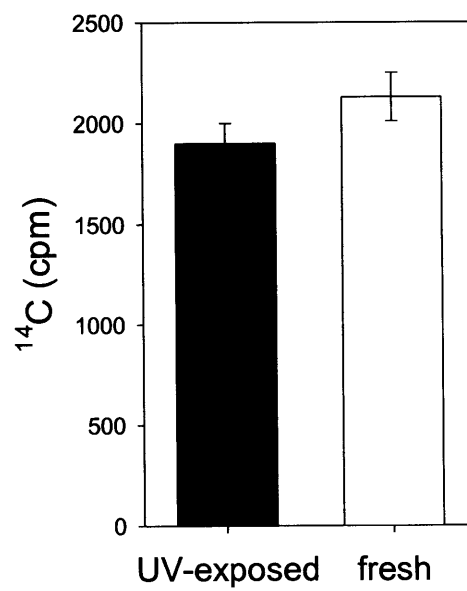
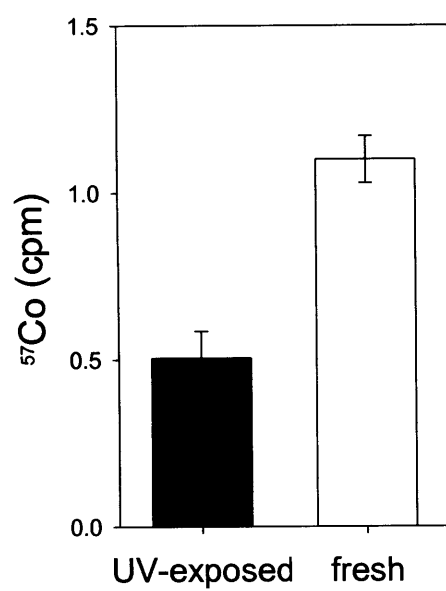


Table 6-1 Cobalt requirements and substitutions in marine phytoplankton

Organism	Distribution	Biogeochemical Influence	Cobalt Requirement	Zinc Substitution	Cadmium Substitution
<i>Prochlorococcus</i> ^a	Global/Subtropical	30-80% GPP*	absolute	no	possible
<i>Synechococcus</i> ^b	Coastal & Global	major cont. GPP	absolute	no	unknown
<i>Emiliana huxleyi</i> ^b	Global	Bloom, CaCO ₃	absolute	yes	unknown
<i>T. weissflogii</i> ^c	Coastal	Bloom, Opal	affects growth	yes	yes
<i>T. oceanica</i> ^b	Global	Bloom, Opal	affects growth	yes	unknown

* refers to gross primary production (Partensky et al., 1999)

^a (Saito, 2000) and Saito et al. unpublished

^b (Sunda and Huntsman, 1995b)

^c (Yee, 1997; Yee and Morel, 1996)

Table 6-2 Conditional Stability Constants for DMG and Teta calibrated using EDTA

Compound	Stoichiometry	log K'(Co(II))
Teta	[ML]/[M][L]	11.2 ± 0.1*
Dimethylglyoxime (pH = 8.0)	[ML ₂]/[M][L] ²	11.5 ± 0.3 ⁺
Co-L	[ML]/[M][L]	16.3 ± 0.9

⁺ error from standard deviation of mean results of three separate calibration curves.

* error from standard deviation of individual points on titration curve n ≥ 3.

Table 6-3 Stimulation of *Prochlorococcus* by Teta additions

Treatment	Cells/mL (max)	Net growth rate (d ⁻¹)	Estimated N use *
Control	140000 ± 13000	0.097 ± 0.08	-- --
50nM Teta	170000 ± 1900	0.19 ± 0.02	20nM (10%)
500nM Teta	210000 ± 15000	0.26 ± 0.05	46nM (2.3%)

* N use estimated using the increase in cells relative to the control, Redfield ratios, and 53fg C/cell. The percentage is the amount of the N needed for the cell number increase relative to the amount added as Teta.

Table 6-4 Application of Liebig's Law of the Minimum to the Sargasso Sea

Element	Cell Quota (mol P ⁻¹)		Sargasso Sea	HNLC	mg POC as C possible:	
Surface	High	Low	Surface Conc.	Surface Conc.	Sargasso	HNLC
C (DIC)	106	106	0.00238M	0.00238	28.6	28.6
C (CO ₂)	106	106	1e-5	1e-5	0.18	0.18
N	16	14.49	12nM	10μM	9.6e-4 - 1.1e-3	0.80 - 0.88
P	1	0.9052	0.4nM	1μM	5.1e-4 - 5.6e-4	1.3 - 1.4
Fe	0.013	5.3e-4	1.0nM	0.05 - 0.7nM	0.10-2.4	5.0e-3 -0.12
Co	0.0012	8.5e-6	0.019nM++	0.021 ± 0.004	0.021-2.9	0.023- 3.1526
Zn	0.0014	2.1e-5	0.07 - 10nM+	0.185 - 10nM	0.065-4.2	0.17 - 11

*Fe cell quotas taken from (Sunda and Huntsman, 1995a)

** Zn and Co cell quotas taken from (Sunda and Huntsman, 1995b)

++ cobalt data: Sargasso Sea data from (Saito and Moffett, 2000b). Annual average at BATS depth 40m, n = 29. HNLC data from (Gordon et al., 1998), outside patch, depth ≤ 40m, n=17.

Appendix I.

Purification of *Prochlorococcus marinus* isolates

J. Waterbury and M. Saito

Introduction

Since the discovery of *Prochlorococcus* (Chisholm et al., 1992), isolates have been cultured from a variety of regions around the world (Moore et al., 1995; Partensky et al., 1999). However, these cultures have all been non-axenic, meaning that they contained heterotrophic bacteria in addition to the *Prochlorococcus* strain of interest. There has been a clear need for axenic cultures in physiological experiments without the potential ambiguities of bacterial effects and for a variety of molecular biology techniques. Yet obtaining pure cultures of *Prochlorococcus* has proven to be non-trivial: efforts to serially dilute or plate strains tried by several research groups have met with little success. Several months before our attempts, Rosie Rippka succeeded in purifying one strain of *Prochlorococcus*, using serial dilution, but has been unable to reproduce these results (pers. comm.). In this appendix, we present the method we developed and utilized to culture *Prochlorococcus* strains on agar plates and resuspend them in solution to achieve two axenic strains, MED4-Ax and MIT9312-Ax.

Methods

Using laboratory isolates that had been in culture for several years and isolated by serial dilution (Chisholm et al., 1992), we tried both serial dilution and plating methods. Prior to plating, MED4 and SS120 (isolated from the Mediterranean Sea and the Sargasso respectively) were grown in K-media with 11.7 μ M EDTA (Chisholm et al., 1992) diluted with tyndallized Milli-Q water (microwave sterilized filtered Milli-Q water) to 75% seawater, and major nutrients (ammonia, urea and phosphate) were then added to K-media concentrations from sterile stock solutions. All glassware was cleaned with overnight soaking in micro or citranox detergent, followed by overnight soaking in 10% HCl (Baker Instra-analyzed), and thorough rinsing with Milli-Q water.

Serial dilutions of MED4 cultures were prepared by diluting to 10^{-5} , 10^{-6} , 10^{-7} from the original culture into sterile polystyrene tubes. Each tube contained 5mL of 75% K-media, half of which were amended with 10% spent media. The spent media amended tubes produced *Prochlorococcus* growth 2-3 weeks sooner than the normal media controls in the most concentrated 10^{-5} dilution. In our trial plating attempts with 75% K-media+, we dedicated half of our plates to spent media enrichments and kept the other half as normal controls. The agar/seawater plating attempts with spent media additions consistently produced vigorous and visibly green growth after 2-3 months while the control plates often did not produce any *Prochlorococcus* growth at all.

The media recipe is equivalent to K-media (Keller et al., 1987; Chisholm et al., 1992) except for three changes: the dilution to 75% seawater, the addition of three vitamins, and the addition of spent media (Table 1). Filtered SSW was microwaved for 10 min/L (Keller et al., 1988) immediately after filtration and was diluted to 75% with tyndallized Q water. The final EDTA concentration is $11.7\mu\text{M}$, however, it should be noted that over the past two decades of manufacturing there have been significant differences in the purity of the Na_2EDTA crystals with respect to trace metal concentrations. The Na_2EDTA used is the SigmaUltra grade (lot 115HO7461 purchased in 1997). 100 μL per 100mL of biotin, B_{12} (cobalamin), and thiamin vitamins were added to the media from their respective 1.5 $\mu\text{g/mL}$ sterile stock solutions. The urea (Sigma cell culture grade lot 73H09525), phosphoric acid (Sigma lot 44H3449 P-5811) and ammonium hydroxide, isothermally distilled Fisher Trace Metal grade were added aseptically using sterile pipettes. Once all the ingredients were added, the media was microwaved again to $\sim 60^\circ\text{C}$ to kill any vegetative cells and left loosely capped overnight to re-equilibrate with air.

Spent media was prepared by growing 25mL of SS120 in the 100% K-media with no added cobalt. When the cultures entered the transition between log phase and stationary phase they were filtered through a 0.2 μm sterile acrodisc syringe filter that had been rinsed with 10% HCl and Milli-Q water, and collected into a sterile acid cleaned polycarbonate container. The spent media was refrigerated and kept in darkness until use.

Agar/seawater plates were prepared as 75% seawater ionic strength, with the Milli-Q water used to dissolve the agar providing the dilution. Invitrogen 'bacclovirus' agar (lot 502183 opened 8/1997) was added to 50mL of Q water (0.35g per 100mL) and microwaved/boiled until dissolved. The agar was then added to 150 mL of 100% K-media+ and placed in a ~35°C water bath, which kept the solution above the 32°C solidifying temperature and cool enough to minimize condensation. ~10mL was poured into each petri dish and allowed to cool overnight.

The plates were streaked using a flamed loop dipped into a 75% K-media culture nearing stationary phase. Four areas were drawn on the underside of the plate to demark the dilutions. Once the first area was streaked, the loop was flamed again cooled by touching the second area, run across the first area, and streaked across the second area. This was repeated for the third and fourth dilution areas. 100% seawater plates were also prepared by dissolving the agar in hot 50mL K-media and then adding 150 of the modified K-media as described above (called K-media+ from hereon). *Prochlorococcus* isolates grown in 100% K-media and transferred to 100% K-media+ plates did successfully form colonies, although their growth was not as vigorous as with isolates grown in 75% media and on 75% K-media+ plates.

The *Prochlorococcus* colonies were picked by cutting a divot of agar out using a flamed tungsten spatula. We noticed that unlike the *Synechococcus* colonies (Waterbury et al., 1986), the MED4 and SS120 colonies were sticky and difficult to remove from the plates. The divot was placed in a sterile clean polycarbonate tube with 5mL of K-media+ of the corresponding salinity.

We checked for axenicity using a marine purity test (Waterbury et al., 1986) and visual inspection of late stationary phase cultures and of the the purity test broth on a Zeiss Standard microscope equipped with epifluorescent illumination and a 100-W mercury lamp for non-coccoid non-fluorescent cells.

Fluorescence emission measurements on dissolved organic matter was measured by excitation at 450nm and scanning between 480-770nm on an HP fluorescence spectrophotometer at a rate of 1000. Filtered aliquots of spent media were added to 1cm quartz cuvettes. A peak was apparent at 680nm and peak height was calculated.

Results

Strain SS120 (Sargasso Sea isolate) was plated at different points in the growth cycle onto 100% seawater/agar plates (Figure 1). When plated only a few days into stationary phase, no growth on the plates was observed. But allowing the culture to stay in stationary phase for 20 additional days yielded SS120 growth on plates.

Prochlorococcus growth on plates streaked from this very late stationary phase cultures was observed repeatedly and occurred two weeks sooner than from an exponentially growing culture streaked under the same conditions.

Prochlorococcus strain MED4 was successfully plated on 75% K-media+ plates and an isolated colony was picked and placed in 5mL of 75% K-media+ . The picked colony took two months to turn the media visibly green, at which point it was transferred to another K-media+ tube followed by 5% and 1% inoculation volume respectively into 20mL of 75% K-media+ and 100% K-media (Figure 2). Axenic MED4 (MED4-Ax) grew faster in the 100% K-media, despite a slightly smaller inoculation volume, thereby showing no difficulty in adjusting to the higher salinity or lack of spent media and vitamins.

Once established in culture, we conducted a minimum inoculation size experiment (Figure 3). Using borosilicate tubes and K-media+, we added between 0.1% and 5% inoculum a late-log phase culture. The expected fluorescence based on dividing the 5% inoculum fluorescence is given by the small open symbols. No growth is observed at the 0.5% and 0.1% inoculation volume. Based on previous lab experience, the axenic MED4 is more prone to fail in transferring with small inoculation volume than the non-axenic culture. Further research is necessary to elucidate the cause of this inoculation size effect. Two hypotheses as to the cause of this effect are 1) there is a minimum cell number needed to transfer, or 2) there was a dilution of dissolved ingredients found in the conditioned media. The second of these possibilities would explain the influence of the spent media effect that we observed. However, the advantage of spent media likely to only be apparent below a threshold inoculum volume when it would be diluted out. An experiment looking at the influence of spent media and vitamin

mix on the growth rate of MED4-Ax culture showed only a small effect on growth rate in each case (Figure 4).

The logic behind using spent media was based on an observation that large amounts of yellow colored organic material is exuded under severe cobalt limiting conditions (Figure 5 and 6). We have noticed a consistent and significant improvement in growth and yield of *Prochlorococcus* on both plates and in serial dilutions amended with 5% spent media relative to controls. It is conceivable that when diluted to single cells on a plate or a few hundred cells from a picked colony in media, free chelators present in the spent media bind up necessary trace metals from the EDTA and increase the bioavailability of those metals. We know that *Synechococcus* can produce siderophore chelators, which can alter the media and pull iron away from the synthetic buffer EDTA (Wilhelm and Trick, 1996). Normally in transfers of cultures a large inoculum is used (e.g. 5% inoculum volume), which would also transfer significant amounts of chelators. When cells are diluted to 1-100 cells, there is no transfer of chelators. Hence, the addition of spent media compensates for this and could increase the bioavailability of nutritive metals.

References

- Chisholm, S.W. et al., 1992. *Prochlorococcus marinus* nov. gen. nov. sp.: An oxyphototrophic marine prokaryote containing divinyl chlorophyll a and b. Arch. Microbiol., 157: 297-300.
- Keller, M.D., Bellows, W.K. and Guillard, R.L., 1988. Microwave treatment for sterilization of phytoplankton culture media. J. Exp. Mar. Biol. Ecol., 117: 279-283.
- Moore, L.J., Goericke, R.E. and Chisholm, S.W., 1995. The comparative physiology of *Synechococcus* and *Prochlorococcus*: influence of light and temperature on growth, pigments, fluorescence and absorptive properties. Mar. Ecol. Prog. Ser., 116: 259-275.
- Partensky, F., Hess, W.R. and Vaulot, D., 1999. *Prochlorococcus*, a Marine Photosynthetic Prokaryote of Global Significance. Microbiology and Molecular Biology Reviews, 63(1): 106-127.
- Waterbury, J.B., Watson, S.W., Valois, F.W. and Franks, D.G. (Editors), 1986. Biological and Ecological Characterization of the Marine Unicellular Cyanobacterium *Synechococcus*. Photosynthetic Picoplankton. Can. Bull. Fish. Aquat. Sci., 583 pp.

Figure I-1

Plating success as a function of growth phase. Plates were streaked from culture at two different times during stationary phase, on day 19 and day 40. The growth curves for this culture is shown in this figure, with duplicate tubes. The open symbol replicate was used for streaking numerous plates. Plates from day 19 did not yield any *Prochlorococcus* growth, as measured by visual inspection for green lawns, and by epi-fluorescent microscopy. Plates from very late stationary phase on day 40 did yield *Prochlorococcus* growth. This phenomenon was observed repeatedly.

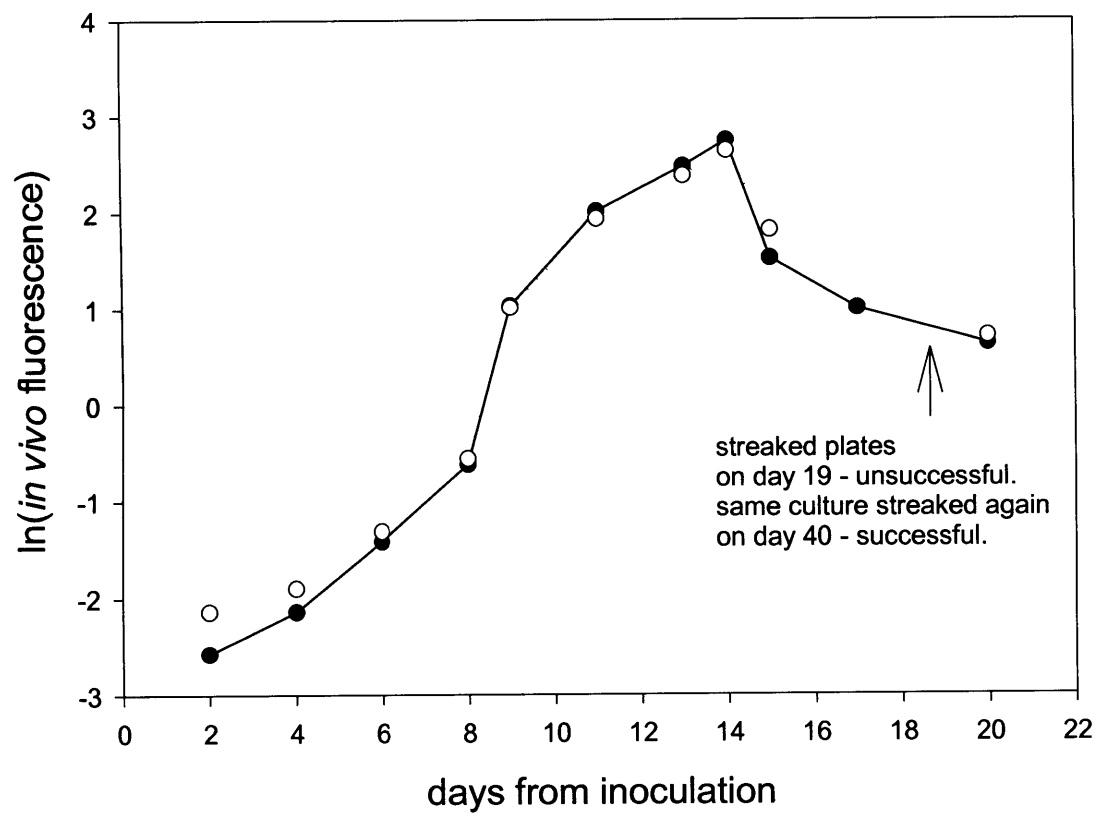


Figure I-2

Transfer of axenic MED4-Ax strain into 100% and 75% seawater media. MED4-Ax had been picked from a colony and transferred into media, transferred once, and then added two these two treatments. Although the plating procedure utilized 75% seawater media, MED4-Ax had no difficulty in adjusting to 100% seawater media soon after its isolation.

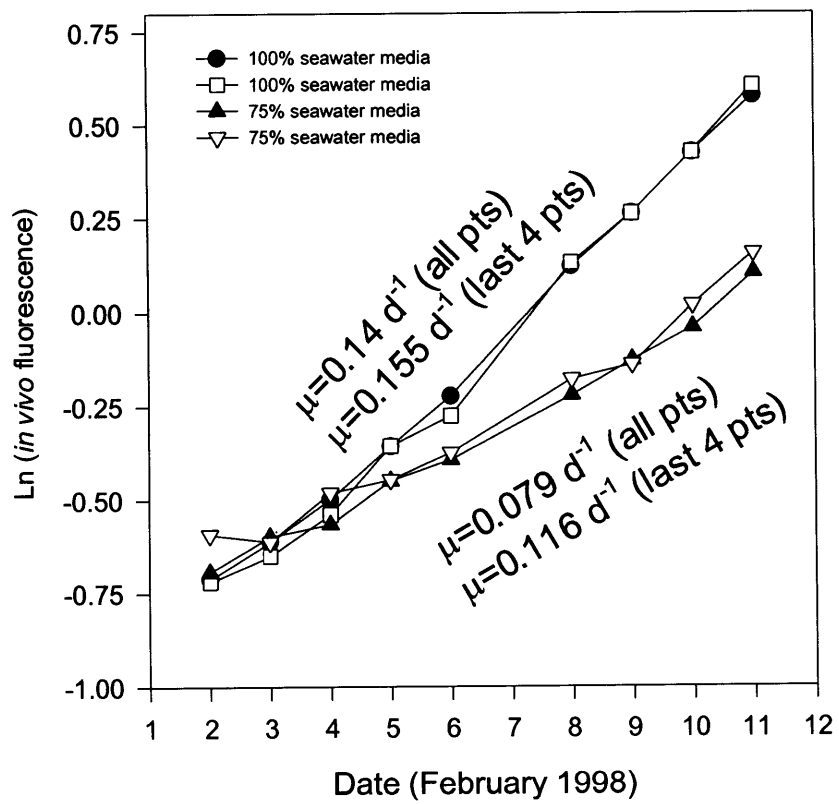


Figure I-3.

The influence of inoculum size on the survival of MED4-Ax *Prochlorococcus* cultures. Large symbols indicate measured data, and small symbols indicate calculated fluorescence based on the dilution of inoculum and a constant growth rate. At small inoculum volumes cultures of *Prochlorococcus* do not grow well. This phenomenon is likely related to the problems associated with plating, where green lawns of *Prochlorococcus* and heterotrophs are readily produced, but individual colonies of *Prochlorococcus* are rare. Cultures were started from a single inocula culture using a range of inocula volumes. Exponential growth was measured using *in vivo* fluorescence, and the 2.5% inoculum volume matched the calculated dilution of *in vivo* fluorescence. The 0.1% and 0.5% inoculum volumes did not survive transferring.

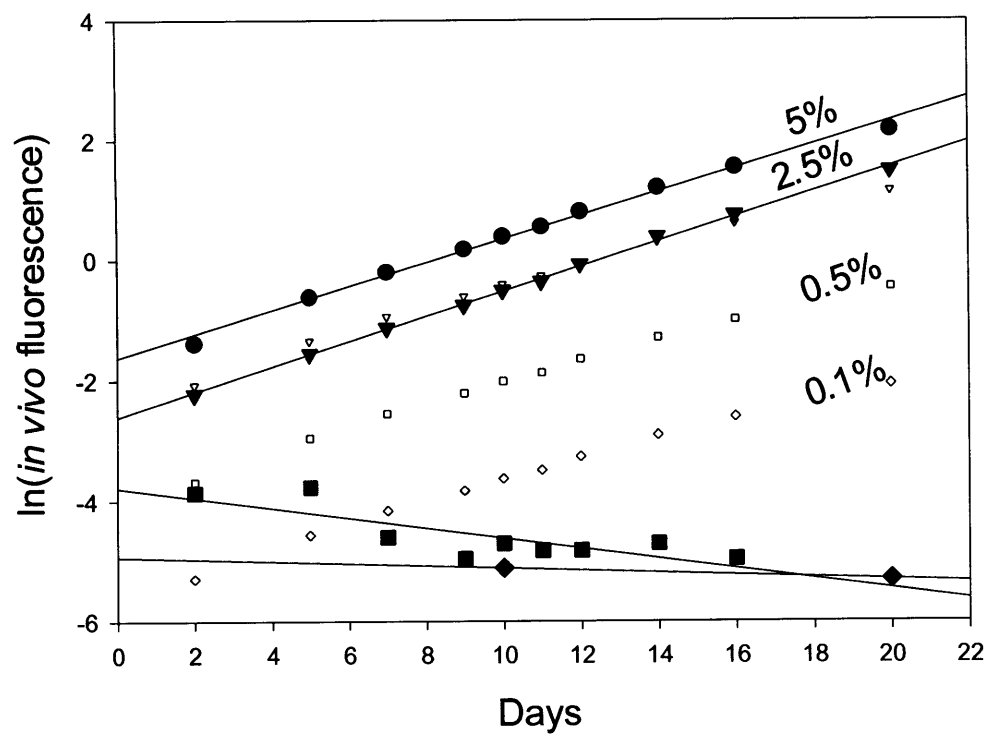


Figure I-4.

The influence of inoculum volume, 10% spent media and vitamin mix (1µg/L biotin, cobalamin, and thiamin) on the growth rate of MED4-Ax cultures. While decreasing spent media significantly affected growth rate, little effect of spent media or vitamin mix was observed. The relatively high cell densities of these cultures likely hides any influence of the spent media.

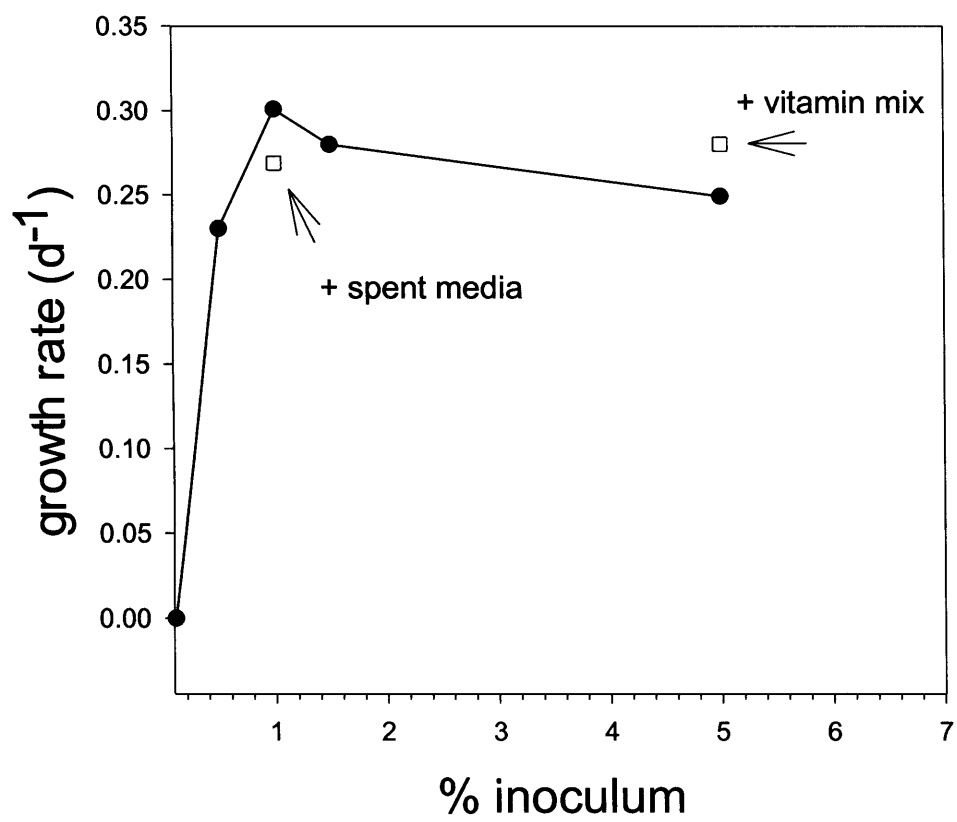


Figure I-5.

Production of colored dissolved organic material in cobalt limited cultures. Cobalt limited cultures in late-log phase were syringe filtered through 0.2µm acrodisk filters and analyzed on a fluorescence spectrophotometer. Fluorescence emission at 680nm increased with the degree of cobalt limitation, suggesting either that cobalt limited cultures were exuding dissolved organic material, that cobalt limited cultures were more susceptible to lysis upon filtration, or that surface bound DOM was being removed by filtration. This material could be related to the improved plating results we observe with the addition of spent media.

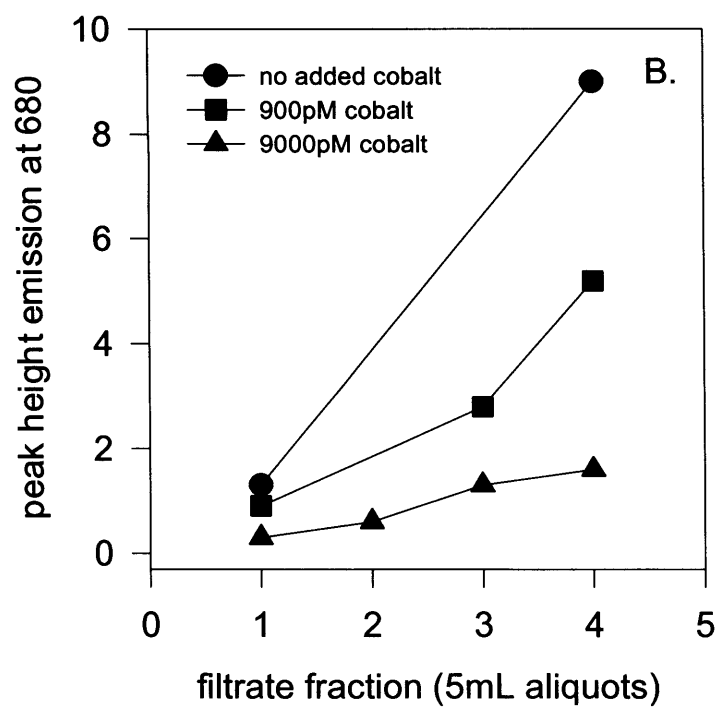
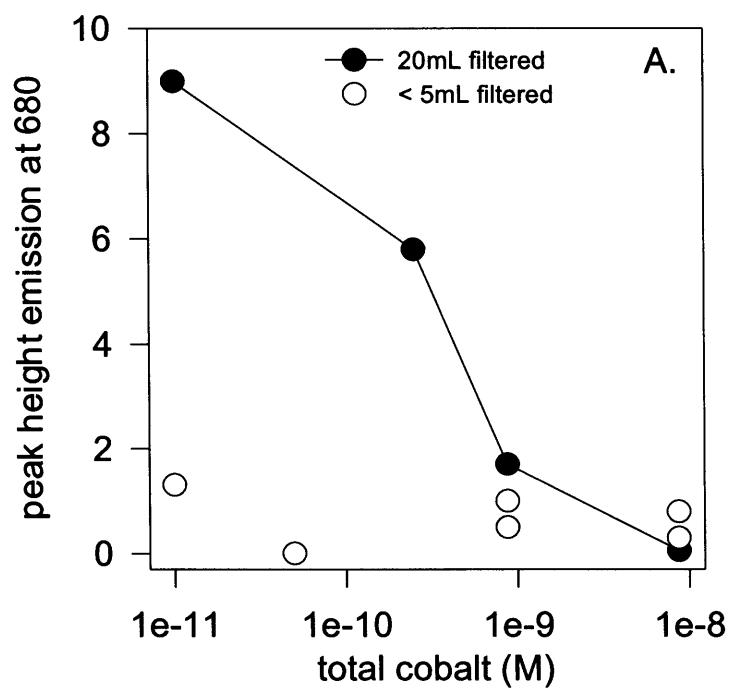


Figure I-6.

Raw fluorescence spectra from a cobalt limited culture with a large peak at 680nm. The fluorescence spectrophotometer was programmed to excite at 430nm and scan for emission between 480-770nm.

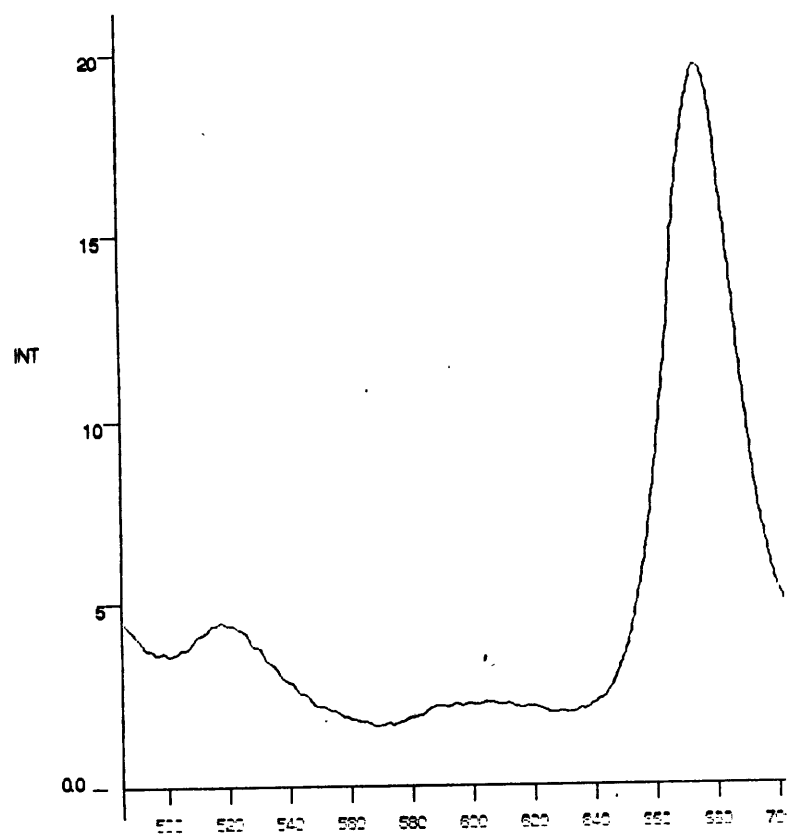


Table I-1 Pro-1 media composition for plating made with 75% Sargasso Seawater

	Concentration
H ₃ PO ₄ ⁻	10 µM
Ammonia	50 µM
Urea	100 µM
Na ₂ EDTA (Sigma Ultra)	11.7 µM
Fe(III)Cl ₃	1.17 µM
Co(II)Cl ₂	5 nM
NiCl ₂	10 nM
ZnCl ₂	8.0 nM
MoO ₄	3.0 nM
Mn	90 nM
Se	10 nM
cobalamin (B ₁₂)	1 µg/L
thiamin	1 µg/L
biotin	1 µg/L
Spent media (filtered)	10%

Appendix II.

A calculation of the fraction of the cobalt that exists as B₁₂ in photosynthetic cyanobacteria

In addition to physiological measurements testing the ability of *Prochlorococcus* or *Synechococcus* to utilize cobalamin (B₁₂), we can compare calculations of the amount of cobalt relative to the amount cobalt in B₁₂ in *Synechococcus*. Cobalt cellular quota data for *Synechococcus bacillus* is from Sunda and Huntsman (1995), and B₁₂ cellular quota data for *Synechococcus* strain PCC7002 is from Wilhelm and Trick (1995). Ideally, the same experimentalist would measure the both the B₁₂ and Co:C quota on the same strain. However, both of these goals are formidable. Hence, this appendix presents a simple calculation in the absence of such a study.

$$256 \text{ B}_{12} \text{ molecules/cell} \times 1\text{Co:1B}_{12} / 2.7 \times 10^9 \text{ C atoms/cell} = 9.6 \times 10^{-8} \text{ Co:C as B}_{12}$$

$$\textit{Prochlorococcus} \text{ volume: } 4/3\pi(0.3)^3 = 0.11 \mu\text{m}^3 \text{ (assuming a diameter of } 0.6\mu\text{m)}$$

$$\textit{Synechococcus} \text{ volume: } 4/3\pi(0.6)^3 = 0.90 \mu\text{m}^3 \text{ (assuming a diameter of } 1.2\mu\text{m)}$$

Prochlorococcus has 53 fg C/cell (Campbell et al., 1994)

Synechococcus should have 8.2 fold higher carbon per cell,
based on volume calculations

$$= 424 \text{ fg C cell}^{-1} = 2.1 \times 10^{10} \text{ C atoms per cell}$$

Synechococcus Co:C, assuming B₁₂ is the sole repository of cobalt in the cell:

$$= 0.012 \mu\text{mol Co mol}^{-1} \text{ C}$$

Sunda and Huntsman Co:C measurements in *Synechococcus bacillus*:

$$\text{from } 0.3 - 11 \mu\text{mol Co mol}^{-1} \text{ C}$$

$$\text{B}_{12} < 4\% \text{ of the cobalt quota in } \textit{Synechococcus}$$

References

- Campbell, L., Nolla, H.A. and Vault, D., 1994. The importance of *Prochlorococcus* to community structure in the central North Pacific Ocean. *Limnol. Oceanogr.*, 39(4): 954-961.
- Sunda, W.G. and Huntsman, S.A., 1995. Cobalt and Zinc interreplacement in marine phytoplankton: biological and geochemical implications. *Limnol. Oceanogr.*, 40: 1404-1417.
- Wilhelm, S.W. and C.G. Trick. 1995. Effects of vitamin B₁₂ concentration on chemostat cultured *Synechococcus* sp. strain PCC7002. *Can. J. Microbiol.* 41. 145-151.

Appendix III.

The relationship between fluorescence per cell and *in vivo* fluorescence

Introduction

Fluorometers and flow cytometers are two instruments that allow estimation of phytoplankton culture growth. Fluorometers measure the relative amount of pigment within a culture of phytoplankton cells by projecting a narrow wavelength range of light on the culture and measuring the fluorescent light emission. This instrument has the advantage of being a non-invasive technique, where the culture tube itself can be placed within the instrument for a brief period of time of the measurement. The culture is not adversely affected by the measurement. In addition, by avoiding opening and subsampling of the culture tube, the risk of trace metal contamination is greatly reduced.

Flow cytometry instruments utilize the same principle of excitation using a laser beam as a light source and measuring fluorescent emission at multiple wavelength ranges (depending on the number of photomultiplier tubes) on *individual cells* as they pass through the flow cell of the instrument. In addition, light scatter can be measured at various angles from the flow cell as a measurement of cell size or texture. More complete descriptions of flow cytometry and its application to the study of marine phytoplankton are available elsewhere (Chisholm et al., 1986; Davey and Kell, 1996; Lepesteur et al., 1993; Marie et al., 1997). Flow cytometry has the advantage of being highly sensitive, being able to measure pigment per cell and cell size, and having small sample sizes (e.g 150µl). The ability to measure cell number directly allows us to avoid concerns of whether the culture is in balanced growth as with fluorometry. Disadvantages to flow cytometry relative to fluorometers include significantly slower sample throughput, invasive sampling, and slightly decreased instrumental precision.

Together these instruments provide an invaluable combination for studies of phytoplankton physiology. Growth rates can be obtained using fluorometry on numerous experimental treatments and replicates, and more detailed information such cell size,

pigment per cell, and DNA per cell can be measured using flow cytometry. However, care must be taken to avoid misinterpretation of fluorometer data due to detection limit problems and variability in fluorescence per cell when cells are not in exponential growth. In this appendix, I discuss the factors that need to be considered when utilizing *in vivo* fluorescence.

Methods

Turner fluorometers (model 10 series and AU-10) were used to measure fluorescence of batch cultures in either borosilicate or polycarbonate tubes. The cultures were grown with media as described in Chapters 4 and 5. Flow cytometry samples were run on a Becton-Dickinson FACScan as described in Chapter 4. FACScan samples were frozen in liquid nitrogen (Lepesteur et al., 1993) and *in vivo* fluorescence measurements were taken within 2h of each other. The *Prochlorococcus* strain SS120 was grown in these experiments in polycarbonate tubes. This strain was not (and still is not) available in axenic cultures. An inoculum volume of 0.08% was used from a single low cobalt culture tube in an effort to try to dilute out the presence of any biogenic cobalt ligands. In addition, high inoculum volume (2.2%) experiments were conducted with *Prochlorococcus* strain MED4-Ax. Each of the fluorometers used in this study had different sensitivities, and hence were compared with flow cytometry separately.

Results and Discussion

In vivo fluorescence and cell number measured on a samples from a variety of cobalt treatments (Figure 1) shows a strong correlation between these two parameters above a $\ln(\text{in vivo fluorescence})$ of value of -1.7 or 1.1×10^6 cells/mL with an r^2 of 0.979 (Figure 2). Below this number of *Prochlorococcus* cells the relationship degenerates with *in vivo* fluorescence values measuring a baseline at the detection limit while cell number continues to decrease. While growth rates at the end of the growth curve can be calculated with fluorescence, the plateau in cell number in the 0.18pM cobalt treatment is not observed in the fluorescence data set due to the detection limit problem. Since these culture treatments all began from with the same inoculum culture and with equal inoculum volumes, it is clear that the treatments are distinct from each other in Figure

1A. If they were not all the lines would be overlapping. Moreover, one can extrapolate the growth rate of the 0.18pM Co^{2+} culture back to day 1 and discern that there must have been a time of lower growth rate that occurred when the culture was below detection limit. It should be noted that the inoculum volumes used in this experiment are only 0.08%. These small inoculum volumes were used to try to dilute out any natural cobalt ligands that may have been produced by *Prochlorococcus* or the heterotrophic bacteria in these cultures.

Another example of the relationship between fluorescence and flow cytometry is evident in Figure 3. In this instance, there is no detection limit problem because the inoculum volume was significantly higher (2.2% inoculum volume) resulting in a higher number of cells at the beginning of experiments.

The regressions shown in Figures 2 and 3 illustrate how cultures grown at a single light intensity can have a relatively constant fluorescence per cell. However, there are two situations where this relationship can degenerate. First, stationary phase caused by nutrient limitation can result in a rapid decrease in fluorescence per cell as the pigment within the cells is degraded (Figure 3) before the cells themselves undergo apoptosis. Second, under severe nutrient limitation cells may adjust their pigment per cell to cope with the nutrient stress. However, such large changes in fluorescence per cell in cultures grown in the same light level are not usually observed (Figure 3C). Exceptions to this include stationary phase (Figure 3A), where fluorescence per cell decreases rapidly, and extreme nutrient limitation.

While the estimation of growth rates and cell number using fluorometry needs to be done with care, there are experimental designs that can avoid complications with variable fluorescence per cell. If differences between experimental treatments is the primary objective, and invasive sampling for flow cytometry is problematic due to the potential for trace metal contamination, *in vivo* fluorescence can be monitored for a numerous treatments provided all of the treatments were started with inocula of equal volumes from the same source. For example, the antagonistic effects of nickel on cobalt limited cultures were explored using treatments inoculated with a 0.08% volume from the same inoculum culture (Figure 5 of Chapter 4). Deviation between treatments shows a significant antagonistic effect. While we cannot specify if the effect due to a change in

growth rate or a decrease in fluorescence per cell when nickel is added, the antagonistic effect itself is unambiguous.

References

- Chisholm, S., Armbrust, E.V. and Olson, R., 1986. The Individual Cell in Phytoplankton Ecology: Cell Cycles and Applications of Flow Cytometry. : 343-369.
- Davey, H. and Kell, D., 1996. Flow Cytometry and Cell Sorting of Heterogeneous Microbial Populations: the Importance of Single-Cell Analyses. Microbiological Reviews, 60: 641-696.
- Lepesteur, M., Martin, J.M. and Fleury, A., 1993. A comparative study of different preservation methods for phytoplankton cell analysis by flow cytometry. Marine Ecology Progress Series, 93: 55-63.
- Marie, D., Partensky, F., Jacquet, S. and Vaultot, D., 1997. Enumeration and cell cycle analysis of natural populations of marine picoplankton by flow cytometry using the nucleic acid stain SYBER Green I. Applied and Environmental Microbiology, 63: 186-193.

Figure III-1.

In vivo fluorescence and flow cytometry measurements on a cobalt limited culture. A) *In vivo* fluorescence measurements of cobalt limited *Prochlorococcus* SS120 cultures with the detection limit of the Turner AU-10 fluorometer for *Prochlorococcus* shown by a dashed line. Data points below the line are inaccurate. Concentrations of cobalt are given as free Co^{2+} ions. All treatments were done in duplicate and started from the from a single low cobalt culture with equal inoculum volumes. B) Flow cytometry data shows a plateau in cell number that is below the detection limit of the fluorometer in the 0.18pM treatment. Since both treatments were started with equal volumes of the same inoculation culture and maximal growth rates of the two treatments are similar, the plateau in cell number below the detection limit explains the temporal offset from the 1.1pM treatment.

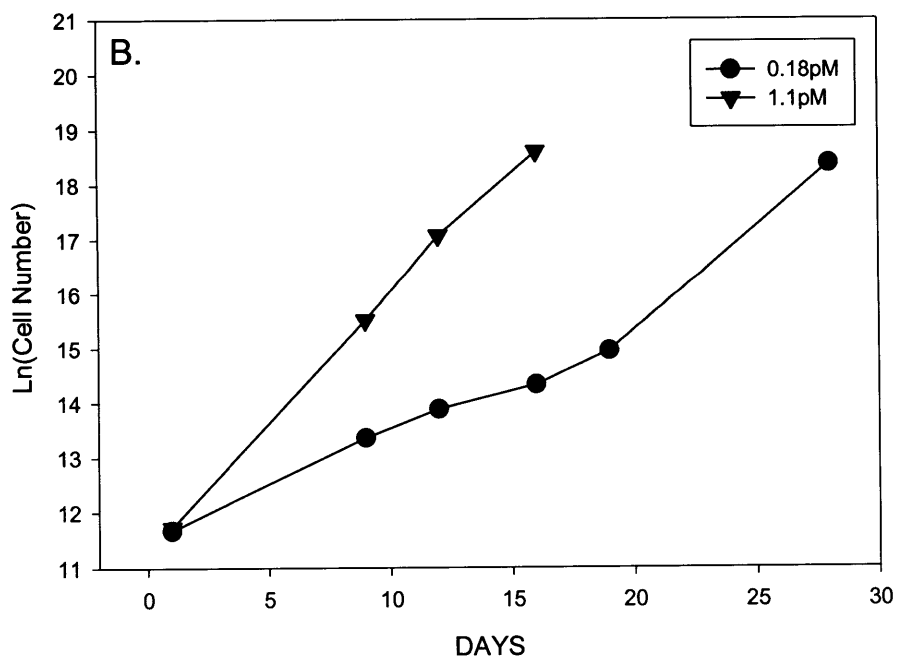
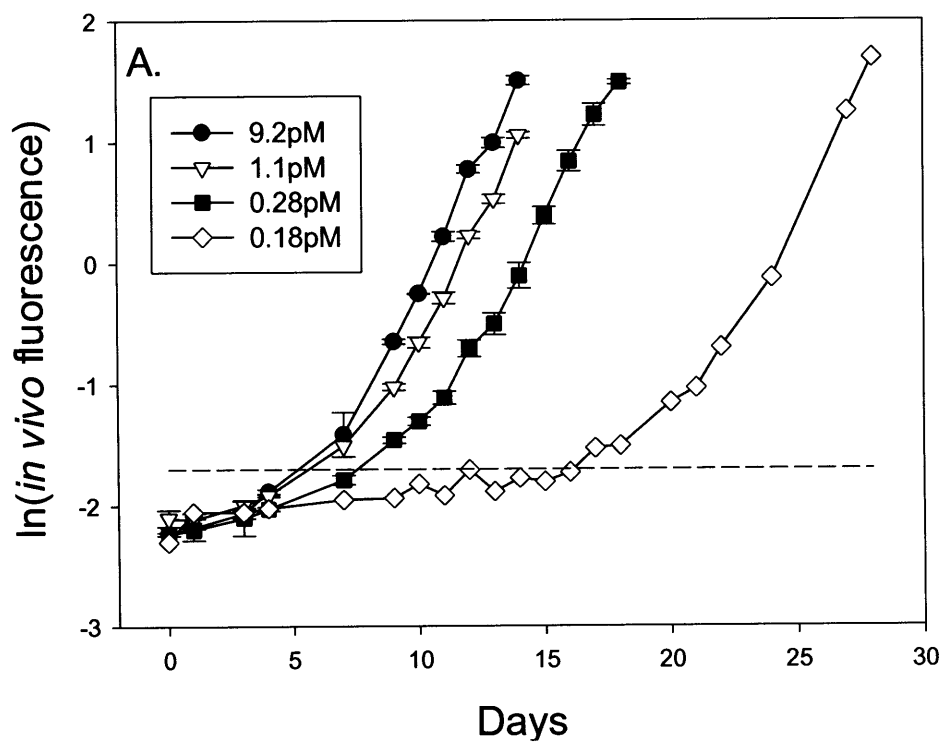


Figure III-2.

Regression of cell number versus *in vivo* fluorescence of *Prochlorococcus* cells. Closed symbols indicate samples that are above the Turner fluorometer detection limit, and open symbols indicate samples below. A linear regression of samples above the detection limit shows a strong correlation with an r^2 of 0.979. Different fluorometers will have different slopes and sensitivity; the Turner fluorometer in the Chisholm Lab was utilized for this calibration.

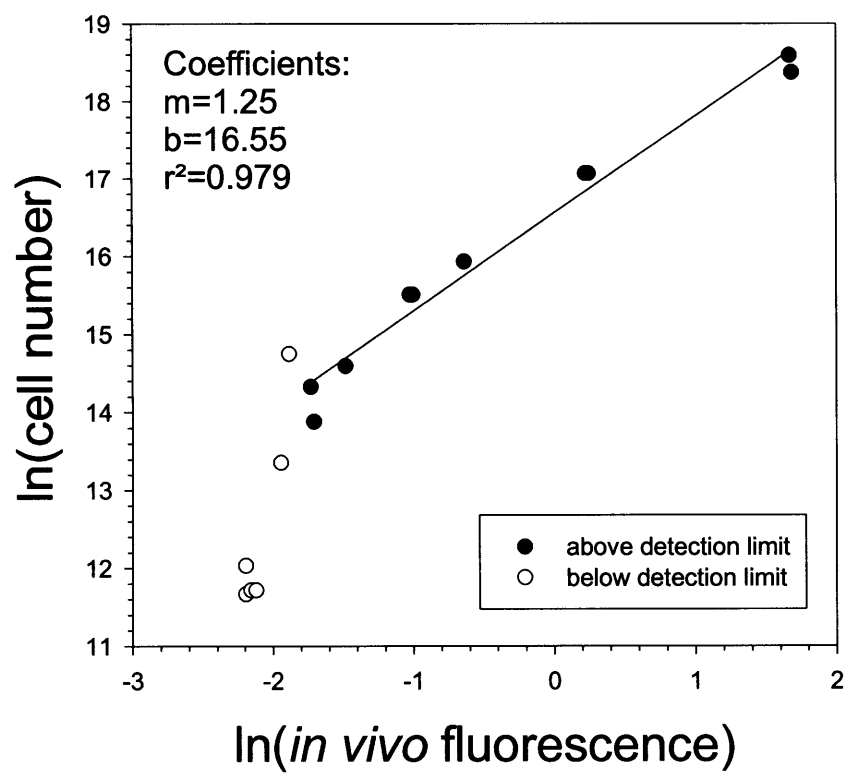
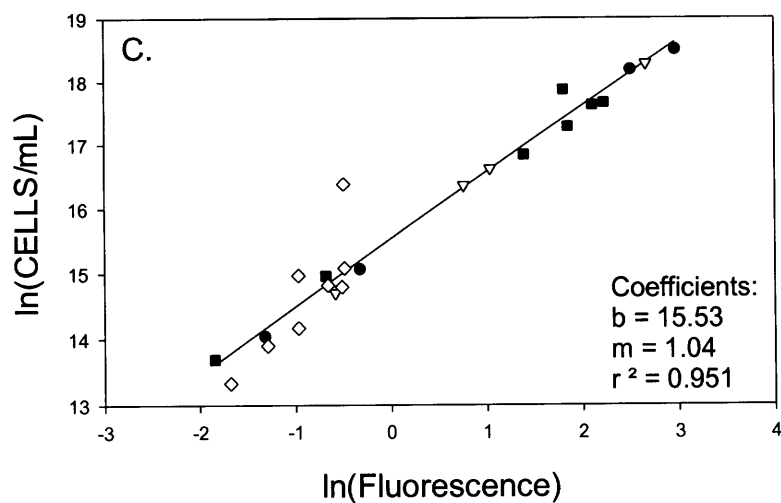
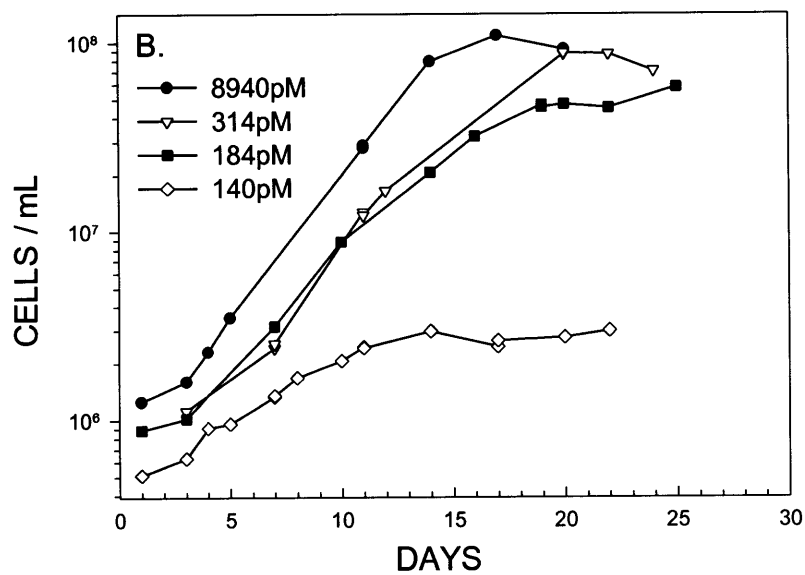
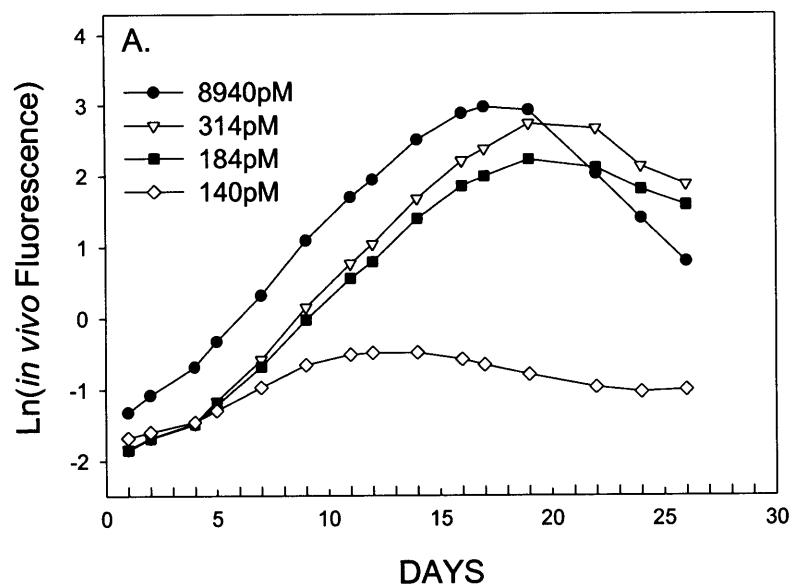


Figure III-3

Growth curves of cobalt-limited *Prochlorococcus* MED4-Ax cultures (2.2% inoculum volume). A) *In vivo* fluorescence for the four cobalt treatments. B) Cell number data as measured by flow cytometry. Comparisons of sampled and unsampled replicates by *in vivo* fluorescence was excellent indicating that the sampling for flow cytometry did not contaminate cultures with cobalt. C) Regression of fluorescence to cell number data. Not every *in vivo* fluorescence data point has a corresponding flow cytometry data point. The large inoculum volumes avoided problems with fluorometer detection limits. The *in vivo* fluorescence data was measured on the Anderson Lab Turner AU-10 fluorometer in the spring of 1999.



Appendix IV.

Long-term cobalt limitation studies of *Prochlorococcus* in
NTA and EDTA media: Raw data

Figure IV-1

Cobalt limited cultures of *Prochlorococcus* SS120 in successive transfers using a 2.5% inoculum volume. Cultures were grown in 10^{-4} M NTA media and under the conditions described in Chapter 4. Raw data is shown to illustrate the absolute requirement of *Prochlorococcus* for cobalt. Low cobalt treatments were inoculated from higher cobalt concentrations when previous transfers did not survive. Cobalt concentrations refer to the total cobalt in the culture media (added plus estimated media blank of 150pM).

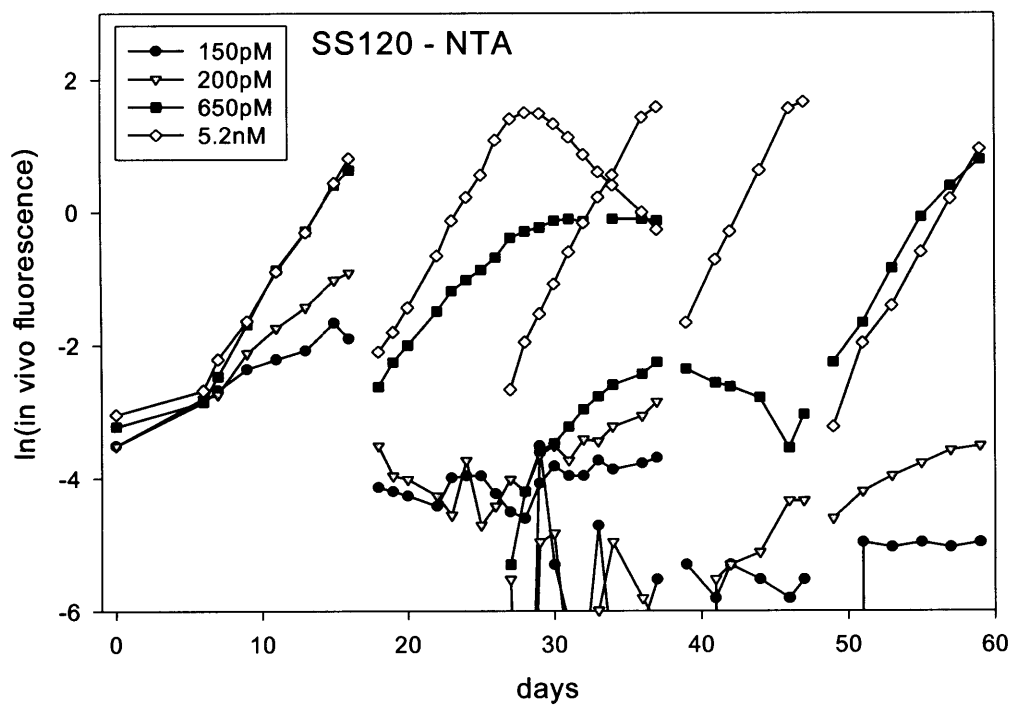


Figure IV-2

Cobalt limited cultures of *Prochlorococcus* MED4-Ax in successive transfers using a 2.2% inoculum volume. The raw data is plotted to illustrate the repeatability of absolute cobalt limitation. Cultures were grown in 11.7 μ M EDTA and under conditions described in Chapter 4. Cobalt concentrations refer to total cobalt added, and a cobalt blank of 140 \pm 13pM was measured. The fifth transfer was used for cell cycle experiment in Chapter 5. Replicates are not plotted in order to simplify the figure. 1st transfer: all from same tube - only low cobalt tubes plotted here. 2nd transfer: highest three concentrations from 45pM, low two from 0pM. 3rd transfer: highest three conc. transferred from tube of same concentration, low two are from 174pM (low culture of previous transfer did not survive). 4th transfer: all but 0pM are transferred from same concentration (no 870pM tubes on this run). 5th transfer: used two high concentrations (only those survived). 6th transfer: each Co level transferred from same level, 0pM was also transferred from 45pM in anticipation of its non-survival from 0pM transfer (both transfers plotted).

